

STUDIES ON CHEMICAL METHODS OF PREPARATION OF FINE CERAMIC POWDERS

**THESIS
SUBMITTED TO
THE UNIVERSITY OF KERALA
IN PARTIAL FULFILMENT
OF THE REQUIREMENTS
FOR THE DEGREE OF
DOCTOR OF PHILOSOPHY IN CHEMISTRY**

BY

HARI KRISHNA VARMA P. R

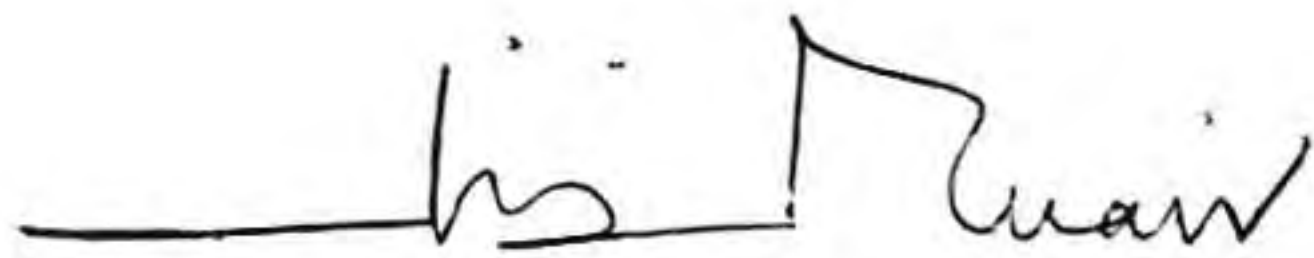
**REGIONAL RESEARCH LABORATORY (CSIR)
TRIVANDRUM - 695 019
INDIA**

AUGUST 1992

.... DEDICATED TO MY PARENTS
AND TEACHERS

CERTIFICATE

This is to certify that the thesis entitled "Studies on Chemical Methods of Preparation of Fine Ceramic Powders" is an authentic record on the research work carried out by Mr. Hari Krishna Varma P.R., M.Sc., under our supervision in partial fulfilment of the requirement for the Degree of Doctor of Philosophy of the University of Kerala and further that no part thereof has been presented before for any other degree.



*Dr. K.G.K. Warriar
Scientist, BSMR Division
Regional Research Laboratory
Trivandrum 695 019*

*Prof. (Dr.) C.G.R. Nair
Professor of Chemistry,
University of Kerala and
Chairman, Kerala State
Committee on Science,
Technology and Environment and
Ex Officio Secretary,
Government of Kerala*

DECLARATION

I, HARI KRISHNA VARMA P.R., hereby declare that this thesis entitled 'Studies on Chemical Methods of Preparation of Fine Ceramic Powders', is a bonafide record of research work done by me and that no part of this thesis has been presented earlier for any degree or diploma of any other Universities.

(HARI KRISHNA VARMA P.R.)

CONTENTS

Acknowledgements	i
Synopsis	iii
List of Publications	vi
List of Figures	ix
List of Tables	xvii

PART A

CHAPTER I CHEMICAL METHODS OF PREPARATION OF CERAMIC POWDERS

Introduction	1
✓ General methods for the preparation of fine ceramic powders	6
Preparation of $\text{YBa}_2\text{Cu}_3\text{O}_{7-x}$ high T_c superconducting particulates - A review	18
Conclusion	31

CHAPTER II METHODS OF CHARACTERISATION OF POWDERS

Introduction	50
Chemical analysis	50
Phase analysis	51
Thermal analysis	52
Particle size analysis	53
Microscopic techniques	54
Density	56
Surface area	57

**CHAPTER III PREPARATION AND PROCESSING OF YBCO AND
YBCO/Ag COMPOSITE BY CITRATE GEL ROUTE**

**Citrate gel route for the preparation of
 $\text{YBa}_2\text{Cu}_3\text{O}_{7-\delta}$ superconducting compound**

Introduction	61
Chemistry of citrate gel	62
Experimental	62
Methods	64
Results and discussion	70
Conclusion	80

**Silver-YBCO composite derived from
citrate precursor route**

Introduction	82
Experimental	83
Results	84
Discussion	100
Conclusion	102

**Processing of citrate gel derived
YBCO wires**

Introduction	102
Experimental	103
Results and discussion	104
Conclusion	113

CHAPTER IV FLASH COMBUSTION SYNTHESIS OF YBCO

Introduction	116
Mechanism of urea-metal nitrate decomposition	117
Experimental	119
Methods	119
Results	120
Discussion	128
Conclusion	129

CHAPTER V MICROWAVE PROCESSING OF YBCO

Introduction	131
Experimental	138
Methods	139
Results and discussion	139
Conclusion	145
 Post sintering treatments in microwave derived YBCO powder	
Melt texturing process	151
Experimental	151
Results and discussion	152
Repeated zone melting process	155
Experimental	155
Results and discussion	158
Conclusion	160

CHAPTER VI	COMPARISON OF PROPERTIES OF YBCO POWDERS AND SINTERED SAMPLES DERIVED THROUGH VARIOUS ROUTES	
	Introduction	169
	Experimental	170
	Results and discussion	171
	Conclusion	195
PART B		
CHAPTER VII	SOL-GEL METHODS AS APPLIED TO PREPARATION OF ALUMINA AND STRONTIUM TITANATE	
	Introduction	200
CHAPTER VIII	STRONTIUM TITANATE CERAMICS FROM MODIFIED METAL ALKOXIDE PRECURSORS	
	Introduction	206
	 Spray drying of redispersed gel	
	Experimental	209
	Methods	209
	Results and discussion	210
	 Spray drying of a metal alkoxide sol	
	Experimental	220
	Results and discussion	221
	Conclusion	232

CHAPTER IX

**PARTICULATE CHARACTERISTICS OF ALUMINA
POWDER PREPARED THROUGH SPRAY DRYING OF
BOEHMITE SOL**

Introduction	239
Experimental	240
Methods	241
Results and discussion	242
Conclusion	255
SUMMARY	258

ACKNOWLEDGEMENTS

It is with great pleasure I express my deep sense of gratitude and respect to Dr. K.G.K. Warriar, Regional Research Laboratory, Trivandrum for his constant encouragement, invaluable guidance and support throughout the course of this work. I am indebted to him for giving me considerable freedom of thought, work and expression I enjoyed during this tenure. He has served as a constant source of ideas and information. I owe my introduction to the emerging area of fine particulate ceramics to him.

I am indebted to Prof. (Dr.) C.G.R. Nair, Professor, University of Kerala, Trivandrum for his guidance and support during this research. Discussions with him, on the scientific work have always been enlightening.

My heart-felt sense of gratitude and indebtedness go to Dr. A.D. Damodaran, Director, Regional Research Laboratory, Trivandrum for his constant encouragement, interest and guidance during the course of this investigation. I am also thankful to him for the whole-hearted discussions and constructive suggestions. I am grateful to him for extending all the facilities of RRL, Trivandrum to carry out my doctoral work.

My sincere thanks are due to Dr. P.S. Mukherjee, Mr. Peter Koshy, Mr. Prabhakara Rao, Dr. K. Raveendran Nair, Dr. (Mrs.) M. Lalithambika, Mr. P. Raghavan, Dr. Suresh Das, Mr. P. Guruswamy, Mr. S.G.K. Pillai and Mrs. Prasanna Kumari of RRL, Trivandrum for their help in different instrumental methods used in this study.

I am thankful to Dr. U. Balachandran, Argonne National Laboratory, USA for the useful discussions and suggestions during the work.

My sincere thanks are due to Messers T.V. Mani, N. Balagopal, B.

Ajit Kumar and S. Sivakumar for the continued help and for providing a friendly atmosphere and excellent company.

I take this opportunity to thank my colleagues of BSMR Division, RRL, Trivandrum, Messers P. Mukundan, P. Krishna Pillai, P. Perumal, S.K. Ghosh and Pazhani for all the technical support they provided and for the affectionate friendship. Thanks are also due to Messers K.R. Prasad and V. Sreekantan, RRL, Trivandrum for their help in using the high temperature furnace facilities. My special thanks are also due to my friends Mrs. Umadevi, Messers K.V. Paulose, Simon Augustin, M. Sankara Sarma, Shinesh Kumar, Sunil Kumar, S. Ananthakumar and Suraj. I acknowledge the numerous timely help rendered by Messers K. Muraleedharan Nair and V.S. Kelukutty of RRL, Trivandrum in this investigation.

My heart-felt thanks go to Mr. K.P. Kumar and Dr. (Mrs.) B. Jalajakumari, University of Twente, The Netherlands for their affectionate friendship and help during this research work. I make use of this opportunity to express my heart-felt thanks to Messers. George John, Anil Kumar and Sreekumar for making my stay at Trivandrum a memorable one. I thank the staff of RRL, Trivandrum, numerous friends specially Messers Manoj and Johnson and well wishers all whom cannot be named here.

Help rendered by Messers. A.V. Thomas, P. Vijayakumar, Sreenivasan, R. Babu, N. Gopinathan and G. Sudhakaran in this thesis preparation is duly acknowledged.

I acknowledge the Council of Scientific and Industrial Research (CSIR), New Delhi for the financial support during the course of this work.

Last but certainly not least, I am thankful to the members of my family for their unwavering moral support.

(HARI KRISHNA VARMA P.R.)

SYNOPSIS

The recent developments in the field of advanced ceramics for electronic and structural applications demand high purity fine powders having specific distribution characteristics as starting materials. Conventional methods based on precipitation and milling introduce impurities and are less effective in producing unagglomerated powders of uniform size, shape and composition. Chemical methods of preparation are found to result in narrow sized powders with desired properties. Solid state decomposition of metal salts, sol-gel methods, vapour phase reaction techniques are a few to mention. Formation of agglomerates during powder processing can be controlled by selecting suitable reaction conditions such as pH, concentration, temperature, medium of formation and controlled heat treatment schedules. In the present investigation, attempt has been made to prepare ceramic powders of strontium titanate, alumina and yttrium barium copper oxide via 'sol-gel' and 'solid state precursor' routes. Powder characteristics such as particle size distribution, morphology, compaction behaviour and sinterability are also studied. Electrical properties of the sintered specimens were also investigated. Characterization methods such as

thermogravimetry, particle size analysis, nephelometry, BET surface area analysis, XRD, SEM were used during this investigation.

The present study is described in two sections. Part A consists of six chapters and Part B has three chapters.

In Part A, Chapter I begins with an introductory section which describes the various chemical methods of preparation available for powders followed by the various methods employed for the preparation of yttrium-barium copper-oxide (123, YBCO, $\text{YBa}_2\text{Cu}_3\text{O}_{7-\delta}$) superconductors.

Chapter II presents a brief outline of the various experimental methods and instrumental techniques used in this work.

Chapter III gives the preparation and characterization of $\text{YBa}_2\text{Cu}_3\text{O}_{7-\delta}$ and Ag- $\text{YBa}_2\text{Cu}_3\text{O}_{7-\delta}$ composite superconducting powders via citrate gel decomposition. A cold extrusion technique for YBCO wires is also described.

Chapter IV presents the preparation and properties of $\text{YBa}_2\text{Cu}_3\text{O}_{7-\delta}$ superconducting powder through a novel flash combustion synthesis.

Chapter V describes the synthesis of $\text{YBa}_2\text{Cu}_3\text{O}_{7-\delta}$ powder using microwave energy, from the mixture of corresponding nitrates of Y, Ba and Cu. It also describes the melt texturing and zone melting processes of YBCO powders derived through microwave decomposition method.

Chapter VI gives a comparative picture of various powders as well as sintered characteristics of $\text{YBa}_2\text{Cu}_3\text{O}_{7-\delta}$ superconducting compound generated through different routes described in the above chapters.

In Part B, Chapter VII starts with a general introduction on sol-gel methods related to preparation of alumina and strontium titanate. Chapter VIII describes the sol-gel synthesis of SrTiO_3 through hydrolysis of alkoxide. A sol spray technique has been adopted to generate submicron powders. Chapter IX deals with the preparation and properties of high purity alumina through a sol-spray technique.

List of Publications

1. Metal nitrate-urea decomposition route for Y-Ba-Cu-O powder. *J. American Ceramic Society*, 73(10) (1990) 3100.
2. Non aqueous cold extrusion as a route for Y-Ba-Cu-O processing. *J. American Ceramic Society*, 73(10)(1990) 3103.
3. Thermal decomposition of citrate precursor for 1-2-3 high Tc superconductor. *J. Mater. Sci. Lett.*, 8(1989) 1313.
4. Silver-YBCO composite derived from citrate gel. *Superconductor Science and Technology*, 3(1990) 73.
5. Preparation of high temperature superconducting composite without oxygen annealing. *J. Mater. Sci. Lett.*, 9 (1990) 1000.
6. Influence of the precipitation medium on the properties of fine alumina powders. *Ceramics International*, 16 (1990) 73.
7. Strontium titanate powder through spray drying of modified metal alkoxide gel. *British Ceramic Transaction and Journal*, 90 (1991) 189.
8. Rapid method for the preparation of 123 superconductor using microwaves. *J. Amer. Ceram. Soc.*, (In press).
9. Spray drying of metal alkoxide-acetate sol for strontium titanate ceramics. *J. Am. Ceram. Soc.* (in press).

10. Preparation of homogeneous metal-YBCO high T_c superconductor powders by sol-gel method. Transactions of PMAI, 17 (1990) 69.
11. Microstructure development in repeated zone refining of microwave derived YBCO bulk compacts. Jap. J. Appl. Phys., 31, 5A (1992) L543.
12. Particulate characteristics of alumina powder prepared through spray drying of boehmite sol. (communicated).
13. Microstructural and electrical properties of melt textured YBCO superconductor. (Communicated).
14. Preparation of $YBa_2Cu_3O_{7-\delta}$ by nonconventional routes - A review. (Communicated).

Conference Presentations

1. Preparation of $YBa_2Cu_3O_{7-\delta}$ superconductor from coprecipitated powders. Seminar on Advances in Ceramics, Banaras Hindu University, February 1988, Varanasi.
2. Thermal behaviour of citrate precursor for 123 high T_c superconductor. National Workshop in Advanced Ceramic Materials, August 1988, Calcutta.
3. Silver-YBCO powder composite through citrate gel route. First International Conference on Superconductivity, American Ceramic Society, October 1989, Anaheim, USA.

4. Flash combustion synthesis of 123 superconducting powder. First SAMPE Symposium, November 1989, Japan.
5. YBCO processing by non aqueous cold extrusion. International Conference on superconductivity, January 1990, Bangalore.
6. Sol-spray as a route for ultrafine SrTiO_3 powders. National Seminar on Materials Processing-Emerging Trends, Indian Institute of Metals Trivandrum Chapter, March 1990, Trivandrum.
7. Mechanical and electrical properties of YBCO-polyethylene composites. International Conference on Advances in Composite Materials, American Society of Metals, India Chapter, January 1990, Bombay.
8. Microwave processed high T_c superconductor powders. 17th National Powder Metallurgy Conference, February 1991, Trivandrum.
9. Microwave melt processing for textured YBCO superconductors. ICAMPS, ASM (India Chapter) Conference, February 1992, Bombay.
10. Sintering studies on tape cast alumina substrate arrived through sol-spray technique. 94th Annual Meeting and Exposition of American Ceramic Society, 1992, Minneapolis, USA.
11. Processing of post sintered microwave derived YBCO powders. 94th Annual Meeting and Exposition of American Ceramic Society, 1992, Minneapolis, USA.

List of Figures

- Fig.I.1 Conventional ceramic technology
- Fig.I.2 Nonconventional ceramic technology
- Fig.I.3 Spray drying set up (Schematic)
- Fig.I.4 Structure of $\text{YBa}_2\text{Cu}_3\text{O}_{7-\delta}$ compounds
- Fig.I.5 XRD patterns of $\text{YBa}_2\text{Cu}_3\text{O}_{7-\delta}$ compounds
- Fig.I.6 Meissner effect: A permanent magnet levitates above a YBCO superconductor bathed in liquid nitrogen because its magnetic field is completely repulsed at the surface of the superconductor
- Fig.III.1 Citrate gel network
- Fig.III.2 (a) Arbitrary shape of a sample with four contacts on the periphery as used in van der Paw's method (b) Resistivity measurement set up and (c) Sample set up used for measuring critical current density (J_c)
- Fig.III.3 Particle size distribution curve of $\text{YBa}_2\text{Cu}_3\text{O}_{7-\delta}$ derived through citrate gel route
- Fig.III.4 TG and DTA curves of citrate precursor
- Fig.III.5 XRD patterns of citrate gel heated at various temperatures
- Fig.III.6 Citrate precursor heated in flowing oxygen at different temperature and heating rate.
 (a) 600°C at $50^\circ/\text{hr}$, (b) 700°C at $50^\circ/\text{hr}$ and
 (c) 700°C at $25^\circ/\text{hr}$

- Fig.III.7** SEM pictures of citrate gel heated at various temperatures. (a) dried gel, (b) at 550°C and (c) at 850°C
- Fig.III.8** Surface morphology of sintered $\text{YBa}_2\text{Cu}_3\text{O}_{7-\delta}$ derived through citrate gel route
- Fig.III.9** Temperature vs resistivity curve of sintered $\text{YBa}_2\text{Cu}_3\text{O}_{7-\delta}$
- Fig.III.10** Tap density vs amount of silver content in the Ag/YBCO precursor powder
- Fig.III.11** Green density variation with applied pressure for the Ag/YBCO composite powder containing various amount of silver
- Fig.III.12** Particle size distribution of Ag/YBCO calcined powder
- Fig.III.13** SEM picture of Ag-YBCO precursor powder (20 wt% Ag/YBCO precursor)
- Fig.III.14** XRD pattern of Ag (20 wt%)/YBCO precursor gel after decomposition at 250°C
- Fig.III.16** Resistance - Temperature curves of sintered pellets (a) 5 wt% Ag-YBCO, (b) 20 wt% Ag-YBCO and (c) 50 wt% Ag-YBCO composite
- Fig.III.15** XRD pattern of sintered (a) YBCO, (b) 5 wt% Ag-YBCO, (c) 20 wt% Ag-YBCO, (d) 50 wt% Ag-YBCO and (e) 20 wt% Ag-YBCO (quenched)
- Fig.III.17** Surface morphology of Ag (20 wt%)-YBCO citrate gel after the heat treatment at 900°C

- Fig.III.18 Fractographs of sintered superconducting composites (a) 5 wt% Ag-YBCO, (b) 20 wt% Ag-YBCO and (c) 50 wt% Ag-YBCO
- Fig.III.19 Energy dispersive X-ray analysis of YBCO rich phase in 50 wt% Ag-YBCO composite
- Fig.III.20 Extrusion set up
- Fig.III.21 Cold extruded wires
- Fig.III.22 Surface morphology of as extruded wires
- Fig.III.23 Heating schedule for the sintering of the extruded wire
- Fig.III.24 Surface morphology of sintered wires in low and high magnification
- Fig.III.25 Polished fractured surface of sintered wire
- Fig.III.26 Temperature vs resistivity of the superconductivity wires
- Fig.III.27 Variation of critical current density with applied magnetic field
- Fig.IV.1 Mechanism of metal nitrate-urea combustion reaction
- Fig.IV.2 Particle size distribution curve of flash combustion YBCO powder
- Fig.IV.3 X-ray diffraction patterns of flash combustion powder at various temperatures (a) 700°C for 5 minutes, (b) 800°C for 5 minutes, (c) 900°C for 5 minutes, and (d) 900°C for 1 hour

- Fig.IV.4 Percentage of BaCO_3 present in the powders as a function of flash combustion temperature assuming maximum at 600°C
- Fig.IV.5 Scanning electron micrograph of flash combustion derived YBCO powder
- Fig.IV.6 Fractured surface of sintered YBCO sample ($930^\circ\text{C}/10$ hr)
- Fig.IV.7 Temperature vs resistivity for sintered YBCO derived through flash combustion route
- Fig.V.1 Dielectric properties of CuO as a function of temperature
- Fig.V.2a Experimental set up
- Fig.V.2b Precursor powder inside the crucible
- Fig.V.3 Weight loss of mixture of nitrates of 123 stoichiometry
- Fig.V.4 XRD patterns of the mixture of nitrates of Y, Ba and Cu after exposing to microwave for (a) 1 minute, (b) 2 minutes, (c) 3 minutes, (d) 4 minutes and (e) after heating the sample at 900°C for 4 hours
- Fig.V.5 Scanning electron micrograph of sample after exposure to microwave (a) after 4 minutes, (b) above sample after annealing at 900°C for 4 hours (c) sample 'a' after grinding and (d) fractured surface of the sintered specimen ($940^\circ\text{C}/4$ hours)

- Fig.V.6 Temperature vs resistance curve of sintered 123 sample
- Fig.V.7 Heating schedule for the melt texturing of the microwave derived sample
- Fig.V.8 Suspension of melt-textured YBCO superconductor sample beneath a rare earth magnet
- Fig.V.9 SEM pictures (a and b) of melt textured YBCO superconductor (c) Frictionless bearing (i) experimental set up and (ii) schematic representation
- Fig.V.10 (a) Experimental set up, (b) temperature profile
- Fig.V.11 Optical micrograph of sintered and zone melted YBCO samples (a) to (f)
- Fig.V.12 SEM pictures of fractured zone refined samples showing bulk oriented YBCO grains
- Fig.VI.1 Particle size distribution curve of various YBCO powders (a) citrate, (b) microwave, (c) flash combustion and (d) conventional solid state route
- Fig.VI.2 Morphology of YBCO powders (a) citrate, (b) flash, (c) microwave and (d) conventional solid state route
- Fig.VI.3 Green density of four YBCO powders as a function of pressure
- Fig.VI.4 Sintering schedule for the YBCO powder compacts
- Fig.VI.5 Sintered density variation with applied pressure for the four YBCO samples sintered at different temperatures and time

- Fig.VI.6 Temperature vs resistivity of sintered YBCO samples
- Fig.VI.7 Fractured surface of sintered YBCO sample derived through (a) solid state route, (b) citrate, (c) flash and (d) microwave methods
- Fig.VIII.1 TGA curve of the spray dried SrTiO_3 gel
- Fig.VIII.2 IR spectra of the gel sprayed powder heated to different temperature (a) as sprayed, (b) 450°C , (c) 650°C and (d) 800°C
- Fig.VIII.3 XRD patterns of the gel sprayed powder heated to different temperatures (a) as sprayed, (b) 650°C , (c) 800°C , (d) 800°C (solid state mixing route) and (e) 1400°C
- Fig.VIII.4 Particle size distribution curve of gel sprayed powder calcined at 1000°C
- Fig.VIII.5 SEM pictures of (a) SrTiO_3 powder calcined at 1000°C , (b) the same at 1200°C and (c) fractograph of sintered SrTiO_3
- Fig.VIII.6 Frequency vs dielectric properties of sintered SrTiO_3 derived through gel spray route
- Fig.VIII.7 Variation of NTU value of sol containing different amount of solvent (isopropanol) with time
- Fig.VIII.8 Variation of NTU value of sol containing different amount of solvent (water) with time

- Fig.VIII.9 Thermal decomposition of sol sprayed SrTiO_3 precursor powder
- Fig.VIII.10 IR spectra of sol sprayed precursor powder calcined at various temperatures (a) spray dried powder, (b) 400°C , (c) 500°C , (d) 700°C , (e) 800°C and (f) 1200°C
- Fig.VIII.11 XRD patterns of sol sprayed precursor powder calcined at various temperatures (a) spray dried powder, (b) 400°C , (c) 550°C , (d) 800°C and (e) 1200°C
- Fig.VIII.12 Particle size distribution curve of sol sprayed powder calcined at 1000°C
- Fig.VIII.13 Variation of sintered density with sintering temperature
- Fig.VIII.14 Dielectric behaviour of SrTiO_3 samples sintered at various temperatures as a function of frequency
- Fig.VIII.15 SEM micrograph of (a) SrTiO_3 powder (calcined at 1000°C) and (b) Fractograph of SrTiO_3 sintered at 1400°C
- Fig.IX.1 XRD patterns of (a) spray dried powder and (b) heated at 1100°C (1 hr)
- Fig.IX.2 Thermogravimetric curve of spray dried powder
- Fig.IX.3 Particle size distribution curves of calcined powders (a) powder as sprayed, (b) treated with acetone, (c) isopropanol and (d) tert. butanol

- Fig.IX.4 Plot of relative density of different alumina powders as a function of compaction pressure (a) without washing (b) acetone washed and (c) isopropanol washed
- Fig.IX.5 SEM picture of the alumina samples obtained after various treatments (a) as sprayed, (b) after washing in acetone, (c) isopropanol and (d) tert. butanol
- Fig.IX.6 Variation of point of zero charge as a function of pH for calcined alumina powders (a) without washing (b) acetone washed (c) isopropanol washed and (d) tert. butanol washed
- Fig.IX.7 Sintered surface microstructure of alumina (1400°C for 3 hours) derived from boehmite (a) without washing and (b) after washing with isopropanol

List of Tables

- Table I.1 Applications of some high performance ceramics
- Table I.2 Lattice parameters and d values of $\text{YBa}_2\text{Cu}_3\text{O}_7$ -
compound
- Table III.1 Various phases detected using XRD during
the heating of Ag/YBCO citrate gel
- Table III.2 T_c and density values of Ag-YBCO composites
(compacted at a pressure of 150 MPa and
sintered at 915°C for 10 hours)
- Table VI.1 Characteristics of various powder preparation
techniques for YBCO
- Table VI.2 Lattice parameters and d values obtained
for powders prepared by different methods
(a) Citrate gel (b) Flash combustion
(c) Microwave decomposition and (d) Solid
state mixing
- Table VI.3 Oxygen content in YBCO derived through
various routes
- Table VI.4 Tap density of YBCO powders derived
through various routes
- Table VI.5 Electrical properties of sintered
YBCO samples
- Table VI.6 Properties of YBCO powders derived through
different powder preparation techniques
- Table VIII.1 Densification characteristics of sol sprayed

SrTiO₃ powder calcined at various temperatures

Table IX.1 Tap densities of various alumina powders
derived through surface treatments
of sol sprayed boehmite powder (calcination
temp. 1100°C/1 hour)

P a r t A

CHAPTER I

CHEMICAL METHODS OF PREPARATION OF CERAMIC POWDERS

I.1 Introduction

The history of ceramic materials is as old as the human civilization. The term ceramic has evolved from the Greek word 'Keramos' which means fired objects made out of clay. According to Kingery(1), ceramics can be given a general definition as the manufacture of shaped inorganic, nonmetallic, high temperature materials traditionally done by three general processes, i.e., preparation of a cementitious powder, shaping of the same to an object and heating it to form a permanent object. Some of the well known features of ceramic materials are low density, high strength at elevated temperature, low electrical and thermal conductivity, brittleness, low toughness and corrosion resistance to environment. Over the ages, man has developed a number of products based on natural materials like clay and silicates. Beginning of the century saw the emergence of ceramics formed from non naturally occurring materials and then properly termed as fine ceramics or engineering ceramics or more recently as advanced ceramics(1). High performance materials are required for a host of engineering applications in the recent times and hence the

ceramic materials based on high purity oxides, carbides and nitrides etc. have been studied in much more detail. Hence to make these materials more functional, extreme care is exercised in various processing steps, the preparation of starting particulates in particular.

Over the years, the technology and science of ceramic fabrication were relatively simple and can be visualized as a four stage process as shown in Figure I.1. The traditional ceramic industry uses natural raw materials, usually clay minerals, sands, feldspar etc. and a series of physical operations such as crushing, milling, floatation and washing etc. to make powders for making satisfactory ceramic wares, construction and refractory materials. Similarly, ceramic industry also uses large quantities of powder for single and multicomponent oxides, carbides, nitrides, borides etc. for making a variety of so called advanced ceramics for a number of functional applications such as structural and electronic uses. Table I.1 gives a brief list of such compounds and its application. Figure I.2 shows a parallel representation as shown in Fig.I.1 for the preparation of these materials. These procedures have been advanced in the last three decades to a great extent in the science of processing ceramic materials. This progressive realization is primarily because of the fact that the final performance of a ceramic depends largely on its microstructural characteristics. For this, the raw material properties to be controlled are chemical composition, particle

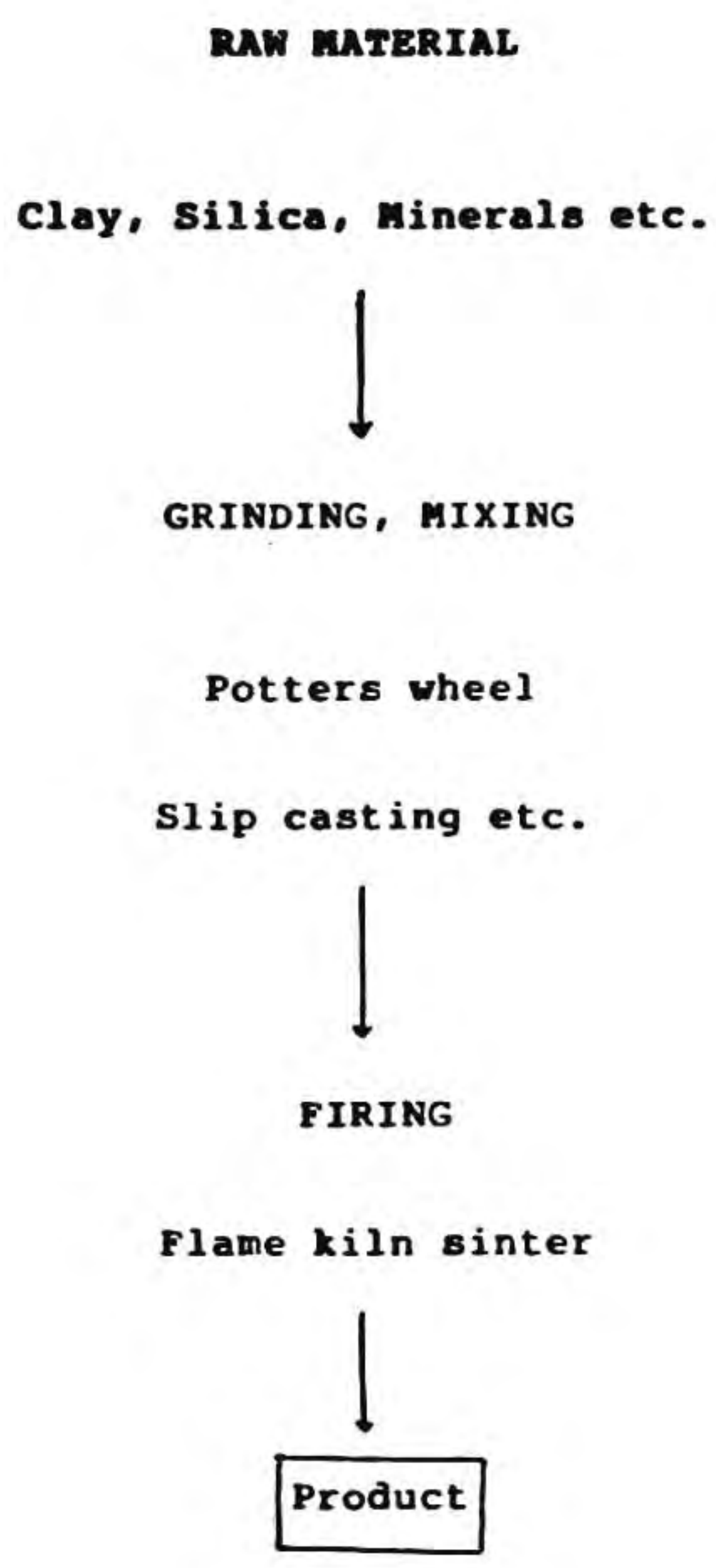


Fig. I.1 Conventional Ceramic Technology

**CHEMICAL METHODS OF PREPARATION OF
FINE POWDERS**

Precipitation, Spray drying, Sol-gel,

Vapour phase reactions etc.



FORMING

Slip casting, Injection moulding, Sol-gel,

Fibre drawing, Gel casting etc.



SINTERING

Electric furnace sinter, HIP, Explosive forming,

Plasma spray etc.



Product

Fig. 1.2 Nonconventional Ceramic Technology

Table I.1 Applications of some high performance ceramics

Function	Materials	Applications
Electrical and Electronic	Al_2O_3 , BeO, MgO, SiC	Substrates
	$BaTiO_3$, $SrTiO_3$	Capacitors
	PZT	Oscillators
	SnO_2 , ZnO, NiO, Stabilized ZrO_2	Sensors
	ZnO, SiC	Varistors
	YBa-Cu-O, Bi-Sr-Ca-Cu-O Tl-Ba-Ca-Cu-O systems	Superconducting materials
Mechanical	Al_2O_3 , ZrO_2 , BN	Wear resistant materials
	TiC, WC, Si_3N_4	Grind stone, Cutting tools
Magnetic	Ferrites	Magnets, Magnetic Cores, Memory Devices
Optical	PLZT, Al_2O_3 , $Y_2O_3-ThO_2$	Optical memory junctions, Optical shutters and valves, laser materials, Special lamp tubes
Thermal	Al_2O_3 , SiC	Heat resistant fixtures
	ZrO_2	Heat engines

size and morphology, crystal structure, lattice defects, surface properties etc. In order to get uniform flaw free microstructures, the need for high quality ceramic powder as starting material is fairly well understood. In general, the kinetics of sintering depends to a large extent on particle size and distribution, shape and consolidation characteristics. Such powders sinter at low temperatures to high density having desired sintered microstructures. Synthetic chemistry has found an ideal tool to produce powders of high purity, uniform size and shape and also of good sinterability. The modern powder synthesis methods can be broadly classified into three major categories, i.e. solid, liquid and vapour phase reactions.

1.2 General methods for the preparation of fine ceramic powders

1.2.i Solid phase reactions

Thermal decomposition of salt(s) or precursor compound is basically the principle behind this technique. A number of conventional techniques(2-4) are based on solid state decomposition. Calcination of hydroxides, halides, carbonates etc. at elevated temperature result in oxidic powder. These techniques are quite general to both single and multicomponent systems. Alumina is produced in tonnage quantities(5) by calcination of aluminium hydroxide followed by grinding.

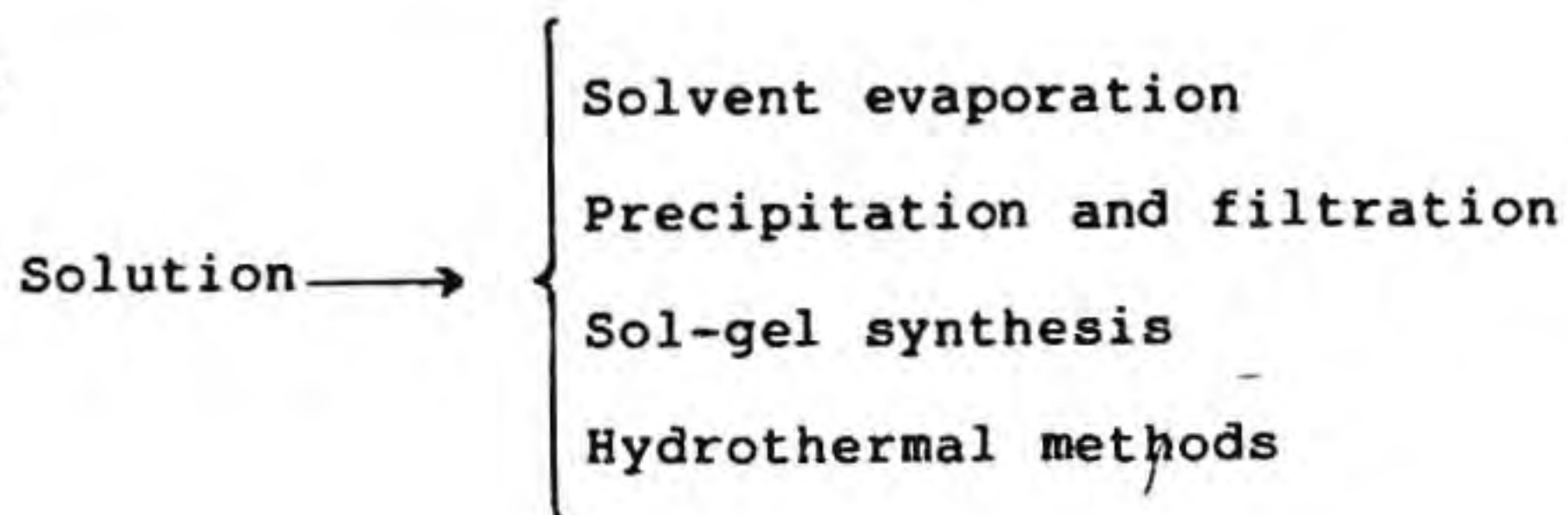
Similarly MgO is produced by heating $Mg(OH)_2$ obtained from brine water. TiO_2 , SiC, $BaTiO_3$, and Ferrites(6-7) are also prepared by the solid state reaction route. A variety of non oxide ceramics are also mainly prepared by solid state reaction at specific atmospheric conditions.

Since the solid state reaction is diffusion controlled, the important parameters that affect the extent of reaction are particle size distribution, the homogeneity of mixing of reactants, the composition and flow of gases. The calcination at higher temperature would result in aggregated particles and so considerable grinding of the hard aggregates is required to produce fine powder, which sometimes re-agglomerate and end up in high energy consuming steps.

I.2.ii Solution phase synthesis

Most of the chemical methods of preparation correspondingly known as wet chemical powder preparation(8) come under this heading. It offers advantages of ease of preparation, high homogeneity and purity, control of composition to any desired level and fine size. The first step of this technique is the preparation of a suitable liquid (aqueous or non aqueous) solution containing cations or anions of interest. In the case of multicomponent systems, the stability of the solution depends on the mutual compatibility of the salts in solutions. The solid particulate powders are then generated from the solution by the removal of the solvent.

The solvent removal procedures can be classified as:



I.2.ii.a Solvent evaporation techniques

The simplest method, the slow evaporation of solvent by drying the solution at an elevated temperature result in solid particulates. The subsequent calcination of such solid particles result in agglomerated powders. In the case of multicomponent systems, the selective or preferential crystallization of components with different solubilities produce inhomogeneous powder mixtures.

I.2.ii.a.i Spray drying:

The aim of this procedure is to prepare uniform homogeneous (many cases spherical agglomerates) powders by spray drying a salt solution above the evaporation point of the solvent. The solution is atomized by means of high pressure air or gases into a chamber kept at elevated temperature. The droplet size will vary depending on parameters like air pressure, concentration of solution, flow rate etc. During evaporation, the solvent vapours are removed and solid material is collected. A schematic diagram of the spray drying set up is

shown in Fig.I.3.

Preparation of a number of oxidic powders, single and multicomponent, have been reported widely(9-13). The spray drying is also performed by spraying the solution into an immiscible liquid. Emulsion drying and hot kerosene process(14-18) are some modifications of this technique. Spray drying of a dispersed gel is also used sometimes. Polymeric solution of nitrates and formates are also used.

I.2.ii.a.ii Spray calcination or spray pyrolysis:

Evaporative decomposition of solutions results in ceramic powders in single step. The principle is same as in the case of spray drying but at a high temperature, i.e. above the decomposition temperature of the salts or compound. Chlorides, nitrates, sulphates etc. are used as salt precursors(19-26). The important parameters such as size of the hot chamber, flow rate, concentration of the solution etc. are to be effectively monitored with respect to reaction time and ultimate uniformity of powder. The short residence time in the hot chamber has two fold effect, i.e. formation of more loose agglomerates as well as incomplete reactions. So it requires judicious selection of the temperature and zone size to achieve optimum powder property.

I.2.ii.a.iii Freeze drying:

Freeze drying is based on the principle by which

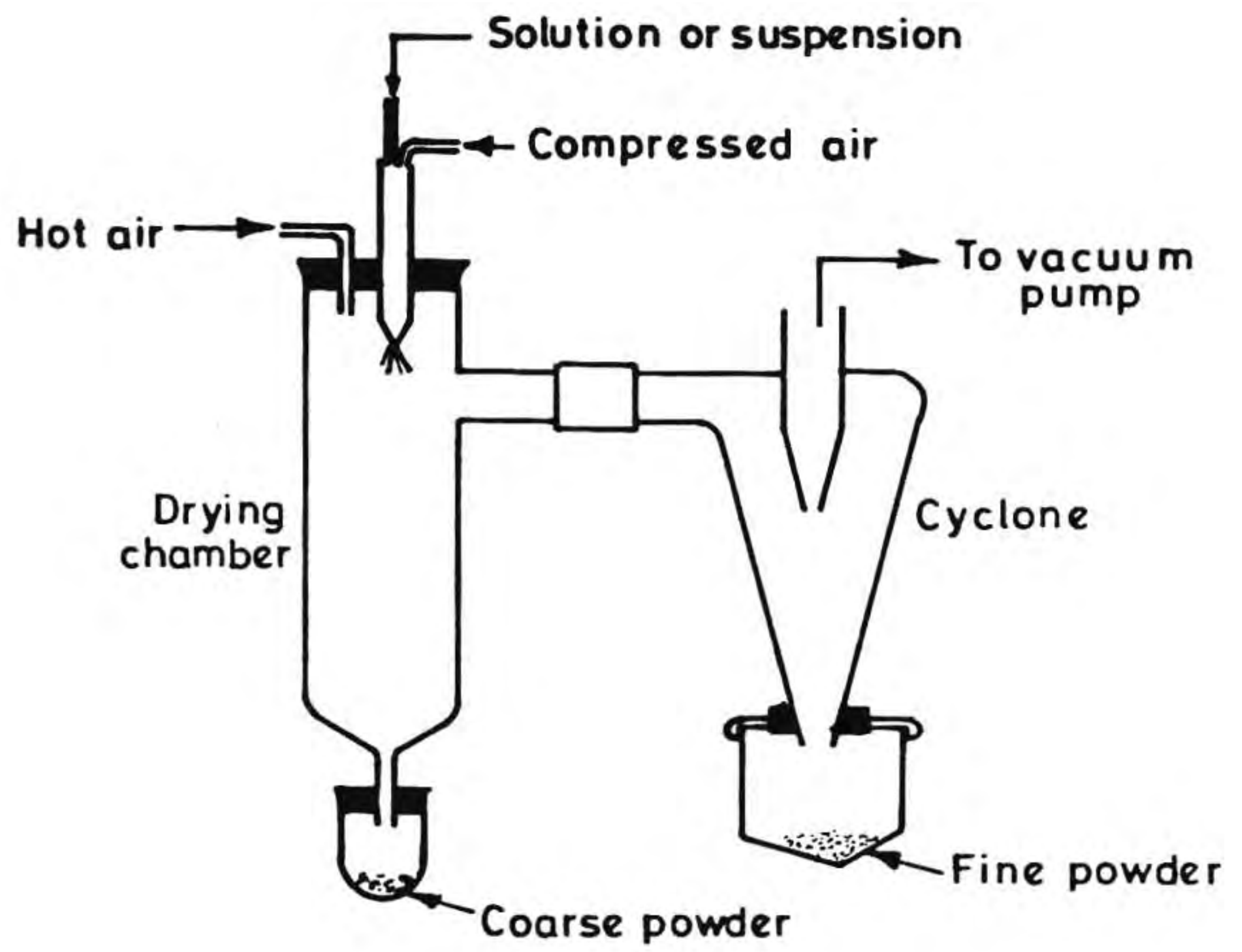


Fig. 1.3 Spray drying set up (Schematic)

concentrated solution of salt(s) is sprayed into a chamber cooled by liquid N_2 or directly sprayed into liquid nitrogen. The solvent will freeze and the inhomogeneity due to the drying within the drops will be prevented. The frozen droplets are then dried in evacuated chambers to sublime off the solvent and then decomposition of salts by controlled calcination(27-29). Freeze drying in different solvent systems could be effectively utilized to improve the sinterability. A number of ceramic oxides such as alumina(30-31), spinel(32) and barium titanate(33) have been prepared through this technique.

I.2.ii.b Precipitation techniques

Precipitation technique is one of the oldest methods of powder preparation. The well known Bayer process(34) for the production of aluminium oxide in which aluminium hydroxide precipitated from sodium aluminate solution by adjusting the concentration, pH and conditions of precipitation demonstrates as the best example of the applicability of both laboratory and industrial scale. The precipitate of more than one component as hydroxide, carbonate, oxalate etc. are studied in detail from the beginning. Even though this technique is simple, a number of factors like pH, mixing of components to get the right homogeneous solution, rate of stirring, temperature etc.(35) should be controlled accurately so that preferential precipitation is avoided and the particle size and distribution is controlled. Also the maximum attention is given to minimise

the agglomerated nature of the filtered powders(36). Washing the precipitate with suitable solvents have been tried with some success to minimise this problem. The homogeneous precipitation technique such as urea method is one in which the precipitant is generated insitu in the solution (to avoid the local supersaturation) in order to get homogeneous powders(37-39).

Oxides such as Al_2O_3 (40), SiO_2 (41), ZrO_2 (42), ZnO (43) and a number of nuclear fuel oxides(44-45) have been investigated in detail based on this technique. Multicomponent oxides such as stabilized ZrO_2 (46-48), ferrites(49-51), titanates(52-55) spinels(56-57), PLZT(58,59), composites(60) etc. have also been prepared with this technique. Matijevic(61) and his group introduced forced hydrolysis by adjusting the pH, concentration, nature of anion and temperature to get monodispersed particles of an array of ceramic systems.

I.2.ii.c Hydrothermal technique

The hydrothermal reaction refers to the reaction taking place in the presence of water at high pressure and temperature. High quality quartz crystals have been synthesized from silica gel in early 1845. The most of the mineralogical transformations occurred in nature also has occurred through this process. In order to make pure, fine crystalline powder at lower temperatures, in both single as well as multicomponent oxide synthesis, it is desirable because

of high endotherm associated with crystallization process. Today hydrothermal methods have been used to prepare barium titanate(61-63), aluminium phosphate(64,65), zirconia(66), titania and alumina(67,68), zirconia-yttria(69) and ferrites(70,71) from their salts. Hydrothermal preparation of powders were also studied from the alloys of the corresponding metals of the ceramic composites(72,73).

I.2.ii.d Sol-gel methods

Sol-gel methods have been investigated over many decades in the past, however, increased emphasis was given for the preparation of the starting materials for advanced technical ceramics, because their possible applications for the preparation of films, filters, fibres and monoliths(74) in addition to the preparation of fine ceramic powders. Elaborate survey over the state of the art of this technique has been presented in a number of symposia(75,76), conferences on ultrastructure processing of glasses, ceramics and polymers(77-81) and the literature cited therein. In general, the process can be broadly seen as one which involves three major steps:

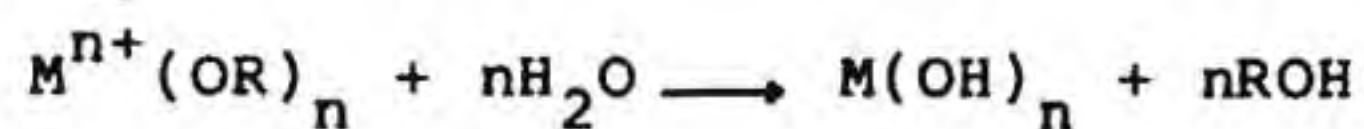
- (i) the preparation of a sol. Sol is a dispersion of solid particles of sizes ranging from 1 to 100 nanometers in a liquid.

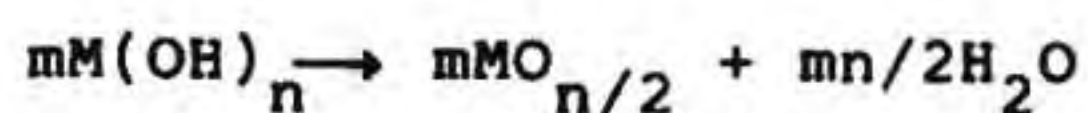
- (ii) evaporation of the solvent or by polymerization of the sol particles, a gel is formed. Gels can be classified as alcogel, aquagel, aerogel etc. depending on in which medium the gel network exists.
- (iii) controlled drying or pyrolysis of the gel yields desired ceramic. A number of deviations are suggested and applied successfully to get optimum results.

I.2.ii.d.i From molecular precursors:

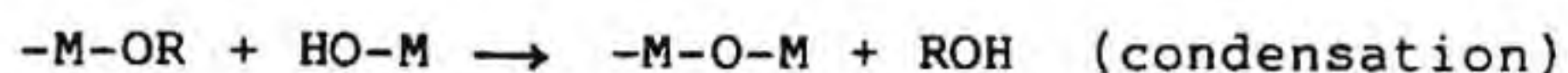
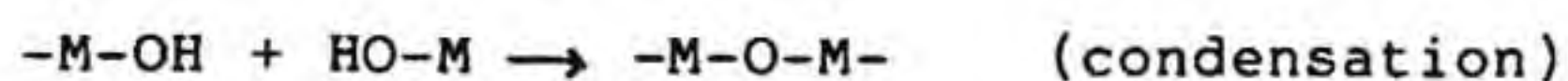
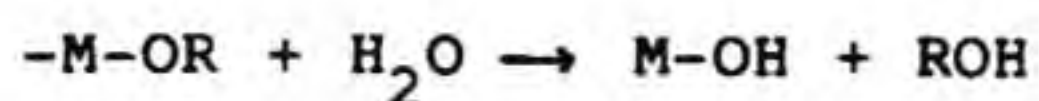
Most of the work related to sol-gel methods have been studied using alkoxides as the starting reagent or as precursor. The advantage of alkoxide route are (1) solubility in a variety of solvent systems (2) possibility of control of rate of hydrolysis and condensation by chemical means(82). Today it is clear that more than half the number of elements can be converted into their corresponding alkoxides(83,84) and can be used as the precursor material for a variety of ceramic compounds by suitable techniques(85-92).

Metal alkoxide or $M^{n+} (OR)_n$ where M is a metal element and R is an alkyl group is a compound in which the metal element is bonded to the organic carbon via oxygen. On hydrolysis it forms metal hydroxides or metal oxide as follows:





The hydrolysis and polycondensation to a gel can be summarised as:



In the over-all process the removal of medium liquid from gel and the rate of removal of liquid are crucial in determining whether a powder or monolith may form. The hydrolysis of alkoxide in controlled conditions such as pH, concentration of medium of gelation, temperature etc. have to be performed to generate spherical particles(93,94). SiO_2 is the most investigated system in sol-gel literature(95,96) but a large number of ceramic oxides such as Al_2O_3 (97-101), TiO_2 (102-104) ZrO_2 (105-107) and many single oxide systems(108-113) have been studied in detail for the preparation of fine powders. Mixed alkoxides were effective in producing a series of compounds such as ferrites(114), titanates(115-119), mullite(120,121), nasicon(122), PLZT(123,124) and a number of composite oxides and mixed oxides(125-128). Preparation of

powders were also performed by the modification of conventional sol-gel process such as, alkoxide sol dispersion in immiscible solvent(129), sol generated from alkoxide and an inorganic salt(130), spray drying of alkoxide generated sols(131) etc.

I.2.ii.d.ii Inorganic precursors:

The sol-gel process involving hydrolysis and polycondensation reactions is not restricted to metal alkoxide as precursor for the single as well as multicomponent ceramic systems. A variety of non alkoxide precursors are inorganic salts like nitrate, chloride, or organic salts like carboxylates, acetyl acetonates, acetates, citrates, acrylates etc. With difference in the chemistry of powder preparation, these precursors also lead to oxides and non oxide ceramic powders with definite particulate characteristics.

NaNO_3 is used(132) for the preparation of $\text{SiO}_2\text{-Na}_2\text{O}$ gels and calcium nitrate was used for preparing gels of $\text{SiO}_2\text{-CaO}$ systems(133-134). Nitrates are also used along with alkoxide for mullite(135) and $\text{SiO}_2\text{-ZrO}_2$ (136). For example aluminium nitrate is partially hydrolysed to get boehmite and the gels were comparable with the alkoxy counterpart(137). Carboxylic acids are also frequently used as precursors for sol-gel synthesis. -COO^- bonds with metal ions in ionic, bridging as well as chelate bonds to obtain homogeneous gels both in the case of single and multicomponent systems(138,139). Pechini process involving citrate and ethylene glycol as

chelating species is a well known technique(140) for the preparation of a number of oxide powders in both laboratory as well as industrial scale. The functionality of the carboxylic acid can be improved by substituting citric acid with poly acrylic acid(141,142).

Silica gel was prepared from silicon tetra acetate(143) and lead acetate for $(\text{CH}_3\text{COO})_2\text{Pb} \cdot \text{Pb}(\text{OH})_2$ gels(144). Chlorides and other inorganic salts were also used for making monolithic transparent gels of $\text{Al}_2\text{O}_3/\text{SiO}_2$ (145).

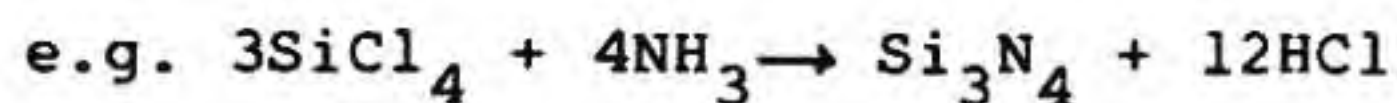
The concept of preparing pure, homogeneous noncrystalline xerogels for crystalline ceramic powder was explored extensively. By using inorganic colloids the diphasic and monophasic systems have been introduced by Roy et. al(146,147).

I.2.iii Gas phase reactions

Vapour techniques are extensively used to produce unagglomerated powders in most cases having spherical shape. Some of the ceramic powders prepared by gas phase reactions at present are Si_3N_4 (148), SiC (149), TaC (150), BN (151) and oxides such as TiO_2 , Al_2O_3 (152-154) etc.

The solid ceramic material is to evaporate or sublime and subsequent condensation of the vapour results in extremely fine powder(155). By injecting the material into a dc arc or electron beam heater, the evaporation of oxides are

possible(156). Direct pyrolysis of alkoxides under suitable conditions is another method of preparation of carbides, nitrides, borides etc(106). Gas phase reaction of a volatile material like metal chloride and the reaction of the vapour with NH_3 or N_2 result in fine powders of nitrides(157,158).



Thermally induced gas phase reactions are also performed by lasers(159,160). This technique is found to be very effective in producing non oxide ceramic powders.

I.3 PREPARATION OF $\text{YBa}_2\text{Cu}_3\text{O}_{7-\delta}$ HIGH T_c SUPERCONDUCTING PARTICULATES - A REVIEW

Discovery of superconductivity in La-Ba-Cu-O system by Bednorz and Muller(161) and subsequent observation of existence of this phenomena above liquid nitrogen temperature by Chu et. al.(162) initiated enormous research effort on the preparation and properties of a series of copper oxide based superconducting materials. Out of the many compounds reported, three most widely studied ones are Y-Ba-Cu-O(YBCO), Bi-Sr-Ca-Cu-O (BSCCO) and Tl-Ba-Ca-Cu-O (TlBCCO) compounds(162-164). All these come under perovskites having related structure as typically provided for YBCO in Fig.I.4. Considerable research input has been involved in their synthesis, processing as well

as the study on their physical and chemical properties and also on the possibility of device fabrication. A number of books were already published dealing with the superconductivity in this class of new compounds(165-173). Among them, Y-Ba-Cu-O (YBa₂Cu₃O_{7-δ} or YBCO or 123) system attracted more attention from the very beginning and is still being investigated in further detail.

I.3.i Structure and properties of YBa₂Cu₃O_{7-δ} compound

YBa₂Cu₃O_{7-δ} exists in two structural form depending on the oxygen content, i.e. tetragonal and orthorhombic phases. The phase transitions are the direct result of the variation of oxygen stoichiometry which results in disorder as well as structural distortion. The oxygen content can be varied from 6 to 7 by appropriate heat treatment and a controlled oxygen atmosphere. The orthorhombic YBa₂Cu₃O_{7-δ} loses oxygen at high temperatures of 950°C and becomes tetragonal and non superconducting with formula YBa₂Cu₃O₆. The decomposition is reversible and while annealing in oxygen at lower temperature of 400-500°C the tetragonal YBa₂Cu₃O₆ absorbs oxygen and converts to YBa₂Cu₃O_{7-δ} (δ close to 0). The structure of the two forms have been schematically depicted in Figure I.4. The X-ray diffraction patterns and lattice parameters are provided in Fig.I.5 and Table I.2.

In the orthorhombic form all the O1 sites are occupied while in tetragonal symmetry these sites are vacant. Since the

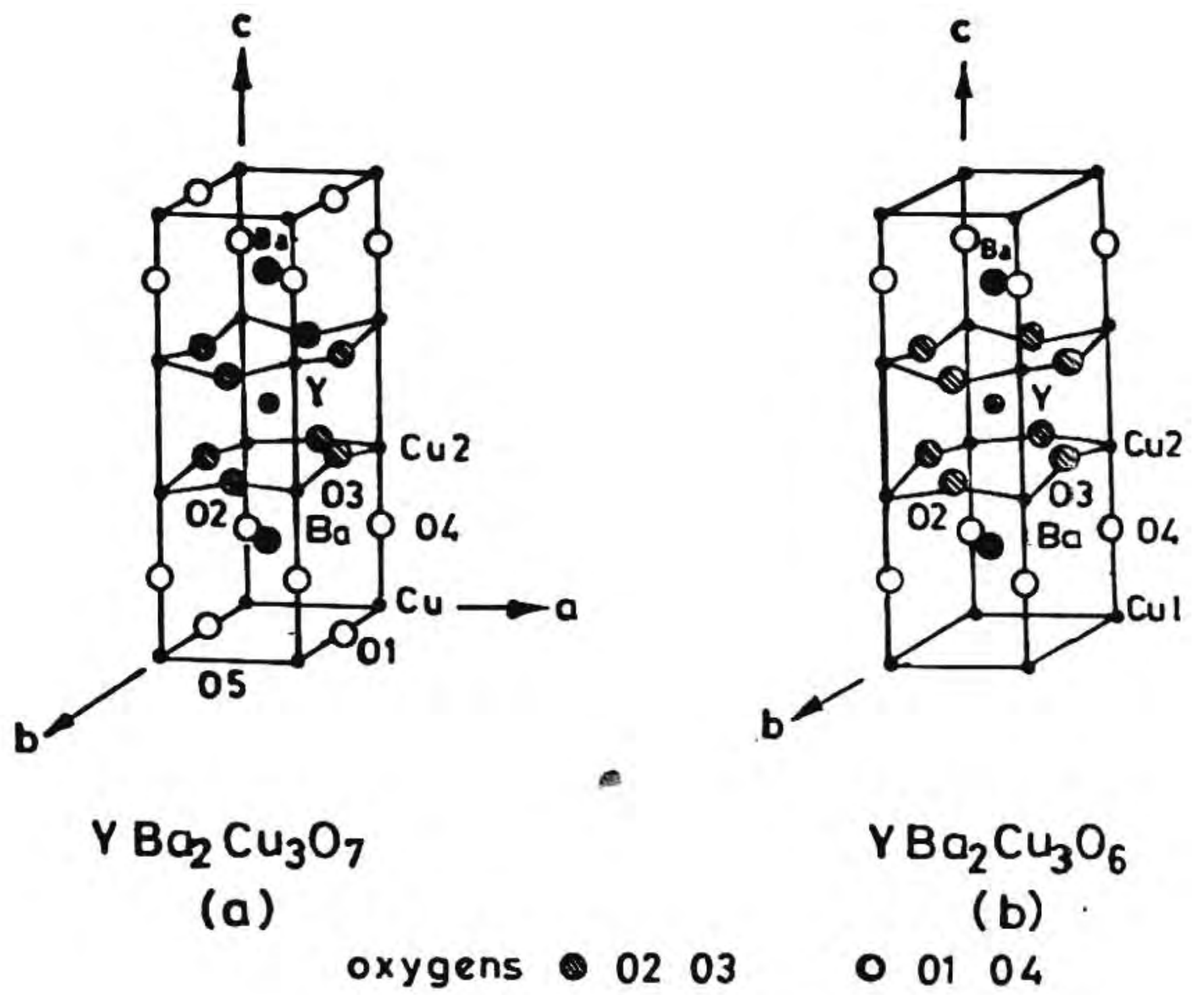


Fig. I.4 Structure of $\text{YBa}_2\text{Cu}_3\text{O}_{7-\delta}$ compounds

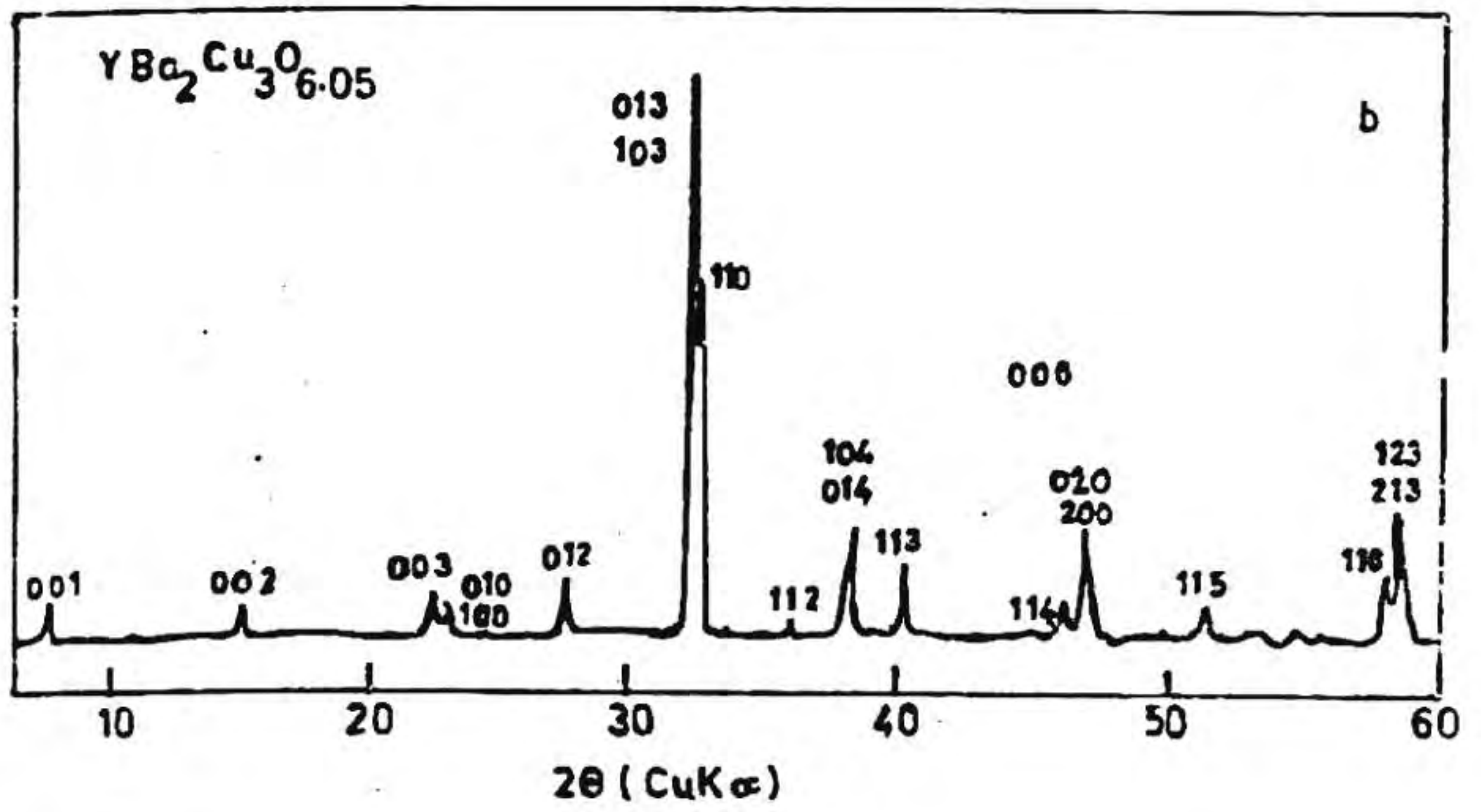
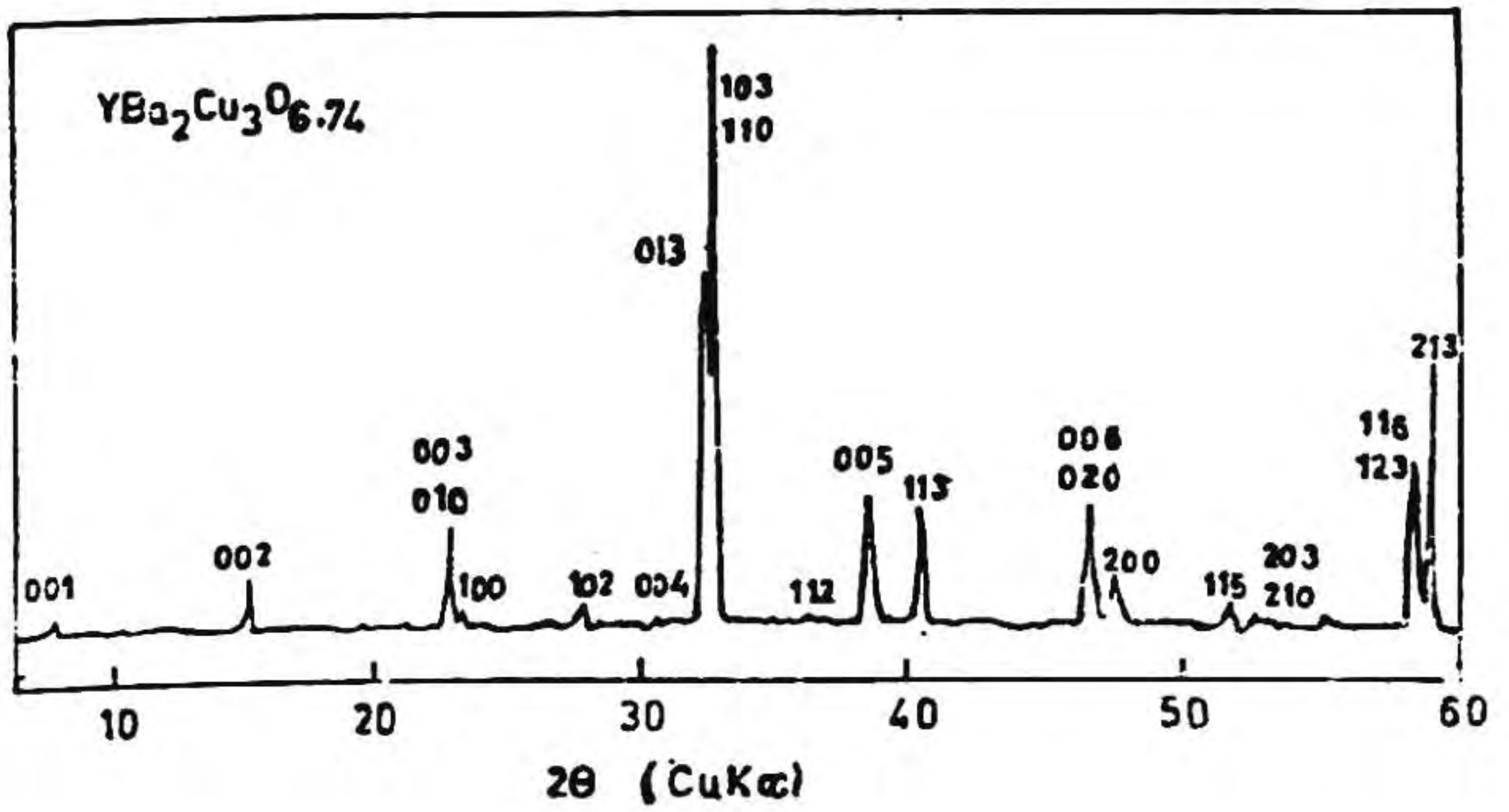


Fig. I.5 XRD patterns of $\text{YBa}_2\text{Cu}_3\text{O}_{7-\delta}$ compounds

Ba ₂ YCu ₃ O ₇ a=3.816Å b=3.883Å c=11.698Å Pmmm						Ba ₂ YCu ₃ O ₆ a=3.853Å c=11.780Å P4/mmm					
2θ		d _{calc}	1/l _o		hkl	hkl	1/l _o		d _{calc}	2θ	
obs	calc		obs	calc			obs	calc		obs	calc
	7.56	11.70		2	001						
	15.15	5.819		3	002						
22.85	22.81	3.899	8	10	010						
	22.90	3.883		8	8	003	003	5	2	3.927	22.70
23.30	23.31	3.816	2	6	100	100	6	11	3.853	23.18	23.08
27.73	27.57	3.235	2	5	012	102	10	8	3.221	27.76	27.67
27.90	27.92	3.196	4	9	102						
32.60	32.54	2.751	50	89	013	103	100	100	2.750	32.65	32.56
32.88	32.84	2.727	100	96	110	110	49	36	2.725	32.95	32.87
	32.91	2.722		100	103						
33.75	33.81	2.651	1	2	111						
36.46	36.41	2.468	3	5	112	112	3	2	2.473	36.37	36.33
38.57	38.48	2.340	17	6	014						
	38.54	2.336		11	005	005	11	6	2.356	38.14	38.20
38.75	38.79	2.321	1	4	104	104	16	3	2.340	38.57	38.48
40.16	40.41	2.232	19	28	113	113	15	12	2.238	40.31	40.29
46.68	46.58	1.950	33	17	006	006	13	8	1.963	46.22	46.21
	46.79	1.911		31	020	200					
47.63	47.66	1.908	17	29	200						
51.58	51.51	1.774	5	6	115	115	8	2	1.782	51.28	51.26
52.68	52.52	1.742	4	2	016	106	1	2	1.749	52.31	52.29
	52.66	1.738		2	023						
52.87	52.91	1.730	3	2	120	210	3	3	1.723	53.07	53.15
53.43	53.46	1.714	6	2	203						
	53.51	1.712		2	210						
55.00	54.91	1.671	3	2	007						
55.37	55.37	1.659	2	3	122	212	5	2	1.654	55.55	55.57
55.88	55.95	1.643	1	2	212						
58.26	58.21	1.585	49	37	116	116	16	13	1.593	57.85	57.89
	58.31	1.582		32	123	213					
58.87	58.90	1.568	25	32	212						

Table I.2 d values and lattice parameters
of YBa₂Cu₃O_{7-δ} compounds

superconductivity of $\text{YBa}_2\text{Cu}_3\text{O}_{7-\delta}$ depends on the oxygen stoichiometry, the electrical properties such as T_c has a direct bearing on the oxygen content and for $\delta = 0-0.2$ T_c remains almost 90-92K and then decreases with decreasing oxygen content. Like other superconducting materials, orthorhombic $\text{YBa}_2\text{Cu}_3\text{O}_{7-\delta}$ is also diamagnetic below its T_c (Fig.I.6).

I.3.ii Preparation of $\text{YBa}_2\text{Cu}_3\text{O}_{7-\delta}$

In practice, a mixture of Y_2O_3 , BaCO_3 and CuO are taken in 1:2:3 stoichiometric proportion and mixed in a mortar, calcined at 900-950°C for 20-50 hrs with repeated grinding operations in order to develop maximum percentage of 123 phase. Long hours of oxygen annealing is required in the temperature range 450-650°C to stabilize orthorhombic $\text{YBa}_2\text{Cu}_3\text{O}_{7-\delta}$ phase. In this method, the high diffusion length between the individual solid particle prevents the formation of single phase compound easily. Therefore, emphasis has been laid on the preparation of YBCO particulates with desirable properties such as high purity and homogeneity, small particle size and narrow distribution and which possess good sinterability at relatively lower temperature. Formation of single phase compound without intermediate grinding and occurrence of minimum microcracks also were found desirable properties for the starting powders. In this regard several novel chemical techniques have emerged. Most of the chemical methods of preparation start from a solution of cations (for atomic scale mixing) and through

Fig. 1.6 Meissner effect: A permanent magnet levitates above a YBCO superconductor bathed in liquid nitrogen because its magnetic field is completely repulsed at the surface of the superconductor

concentration or precipitation, generate a solid precursor. Another direct way of making fine powder is from a mixture of cationic salts through direct high temperature oxidation. The various techniques can be classified broadly into a few sub-headings in order to make them precise.

Classification

Chemical methods of preparation of fine superconducting powders can be broadly classified into two major types, (a) through precursor and (b) direct synthesis.

I.3.ii.a Preparation through chemical precursors

The first step involves making a right solution of Y, Ba and Cu.

Solution preparation:

The choice of right metal salts and solvent medium are the two important factors in the solution preparation. Water or water/alcohol mixture is employed if the salts are inorganic (ionic precursors) and non aqueous solvents if metal alkoxides (molecular precursors) are used. Preferential crystallization or precipitation of the component cations have been avoided (mutually compatible) by adjusting the parameters like concentration, pH, atmosphere etc. Preferred anionic salts employed are nitrates, acetates, oxalates, carbonates or citrates. Butoxides, hexanates, acetyl acetonates,

naphthanates etc. are commonly used alkoxide systems. Once a stable solution is made, solvent is removed to prepare solid precursors while keeping the chemical homogeneity of the liquid solution as far as possible. Thermal decomposition of the precursor results in the single phase YBCO. Solid precursors are made from the solutions by

- (i) spray drying/calcination
- (ii) coprecipitation
- (iii) sol-gel decomposition and
- (iv) polymer precursor decomposition

I.3.ii.a.i Spray drying/calcination

In spray drying technique, the atomization of a solution of cations into a hot chamber favours rapid removal of the solvent giving fine spherical agglomerates. For example, when the temperature in the chamber is between 200-400°C, spray dried powder requires further heat treatment in the range 850-900°C in order to form pure 123 phase(174). On the contrary, the solution can be sprayed into a chamber kept above 800-1000°C, YBCO phase is reported to form in single step(175). Both atomic or molecular precursor solutions can be used for spraying(176). This method has shown possibility of scale up. Agglomeration of the sprayed powders has been reduced by spraying the solution into a dehydrating solvent, or immiscible liquid resulting in particles of spherical morphology. A citrate solution of Y, Ba and Cu was sprayed into a dry ethanol solution(177), powder was

filtered out and heat treated at 920°C for 3 hrs, resulting in YBCO particles of 0.3 to 0.5 microns.

I.3.ii.a.ii Coprecipitation:

Simultaneous precipitation of yttrium barium and copper from a solution of nitrate or acetate as oxalate(178,179), carbonate(180) or as hydroxide(181) is well established. Preferential precipitation of individual constituents and selective solubility of the components in the solvent system are the two major problems identified as the factors affecting the homogeneity. Simultaneous precipitation of yttrium, barium and copper as hydroxide is known to be difficult because of high solubility of $Ba(OH)_2$ in water. This problem has been successfully overcome by selecting an isopropanol/water (3:1) solvent system for the complete precipitation(182). Coprecipitation as carbonate using sodium carbonate(183) or organic carbonate(184) as precipitating agent is another route because all three carbonates are insoluble in aqueous medium at relatively high pH. The sluggish $BaCO_3$ decomposition actually limits the otherwise advantageous coprecipitation in this case. Calcination at reduced pressure (preferably dynamic vacuum) will increase the decomposition rate of $BaCO_3$ (185).

I.3.iii.a.iii Sol-gel synthesis:

Preparation of superconducting oxides by sol-gel techniques has been done in two ways; one starting from

molecular precursors such as metal alkoxides by controlled hydrolysis and condensation or by direct pyrolysis of the mixed alkoxide gel. Sometimes ionic precursors like metal acetates or nitrates are converted to gels by addition of organic acids, ammonia or suitable chelating agents. Further pyrolysis of gels gives the required powder.

I.3.ii.a.iii(a) Alkoxide route:

Horowitz et.al.(186) in one of the early reports on low temperature sol-gel preparation of YBCO used a solution of Y $(\text{OCH Me}_2)_3$, Ba $(\text{OCH Me}_2)_3$ and Cu $(\text{OC}(\text{CH}_3))_2$ in tetrahydrofuran. Controlled hydrolysis and subsequent heat treatment of the precursor at 750°C for 5 hours, tetragonal 123 phase has formed with less impurity phases. Shibata et.al.(187) synthesized homogeneous Y, Ba and Cu butoxide gel using butanol as solvent. Laurates(188), naphthanates(189), acetyl acetonates(190,191) and certain carboxylates are commonly used as organometallic compounds for 123 preparation. In all these methods, the homogeneous gel undergoes a decomposition to a finely dispersed mixture of oxides before reacting to form final compound. In the case of controlled hydrolysis of mixed alkoxide solution, water soluble $\text{Ba}(\text{OH})_2$ strongly adsorb over (Y,Cu) hydroxides so that complete removal of the solvent by filtration become feasible and the solvent free precursor react at as low a temperature as 700°C to pure 123 compound(186). This temperature is one of the lowest reported formation

temperature. It has not been possible, however, to achieve a homogeneous network of -O- bonds with Y, Ba and Cu in the gel structure, but on the other hand, they keep their independent identity as oxide, hydroxide or carbonate.

I.3.ii.a.iii(b) Other sol-gel methods:

Polymeric gels derived from ionic salts also offer intimate mixing of cations in atomic level. The well known example is 'citrate gel' route. Mixture of nitrate solution is allowed to complex with citric acid. Solution is concentrated to a rigid blue green gel which on pyrolysis at 800-900°C result in extremely fine superconducting powders(192). Modifications of this process by introducing ethylene glycol(193) or gelation at high pH(194,195) (addition of NH_3 to keep pH above 6) also offer a wide range of citrate gels.

The effect of processing variables such as nitrate content, rate of decomposition, temperature of decomposition etc. play a major role in the ultimate microstructure development of the precursor YBCO powders. Inorganic gels can be formed by simple techniques like concentrating an ammoniated (pH near 6) acetate solution(196). In place of citric acid (functionality 4) poly acrylic acid (functionality 28) can be used for better cross linked polymeric gels. Chelating agents such as EDTA have been effectively utilized for getting homogeneous complex from the nitrate solution(197). All these gels require heat treatment at 850-930°C for 2 to 10 hours

followed by oxygen annealing step.

All these methods are characterised by the fact that they require only single step calcination relatively at lower temperature than that of a solid state reaction method.

I.3.ii.a.iv Polymer-metal complex precursor synthesis:

Yang(198) and his group synthesized 123 compound from polymer-metal complex (PMC) precursor between 860 to 950°C using a reaction time as short as 0.5 hours. They used PMMA, poly amic acid etc as the synthetic organic polymers which has got strong complexation affinities for metal ions. When metal solution is added to certain polymers dissolved in suitable solvents, homogeneous molecular complexes are formed.

I.3.ii.b Direct synthesis:

Certain attempts have been reported on the preparation of YBCO superconductor starting from decomposition of mixture of salts(199). Such methods are attractive since they do not involve solutions or gels and hence large volumes. Further, the evolution of the gaseous decomposition products at low temperature will assist nascent oxide surfaces to react at faster kinetics. Since moisture is minimum, formation of $BaCO_3$ phase also could be brought to minimum. Gallagher et.al.(200) reported a novel, low temperature oxidation-reduction reaction at about 200°C between anionic components of yttrium, barium and copper salts (acetates and nitrates in definite ratio) to

their mixed oxide having surface area 30 gm/cc.

Capacity for absorbing high order of microwaves by the constituents of YBCO superconductor, copper oxide in particular, has been utilised to prepare high purity YBCO compound recently(201). A mixture of oxides/carbonates of Cu, Ba and Y have been subjected to microwaves where the phases were formed after 60-70 minutes. These methods are found to be superior to many others based on solution as well as gel decomposition due to the near absence of $BaCO_3$ formation.

I.4 Conclusion

A number of chemical techniques have been investigated over the years for the preparation of fine powders. There have been minor modifications introduced in the main flow sheet for attaining certain desirable properties in specific cases. The idea of generating fine particle is ultimately to produce homogeneous, pure low temperature sinterable ceramic and to achieve the functionality of the desired ceramic in the most appropriate way. Although many of the above methods nucleate submicron to nano size particles, considerable powder agglomeration takes place during drying/calcination due to the increased surface activity of such particles. Hence the success of any process for fine particulates is preparing the powder of desirable characteristics which will further provide the right compaction and sintering behaviour alongwith the desirable phase composition. In this respect, there exists still many

questions unanswered. Further, it has been difficult to arrive at a clear distinction in terms of powder properties based on the specific routes followed. This study therefore is an attempt to select three different routes, sol-gel, flash combustion and microwave decomposition on three different systems involving single component, double and tripple component systems. Powders have been prepared and a critical evaluation of the powder as well as sintered properties of such particulates are studied.

References

1. W.D. Kingery, pp. 1-29, *Ultrastructure processing of advanced ceramics*. Eds. J.D. Mackenzie and D.R. Ulrich, Wiley Interscience, New York, 1988.
2. D.A. Young, *Decomposition of Solids*, Pergamon Press, New York, 1966.
3. F.H. Norton, *Fine Ceramics*, Krieger, Malabar FL, 1978.
4. W.D. Kingery, D.R. Uhlmann and H.K. Bowen, *Introduction to Ceramics*, 2nd Ed. Wiley Interscience, New York, 1976.
5. W.H. Gitzen, *Alumina as a Ceramic Material*, The American Ceramic Soc. Inc., Ohio (1970).
6. J.S. Reed, *Introduction to the principles of ceramic processing*, pp. 37-44, Wiley Interscience, New York, 1988.
7. R.E. Kirk, D.F. Othmer, M. Grayson and D. Eckroth, *Kirk-Othmer, Encyclopedias of Chemical Technology*, Wiley Interscience, New York (1983).
8. D.W. Johnson Jr., *Am. Ceram. Soc. Bull.*, 60(2) (1981) 221.
9. J.G.M. deLau, *Am. Ceram. Soc. Bull.*, 49(6) (1970) 570.
10. J.G.M. deLau, P.F.G. Bongaerts, J.L.H.M. Wijgergaugs and A.L. Stuijts, *Ber. Dtsch. Keram. Ges.*, 52(7) (1975) 207.

11. J. Thomson Jr., *Am. Ceram. Soc. Bull.*, 53(5) (1974) 421.
12. M.T. Goosey, I.M. Watson, R.W. Whatmore, U.K. Pat. GB 2196621 (1988).
13. L.M. Sheppard, *Am. Ceram. Soc. Bull.*, 68(5) (1989) 979.
14. P. Reynen and H. Bostius, *Powder Metall. Int.*, 8(2) (1976) 91.
15. P. Reynen and H. Von Kamptz, *Ber. Dtsch. Keram. Ges.*, 53(10) (1976) 326.
16. A. Metzger and C. Gorin, *Dig. Intermag. Conf.*, 34(6) (1975).
17. M. Akinc, Report, ARO-21718 3-MS., Order No.A.D-A185140, pp.62, NTIS (1987).
18. Y. Ozaki, M. Wadasako, T. Kasai and Y. Schinohara, *Ger. Offen.*, pp.12 DE 3616503 A1 20 Nov., 1986.
19. K. Richardson and M. Akinc, *Ceram. Inter.*, 13, (1987) 253.
20. D.M. Roy, R.R. Neurgoankar, T.P.O'Hollaran and R. Roy, *Am. Ceram. Soc. Bull.*, 56(11) (1977) 1023.
21. D.M. Roy and S.O. Oyefesobi, *J. Am. Ceram. Soc.*, 60(3-4) (1977) 178.
22. S.C. Zhang and G.L. Messing, *Ceram. Trans.*, 12, (1990) 49.
23. M.J. Ruthner, *Sci. Sintering*, 6, (1974) 81.
24. W.R. Marshall and D.W. Charlesworth, *AIChE J.*, 6, (1984) 44.

25. D.W. Sproson, G.L. Messing and T.J. Gardner, *Ceram. Inter.*, 12, (1986) 3.
26. H. Ishizawa, O. Sakurai, N. Mizutani and M. Kato, *Am. Ceram. Soc. Bull.*, 65, (1986) 1399.
27. F.J. Schnettler, F.R. Monforte and W.W. Rhodes, pp. 79-90, *Science of Ceramics, Vol.4*, Ed. G.H. Stewart, Brit. Ceram. Soc., Stoke on Trent, U.K. (1968).
28. H.A. Sauer and J.A. Lewis, *Am. Inst. Chem. Engg. J.*, 18(2) (1972) 435.
29. M.D. Rigterink, *Am. Ceram. Soc. Bull.*, 51(2) (1972) 158.
30. D.W. Johnson Jr. and F.J. Schnettler, *J. Am. Ceram. Soc.*, 53(8) (1970) 440.
31. Y.S. Kim and F.R. Monforte, *Am. Ceram. Soc. Bull.*, 50(6) (1971) 532.
32. C.S. Tao, *Tech. Rept. No. LBL 3978* (1976).
33. L.A. Xue, F.L. Riley and R.J. Brook, *Br. Ceram. Trans. J.*, 85, (1986) 47.
34. W.M. Flock, *Bayer Processed Aluminas*, pp.85-100 in *Ceramic Processing Before firing*, Eds. G.Y. Onada Jr. and L.L. Hench, John Wiley and Sons, New York, 1978.
35. P.E.D. Morgan, pp.67-76 in *Processing of Crystalline Ceramics*, Ed. H. Palmour III, R.F. Davis and T.M. Hare, Plenum, New York, 1978.
36. K.D. Reeve, *Am. Ceram. Soc. Bull.*, 42(8) (1963) 452.

37. H.N. Willard and N.K. Tang, *J. Am. Chem. Soc.*, 59, (1937) 1190.
38. L. Gordon, M.L. Salutsky and H.H. Willard, *Precipitation from homogeneous solutions*, Wiley Interscience, New York, 1959.
39. J.E. Blendell, H.K. Bowen and R.L. Coble, *Am. Ceram. Soc. Bull.*, 63(6) (1984) 797.
40. B. Cornilsen and J.S. Reed, *Am. Ceram. Soc. Bull.*, 58(12) (1979) 1199.
41. W. Stober, A. Fink and E. Bohn, *J. Coll. Int. Sci.*, 26, (1968) 62.
42. K. Haberko, *Ceramurgia International*, 5(4) (1979) 148.
43. M.E.V. Costa, H.M.M. Diz and J.L. Baptista, *Sci. Ceram.*, 14, (1988) 299.
44. D.T. Rankin, G.B. Burney, P.K. Smith and R.D. Sission Jr., *Am. Ceram. Soc. Bull.*, 56(5) (1977) 478.
45. J.L. Woolfrey, *J. Nucl. Mater.*, 74(1) (1978) 123.
46. M.P. Anderson, *Eur. Pat.* (EP, 294988 A2 14 Dec., 1988), 1988.
47. P. Duran, M. Gonzalez, J.R. Jurado and C. Moore, *Ceram. Trans.*, 12, (1990) 945.
48. A. Kato, K. Inoue and Y. Katatoe, *Mater. Res. Bull.*, 22(9) (1987) 1275.
49. M.I. Mendelson, *J. Am. Ceram. Soc.*, 59(5-6) (1976) 219.
50. M. Kiyama, *Bull. Chem. Soc. Jpn.*, 51(1) (1978) 134.

51. A. Goldman and A.M. Laing, *J. Phys. (Paris) Colloq.*, 1, (1977) 297.
52. W. Roos, H. Haak, C. Voigt and K.A. Hempel, *J. Phys. (Paris) Colloq.*, 1, (1977) 35.
53. W. Brand, D. Hennings, M. Klee and H. Schreinmacher, *Eur. Pat. (EP 304128 A1 22 Feb., 1989)* 1989.
54. M.D. Rigterink, *J. Can. Ceram. Soc.*, 37, LVI-LX (1968).
55. B.J. Mulder, *Amer. Ceram. Soc. Bull.*, 42(11) (1970) 993.
56. V.A. Amelina, V.I. Vereshchagin and P.G. Usov, *Izv. Tomsk. Politekh. Inst.*, 259, (1975) *Chem. Abstr. No.86* 173675 C (1977).
57. V.P. Chalyi and Z. Ya Makarova, *Ukr. Khim. Zh.*, 35(5) (1969) 497 (Russ.), *Chem. Abstr. No. 71 74987 q* (1969).
58. M. Murata, K. Wakino, K. Tanaka and Y. Hamakawa, *Mater. Res. Bull.*, 11, (1976) 323.
59. H. Yamamura, M. Tanada, H. Haneda, S. Shirasaki and Y. Moriyoshi, *Ceram. Int.*, 11(1) (1985) 23.
60. H.L. Lee, G.G. Hong and H.J. Jung, *Yoop Hukhoechi*, 23(3) (1986) 44.
61. E. Matijevic, *Acc. Chem. Res.*, 14 (1981) 22.
62. T. Kubo, M. Kato and T. Fujita, *Kogyo Kagaku Zasshi (in Japanese)*, 71(1) (1969) 114.
63. R. Vivekanandan, S. Philip and T.R.N. Kutty, *Mater. Res. Bull.*, 22, (1987) 99.
64. J.M. Stanley, *Ind. Eng. Chem.*, 46 (1954) 1684.

65. S. Hirano, K. Shibata and S. Naka, Abstract of 22nd Yogyo Kiso-Toronkai, 111 (1984).
66. N.T. Okopnaya, V.I. Zelentosov, V.M. Chertor and B.N. Lyashkevich, Adsorbtsiya Adsorbentry, 2, 108 (1974), Chem. Abstr. No. 111783 z (1974).
67. E.P. Stambaugh, U.S. Pat. 3,607,006.
68. F.A. Foos and E.P. Stambaugh, U.S. Pat. 3,065,095.
69. L. Michalowsky and H.D. Schnabd, Ceram. Inter., 16(1) (1990) 33.
70. A.A. Van Der Giessen, Klei Keram., 20(2) (1970) 30, Chem. Abstr. No. 72 114604 s (1970).
71. F. Schrey, Paper 17-EI-67F, 1967, Annual Meeting of the American Ceram. Soc., Am. Ceram. Soc. Bull., 46(4) (1967) 788.
72. S. Hirano and S. Somiya, J. Cryst. Growth, 35 (1976) 273.
73. H. Toraya, M. Yoshimura and S. Somiya, Am. Ceram. Soc. Bull., 65 (1982) C72.
74. I.J. Mc Colm and N.J. Clark, pp. 90-94 in Forming, Shaping and Working of High Performance Ceramics, Blackie, Chapman and Hall, New York, 1988.
75. H. Palmour III, R.F. Davis and T.M. Hare, Eds. Processing of Crystalline Ceramics, Materials Science Research., 11, Plenum, New York (1978).

76. L.L. Hench and D.K. Ulrich, Eds. Proc. Int. Congress on Science of Ceramic Chemical Processing, Wiley, New York, 1986.
77. C.J. Brinker, D.E. Clark and D.R. Ulrich, Eds. Better Ceramics through Chemistry, Mat. Res. Soc. Symp. Proc., 32, North Holland, New York, 1984.
78. C.J. Brinker, D.E. Clark and D.R. Ulrich, Eds. Better Ceramics through Chemistry II, Mat. Res. Soc. Symp. Proc., 73, MRS, Pittsburgh, 1986.
79. L.L. Hench and D.R. Ulrich, Eds. Proc. Int. Congress on Ultrastructure Processing of Ceramics, Glasses and Composites, Wiley, New York, 1984.
80. J.D. Mackenzie and D.R. Ulrich, Eds. Proc. Int. Congress on Ultrastructure Processing of Ceramics, Glasses and Composites, 1987.
81. P. Vincenzini Ed. Ceramics Today-Tomorrow's Ceramics, Proceedings of CIMTEC, Italy, 1990, Elsevier Science Publishers, the Netherlands, 1991.
82. H. Schmidt, J. Non-Crystalline Solids, 100, (1985) 51.
83. D.E. Bradley, R.C. Mehrotra and D.P. Gaur, Metal Alkoxides, Academic Press, London, 1978.
84. H. Okamura and H.K. Bowen, Ceram. Inter., 12(3) (1986) 161.
85. M.E.A. Hermans, Powder Metall. Inter., 5(3) (1973) 137.
86. A.C. Pierre, Am. Ceram. Soc. Bull., 70(8) (1991) 1281.

87. L. Livage, M. Henry and C. Sanchez, *Prog. Solid State Chemistry*, 18, (1988) 259.
88. K.S. Mazdidasni, *Ceram. Inter.*, 8(2) (1982) 42.
89. G.L. Messing, J.W. McCauley, K.S. Mazdidasni and R.H. Haber, *Advances in Ceramics, Vol.21, Ceramic Powder Science*, American Ceramic Society, Westerville, OH, 1987.
90. W.E. Rhine and H.K. Bowen, *Ceram. Inter.*, 17(3) (1991) 143.
91. G. Pouskouleli, *Ceram. Inter.*, 15(5) (1989) 255.
92. G. Pouskouleli, *Ceram. Inter.*, 15(4) (1989) 213.
93. C.J. Brinker and G.W. Scherer, *Sol-gel Science*, Academic Press, New York, 1989.
94. S. Sakka and T. Yoko, *Ceram. Inter.*, 17(4) (1991) 217.
95. R.K. Iler, *The Chemistry of Silica*, Wiley Interscience, New York, 1979.
96. L.L. Hench and J.K. West, *Chem. Rev.*, 90, (1990) 33.
97. P.A. Thiessen and K.L. Thater, *Anorg. Allg. Chem.*, 181, (1929) 417.
98. F. Tebbe, P.A. Morris, R.H. French, U. Chowdhry and R.L. Coble, *J. Am. Ceram. Soc.*, 71, (1988) C204.
99. B.E. Yoldas, *J. Appl. Chem. Biotechnol.*, 23, (1973) 803.
100. B.E. Yoldas, *Am. Ceram. Soc. Bull.*, 54, (1975) 289.
101. H. Endl, B.D. Krude and H. Housner, *Ber. Dtsch. Keram. Ges.*, 54, (1977) 105.

102. E.A. Barringer and H.K. Bowen, *J. Am. Ceram. Soc.*, 65, (1983) C199.
103. S. Komerneni and R. Roy, *Mater. Lett.*, 3, (1985) 165.
104. J.L. Woodhead, pp.29-37 in *Science of Ceramics 9*, Ed. K.J. de Vries, *Nederlandse Keramische Vereniging, the Netherlands*, 1977.
105. B. Fegley, P. White and H.K. Bowen, *Am. Ceram. Soc. Bull.*, 64, (1985) 1115.
106. K.S. Mazdidasni, C.T. Lynch and J.S. Smith II, *J. Am. Ceram. Soc.*, 48, (1965) 372.
107. B.E. Yoldas, *J. Mater. Sci.*, 21, (1986) 35.
108. D.W. Edenborough, A.S. Malin and R.G. Robin, *J. Nucl. Mater.*, 48(2) (1973) 210.
109. R.B. Mathews and M.L. Swanson, *Am. Ceram. Soc. Bull.*, 58(2) (1978) 223.
110. J.L. Woodhead and D.L. Segal, *Brit. Ceram. Proc.*, 36, (1985) 123.
111. E.M. Vogel, N.C. Andreadris, W.E. Quinn and T.J. Nelson in *Advances in Ceramics*, 22, *Ceramic Powder Science*, Eds. G.L. Messing, J.W. McCauley, K.S. Mazdidasni and R.A. Haber, ACS Inc., Westerville, Ohio, 1987.
112. M. Hoch, pp.13, *Science of Ceramics 9*, ed. K.J. de Vries, *the Nederlandse Keramische Vereniging, the Netherlands*, 1977.
113. O. Yamaguchi, D. Tomihisa and H. Kawabata, *J. Am. Ceram. Soc.*, 70, (1987) C94.

114. S. Naka, S. Hirano and Y. Suwa, Preprints of the Annual Meeting of Japan Ceramic Society, 11131, Tokyo, Japan, 1983.
115. J.S. Smith II, R.T. Dolloff and K.S. Mazdiasni, Am. Ceram. Soc., 53(1) (1970) 91.
116. K.S. Mazdiasni, K.T. Dolloff and J.S. Smith II, J. Am. Ceram. Soc., 52(10) (1969) 523.
117. A.R. Hardy, G. Gowda, T.J. McMohan, R.E. Riman, W.E. Rhine and H.K. Bowen, pp.407, Ultrastructure Processing of Advanced Ceramics, Eds. J.D. Mackenzie and D.R. Ulrich, John Wiley, New York, 1988.
118. F. Schmidt and A. Feltz, Z. Anorg. Alleg. Chem., 573, (1989) 208.
119. Z.Q. Zhuang, M.J. Huan, S.J. Jang and L.E. Cross, Adv. Ceram. Mater., 3(5) (1988) 485.
120. K.S. Mazdiasni and L.M. Brown, J. Am. Ceram. Soc., 55(11) (1972) 548.
121. B.E. Yoldas, Am. Ceram. Soc. Bull., 59(4) (1980) 479.
122. P. Colomban, Adv. Ceram., 21 (Ceram. Powder Sci.) (1987) 139.
123. G.H. Heartling and C.E. Land, Ferroelectrics, 3, (1972) 261.
124. L.M. Brown and K.S. Mazdiasni, J. Am. Ceram. Soc., 55 (1972) 541.
125. I.M.M. Salvado, C.J. Serna and J.M.F. Navarro, J. Non-Crystalline Solids, 100, (1988) 330.

126. J.L. Woolfrey, W.J. Buylex and J.R. Bartlett, *Mater. Sci. Forum.*, 34-36 (Int. Ceram. Conf. AUSTCERAM 88, Pt.1) 583 (1988).
127. D.E. Clark, pp.237-246, *Science of Ceramic Chemical Processing*, Eds. L.L. Hench and D.R. Ulrich, John Wiley and Sons Inc., New York, 1986.
128. P.F. Becher, *Mater. Sci. Res.*, 11, (1978) 79.
129. F.G. Sherif, *European Patent*, EP 36962 A 11 Apr. 1990.
130. D.W. Hoffman, R. Roy and S. Komarneni, *J. Am. Ceram.Soc.*, 67(7) (1984) 468.
131. H. Yoshimatsu, T. Yabuki and H. Kawasaki, *J. Non-Crystalline Solids*, 10, (1988) 413.
132. J. Phalippou, M. Prassas and J. Zarzycki, *J. Non-Crystalline Solids*, 48, (1982) 17.
133. T. Hayashi and H. Saito, *J. Mater. Sci.*, 15 (1980) 1971.
134. F. Pancrazi, J. Phalippou, F. Sorrentino and J. Zarzycki, *J. Non-Crystalline Solids*, 63, (1984) 81.
135. M.S.J. Gani and R. Mcherson, *J. Mater. Sci.*, 12(5) (1977) 999.
136. T. Osuka, H. Morikawa, F. Marumo, K. Toliji, Y. Udagannu, A. Tasumori and M. Yamane, *J. Non-Crystalline Solids*, 82, (1986) 154.

137. A.C. Pierre and D.R. Uhlmann, pp. 865-872, *Ultrastructure Processing of Advanced Ceramics*, Eds. J.D. Mckenzie and D.R. Ulrich, Wiley Interscience Publications, New York, 1988.
138. C. Marcilly, P. Courty and B. Delmon, *J. Am. Ceram. Soc.*, 53(1) (1970) 56.
139. O.J. Anderton and F.R. Sale, *Powder Metall.*, 1, (1979) 8.
140. M. Pechini, U.S. Pat. No. 3330697, July 11, 1967.
141. P.A. Lessing, *Am. Ceram. Soc. Bull.*, 68(5) (1989) 1002.
142. A.L. Micheli, *Ceram. Inter.*, 15(3) (1989) 131.
143. K.C. Chen, T. Tsuchiya and J.D. Mackenzie, *J. Non-Crystalline Solids*, 81, (1986) 227.
144. S.P. Mukherjee, *J. Non-Crystalline Solids*, 82, (1986) 293.
145. H. Suzuki, H. Saito and T. Hayashi, *J. Mater. Sci.*, 19, (1984) 396.
146. R. Roy, *J. Am. Ceram. Soc.*, 52, (1969) 344.
147. S. Komerneni, S. Suwa and R. Roy, *J. Am. Ceram. Soc.*, 69, (1986) C155.
148. K.S. Mazdidasni and C.M. Cook, *J. Am. Ceram. Soc.*, 56(12) (1973) 628.
149. O. De Pous-Battelle, *Ceram. Inf.*, 13(143) (1978) 283.
150. J. Canteloup and A. Mocellin, *J. Mater. Sci.*, 11, (1974) 2352.

151. W.E. Kuhn (ed) pp.81-94 Fine Particles, 2nd International Conference, Electrochemical Society, Princeton, N.J., 1974.
152. A. Kato, I. Mochida, J. Tanaka, H. Takeuchi and S. Kawasoe, Asaki Garasu Kogyo Gijutso Shoreikai Kenkyo Hokoko, 21, (1972) 151.
153. A. Kato and Y. Suyama, Chem. Lett., (1974) 961.
154. M.S.J. Gani and R. McPherson, J. Aust. Ceram. Soc., 8(3) (1972) 65.
155. J.D. Holmgren, J.O. Gibson and C. Sheer, J. Electrochem Soc., 111(3) (1964) 362.
156. C. Sheer, S. Korman, D.J. Angier and R.P. Cahn, pp.133-152, Fine Particles, ed. W.E. Kuhn, Electrochemical Society, Princeton, N.J., 1974.
157. J. Canteloup and A. Mocellin, pp.209-222, Special Ceramics 6, Ed. P. Popper, British Ceramic Research Association, Stoke-on-Trent, 1975.
158. A. Kato, M. Iwata, J. Hojo and M. Nagano, Yogyo Kyokai Shi, 83(9) (1975) 453.
159. W.R. Cannon, S.C. Danforth, J.H. Flint, J.S. Haggerty and R.A. Marra, J. Am. Ceram. Soc., 6 (1982) 324.
160. M. Cauchetier, O. Croiu, M. Luce, M. Michon, J. Raris and S. Tistochenko, Ceram. Inter., 13(1) (1987) 13.
161. J.B. Bednorz and K.A. Muller, Z. Phys. B., 64, (1986) 189.

162. M.K. Wu, J.R. Ashburn, C.J. Torng, P.H. Hor, R.L. Meng, L. Gao, Z.J. Huang, Y.Q. Wang and C.W. Chu, *Phys. Rev. Lett.*, 58, (1987) 908.
163. H. Maeda, Y. Tanaka, M. Fukutomi and T. Asano, *Jpn. J. Appl. Phys.*, L209 (1988).
164. Z.Z. Sheng and A.M. Herman, *Nature*, 332, (1988) 55.
165. A. Nerlikar, *Studies of High Temperature Superconductor*, Vol.1-4, Nova Science Publishers Inc., New York, 1989.
166. V.D. Hunt, *Superconductivity Source Book*, John Wiley and Sons Inc., New York, 1989.
167. M.F. Yan (Ed.), *Ceramic Superconductors, Research Update*, The American Ceramic Society Inc., Westerville, Oh, 1988.
168. *Advanced Ceramic Materials*, American Ceramic Society, 2(3B) (1987).
169. J.W. Halley (Ed.), *Theories of High Temperature Superconductivity*, Addison-Wesley Publishing Co. Inc., CL 1988.
170. J. Muller and J.L. Olsen (Eds.), *Proceedings of the International Conference on High Temperature Superconductors and Materials and Mechanisms of Superconductivity*, Part 1 and 2, Switzerland, 1988, North-Holland, Amsterdam, 1988.

171. Proceedings in High Temperature Superconductivity, Vols.1-24, World Scientific Publishing Co. Pvt. Ltd., LH, Singapore.
172. W.E. Mayo (Ed.), Processing and Applications of High Tc Superconductors, The Metallurgical Society Inc., PA, 1988.
173. High Temperature Superconductivity Reprints from Phy. Rev. Lett. and Phy. Rev., Vols. 1-II, The American Physical Society, New York, 1988.
174. N. Nakahara, T. Nakano, S. Gotoh and M. Shitomi, High Tc oxide Superconductor by spray drying method. Processing and application of high Tc superconductors, Page 23-30, Ed. W.E. Mayo, Metallurgical Society Publication, 1988.
175. P.A. Fuierer, T.T. Srinivasan and R.E. Newnham, Ceramic Superconductors II Research update 1988, pp. 156, Ed. M.F. Yan, The Amer. Ceram. Soc., Ohio, U.S.A.
176. A. Pebler and R.G. Charles, Mater. Res. Bull., 23(9) (1988) 1337.
177. J.H. Jean, J. Mater. Sci. Lett., 8, (1989) 751.
178. S. Yilminot, S.E. Hadigui, A. Derory, M. Drillon, J.C. Bernier, J.P. Kappler, R. Kuentzler and Y. Dossmann, Mat. Res. Bull., 23(4) (1988) 521.
179. A. Manthiram and J.B. Goodenough, Nature, 329, (1987) 701.

180. H.H. Wang, and K.D. Carlson, *Inorg. Chem.*, 26, (1987) 1474.
181. P. Barboux, J.M. Tarascon, L.H. Greene, G.W. Hull and B.G. Bagley, *J. Appl. Phys.*, 63, (1988) 2725.
182. H.K. Varma, K.G.K. Warriar, K.R. Nair and A.D. Damodaran, *Proc. Seminar on Advanced Ceramics, BHU, 1988.*
183. S. Baik, J.H. Moon and H.M. Jang, *Ceramic Superconductors II, Page 186, Research update, American Ceramic Society, 1988.*
184. P. Pramanik, S. Biswas, S. Chakrabarti, B.K. Raul and K.L. Chopra, *Mater. Res. Bull.*, 25(7) (1990) 877.
185. J.R. Spann, I.K. Lloyd, M. Kahn and M.T. Chase, *J. Am. Ceram. Soc.*, 73(2) (1990) 435.
186. H.S. Horowitz, S.J. McLain, A.W. Sliight, J.D. Druliner, P.L. Gai, M.J. Van kavelaar, J.L. Wagner, B.D. Biggs and S.J. Poon, *Science*, 243, (1989) 66.
187. S. Shibata, T. Kitagawa, H. Okazaki, T. Kimura and T. Murakami, *Jpn. J. Appl. Phys.*, 27, (1988) L53.
188. T. Manabe, H. Yokota, T. Kumagai, W. Kondo and S. Mizuta, *J. Ceramic Society, Japan*, 28, (1990) 229.
189. T. Kumagaya, K. Kondoh, Y. Yokota, H. Minakami and S. Mizuta, *Sermikkusu Ronbun-Shi*, 97, (1989) 454.
190. P. Catania, N. Hovnamian, L. Cot, M.P. Thi, R. Kormann and J.P. Ganne, *Mat. Res. Bull.*, 25(5) (1990) 631.
191. R.M. Laine, K.A. Youngdahl, W.M. Carty, G.C. Stangle,

- C. Han, R.A. Kennish, S. McElhancy, T.K. Yin, T. Yogo and M. Sarikaya, *Ceramic Superconductor II, Research update*, Page 450, American Ceramic Society, 1988.
192. F. Mahloojchi, T.R. Sale, N.J. Shah and J.W. Ross, *Superconducting Ceramics*, Page 1, British Ceramic Proceedings No.40, 1988.
193. M. Nagano and M. Greenblatt, pp. 43-53, *Processing and applications of high Tc superconductors*, (ed.) W.E. Mayo, The Metallurgical Society Inc., PA, (1988).
194. C. Chu and B. Dunn, *J. Am. Ceram. Soc.*, 70(12) (1987) 375.
195. D.H.A. Blank, H. Krnidhof and J. Flokstra, *J. Phys. D: Appl. Phys.*, 21, (1988) 226.
196. T. Umeda, H. Kozuka and S. Sakka, *Ad. Ceram. Mater.*, 3, (1988) 520.
197. D.B. Porter, C.M. Tamayo, R. Ibanez, A.B. Porter, J.V. Folgado, E. Escriva, V. Munoz, A. Segura and A. Cantarevo, *Mat. Res. Bull.*, 23(7) (1988) 987.
198. J.C.W. Chein, B.M. Gong, X. Mu and Y. Yang, *J. Polymer Sci., Part A. Polymer Chemistry*, 28, (1990) 1999.
199. M.L. Kaplan and J.J. Hauser, *Mater, Res. Bull.*, 23(2) (1988) 290.
200. K. Kourtakis, M. Robbins and P.K. Gallagher, *J. Solid State Chemistry*, 82, (1989) 290.
201. D.R. Baghurst, A.M. Chippindale and D.M.P. Mingos, *Nature*, 332, (1988) 311.

CHAPTER II

METHODS OF CHARACTERISATION OF POWDERS

II.1 Introduction

A few of the most important informations for easy characterisation of fine ceramic powders are particle size distribution, surface area, crystallite size, porosity, density, surface morphology and surface charge, compaction and sintering features. Various methods are being practised to arrive at these informations. This chapter gives some of the most important methods used in the present work for characterisation of the various ceramic oxides prepared by chemical methods. However, the specific sample preparation techniques and measurements adopted in individual cases are discussed in respective chapters.

II.2 Chemical analysis

The precursor as well as ceramic materials were analysed by wet chemical methods reported in standard text books for quantitative analysis(1,2). The material in some cases requires fusion in presence of a flux to bring into solution. The colorimetric analyser also was used for easy quantitative estimation other than usual precipitation or titration methods. A number of instrumental spectroscopic techniques are



also used for qualitative as well as quantitative analysis(3).
Some of them are listed in the table given below.

Method	Principle
Emission Spectroscopy (Powder)	Thermal, stimulation of electrons or atoms
Flame emission Spectroscopy (liquid)	
Atomic Absorption	
X-ray Fluorescence (powder)	X-ray, stimulation of atoms or electrons
Infrared Spectroscopy (gas, liquid or solid)	Molecular vibration with a change in dipole moment absorb IR radiation

II.3 Phase analysis

Since the ceramic materials are crystalline in nature, the best used technique for the analysis of phases is X-ray diffraction technique.

The well known Bragg law states,

$$n\lambda = 2d \sin \theta$$

where θ is the diffraction angle for a lattice spacing d , λ the wave length of X-rays and n is an integer. Powder or polished specimens are normally used and the diffraction intensity is

recorded as a function of X-ray reflection angle. The identification of phases is done by comparing the d spacings and relative intensities of the sample with standard reference data. The broadening of X-ray diffraction line profiles help in calculating crystallite size in polycrystalline materials(4).

In the present study, XRD patterns were taken in Philips Model PW1710 X-ray diffractometer with $\text{CuK}\alpha$ radiation using nickel as filter at a setting of 40 KV and 20 mA. Powder samples for the XRD were prepared by putting a thin layer of powder smeared over a glass plate. The glass plate was previously coated with paraffin wax to get good adhesion. XRD of the sintered surface was taken by inserting the sample directly in the machine.

II.4 Thermal analysis

The thermodynamical changes in solids and reaction between the materials are determined by thermogravimetric analysis (TGA) and differential thermal analysis (DTA) methods. In TGA, the weight of a material is determined as a function of temperature, while in the case of DTA Differential temperature due to endothermic or exothermic transition or reaction in the sample is plotted as a function of temperature or time with respect to an inert reference powder (eg. alumina)(5). Thermochemical methods give information due to decomposition of material, oxidation or vaporization, phase transition, reaction, vitrification and crystallization etc.

Differential Scanning Colorimetry is usually used for enthalpy change determination. Thermo mechanical analysis (TMA) gives information about the expansion or shrinkage during heating or cooling and the resistance to mechanical penetrations or transmission of mechanical vibrations. The simultaneous thermal analysis of precursors as well as various ceramic powders was carried out using Dupont thermal analyser (Thermal Analyst 2000). The heating rate was 20°C/min in air.

II.5 Particle size analysis

The particle size determination is done mainly by sieving techniques, sedimentation techniques, laser diffraction, light intensity fluctuation techniques etc(6-8). The Sedimentation technique is based on Stoke's law which is the most widely used particle size measurement technique.

The terminal velocity of a particle settling under the influence of gravity is given by $V = a^2(D_p - D_L) g/18\eta$ where V the terminal velocity, D_p and D_L are the densities of solids and liquid, 'a' is the diameter of the particle and η is the viscosity of the suspending medium. g is acceleration due to gravity

The stokes diameter 'a' of the particle is given by

$$a = \sqrt{\frac{18\eta V}{(D_p - D_L) g}}$$

The particle sizes ranging from 40 microns to 0.02

microns is possible with commercial instruments. In the sedimentation technique, the particle interactions and tendency of agglomeration is predominant in the case of sub micron powders. Ultrasonic dispersing in presence of specific defloculants is employed in most cases for getting good powder dispersions.

In the present study, the particle size measurement of the powder was made by using Micromeritics Model Sedigraph 5000D particle size analyser and particle size distribution of the powder was obtained in a graph with cumulative mass percent versus particle diameter in microns. Stable suspensions of the powder in both glycerol-water and in pure glycerol (in the case of YBCO powder) was prepared by putting the powder in solvent and sonicating it with an ultrasonicator for 2 minutes. In the case of alumina and strontium titanate powder, a defloculant (Tetrasodium Pyrophosphate) was also used.

II.6 Microscopic techniques

Microscopic techniques are very good tools for the accurate observation of particle morphology, shape, size and surface properties(9). For this, micrographs, at desirable magnification are required in order to get the details one is looking for. The full range and sizes can be examined using optical and electron microscopes. Optical microscopy is usually adequate for characterisation of particles greater than 0.5 - 1 micron in size. Electron microscopes (both

transmission and scanning) can measure particles as low as 0.001 micron.

The scanning electron microscope manufactured by JEOL was used (Model JEOL 35C). The electron gun is operated at an electron energy of 20 keV with a beam diameter of 20-25 nm. The surface of the sample is coated by sputtering with gold using an ion Sputtering equipment (JEOL, Fine Coat JFC1100, Japan) to make it conductive. The unit is operated at 1 KV and 10 mA current. Initially, the bell jar is evacuated to 10^{-4} torr pressure and then the samples are sputtered. The surface is coated with a thin gold film (10-20 nm thick). This helps to remove the charging effect, which is produced on the sample surface due to high energetic beam, by earthing it. The gold coated samples are mounted in the SEM chamber and the system is evacuated. The electron beam is scanned on the samples and the samples are photographed at appropriate magnifications. EPMA studies were also performed in the same instrument.

In the present study dry powders were mounted on the sample stud by inserting a stud coated with an adhesive into the powder. It was also prepared by placing a dilute suspension of particles in a polished stud which will form a deposit of particles on evaporation of the liquid. Polished as well as fractured samples were used for the characterisation of sintered powder compacts.

The optical micrographs of the samples were taken in a Leitz instrument. Samples were polished with various grades of

polishing papers and finally in polishing cloths using fine alumina powder in liquid paraffin medium. Both polarized as well as normal light was used.

II.7 Density

In the case of fine powders the density is measured by different methods, ie. tap density, bulk density, apparent density and X-ray density, depending on how the volume is determined and each term has got its own significance. Apparent density is a measure of the basic powder or granule density which includes the material volume and volume of the trapped pores. Liquid pycnometry is commercially used for determining the apparent density.

In the present study the powder density was measured using Archimedis principle with a pycnometer and isopropanol as a liquid medium. The density was calculated as follows.

wt. of bottle = W

wt. of bottle + substance = W_1

wt. of bottle + substance + isopropanol = W_2

wt. of bottle + isopropanol = W_3

Density of isopropanol = ρ_p

Density of sample $\rho_s = \frac{(W_1 - W) \rho_p}{(W_3 - W_2) + (W_1 - W)}$

The tap density of a powder is measured by putting the same in a graduated cylinder or container and tapping the

container for a given time or number. Because it is easy to obtain, the tap density of a powder has been commonly used for characterisation and it gives much information about the powder compaction behaviour, ie. those which are not obtained from particle size analysis. A laboratory model densitometer instrument was used in this study. The density calculated from the chemical formula weight and the volume of the unit cell is termed the X-ray density. The bulk density is a measure of the ratio of powder weight to volume before any compaction by tapping.

II.8 Surface area

Surface area of the powder is the surface area per unit mass or volume of the material. It is measured from the amount of gas or dye adsorbed on the surface of particles(10,11). The adsorption can be physical as well as chemical. While chemical adsorption is monolayer, multilayer adsorption is possible physically. Chemisorption of a gas over the surface is irreversible and it is difficult to remove. The best example is hydration of oxides.

In order to determine the surface area of powder as well as porous ceramic materials, physical adsorption of gases is made use of. Physical adsorption is rapid and reversible. The dynamic process of adsorption of gases is considered in Langmuir adsorption.

The rate of adsorption and desorption are equal, when

adsorption takes place in equilibrium

$$\text{so that } \frac{V_a / V_m}{1 - V_a / V_m} = bP$$

where V_a is amount of gas adsorbed in the surface of adsorbent at a pressure P , V_m is the volume of gas required for monolayer coverage and b is a constant for particular system and temperature. Brunauer, Emmet and Teller (BET equation) expanded this dynamic model for monolayer adsorption to understand multilayer adsorption,

$$\text{i.e. } \frac{P/P_s}{V_a (1 - P/P_s)} = \frac{1}{V_m C} + \frac{(P/P_s) (C-1)}{V_m C}$$

where P_s is the saturation vapour pressure and C is a constant. Various types of adsorption isotherms are studied. In the process of determining surface area of ceramic powder using BET(12) technique, the volume of a gas required to make a monolayer adsorption is measured by cooling the powder in liquid nitrogen temperature and by desorption of the gases by heating. Determination of surface area by this technique is dealt in a number of articles and good instrumentation is available at present. Surface area was measured by nitrogen adsorption employing micromeritics Accusorb 2100E instrument in the present work.

References

1. A.I. Vogel, 'A Text Book of quantitative inorganic analysis including elementary instrumental analysis', The English Language Book Society and Longman, 3rd Ed., 1961.
2. Systematic Materials Analysis, Vol.4, Eds. J.H. Richardson and R.V. Paterson, Academic Press, New York, 1978.
3. J.S. Reed, Introduction to the principles of ceramic processing, John Wiley and Sons, 1988.
4. H. Klug and L. Alexander, X-ray Diffraction Procedures, John Wiley and Sons, New York, 1962.
5. W.W. Wendlandt, Thermal methods of analysis, 2nd ed. Wiley-Interscience, New York, 1974.
6. R.R. Irani and C.F. Callis, Particle size: Measurement, Interpretation and Application, John Wiley and Sons, New York, 1963.
7. T. Allen, Particle Size Measurement, Wiley Interscience, New York, 1981.
8. Modern Methods of Particle Size Analysis, Ed. H. Barth, Wiley Interscience, New York, 1985.
9. R.M. Fulrath and J.A. Pask (Eds.), Ceramic Microstructures, Robert E. Krieger Publishing Co., Huntington, New York, 1968.

10. S. Lowell and J.E. Shields, Powder Surface area and Porosity, Chapman and Hall, New York, 1984.
11. C. Orr Jr., Physical characterization techniques for particles, Chapter 6 in ceramic processing before firing, Eds. G.Y. Onada Jr. and L.L. Hench, Wiley Interscience, New York, 1978.
12. B. Brunauer, P.H. Emmet and E. Teller, J. Am. Chem. Soc., 60, (1938) 309.

CHAPTER III

PREPARATION AND PROCESSING OF YBCO AND YBCO/Ag COMPOSITE BY CITRATE GEL ROUTE

This chapter describes the preparation of YBCO and YBCO/Ag composite by citrate gel technique. YBCO powder derived through this method is also processed through a cold extrusion technique.

III.1 Citrate gel route for the preparation of $\text{YBa}_2\text{Cu}_3\text{O}_{7-\delta}$ superconducting compound

III.1.i Introduction

This section presents the citrate precursor method for preparing YBCO. The solid precursor is prepared first by dehydration of gels from the reaction between a polyfunctional hydroxy carboxylic acid and a solution containing metal salt or salts such as nitrates. The solids thus obtained yield extremely fine oxide powder on decomposition by calcination. A variety of acids such as glycolic acid, malic acid, acrylic acid, lactic acid etc. can be successfully used as the hydroxy carboxylic acid. However, citric acid is studied widely(1). Since the appearance of the first paper(2) a number of single

This work was published

* *Journal of Materials Science Letters*, 8 (1989) 1313.

* *Superconductor Science and Technology*, 3 (1990) 73.

* *Journal of Materials Science Letters*, 9 (1990) 1000.

* *Journal of American Ceramic Society*, 73(10) (1990) 3100.

and binary ceramic oxides such as CoO , Cr_2O_3 , LaCoO_3 , SrTiO_3 , Y_2O_3 , Y_2AlO_4 (3,4) etc. have been prepared. In the present investigation, precursors of $\text{YBa}_2\text{Cu}_3\text{O}_{7-\delta}$ and $\text{Ag-YBa}_2\text{Cu}_3\text{O}_{7-\delta}$ superconducting compounds have been synthesized and then powders were heat treated under appropriate conditions to evaluate their superconducting properties.

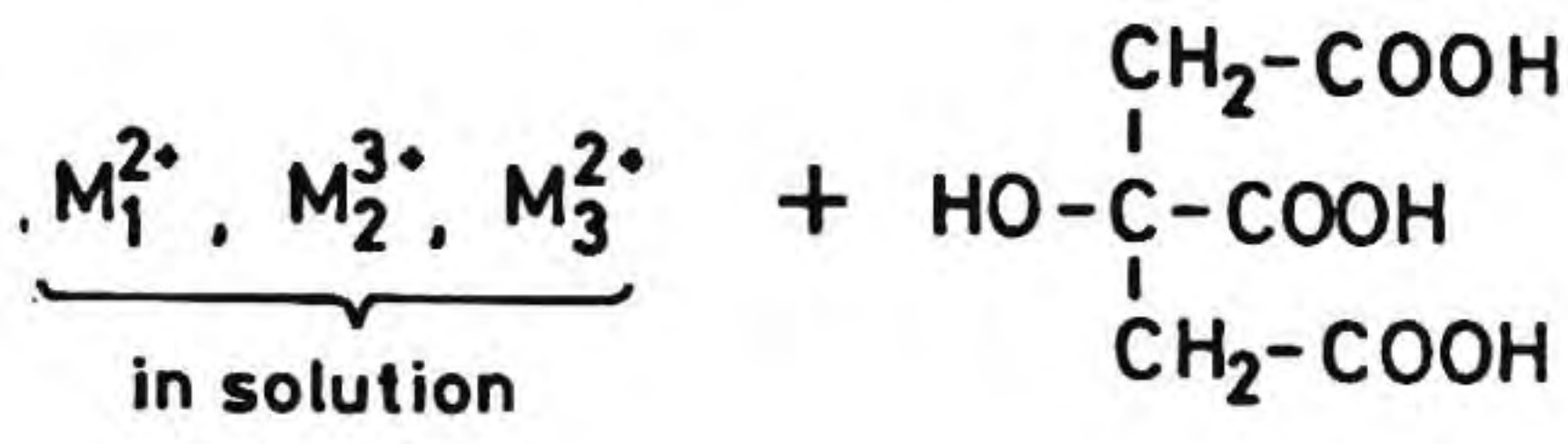
III.1.ii Chemistry of citrate gel

Citric acid has the formula and a functionality of 4, 3 arising from the $-\text{COOH}$ and one from the OH group. When mixed with cation solutions and on concentration, chelates are formed between metal ions facilitating atomic scale distribution of ions in polymer network structure as shown in Fig.III.1. Heating of this resin causes the breakdown of the polymer and charring occurs. On subsequent heating the cations oxidized to form the cation oxides at 500°C to 900°C

III.1.iii Experimental

In the present investigation citric acid is expected to chelate all the ions, and was selected according to the ratio
moles of x $1/3$ citric acid = sums of (moles of
 x $1/3$ Y nitrate + moles of x $1/2$ Cu nitrate +
moles of x $1/2$ Ba nitrate).

$\text{Y}(\text{NO}_3)_3 \cdot 5\text{H}_2\text{O}$ (Aldrich 99.9%), $\text{Ba}(\text{NO}_3)_2$ (CDH Chemical 99.5%), $\text{Cu}(\text{NO}_3)_2 \cdot 3\text{H}_2\text{O}$ (Glaxo 99%), citric acid (CDH Chemical 99%) were used in the present study. In a typical experiment,



- ① Solution
- ② Concentration
- ③ Gelation

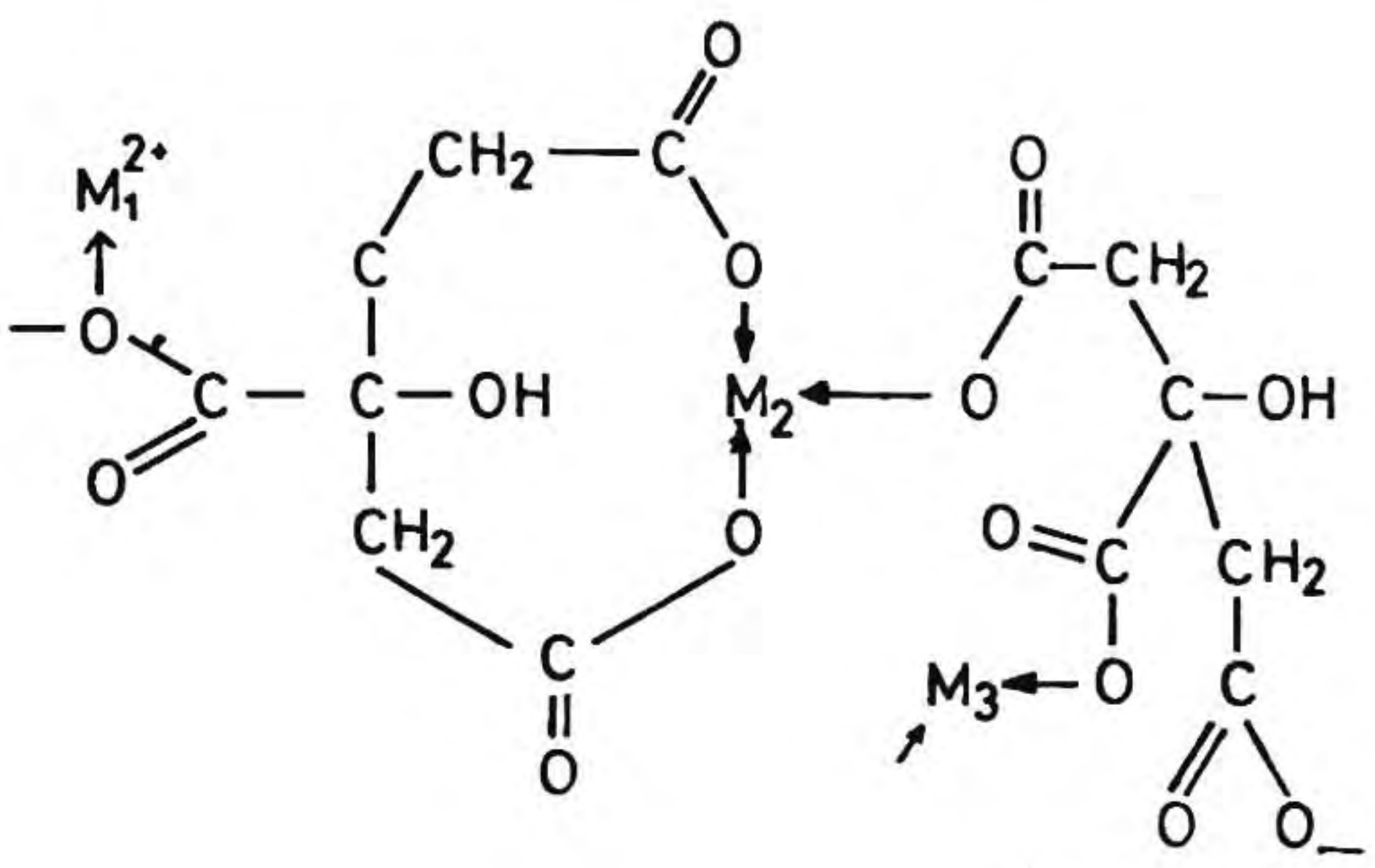


Fig. III.1 Citrate gel network

nitrates of Y, Ba and Cu dissolved [(1:2:3 ratio) 4.54 gm of yttrium nitrate + 6.48 gm of barium nitrate + 8.98 gm of copper nitrate] in minimum amount of distilled water in a 1 litre beaker. To this solution calculated quantity of citric acid was added(11 gms). The solution was kept over a hot plate at 100°C and concentrated under vigorous stirring. A viscous blue green resin was obtained. This resin kept in an air oven at 90°C for 12 hours resulted in a rigid green gel. The gel was decomposed at 250°C by introducing into a muffle furnace. The precursor powder obtained was heat treated at various temperatures to study the extent of reaction. The calcined precursor gave single phase YBCO powder when heat treated at 900°C for 12 hours. The powder compacted to rods of dimension 15 x 4 x 2 mm using uniaxial press in a stainless steel die. The green rods were sintered at 940°C in oxygen (1 atmos) for 12 hours. Such sintered pellets were used for the electrical measurement purpose.

III.1.iv Methods

Chemical analysis, bulk and tap densities, particle size analysis, TGA/DTA, scanning electron microscopy and surface area were obtained as described in chapter II. The XRD patterns were taken as described in chapter II. The identification of the phases were done using ASTM card index of powder diffraction patterns and also from available literature(5).

III.1.iv.a Electrical measurements:

Resistivity measurements on samples in the form of rods and discs were done by d.c four probe method in van der Pauw geometry(6), which is very commonly used in resistivity measurements on solids. Van der Pauw reported the resistivity of a flat lamella of any shape, free of holes can be measured by the following technique.

Assure the four silver contacts M, N, O and P at arbitrary places on the periphery of the sample (Fig.III.2a). Current i_{MN} is applied to contact M and taken off at contact N. The potential difference $V_p - V_o$ measured between P and O is given by

$$R_{MN,OP} = \frac{V_p - V_o}{I_{MN}}$$

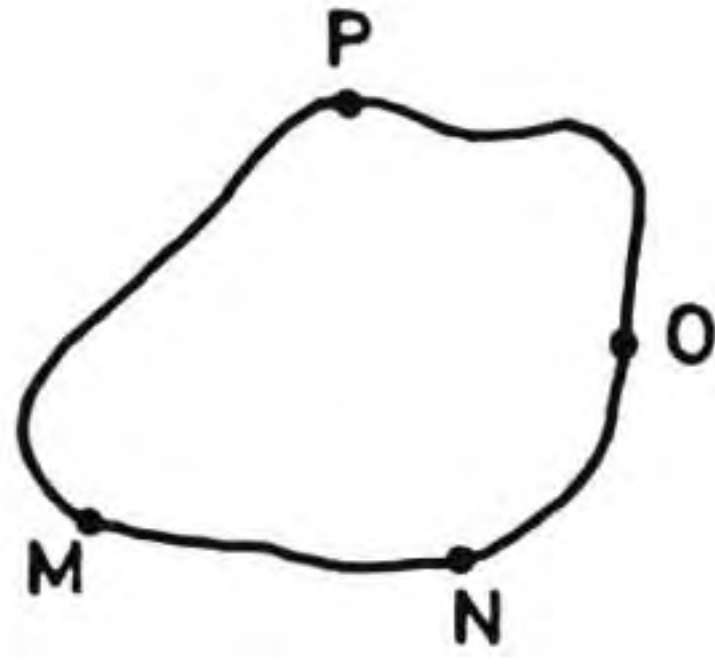
$$R_{NO,PM} = \frac{V_M - V_P}{I_{NO}}$$

from this resistivity can be calculated as

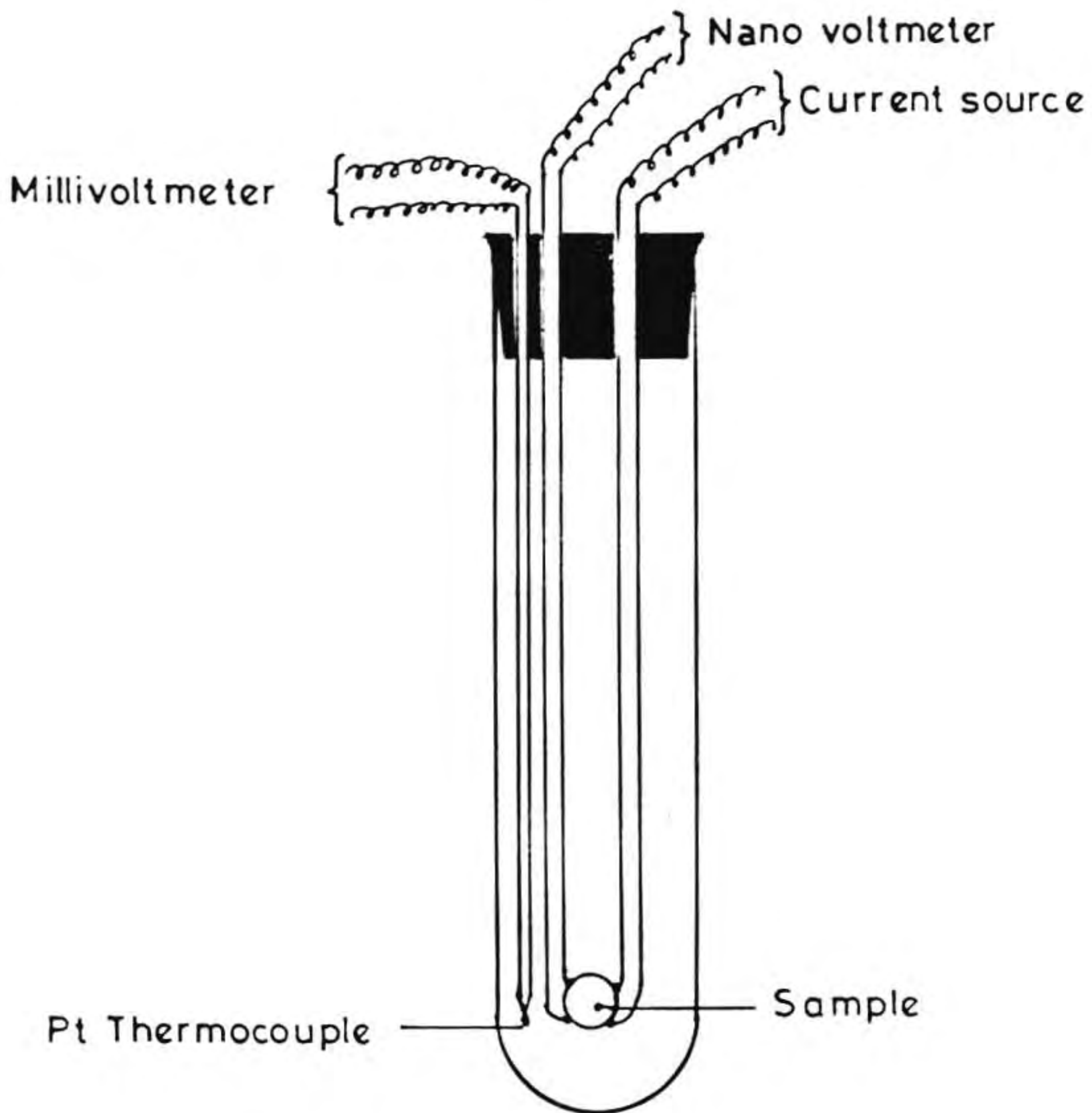
$$\rho = \frac{\pi d}{\ln 2} \frac{R_{MN,OP} + R_{NO,PM}}{2}$$

d is the thickness of the sample

Measurement set up used in the study is given in Fig.III.2b. To measure resistivity a constant dc current (in the range 1-10 mA) was set through the contact from a Keithely



(a)



(b)

Fig. III.2 (a) Arbitrary shape of a sample with four contacts on the periphery as used in van der Paw's method (b) Resistivity measurement set up

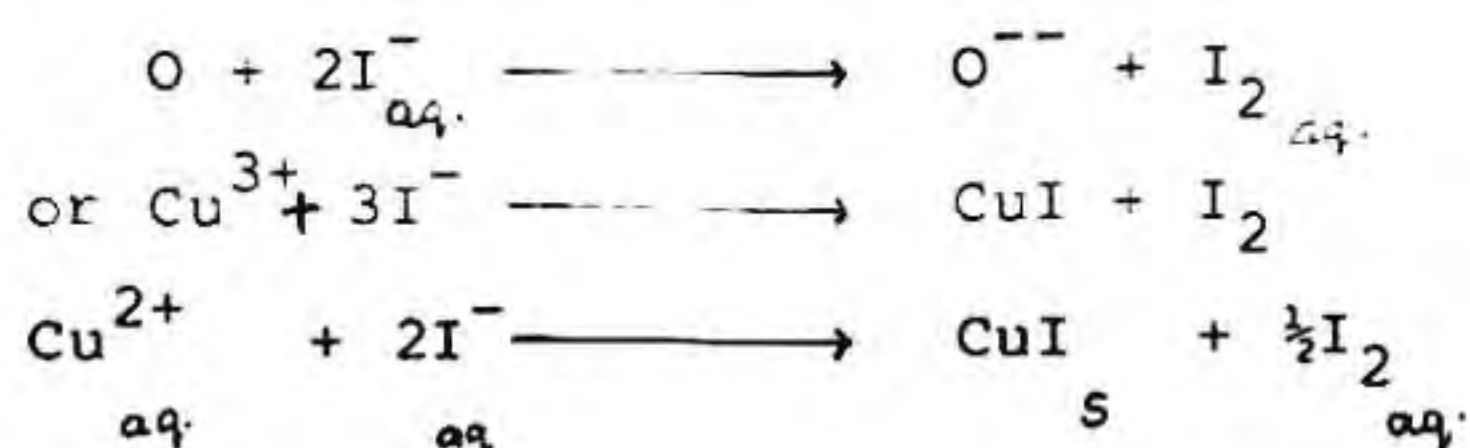
constant current source (model 200). The voltage drop was measured between the other two contacts with a Keithely 181 Nanovoltmeter after zeroing the nanovoltmeter. At the superconducting transition temperature T_c , the voltmeter reading suddenly dropped to zero while a current was passing through the sample.

To measure J_c (critical current density, A/cm^2) in the bulk samples the above experimental set up was modified according to Fig.III.2c. The current was increased till there is a measurable (in the nanovolt range) voltage develops. This current is the critical current and from the dimension J_c , critical current density A/cm^2 was calculated. The whole set up was immersed in liquid nitrogen while measuring the above readings.

III.1.iv.b Determination of oxygen content in $YBa_2Cu_3O_{7-\delta}$
by iodometric titration method:

The techniques have developed by Harris and coworkers(7) and employed by others(8,9).

The Cu^{2+} and excess oxygen content (Cu^{3+}) of $YBa_2Cu_3O_{7-\delta}$ were measured as follows:



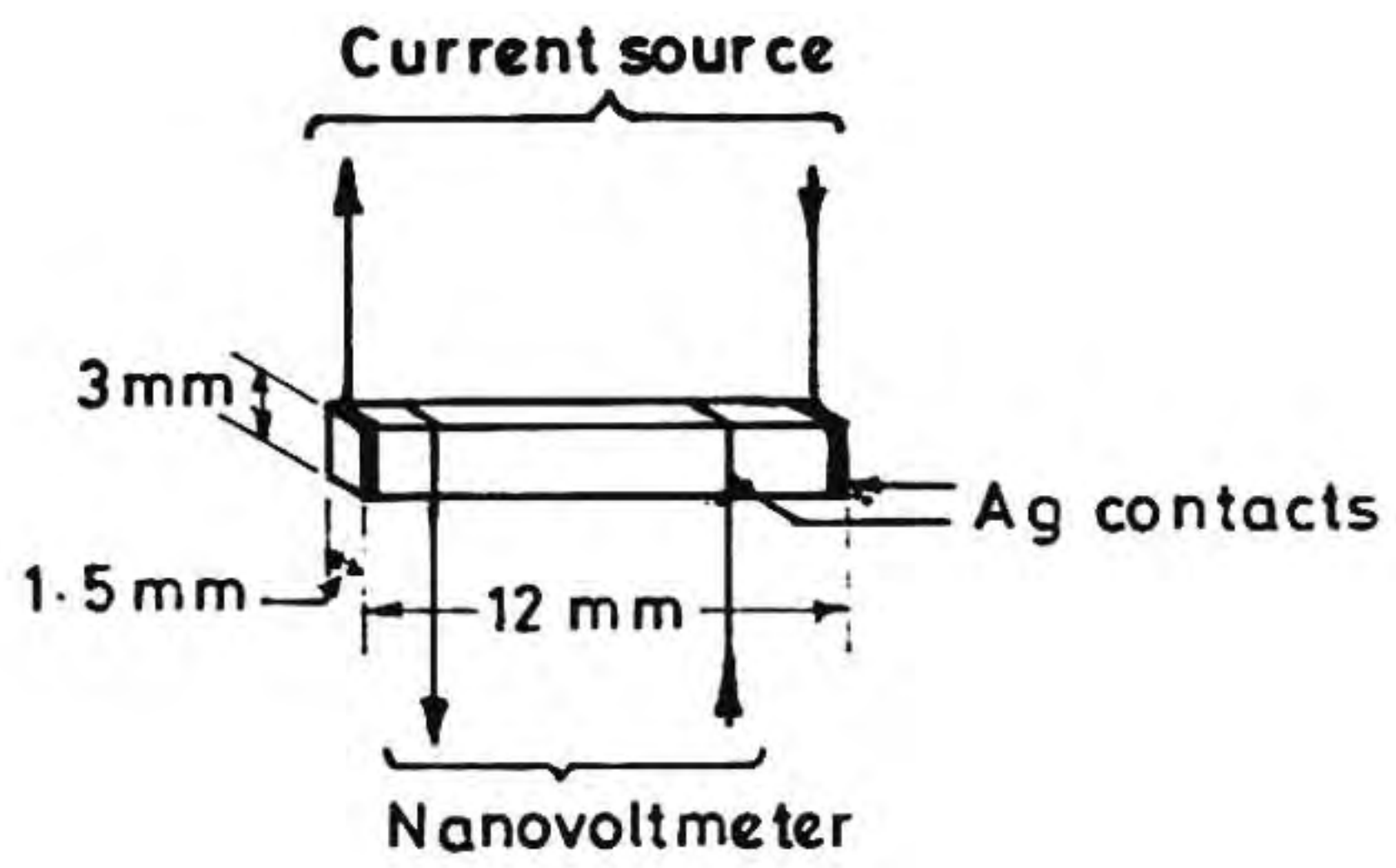
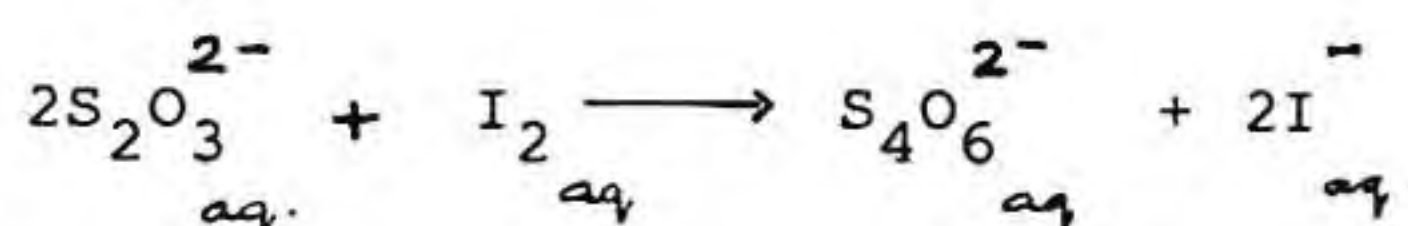


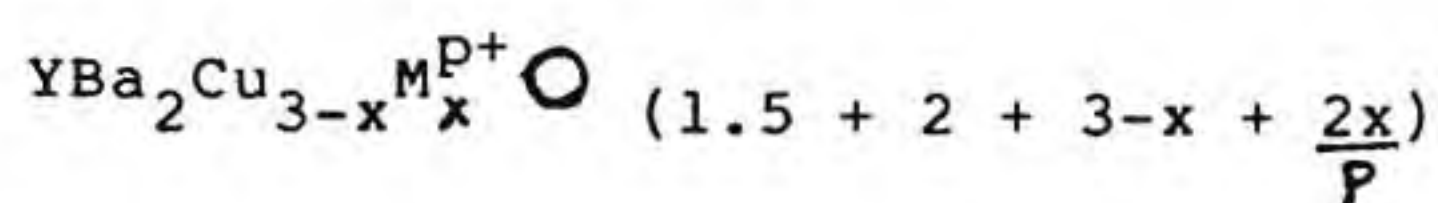
Fig. III.2 (c) Sample set up used for measuring critical current density (J_c)

For this (experiment A) approximately 25 gms of $\text{YBa}_2\text{Cu}_3\text{O}_{7-\delta}$ powder was dissolved in 7 ml of 1 M KI + 0.7 M HCl solution in nitrogen atmosphere. Cu^{3+} or excess oxygen behaves as a two electron oxidant and Cu^{2+} as one electron oxidant. The solution was diluted with 8 ml of water and the iodine liberated was titrated with sodium thiosulphate and starch as indicator. One mole of thiosulphate corresponds to one equivalent of oxidant in the original sample.



In experiment B, the same amount of $\text{YBa}_2\text{Cu}_3\text{O}_{7-\delta}$ powder was dissolved in 1 M HCl in air and boiled gently for 10 minutes. By this, excess Cu^{3+} or excess oxygen in $\text{YBa}_2\text{Cu}_3\text{O}_{7-\delta}$ react with acid to liberate oxygen and is reduced to Cu^{2+} or O^{2-} . This is followed by the iodometric titration as above. From the fraction as in the trivalent state is $A-B/A$ where A and B represent the moles of titrant required per gram of sample in experiments A and B.

Assuming the formula as:



the oxygen content was calculated from the difference in the amount of copper calculated by the formula and the amount obtained by iodometric titration.

III.1.v Results and discussion

The particle size analysis of the YBCO powder calcined at 900°C for 12 hours is given in Fig.III.3. The average particle size is 1.5 microns and maximum particle size is 10 microns. The tap density was measured to as 2.00 gm/cc and compacted density (green density) at a pressure of 100 MPa is 3.9 gm/cc.

The thermogravimetric scan in Fig.III.4 shows a three stage decomposition of the gel. The first stage below 150°C is mainly due to the adsorbed water and free nitrates in the gel network. In the second stage, the citrate gel network collapses with the decomposition of citrates and nitrates resulting in oxides of yttrium and copper and carbonate of barium. This is a major weight loss occurring in the range 150-300°C, which accounts 40% for the total wt of the gel. The exothermic peaks (DTA) at 181°C, 237°C, 280°C and 386°C is due to reactions involving decomposition of citrates, formation of barium carbonate and free carbon which will further decompose to carbon dioxide at around 600°C. Hence it is found that the major decomposition reactions are occurring at temperatures less than 500°C, in accordance with observation of Chu et.al.(10). In the last stage free carbon and barium carbonate decomposes due to the ternary phase formation with Y and Cu.

In Fig.III.5 the XRD patterns of the citrate gel heated at various temperatures at a rate of 120°C per hour are given.

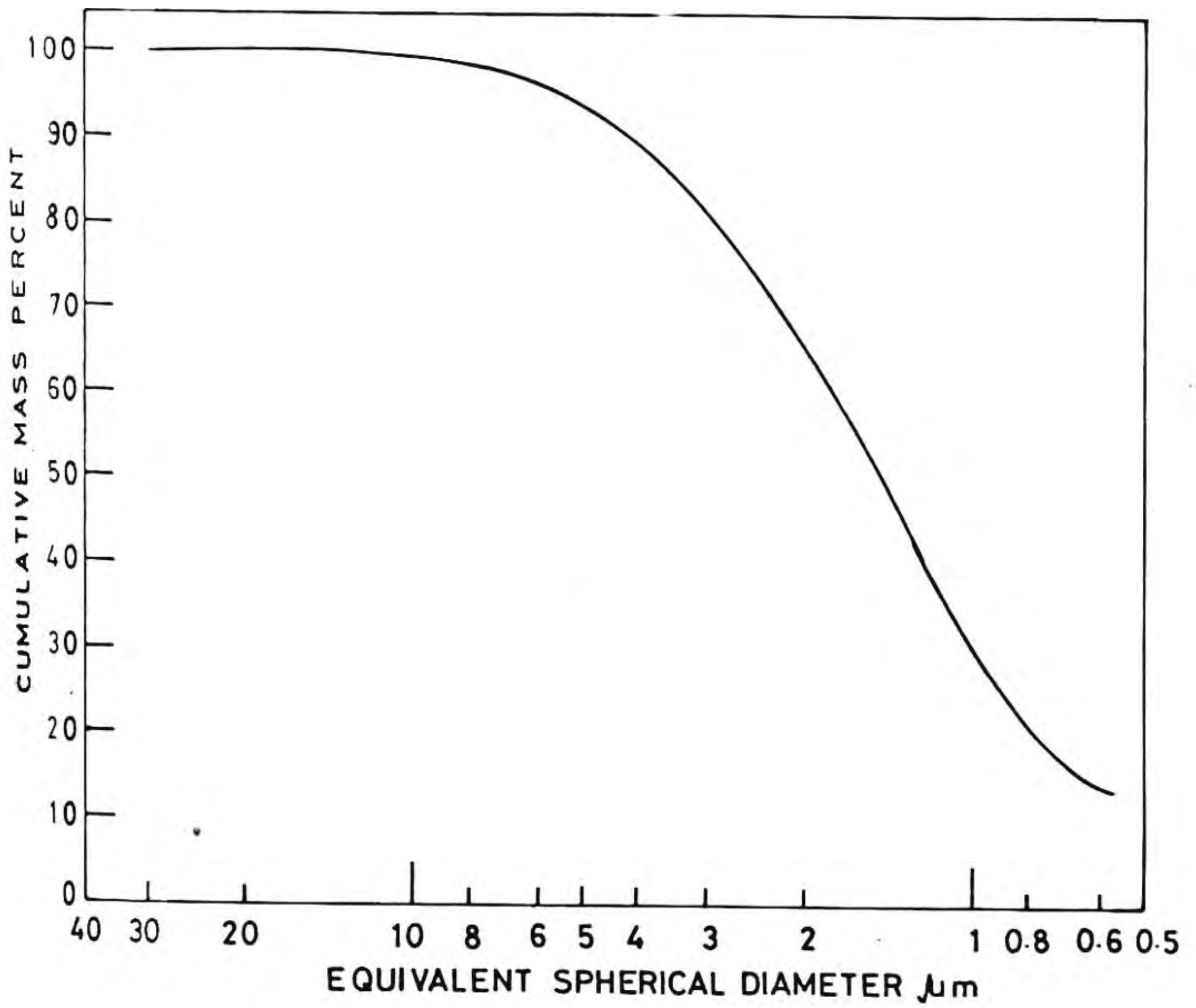


Fig. III.3 Particle size distribution curve of $\text{YBa}_2\text{Cu}_3\text{O}_{7-\delta}$ derived through citrate gel route

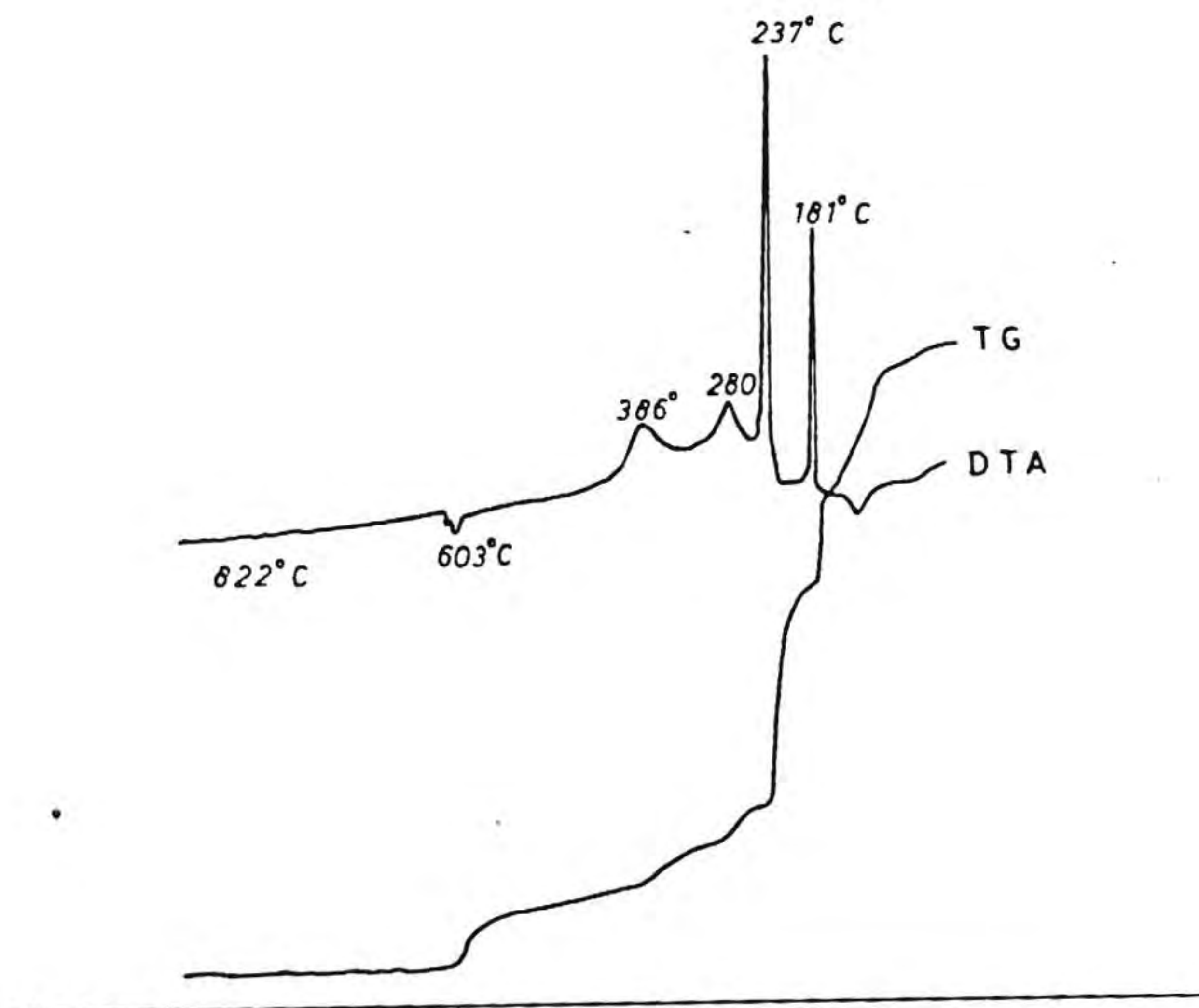


Fig. III.4 TG and DTA curves of citrate precursor

The high hygroscopic nature of citrate gel made it difficult to take the XRD pattern. Still, the XRD shows amorphous to Xrays with presence of barium nitrate. In Fig.III.5a, the gel heated at 250°C is given. It clearly shows the peaks corresponding to the copper oxide ($2\theta=35.5, 38.7$), yttrium oxide ($2\theta=29.1, 33.7$) and barium carbonate ($2\theta=24.09, 42.5$). Unlike in many other reported literatures, there is no major peak assigned to barium nitrate is seen ($2\theta=18.9, 37.1$). When the gel is heated at 550°C, additional peaks of $BaCuO_2$ and Ba_2CuO_3 are coming up. It is interesting to note that even though the intensity is very low there is a peak at $2\theta= 32.8$ which shows the presence of 123 phase. When the gel is heated at 850°C, the intensity of barium carbonate peak along with other predominant phases get reduced while 123 became the major phase. When the gel is heated at 900°C, 123 is the only phase that exists.

Figure III.6 shows the effect of temperature and rate of heating on the citrate gel in the range 600 and 700°C. The Figs.III.6a and III.6b are that of gel heated at 600° and 700°C at a rate of 50°C per hour. There is no appreciable difference between the two charts which resembles with one heated at 550°C in the previous figure (Fig.III.5b). Figure III.6c is the pattern of the citrate sample heated at 700°C at a rate of 25°C per hour. The pattern is similar to that of Fig.III.a.

The thermal changes were observed on heat treated gels by observing the morphology under the scanning electron microscope and are given in Figs. III.7a to c. The dried gel has

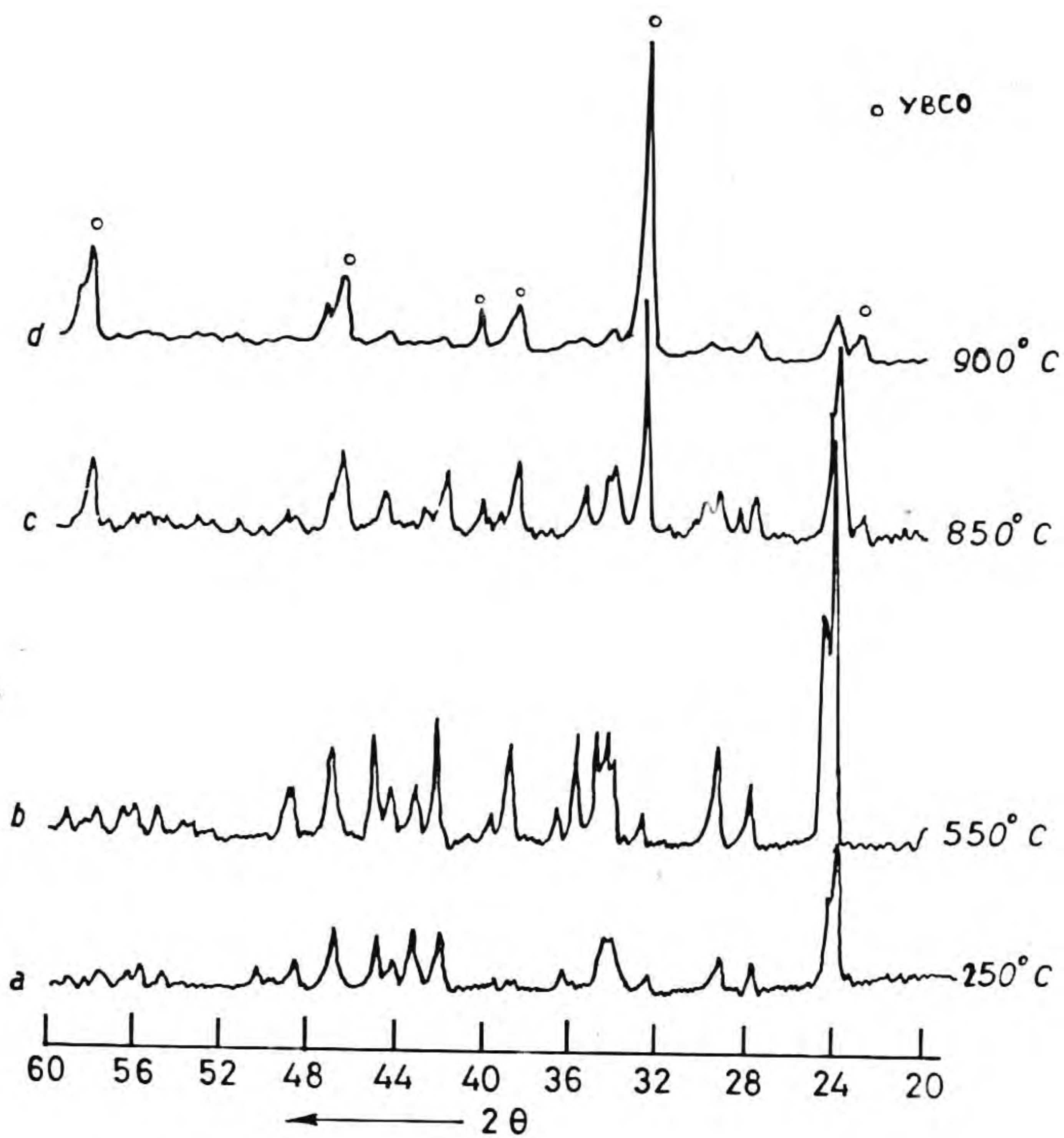


Fig. III.5 XRD patterns of citrate gel heated at various temperatures

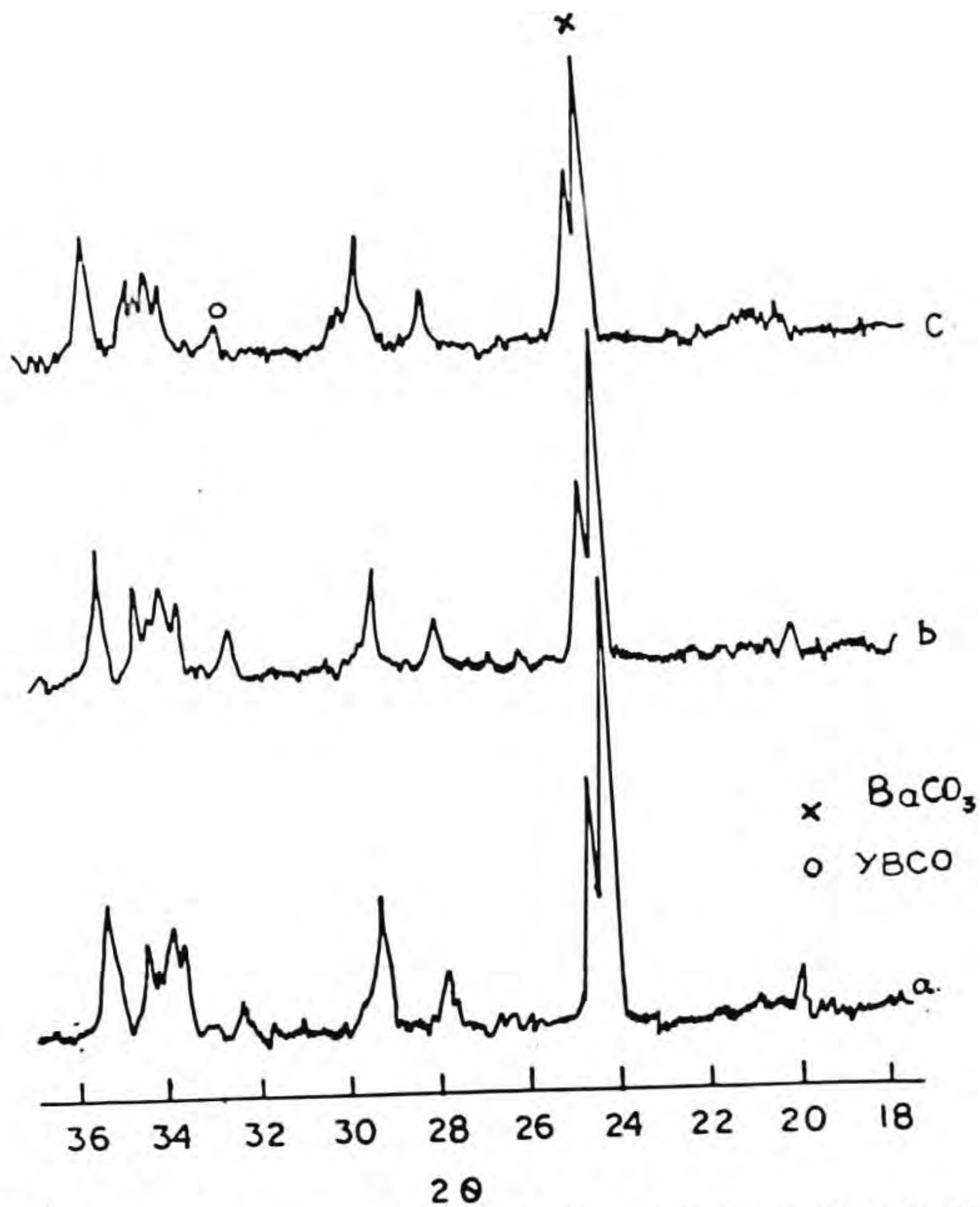
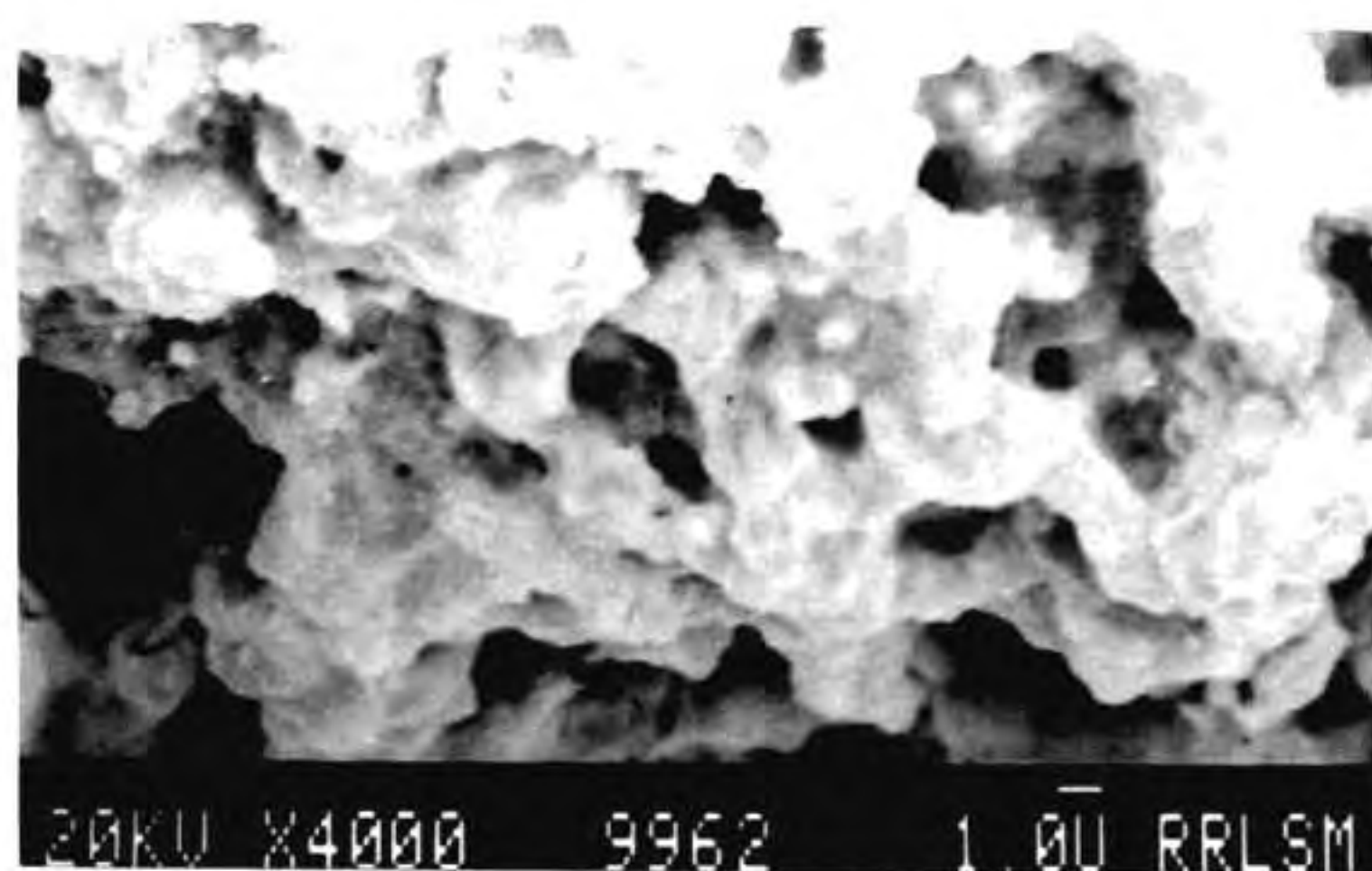


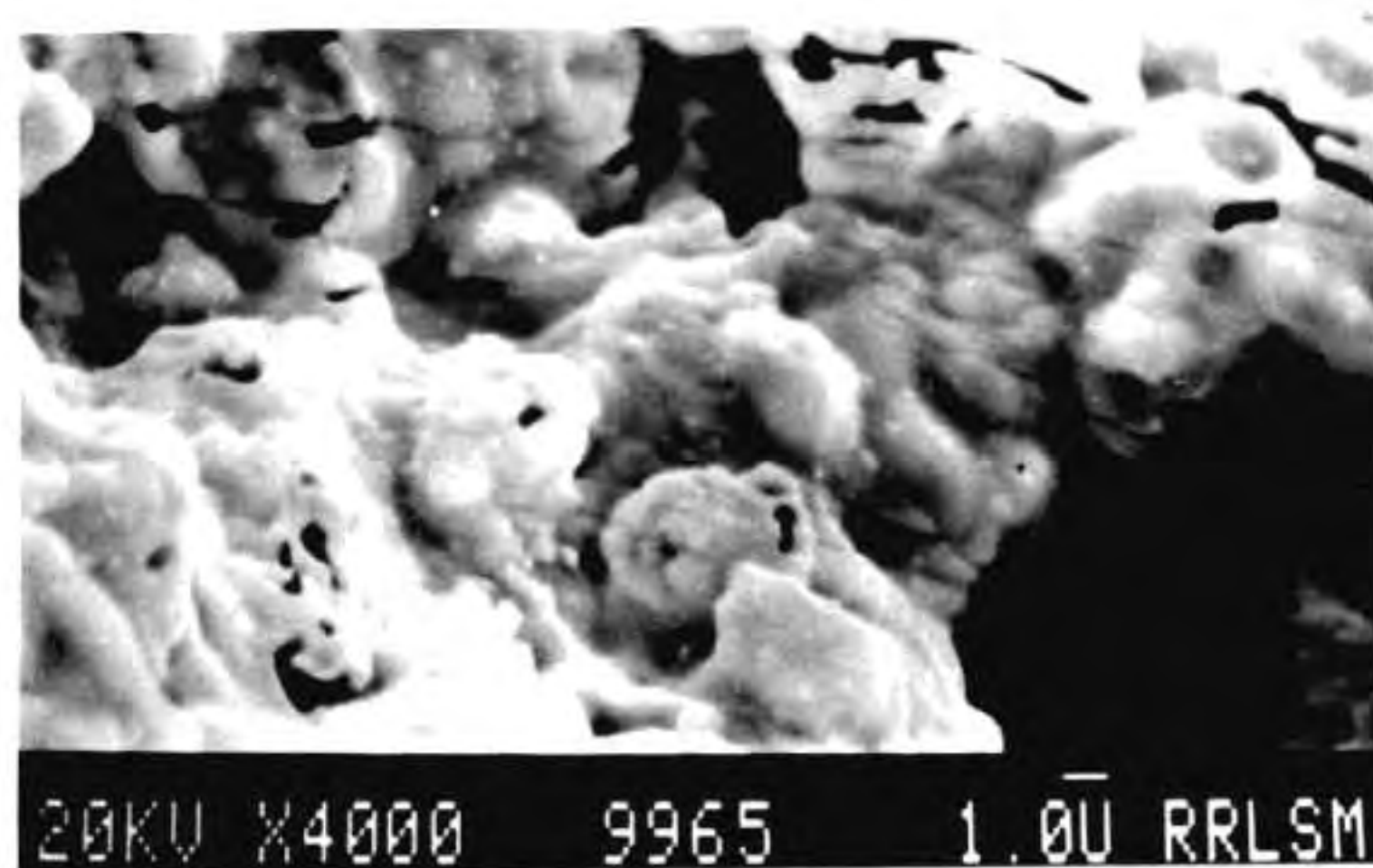
Fig. III.6 Citrate precursor heated in flowing oxygen at different temperature and heating rate.
 (a) 600°C at 50°/hr, (b) 700°C at 50°/hr and
 (c) 700°C at 25°/hr

a fluffy appearance (Fig.III.7a) with amorphous as well as crystalline phases. The crystalline phase could consist of particles less than one micron. The dark areas show the highly porous nature of the dried gel. Figure III.7b shows a partly decomposed and reacted morphology, much different from Fig.III.7a. Further, as a result of the thermal reactions, the gel has become coarse and finger like, and acicular formation has started showing up. On further heating the sample at 850°C, it is found that a purely crystalline morphology (Fig.III.7c) with rod like reacted single phase areas having aspect ratio 5 are being developed. Comparing the morphological features of the decomposed gel at 550°C and 850°C (Figs. III.7b and c), it could be inferred that the formation seems to have already started at 550°C.

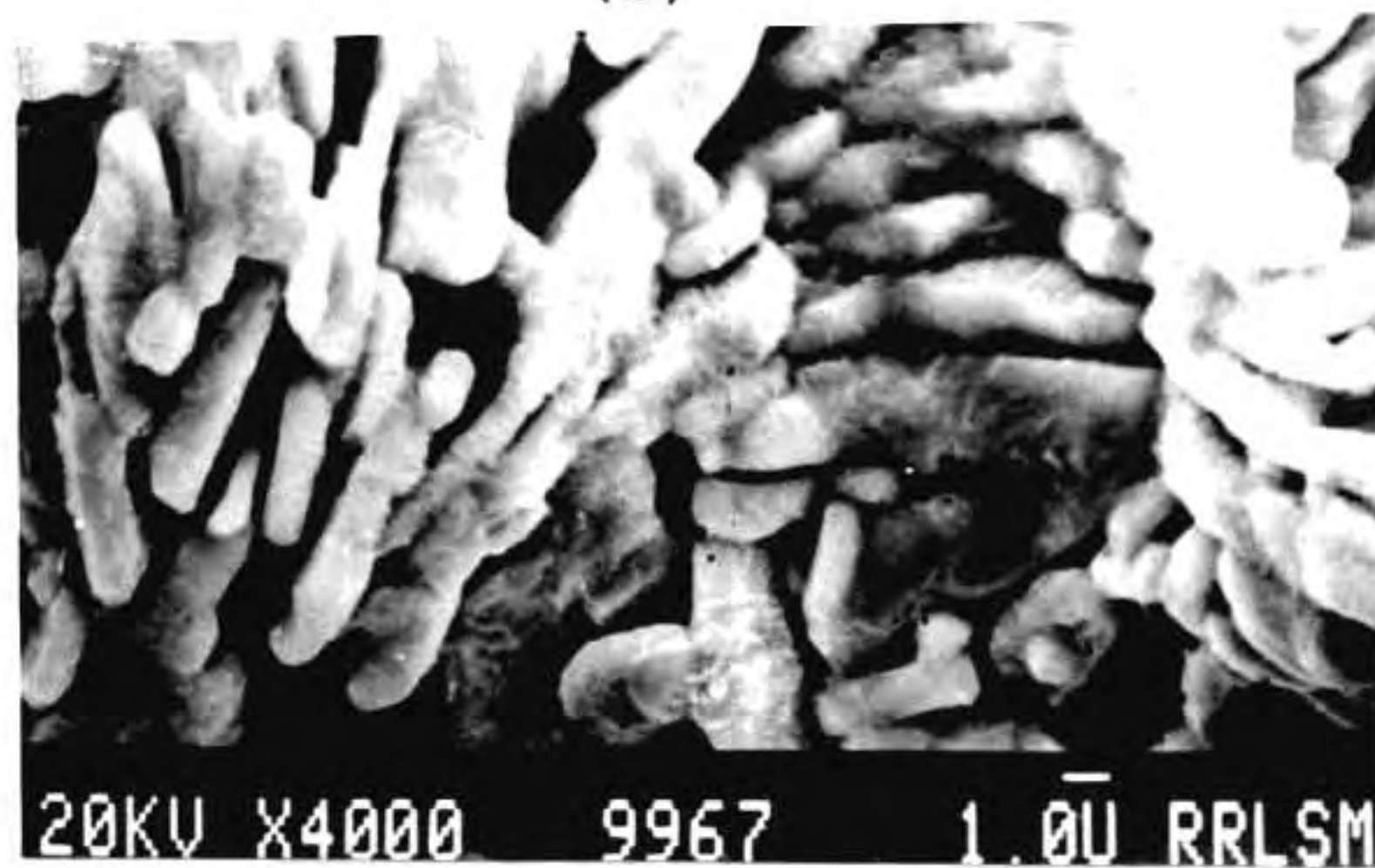
The gel in the as prepared condition was blue-green in colour. The citrates of yttrium and copper are quite easily formed in the acidic environment because of their formation constants while barium does not form citrate completely as (BaCit^{2-}) because of the lower formation constant(10) ($\log K_{\text{BaH}_2\text{Cit}} = 0.6$). This is the reason for the presence of barium nitrate in the undecomposed gel. Since the evaporation of solution is done with continuous stirring whatever barium nitrate formed should uniformly distribute in the gel matrix. So the fine crystallites will also decompose along with citrate gel. This reasons for the presence of very small amount of barium nitrate after decomposing at 250°C, while the



(a)



(b)



(c)

Fig. III.7 SEM pictures of citrate gel heated at various temperatures. (a) dried gel, (b) at 550°C and (c) at 850°C

decomposition temperature of free barium nitrate is well above 500°C. This is believed to be the initial formation of the superconducting phase since there is evidence of formation of the characteristic peak of superconducting phase at $2\theta=32.8^\circ$ in the XRD pattern. The decomposition of citrate gel is accompanied by the evolution of a large amount of oxides of carbon and nitrogen gases, barium ions converted itself into more stable barium carbonate. In the case of preparation of SrMnO_3 Sale et al.(11) observed a similar behaviour. Stable SrCO_3 was reported during the decomposition of citrate gel of Sr, Mn nitrates. A high temperature (1000°C) was necessitated for the completion of the reaction. In the present study, even though high concentration of BaCO_3 prevent the formation of $\text{YBa}_2\text{Cu}_3\text{O}_{3-\delta}$ at moderate temperatures, but the high uniformity in the precursor made it possible for the completion of reaction at 900°C within 10 hours. Also there is no need of any intermediate mixing during the calcination and subsequent solid state reaction.

The citrate gel was heated at 900°C for 12 hours to obtain tetragonal $\text{YBa}_2\text{Cu}_3\text{O}_{7-\delta}$ phase. The powder obtained was crushed in an agate mortar and made into rectangular rods of dimension 15 x 4 x 2 mm. The pressed samples sintered at 940°C for 12 hours in flowing oxygen. The samples were cooled down to room temperature at a rate of 75°C in the oxygen flowing furnace atmosphere. Figure III.8 shows the surface morphology of the sintered specimen. The characteristic shape of the

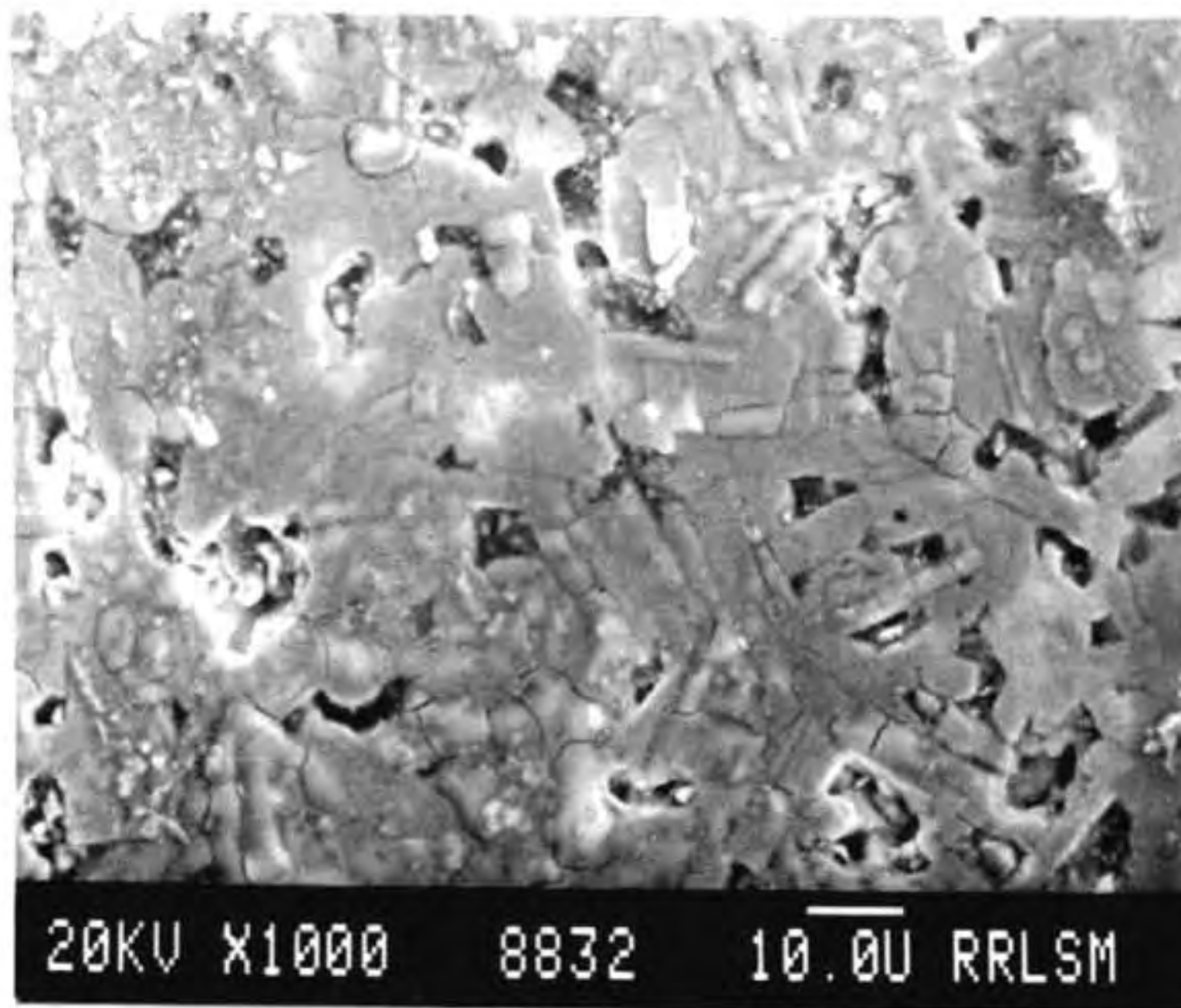


Fig. III.8 Surface morphology of sintered $\text{YBa}_2\text{Cu}_3\text{O}_{7-\delta}$ derived through citrate gel route

superconducting grains developed at 850°C are more or less retained. Since the powders could be compacted to a high green density, the sintered density is very high. Very little intergranular porosity is showing up.

The temperature dependence of the resistivity of the YBCO sample obtained using the above powder is shown in Fig.III.9. The resistance began to drop at 92 K and completely reduced to zero at 90 K. During the measurement, when the temperature was decreased or increased did not alter the resistivity behaviour, ie. no appreciable hysteresis. This could be explained by the fact that there is no undesirable non superconducting phases retained in the sintered specimen revealing the high homogeneity. From the figure it is also clear that above T_c , the sample shows good metallic character.

III.1.vi Conclusion

The citrate precursor route seems to be promising in the preparation of 123 superconducting ceramic material in view of the high order of homogeneity of the phases as well as the process simplicity. Information on thermal decomposition characteristics of the precursor gel is most important to understand the formation of the various phases formed during heat treatment. In the present study, although superconducting phase starts forming as early as at 550°C, rate and atmosphere of decomposition had no significant influence on the suppression of the formation of $BaCO_3$. Single phase

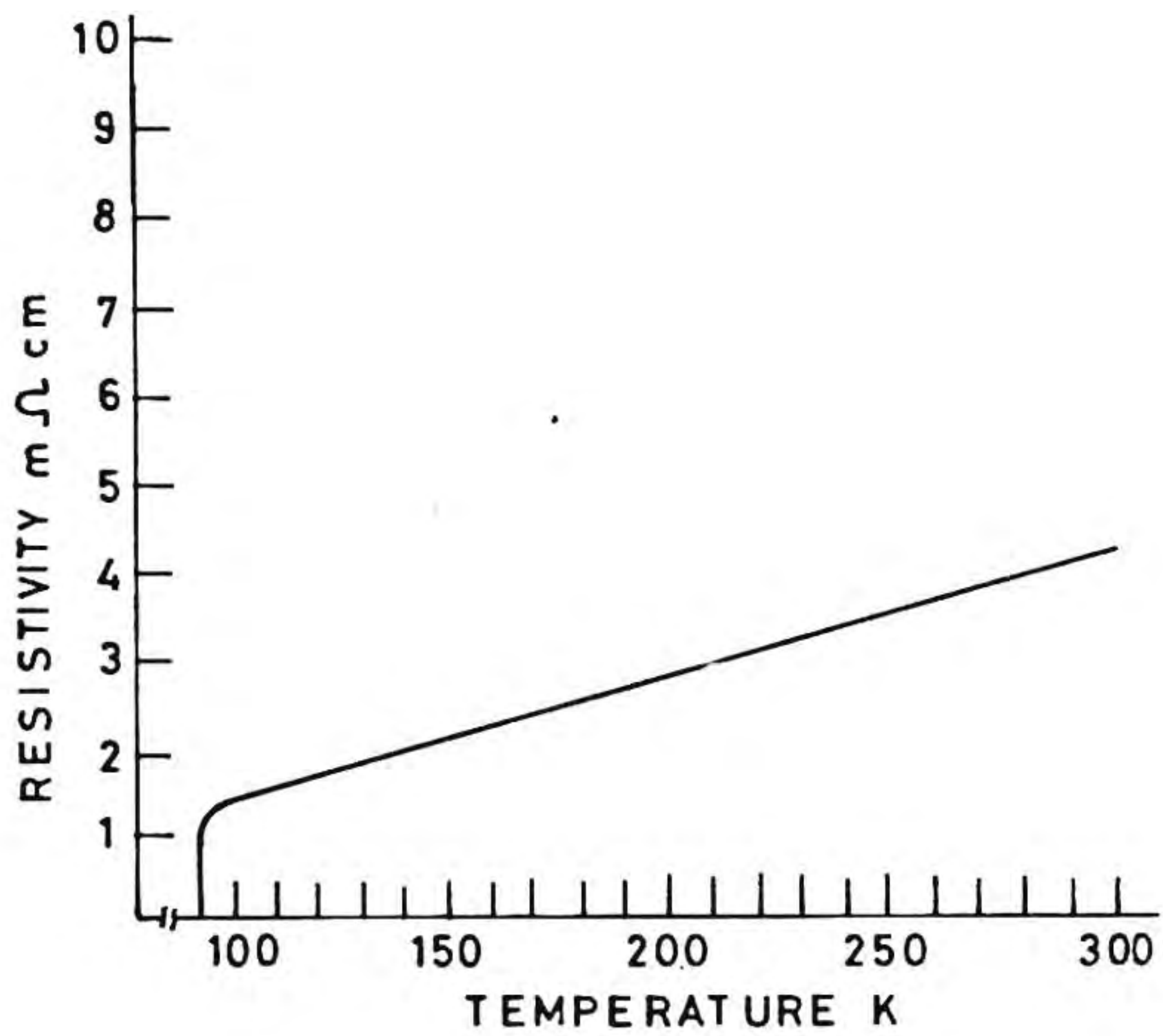


Fig. III.9 Temperature vs resistivity curve of sintered $\text{YBa}_2\text{Cu}_3\text{O}_{7-\delta}$

superconductors were prepared at 900°C showing good thermal stability, sinterability and small particle size.

III.2 Silver-YBCO composite derived from citrate precursor route

III.2.i Introduction

Like almost all ceramic materials, the very brittle behaviour and low strength of YBCO high T_c superconductors makes it difficult for them to meet the necessary engineering requirements. The usual sintering procedures(12) were not able to produce a fully densified product. While one approach has been to increase densification by selecting suitable powders(12), another was to choose appropriate processes such as sintering at near the melt temperatures(13) or hot forging(14). The problem of diffusion of oxygen in dense sintered YBCO is another aspect which required attention. Metal-ceramic composites in general are reported to possess increased ductility and strength, thus facilitating further processing(15). YBCO composites involving Sr, Ni and Cu prepared through the powder metallurgy route have shown certain superconductor and electrical characteristics(16). The addition of silver upto 2 at.% of copper in YBCO results in substitution of copper(17,18). However, Ag-YBCO composites upto 20 vol % of silver have been reported by mixing YBCO and silver powders(19). The uniform mixing of Ag and YBCO powder is

the primary requirement for obtaining a desirable composite. In the present study Ag-YBCO composite powders containing 5-75 wt% of silver have been prepared through citrate gel. The nature of distribution of phases in the sintered composites have also been studied in addition to the superconducting behaviour exhibited by such specimens. The important observation in this study is the fact that there is no need of any external oxygen annealing for getting superconducting sintered Ag-YBCO composite samples.

III.2.ii Experimental

III.2.ii.a Preparation of citrate gel and

Ag-YBCO precursor powder:

Details of chemicals, cupric nitrate, yttrium nitrate, barium nitrate and citric acid were presented in above section. Silver nitrate was AR grade Qualigens, Bombay.

The nitrates of Y, Ba, Cu and Ag were dissolved in double distilled water and stoichiometric amount of citric acid was added. The addition of silver nitrate was adjusted to maintain a 5 wt%, 20 wt%, 50 wt% and 75 wt% of Ag in the YBCO composite. The above clear blue solution was concentrated to a viscous state on a steam bath and in an air oven at 80°C for 24 hours to get a fluffy citrate gel. The gel was decomposed at 300°C in a muffle furnace in air. The powder was gently ground in an agate mortar. Powders containing lower silver content appears

as brownish black while the higher ones appeared as grey.

III.2.ii.b Sintering of composite powders:

The above powders were pressed to samples having 10 mm in diameter and 3 mm thickness in a steel die applying a uniaxial load. The pellets were pressed in different applied pressures of 50 MPa, 100 MPa and 150 MPa. Such pellets were sintered at 915°C for a period of 10 hours in a tube furnace equipped with a programmable temperature controller. The sintering was carried out in static air atmosphere by closing both ends of the furnace with ceramic wool Pads. The heating and cooling rate was 150°C per hour with an accuracy of $\pm 1^\circ\text{C}$. One sample (containing 20 % Ag) was quenched to room temperature from 915°C by taking the sample out using platinum tipped tongs into a copper plate. The sample attained ambient temperature within 10 minutes.

III.2.iii Results

III.2.iii.a Powder characteristics of composite precursors:

III.2.iii.a(i) Tap density:

Figure III.10 gives the tap density variation with amount of silver content in the precursor. Since this precursor powder is a composite powder of Ag and prereacted forms of Y, Ba and Cu citrates, the percentage theoretical density calculation is difficult in this case.

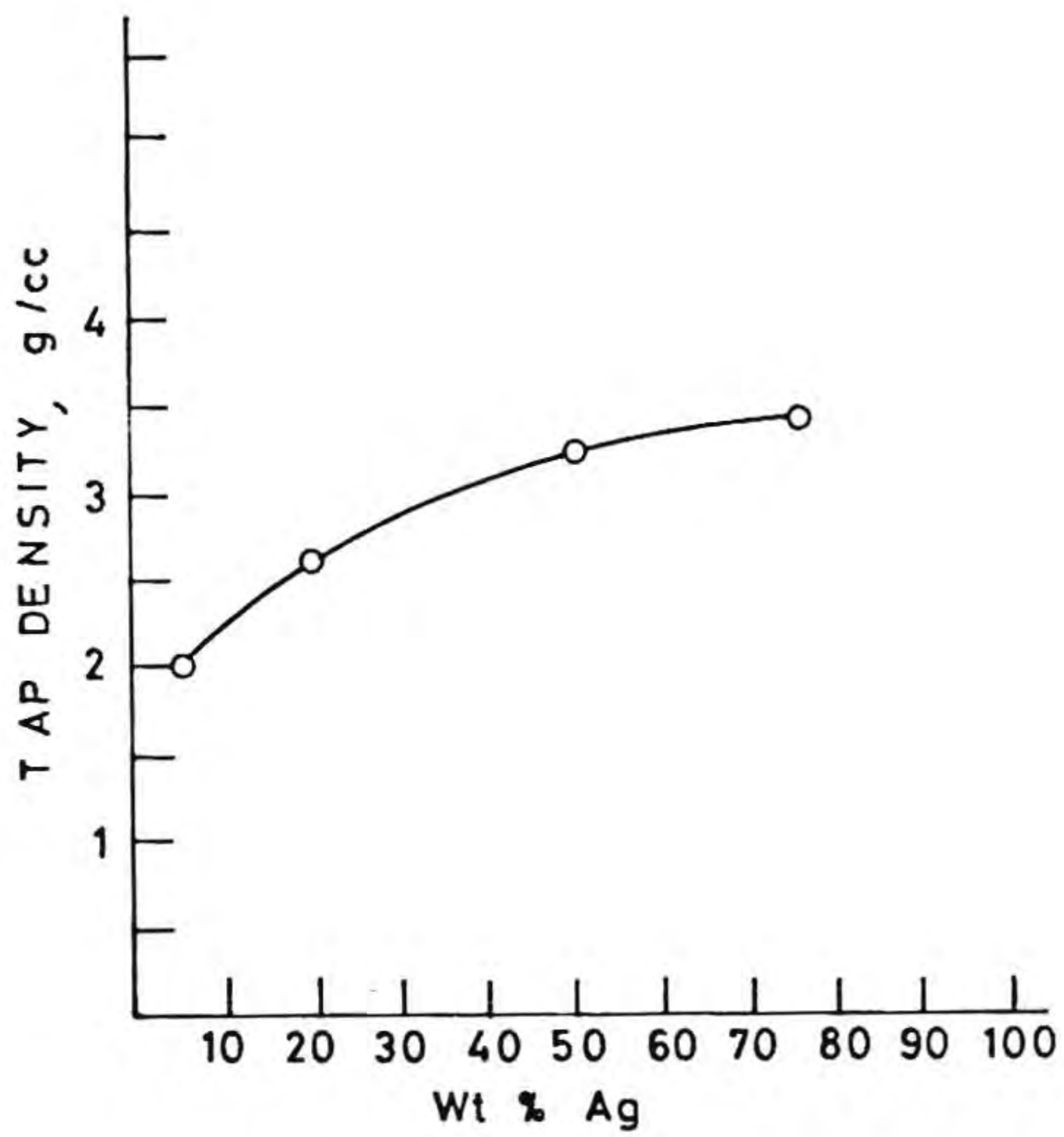


Fig. III.10 Tap density vs amount of silver content in the Ag/YBCO precursor powder

III.2.iii.a(ii) Green density:

Figure III.11 gives the results of green density of this precursor containing different amounts of silver. The density varies linearly with applied pressure in all the samples. Precursor containing higher silver content shows very high green density because of high rate of plastic deformation of the metallic silver in precursor powder. In the case of precursor containing less silver, the densification is rather low.

III.2.iii.a(iii) Particle size distribution:

Figure III.12 gives the particle size distribution of a representative sample ie. 20 wt% Ag. While the maximum particle size is in the order of 7 microns the average particle size is 2.8 microns.

III.2.iii.a(iv) SEM observation:

Figure III.13 shows the scanning microscopic picture of a precursor powder containing 20% Ag. The particles are uniform and spherical. The particle size is about 1.5 microns.

III.2.iii.a(v) X-ray diffraction studies:

Powder XRD patterns of the precursor powder (20 wt% Ag) is provided in Fig.III.14. The peaks corresponding to 2θ values 38.11 and 44.2 are for the metallic Ag, the values for CuO 35.5, 38.7 and 2θ value of BaCO_3 is 23.91 and $2\theta = 29.1$ and 33.7

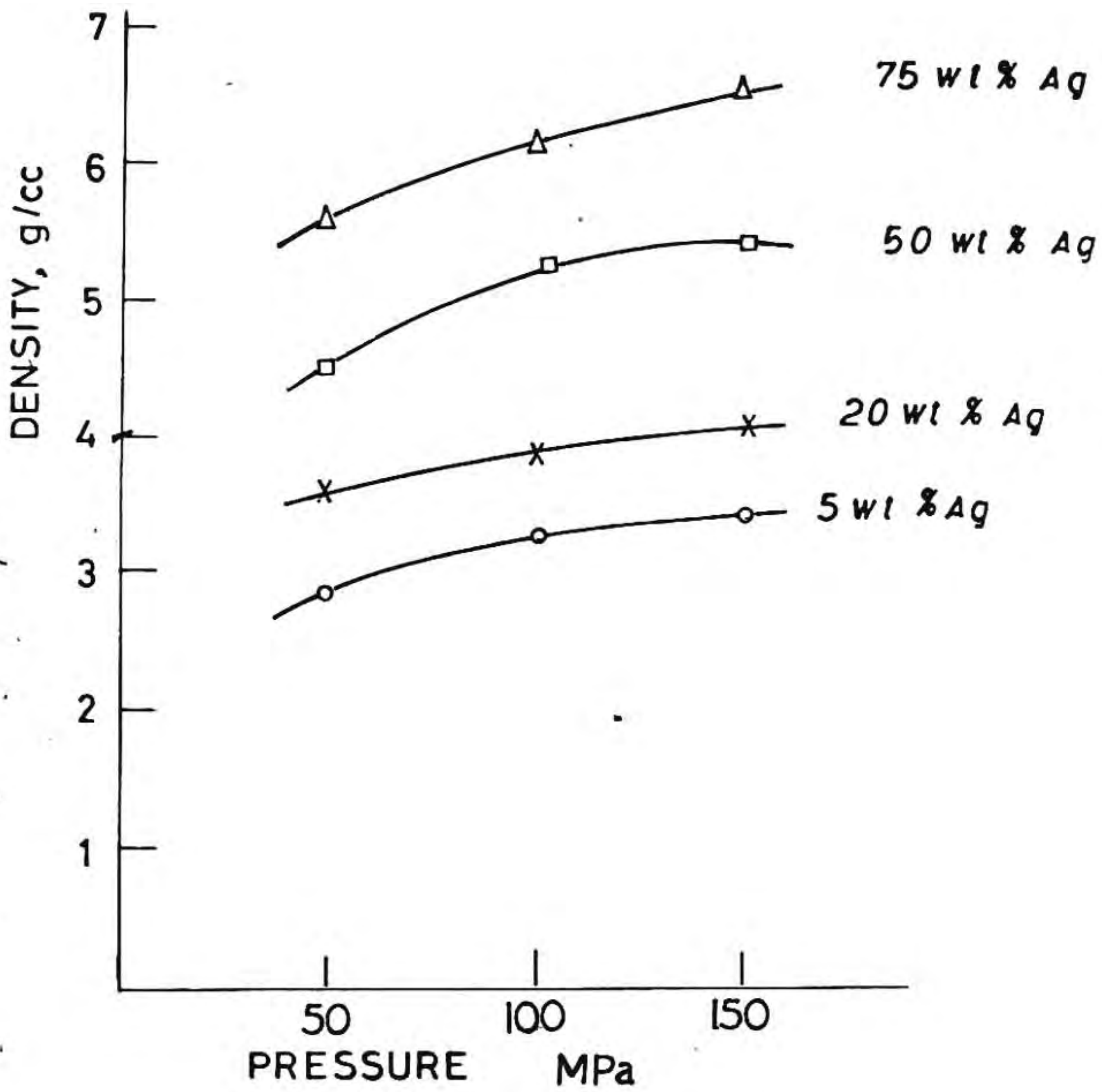


Fig. III.11 Green density variation with applied pressure for the Ag/YBCO composite powder containing various amounts of silver

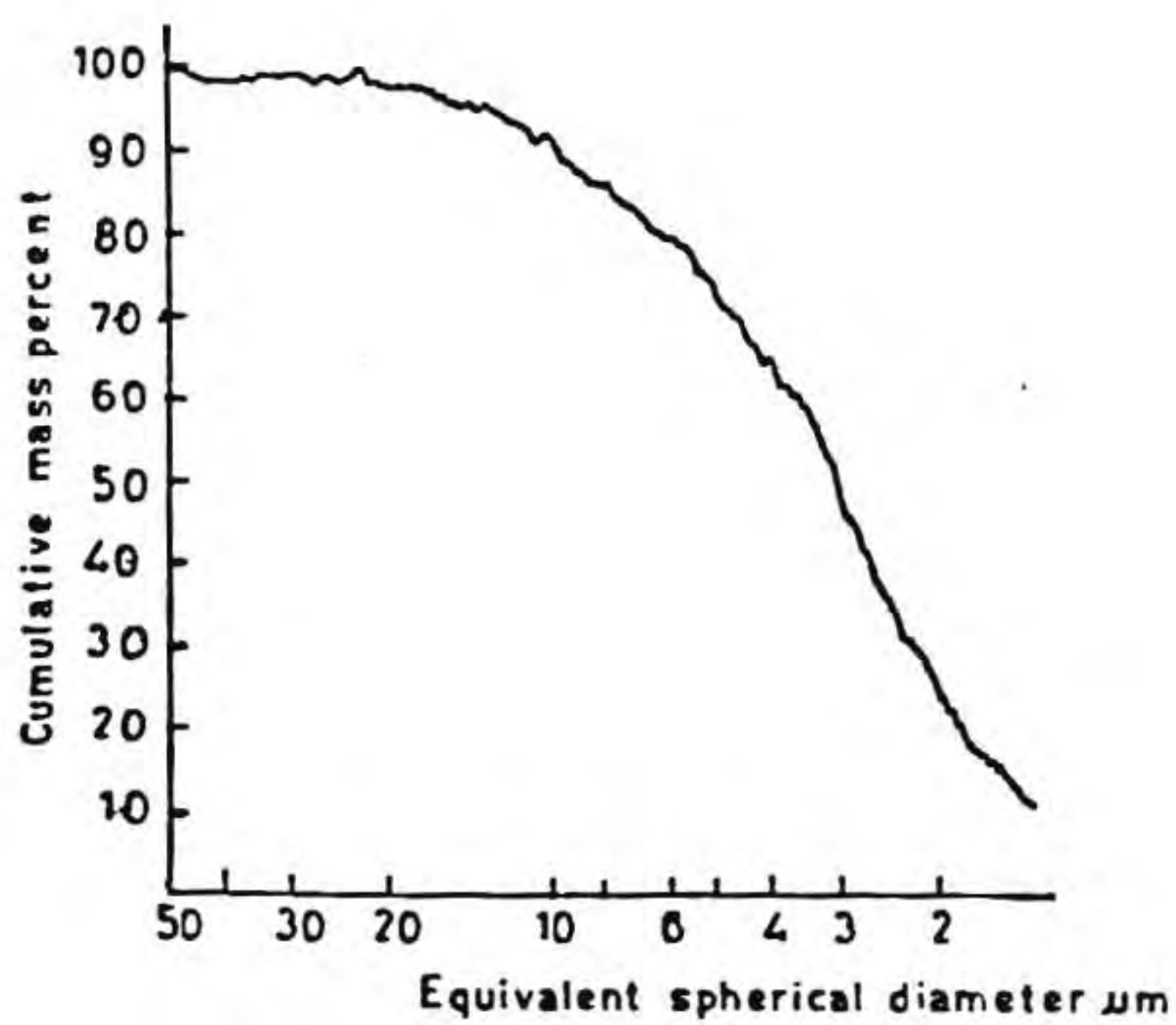


Fig. III.12 Particle size distribution of Ag/YBCO calcined powder

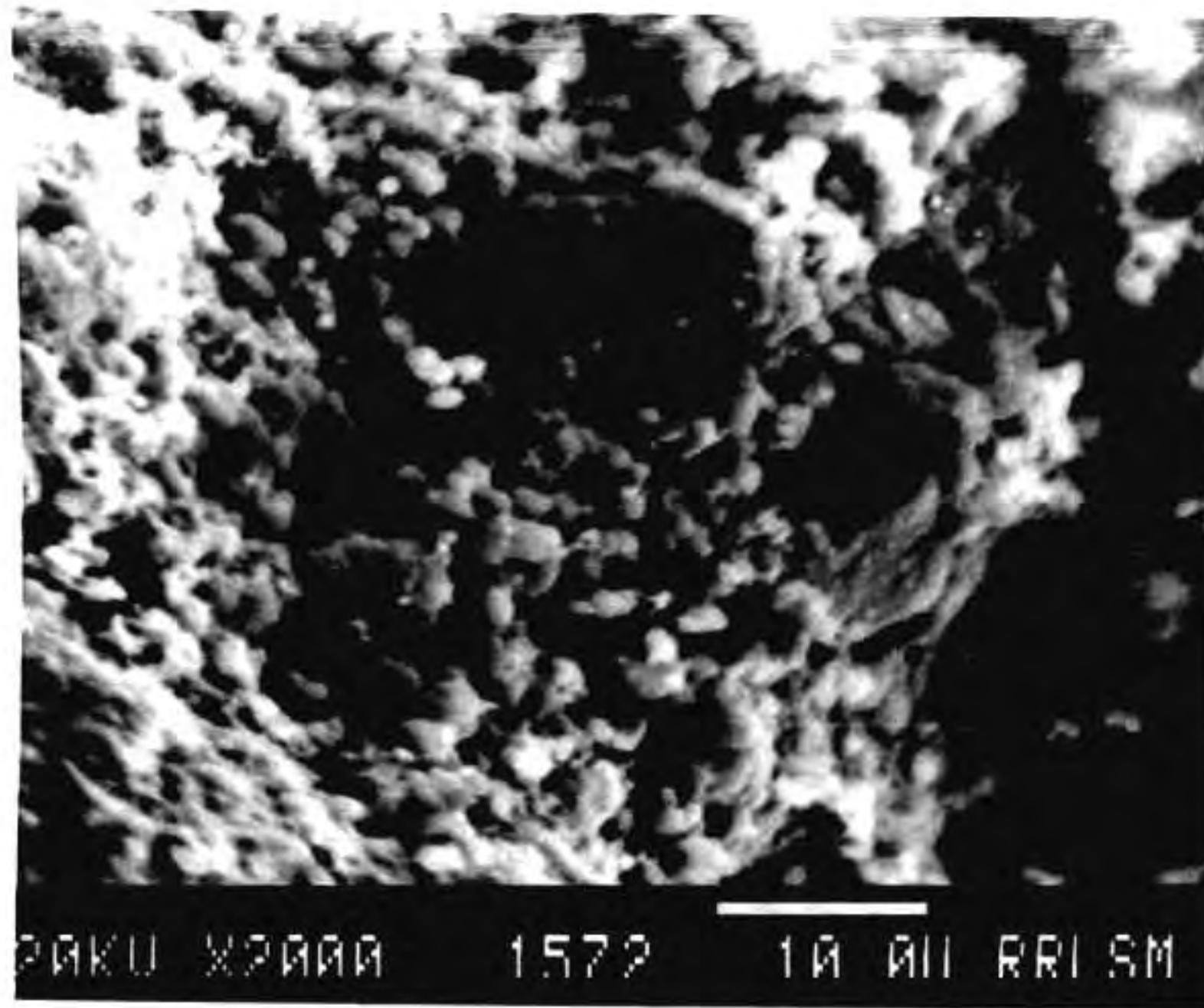


Fig. III.13 SEM picture of Ag-YBCO precursor powder
(20 wt% Ag/YBCO precursor)

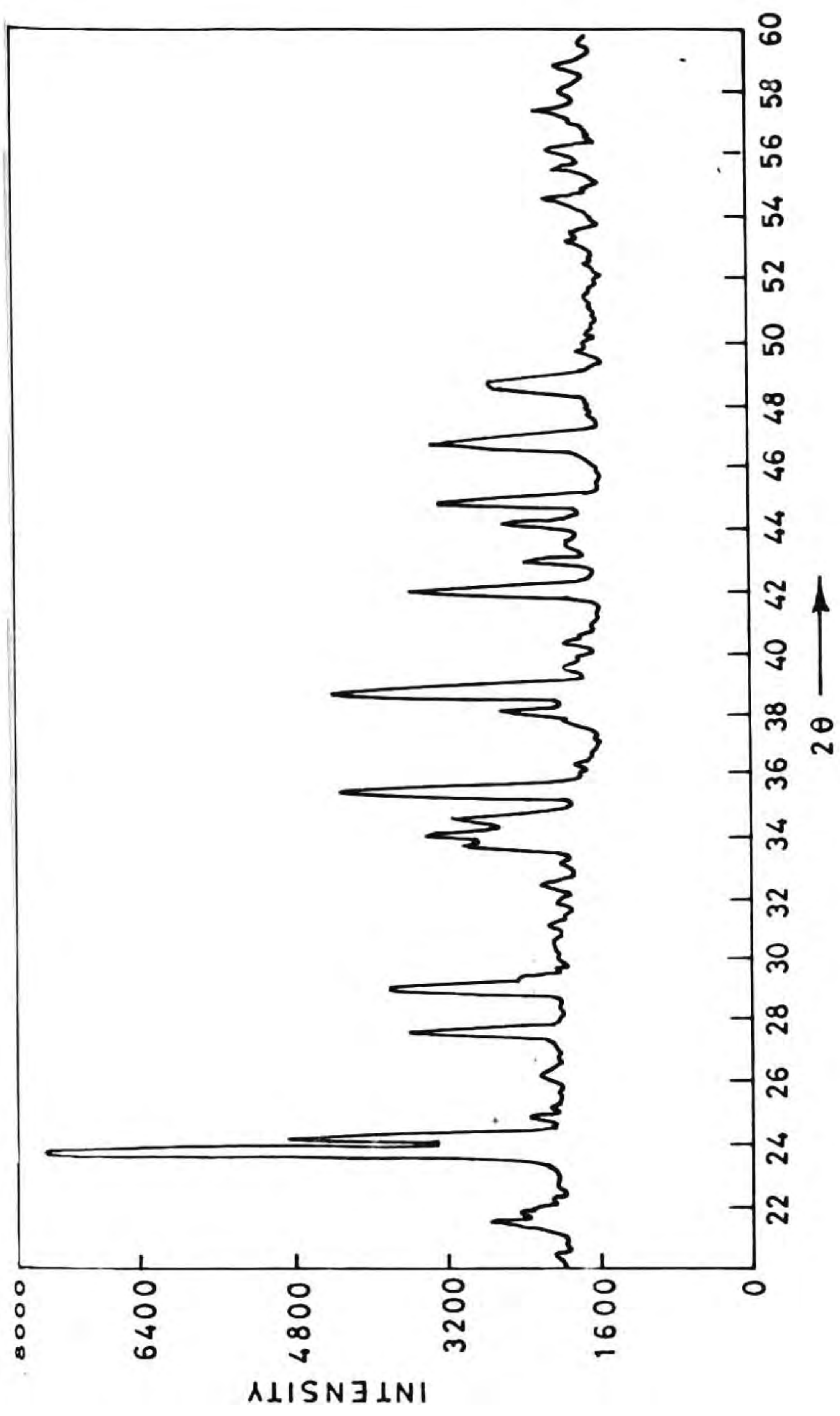


Fig. III.14 XRD pattern of Ag (20 wt%)/YBCO precursor gel after decomposition at 250°C

correspond to Y_2O_3 . Additional peaks corresponding to Ag_2O (14.94, 24.51) and $BaCuO_3$ (29.3, 40.09) are also observed. This shows that the precursor is an intimate mixture of all these phases. Table III.1 gives the various crystalline phases detected by X-ray diffraction technique in the products of decomposition of the citrate gel at various temperatures.

III.2.iii.b Properties of sintered Ag-YBCO composite:

III.2.iii.b(i) Sintered density:

Table III.2 gives the density values of the YBCO samples containing different amounts of silver. The sintered densities of the composite samples increased from 85% to 95% over an increase in silver from 5 to 50 wt%.

III.2.iii.b(ii) XRD observation:

Figure III.15 shows the sintered XRD pattern of the pure YBCO sample prepared through the same citrate gel method. This sample was also sintered along with the composite ones. All the peaks (32.8, 32.5, 46.6 etc) showed that the compound is a pure $YBa_2Cu_3O_{7-\delta}$ phase in the tetragonal phase. The other patterns for 5, 20 and 50 wt% Ag/YBCO composites are showing peaks for YBCO phase and Ag without the presence of any impurity phase. $2\theta = 38.11$ and 44.2 corresponds to metallic silver which is progressively increasing with amount of Ag in the composite, which is expected. The peaks correspond to YBCO ($2\theta = 32.8(100)$, $32.5(50)$) are clearly assigned for the orthorhombic phase.

Table III.1 Various phases detected using XRD during the heating of Ag/YBCO citrate gel

Temperature of heating	Phases detected
250°C	CuO, Y ₂ O ₃ , BaCO ₃ , BaCuO ₂ , Ag ₂ O, Ag
500°C	BaCuO ₂ , Y ₂ O ₃ , BaCO ₃ , Ag + minor amount of other phases
800°C	YBa ₂ Cu ₃ O _{7-δ} , Ag, Y ₂ BaCuO ₅ , BaCuO ₂ , BaCO ₃
900°C	YBa ₂ Cu ₃ O _{7-δ} , Ag

Table III.2 Tc and density values of Ag-YBCO composites
(compacted at a pressure of 150 MPa and
sintered at 915°C for 10 hours)

Sample	Tc K	% theoretical density of sintered samples
5 wt% Ag-YBCO	89.0	85
20 wt% Ag-YBCO	91.0	91
50 wt% Ag-YBCO	90.0	95
20 wt% Ag-YBCO (quenched)	87.5	91

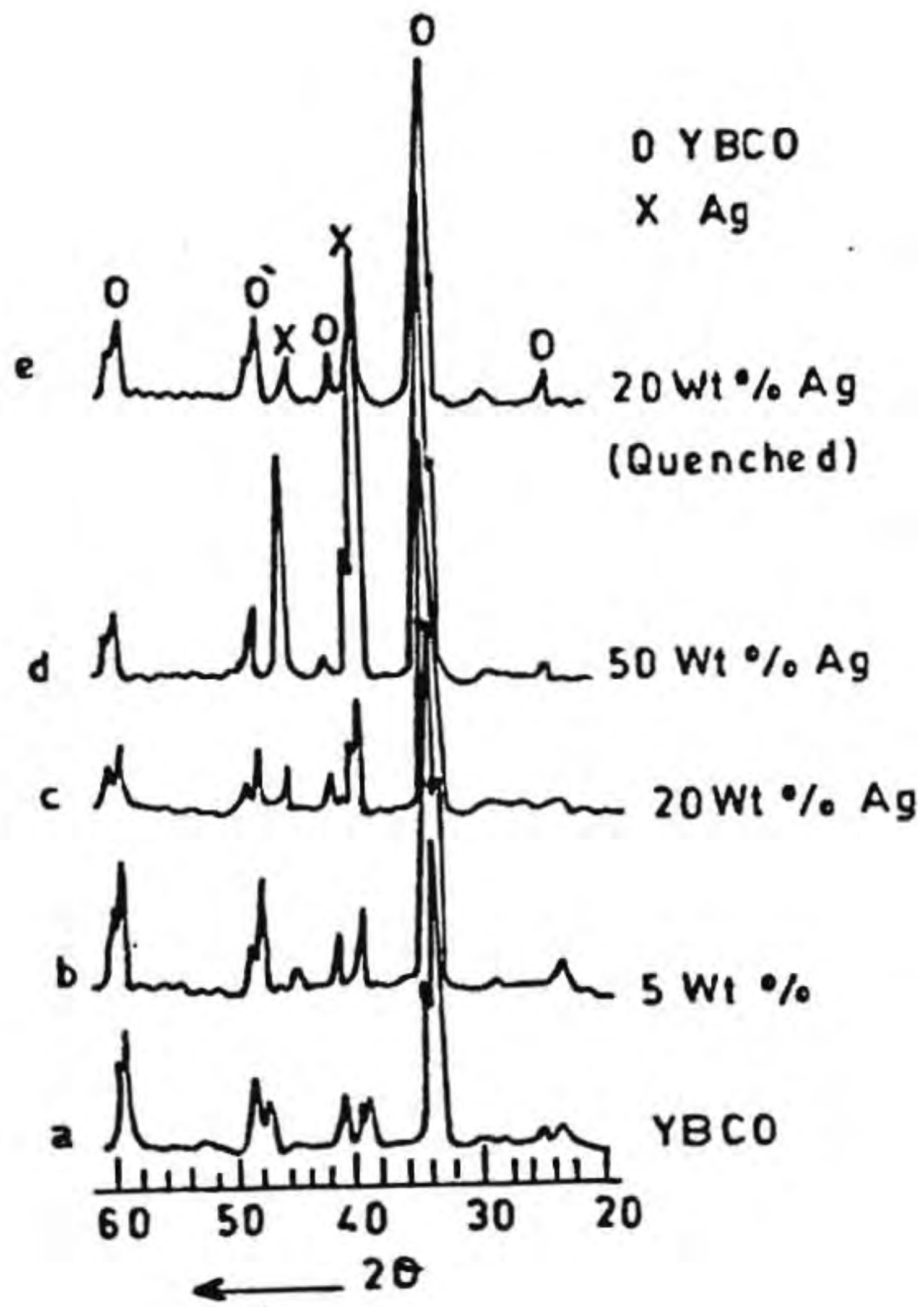


Fig. III.15 XRD pattern of sintered (a) YBCO, (b) 5 wt% Ag-YBCO, (c) 20 wt% Ag-YBCO, (d) 50 wt% Ag-YBCO and (e) 20 wt% Ag-YBCO (quenched)

III.2.iii.b(iii) Meissner effect:

All composites containing 5, 20, 50 and 75 wt% silver and the quenched sample (20 wt% Ag) are showing good Meissner repulsion. The pure YBCO kept along with the composites during the sintering did not show any Meissner effect.

III.2.iii.b(iv) Electrical measurements:

Figure III.16 shows the temperature against electrical resistivity of the Ag-YBCO composites. The bulk resistance of the material decreases as the amount of silver increases. The T_c is $90 \pm 1K$, in all the samples except the quenched sample.

III.2.iii.b(v) SEM analysis:

Figure III.17 shows the morphology of the citrate gel (20 wt% Ag) heat treated at $900^\circ C$ to see the phase formation from a homogeneous gel. The white particles are corresponding to metallic silver while the matrix composed of YBCO grains.

Figures III.18a, b and c are the fractographs of sintered superconducting composite. The transition from brittle fracture to ductile one with increase of silver is clearly visible. The silver is uniformly distributed between the grain boundaries of YBCO grains.

The EDAX pattern given in Fig.III.19 is that of a YBCO rich area in the fractograph of Fig.III.18c. The Y, Ba and Cu peaks are well matched with the 123 stoichiometry with small

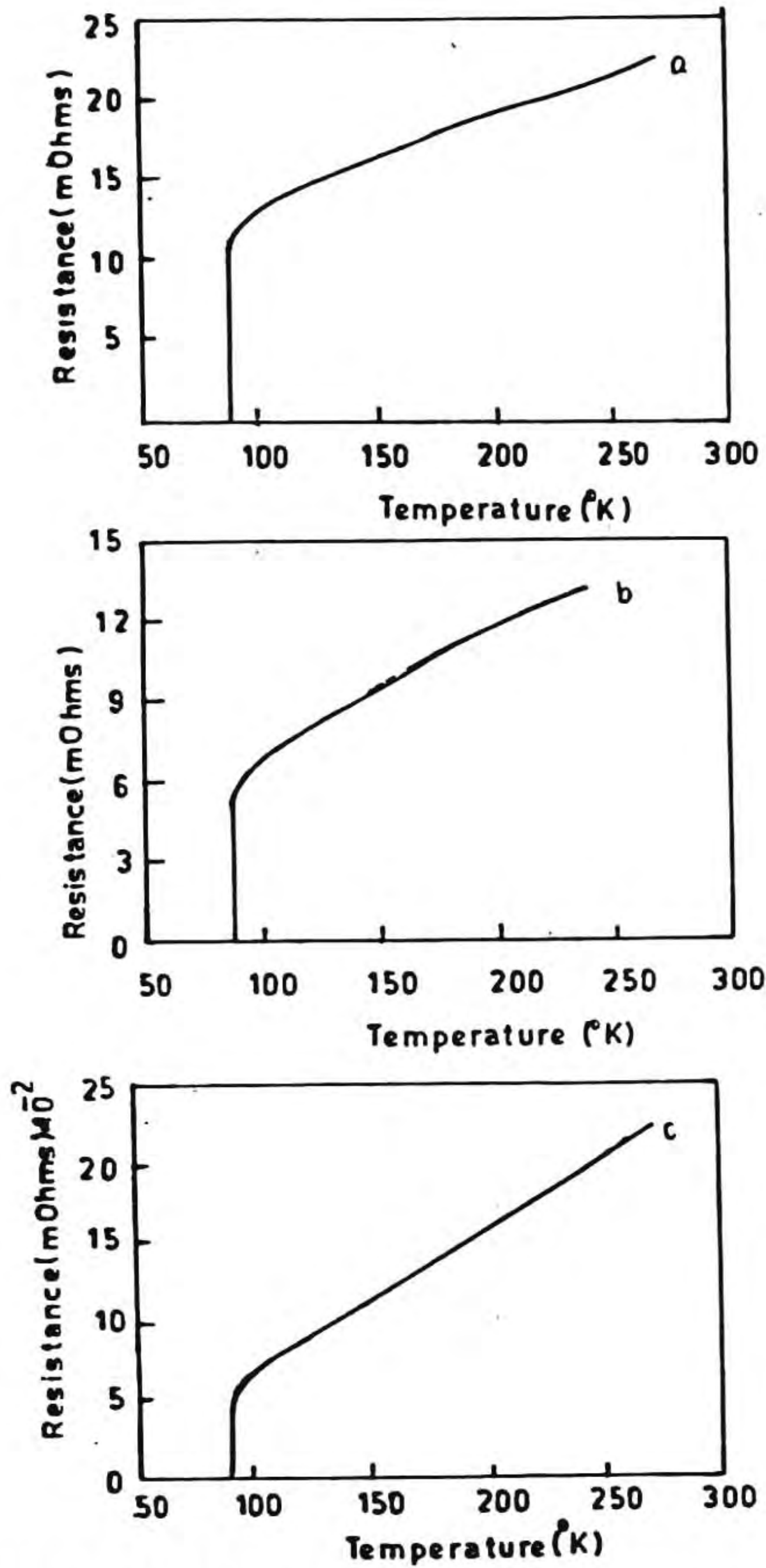


Fig. III.16 Resistance - Temperature curves of sintered pellets (a) 5 wt% Ag-YBCO, (b) 20 wt% Ag-YBCO and (c) 50 wt% Ag-YBCO composite

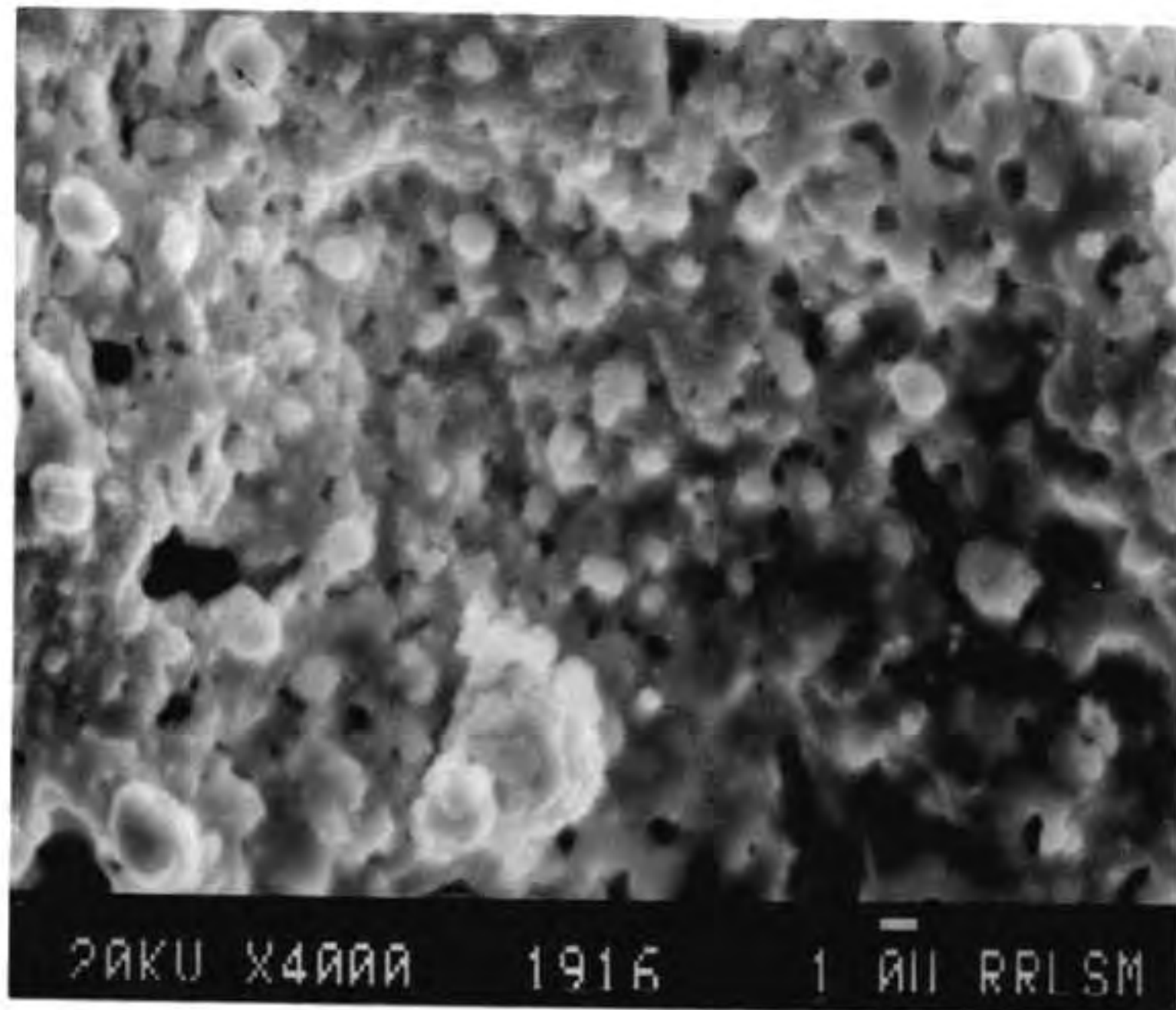
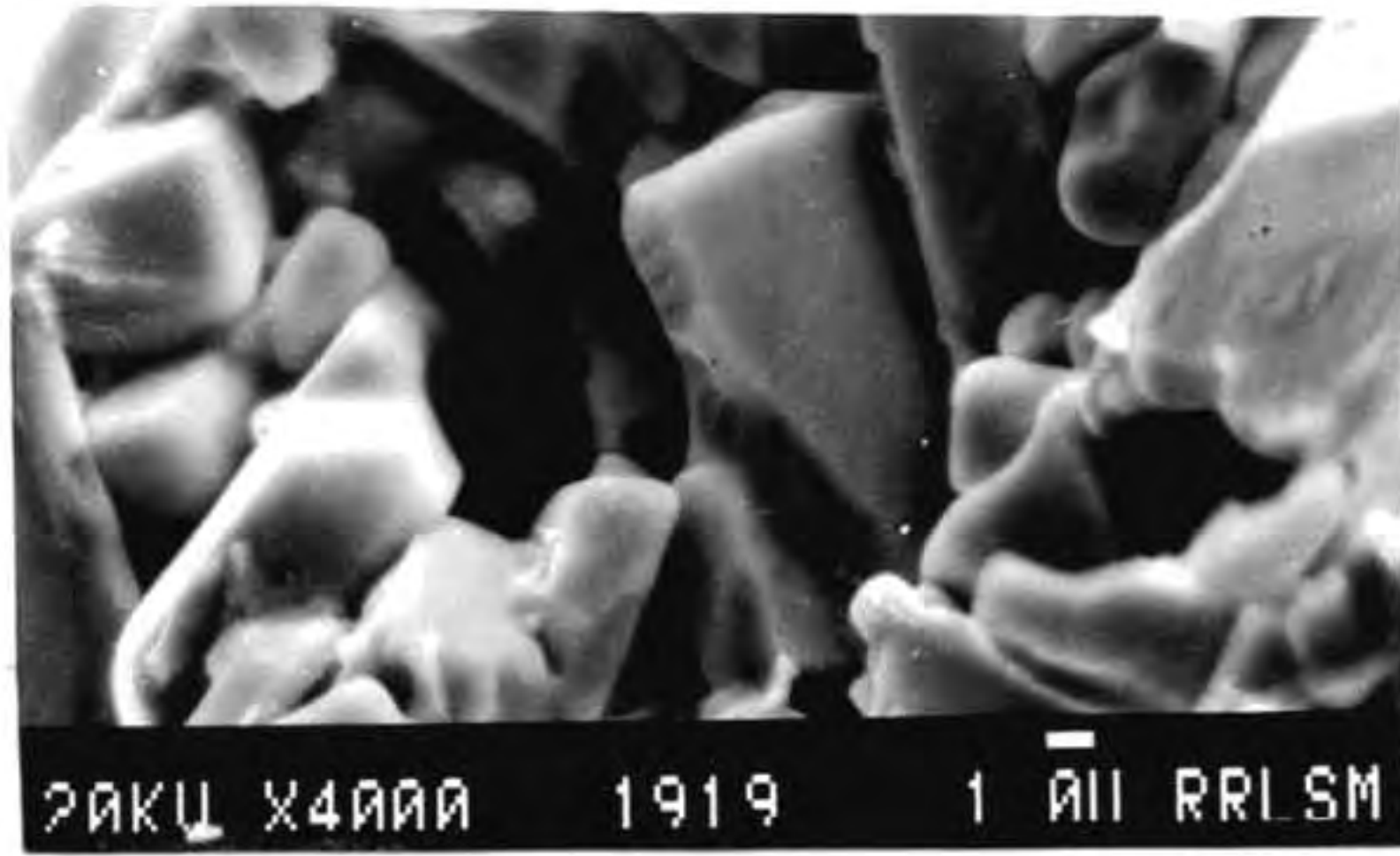
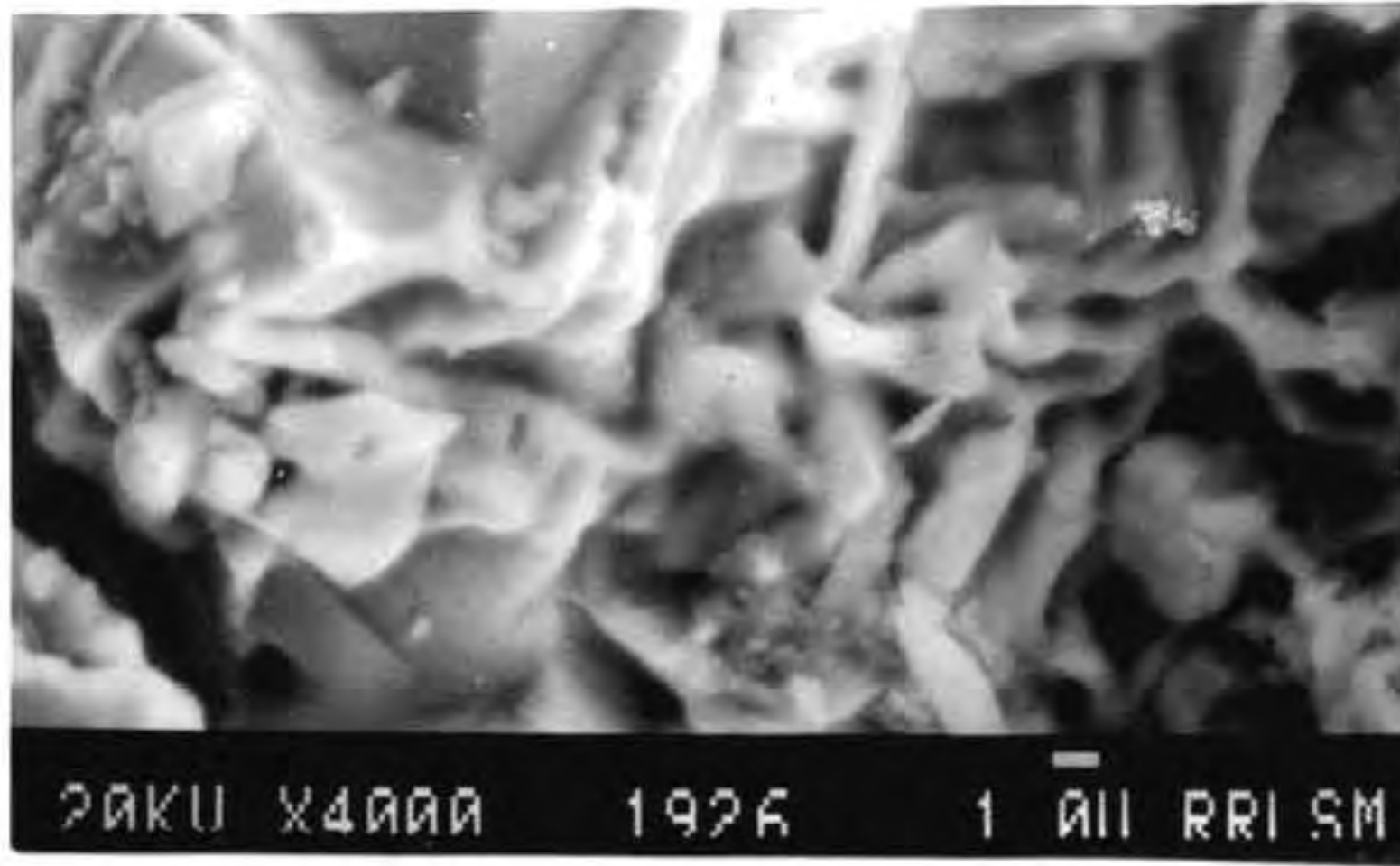


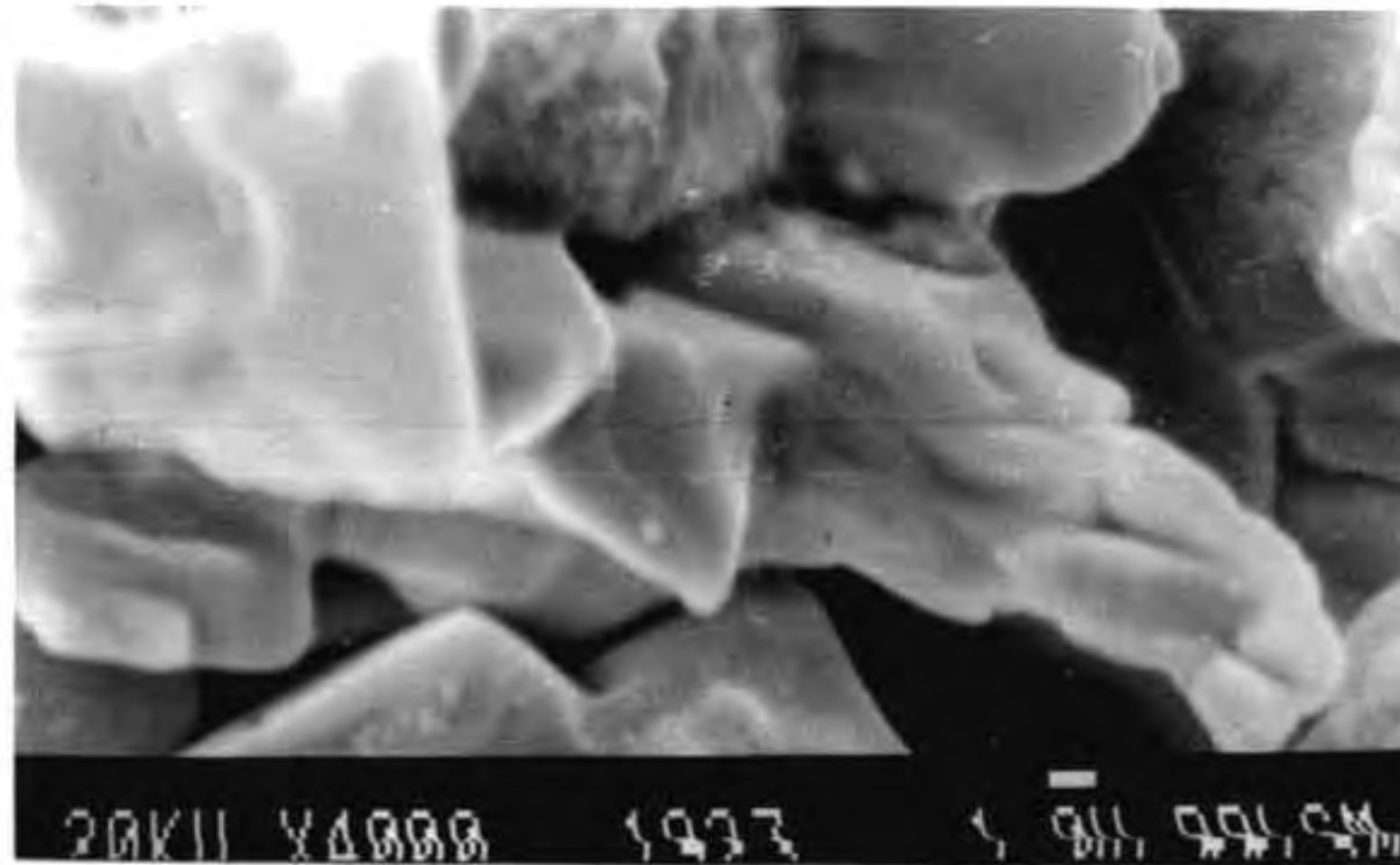
Fig. III.17 Surface morphology of Ag (20 wt%)-YBCO citrate gel after the heat treatment at 900°C



(a)



(b)



(c)

Fig. III.18 Fractograph of sintered superconducting composites (a) 5 wt% Ag-YBCO, (b) 20 wt% Ag-YBCO and (c) 50 wt% Ag-YBCO

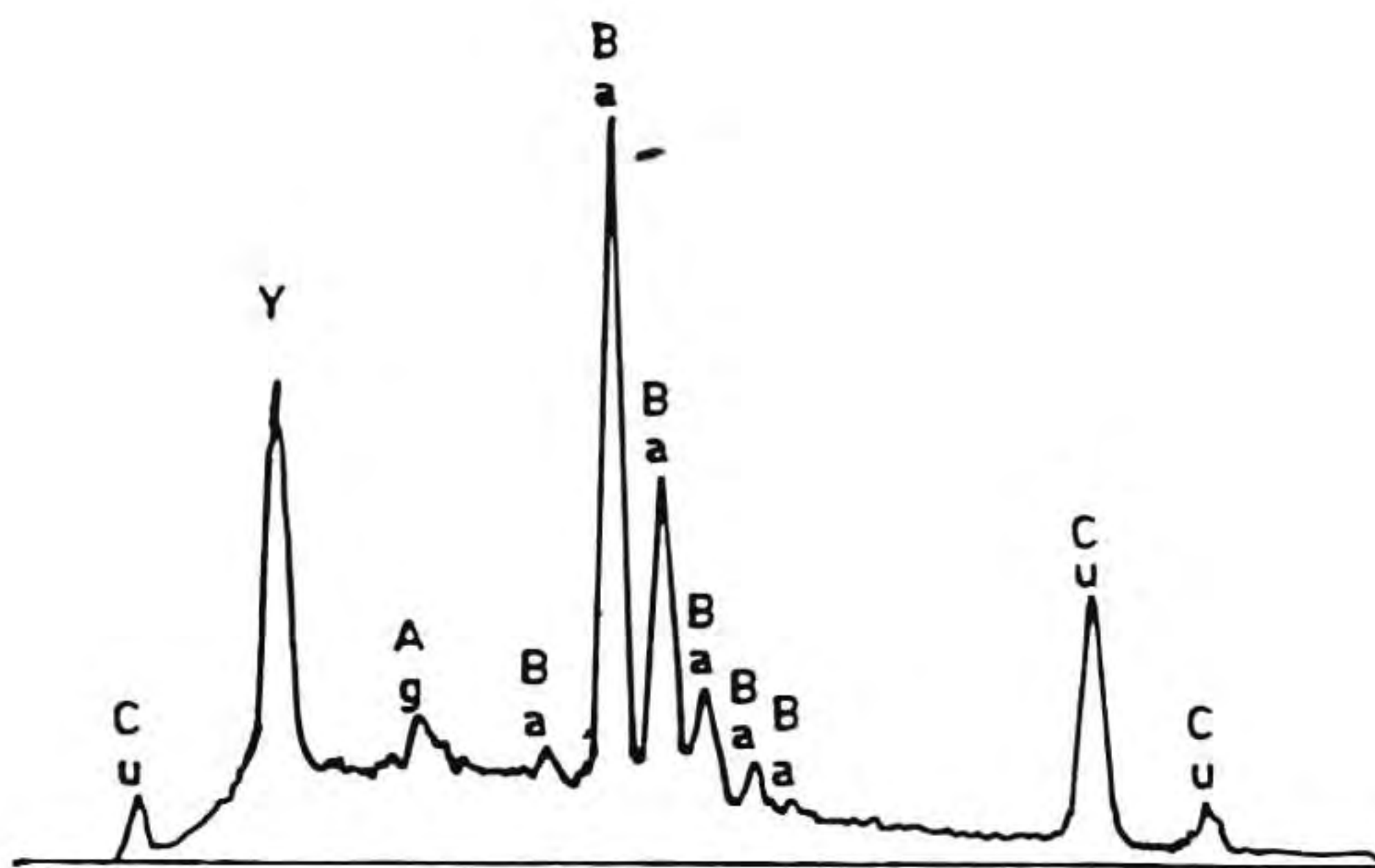


Fig. III.19 Energy dispersive X-ray analysis of YBCO rich phase in 50 wt% Ag-YBCO composite

peaks corresponding to Ag.

III.2.iv Discussion

The high uniformity of phases and narrow particle size distribution are the advantages of this method as seen from the gel morphology and particle size distribution curves. Since the very small chance of substitution of silver in $\text{YBa}_2\text{Cu}_3\text{O}_{7-\delta}$, this method leads to the preparation of composites at any composition ratios. The precursor powders have got varied tap densities and green compaction density depending on the amount of silver present in the final YBCO-Ag composite. The silver percentage has also got profound impact on the final sintered density of the Ag-YBCO composite.

Most important observation in this study is the preparation of YBCO-Ag composite without any oxygen annealing. The result support this observation by the fact that only composite containing the silver showed superconductivity while the pure YBCO showed non superconducting characteristics made under same reaction and sintering conditions. Silver oxide or compounds (as in this case) formed at lower temperature, and under normal conditions, one does not expect the oxygen released from Ag_2O decomposition to contribute to the tetragonal to orthorhombic conversion of YBCO at the sintering temperatures. Although actual mechanism by which Ag_2O acts as an internal oxidiser(20) is speculative, high oxygen gain rates in the YBCO/Ag composites are reported(21). This behaviour

could be explained from the particular microstructure of composite with continuous silver particles interspaced between the grains may allow a better and fast transport of the O_2 into the bulk of the YBCO grains. When discussing about the transport properties of 123/Ag composite, which comprises binary random mixtures of two phases a percolation model is ideal. The clusters of randomly distributed minor phase is a well connected particle of the second phase. As the concentration of the first phase (ie. clusters) increases at a point long scale connectivity is reached called percolation threshold. Above T_c we have a good conductor (Ag) to a bad conductor transition as predicted at a particular value of silver. This is clear because the room temperature resistivity of Ag-YBCO composite containing 20 wt% Ag is about two fold greater than that of 50 wt% Ag YBCO sample. Due to small ratio of respective conductivities of Ag and YBCO, this transition is smooth. This is very clear from the graphs.

The sintering temperature ($915^\circ C$) is very close to the melting point of silver ($962^\circ C$), the metal almost behaves like a liquid during the sintering so the fluid effectively oozes inwards to fill the voids and capillaries. The result is a highly dense and tough composite. Figure III.18 shows the fractured SEM micrographs of Ag-YBCO sample containing various amount of silver. The sample containing less amount of silver has got large porosities in the structure while the high silver content ones are of highly sintered or compacted

microstructure. This is due to the liquid phase sintering. As silver content increases the process of the direct contact of YBCO lessen, at about 70 vol % of Ag Tc drops sharply. It is also observed by other authors that there is a good tendency for growing the grain when they are close together through a clean and well sintered grain boundary.

III.2.v Conclusion

The present study has shown the possibility of preparing micron size homogeneous Ag-YBCO composite precursor powder with silver 5 to 75 wt % by a simple gel decomposition technique. The important observation in this study is, possibility to obtain superconducting Ag-YBCO composite without any oxygen annealing. The high oxygen gain rate (high solubility of O₂ in metallic silver) in the Ag/YBCO composite compound to pure YBCO is a possible explanation. High density sintered composites derived at a lower temperature. Some reaction of silver with bulk grains are nearly negligible, the effect of Ag addition to 20 wt % will improve the electrical and mechanical property by a more sintered microstructure.

III.3 Processing of citrate gel derived YBCO wires

III.3.i Introduction

For any practical application, ceramic superconductors must be fabricated to any useful forms like, wires, tapes or

films. While the preparation of high T_c superconducting films has advanced to reasonably satisfactory levels with critical current density in the range 10^6 A/cm^2 , fabrication of bulk forms face many material problems before shaping to forms like wires, tapes or bulk sintered shape(22). Attempts have been done to process superconductor powders into metal clad composite wires, metal core wires, metal substrate composite ribbons or bare wire or tapes. Another approach widely being attempted to draw wires by first introducing the powders into metal tubes (in most cases, silver tubes) followed by swagging and drawing progressively into thin wires which are finally subjected to sintering. Some authors have indicated the use of novel processing techniques such as tape casting, slip casting and extrusion of YBCO-polymer mixes to desired shapes(23). During extrusion the YBCO particles can align themselves because of shear stresses which may ultimately result in high current densities.

The present investigation concerns the possibility of drawing wires from a mixture of polymer and YBCO at room temperature (30°C) from a nonaqueous viscous mass by an extrusion technique.

III.3.ii Experimental

Finely ground YBCO derived by the citrate decomposition method was mixed with a long-chain polymer such as polypropylene carbonate in the presence of a solvent (ethyl

methyl ketone) by ball milling in a PVC bottle using zirconia balls as the grinding media. Certain minor additives such as polyethylene glycol (0.5%) and stearic acid (0.2%) were also incorporated as extrusion aids. The mixture was evaporated gradually until a highly viscous mass remained, which was further extruded in a stainless steel extruder having a nozzle size ranging from 0.2 to 1 mm in diameter. The wires were wound on glass rods or polyethylene rods of desired diameter and allowed to dry. These spirals were then heat-treated at controlled rates for binder burnout and then sintered at 940°C in flowing oxygen for 10 h. The wires were tested for the Meisner effect and then for T_c measurement. Current density was measured at small applied magnetic field on 3 cm-long spiral wire having a cross-sectional area of 0.0039 cm^2 . Further, the morphology of the extruded wires of YBCO-polypropylene composite before and after the heat treatment and the polished microstructure of the sintered samples were observed in a scanning electron microscope.

III.3.iii Results and discussion

The setup in which the YBCO-polypropylene mixture was extruded and wound in spiral forms is shown in Fig.III.20. The mixing of the polymer and YBCO powder as well as the rate of evaporation of the solvent (ethyl methyl ketone) are very carefully performed in this experiment in order to avoid segregation of the YBCO particles. Further, the particle size

distribution of the YBCO powder is adjusted such that the average particle size is about 1 micron. Figure III.21 presents the wire drawn using the present setup. The diameter of the wire was varied by changing the nozzle size. Morphological features of the wire presented in Fig.III.22 reveal a continuous polymer-YBCO distribution with periodic deep tracks caused by the irregularity on the inner surface of the nozzle. On heat treatment, the binder decomposes slowly without disturbing the YBCO particles due to the very slow burnout schedule presented in Fig.III.23 arrived at after various trials. A partial vacuum in the range 3 to 10 mmHg (400 to 1300 Pa) was applied during the binder burnout stage in order to make the process smooth. The cooling schedule and oxygen annealing were arrived at from various experiments. At higher temperatures sintering takes place and the surface of the wire presented in Fig.III.24 shows well-formed YBCO grains. The polished surface of a cross section of the wire (Fig.III.25) reveals the appreciably compact microstructure. The sintered wires annealed in oxygen were single-phase orthorhombic according to the XRD pattern and also exhibited the Meisner effect. The resistance vs temperature curve provided in Fig.III.26 shows the T_c to be 89.5K. The current density was measured based on magnetic behaviour in small applied magnetic fields in the range 0 to 13 G (0 to 1.3×10^{-3} T) and the sample exhibited a J_c value of over 223 A/cm^2 at zero field. The decrease in the value of J_c with increasing field is given in Fig.III.27.



Fig. III.20 Extrusion set up

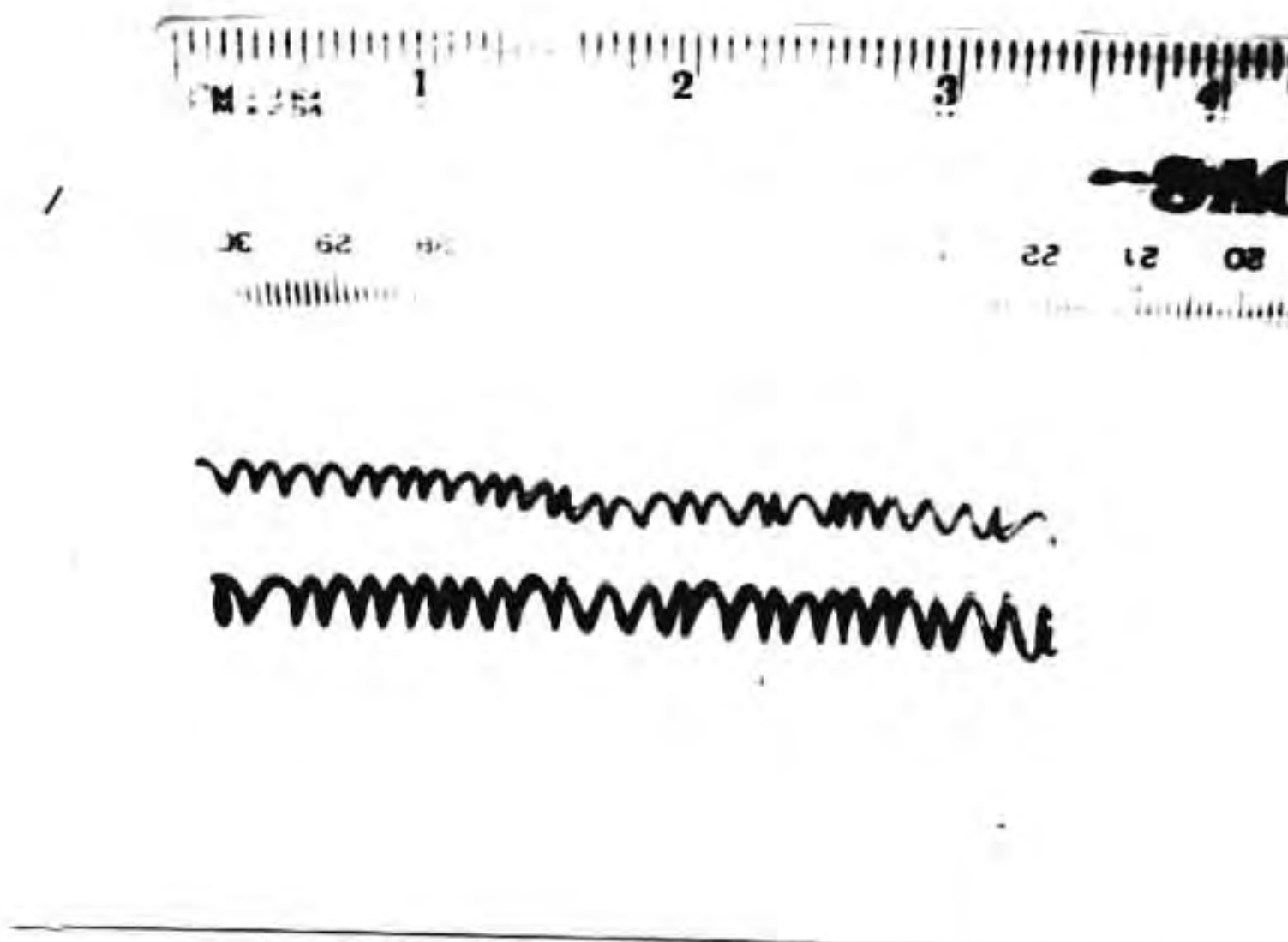


Fig. III.21 Cold extruded wires

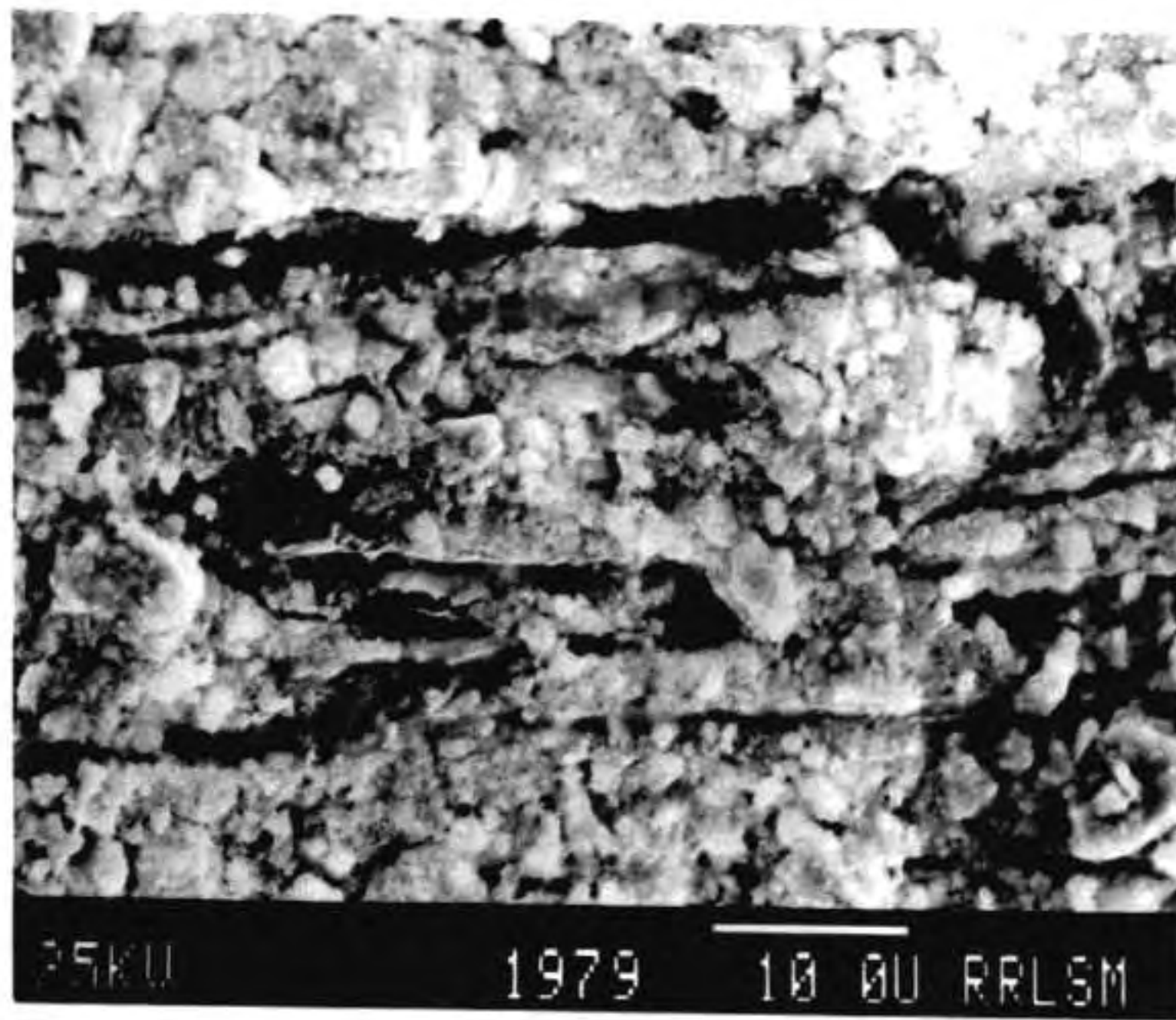


Fig. III.22 Surface morphology of as extruded wires

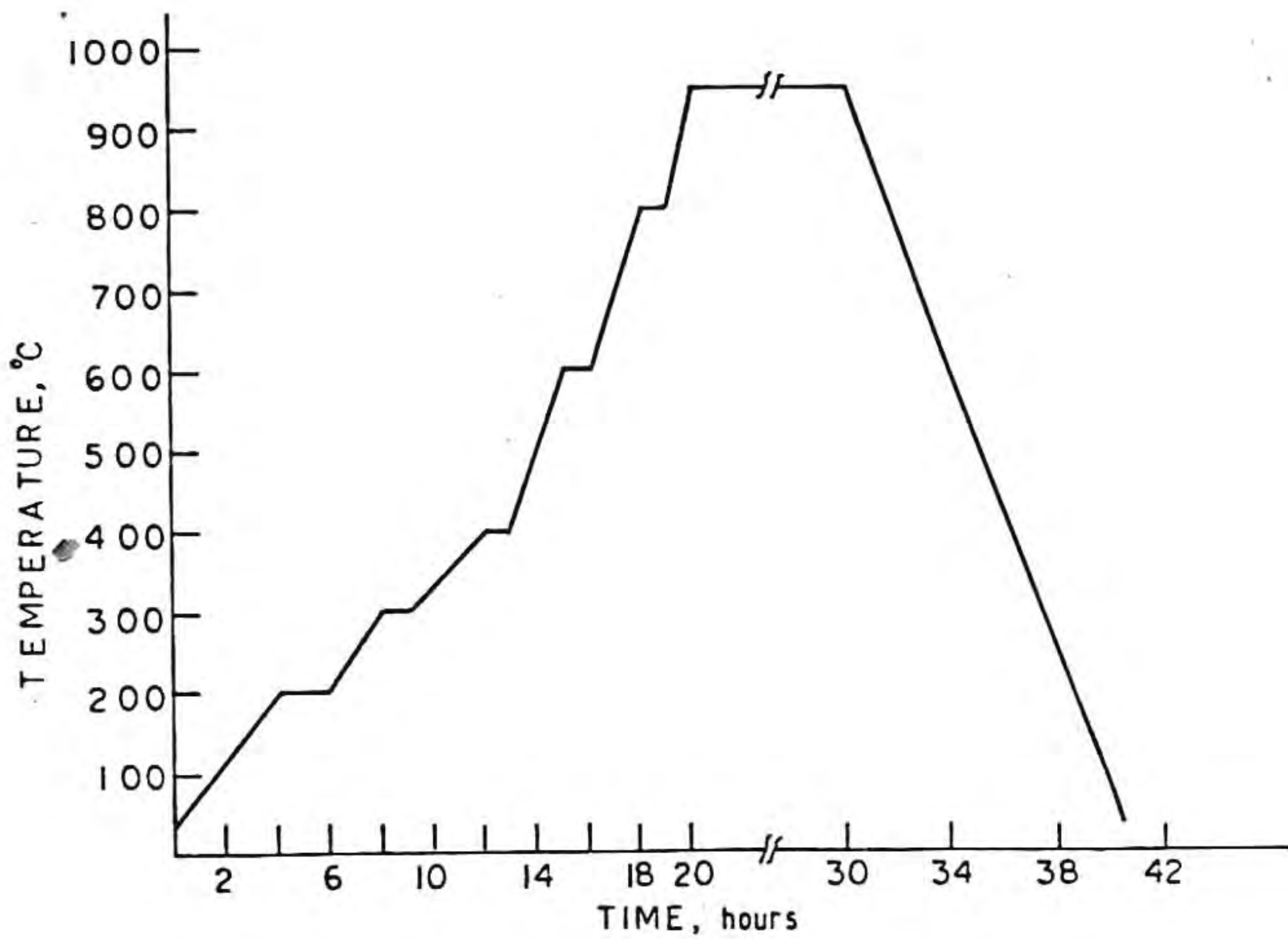
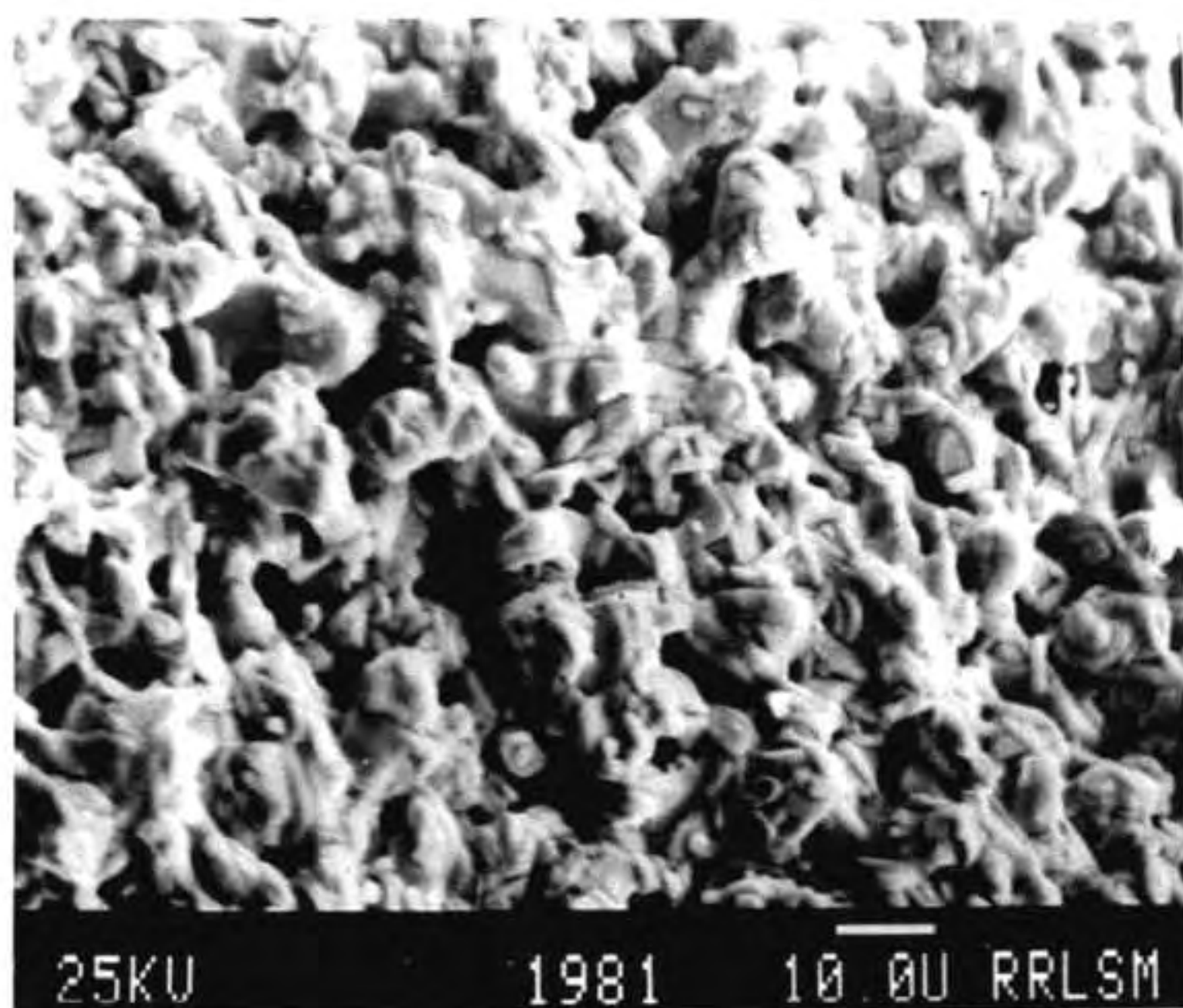
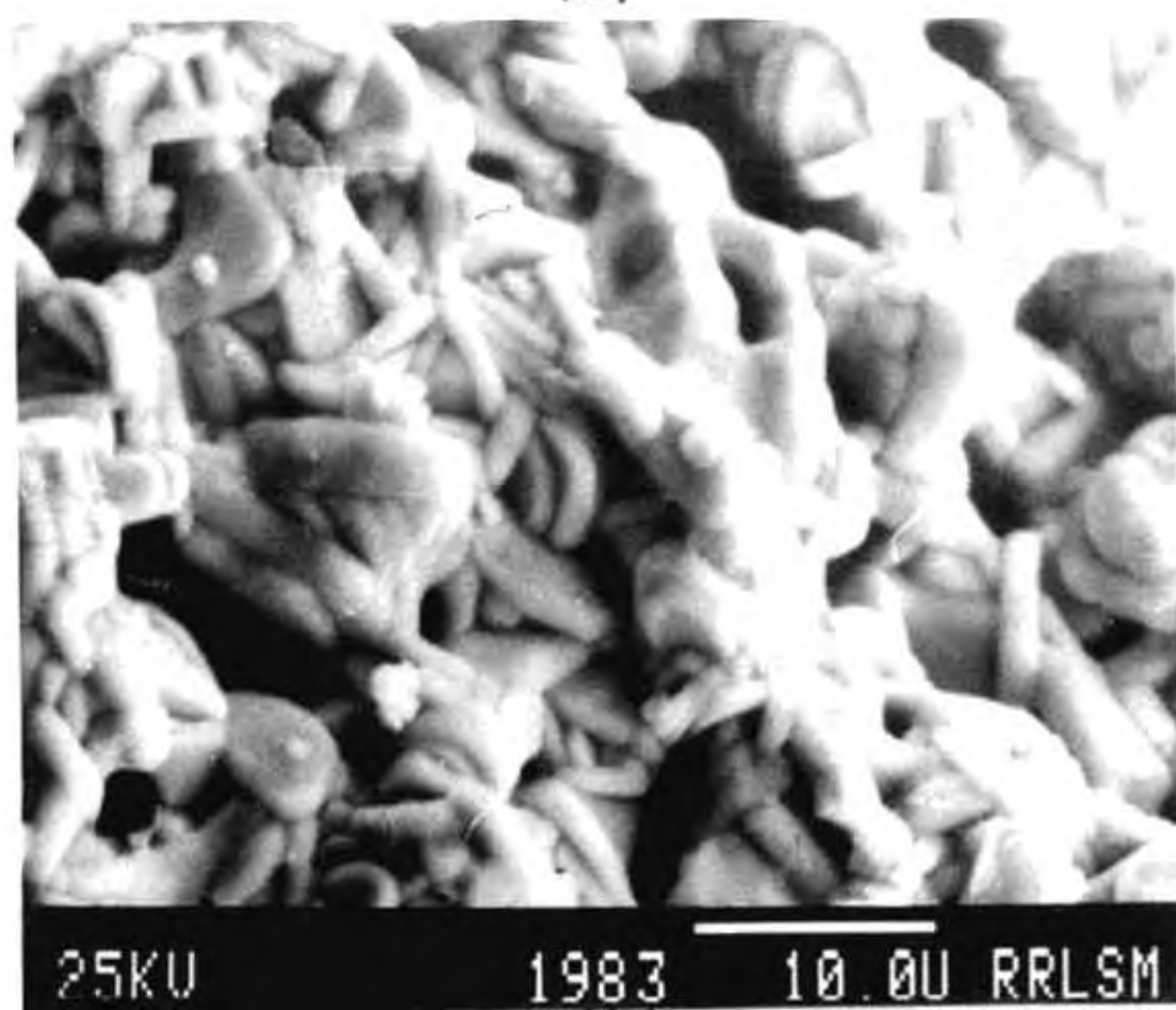


Fig. III.23 Heating schedule for the sintering of the extruded wire



(a)



(b)

Fig. III.24 Surface morphology of sintered wires in low and high magnification

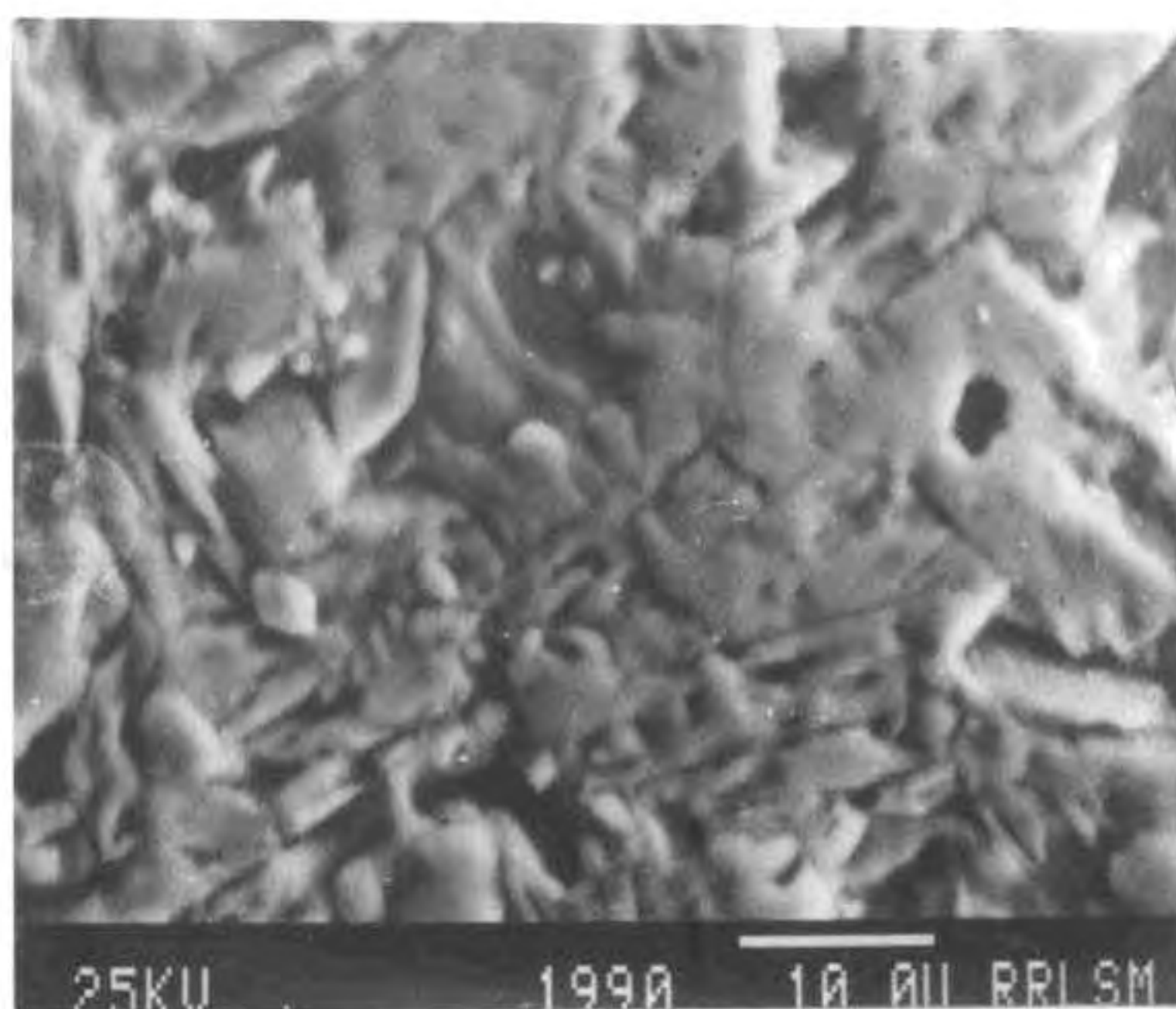


Fig. III.25 Polished fractured surface of sintered wire

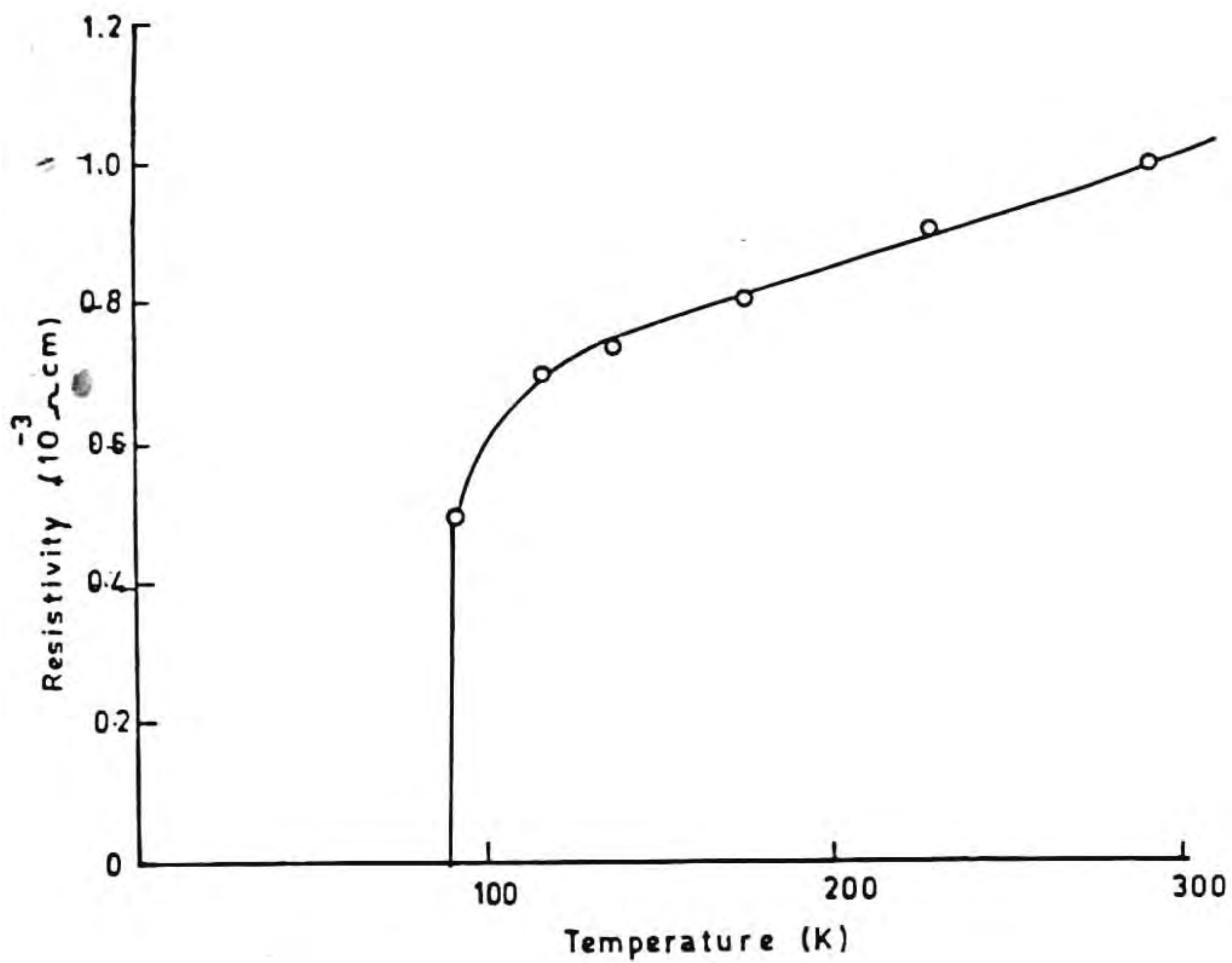


Fig. III.26 Temperature vs resistivity of the superconducting wires

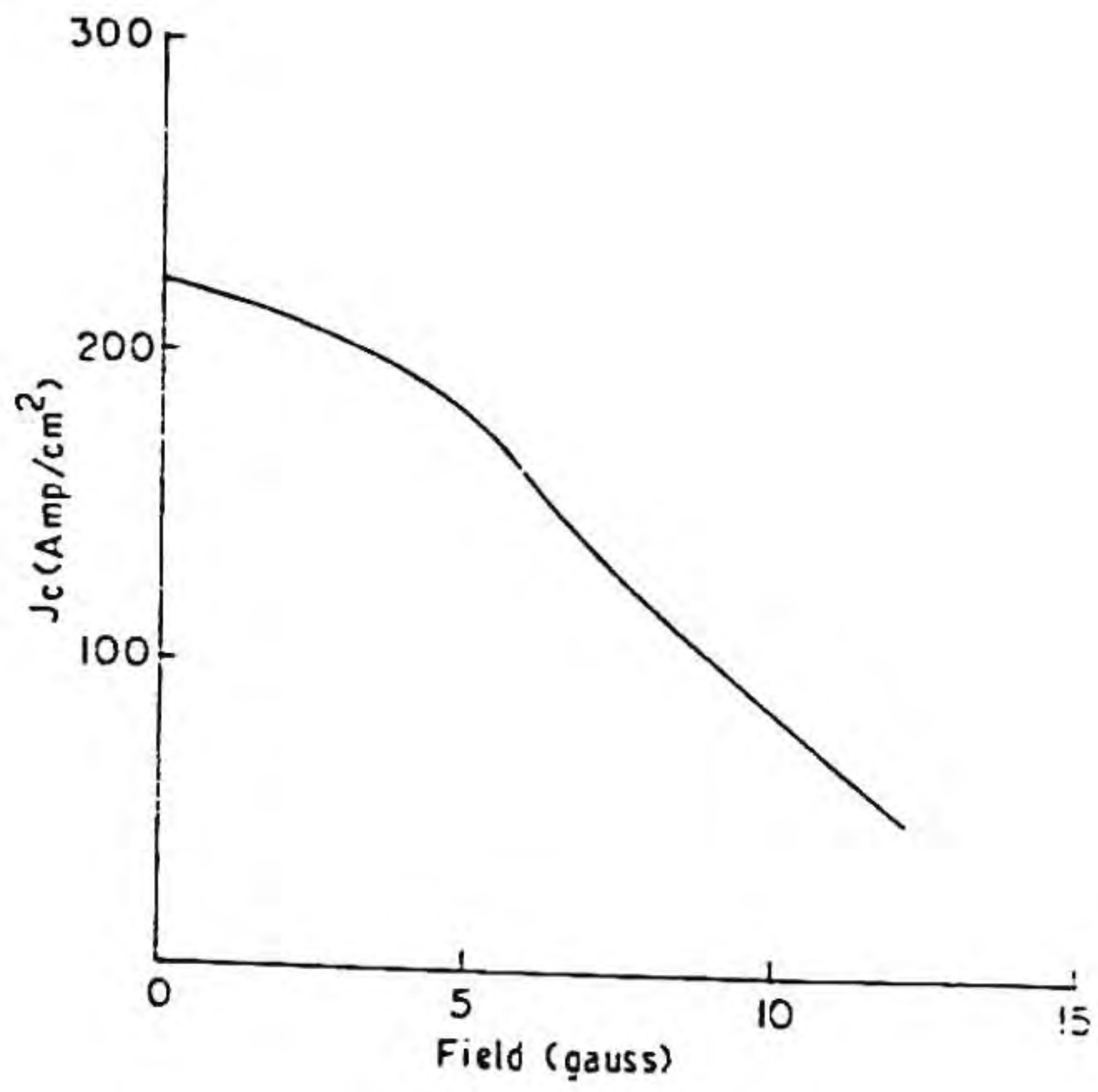


Fig. III.27 Variation of critical current density with applied magnetic field

III.3.iv Conclusion

The present study has therefore shown the possibility of drawing citrate gel derived YBCO wires as a composite with polypropylene at 30°C and the process is very simple and energy efficient. Further, these wires could be wound into spirals which on further heat treatment and annealing resulted in superconducting wires with a Tc of 89.5K and a Jc of 223 A/cm².

References

1. P.A. Lessing, *Am. Ceram. Soc. Bull.*, 68(5) (1989) 1002.
2. C. Marcelly, P. Courty and B. Delmon, *J. Am. Ceram. Soc.*, 53(1) (1970) 56.
3. N.G. Eror and H.U. Anderson, pp.571-577 in *Better ceramics through chemistry II*, MRS Proceedings, Vol.73, Eds. C.J. Brinker, D.E. Clark and D.R. Ulrich, Materials Research Society, Pittsburgh, PA, 1986.
4. D.J. Anderton and F.R. Sale, *Powder Metall.*, 22, (1979) 14.
5. A.M.T. Bell, *Supercond. Sci. Technol.*, 3, (1990) 55.
6. L.J. Van der Pauw, *Philips Res. Rep.*, 13, (1958) 1.
7. D.C. Harris and T.A. Hewston, *J. Solid State Chem.*, 69, (1987) 182.
8. A. Manthiram, J. Swinnea, Z.T. Sui, H. Steinfink and J.B. Goodenough, *J. Am. Chem. Soc.*, 109, (1987) 6667.
9. J.D. Jorgensen, B.W. Veal, A.P. Paulikas, L.J. Nowicki, G.W. Crabtree, H. Claus and W.K. Kwok, *Phys. Rev. B.*, 41, (1990) 1863.
10. C. Chu and B. Dunn, *J. Am. Ceram. Soc.*, 70(12), (1987) C375.
11. M.S.G. Baythoun and F.R. Sale, *J. Mater. Sci.*, 17, (1982) 2757.
12. M.F. Yan, H.C. Ling, H.M. O'Bryan, P.K. Gallagher and W.W. Rhodes, *Mater. Sci. Engg.*, B1, (1988) 119.
13. M.N. Rahman, C. Lutgard, De Jonghe and M. Chu,

- Adv.Ceram. Mater., 2, (1988) 380.
14. Q. Robinson, P. Georgopoulos and D.L. Johnson, Adv. Ceram. Mater., 2, (1987) 380.
 15. K.G.K. Warriar and P.K. Rohatgi, Powder Metall., 9, (1986) 65.
 16. A. Goyal, P.D. Funkenbusch, G.O.S. Chang and W.J. Burns, Proc. 2nd Ann. Conf. on superconductivity and application, Baffalo, Eds. H. Kwok and D.T. Shan, Elsevier, Amsterdam, 1988.
 17. D. Cahen, Z. Moisi and M. Schwarts, Mat. Res. Bull., 22, (1987) 1581.
 18. S.L. Shinde, D. Goland, D. Chance and T.J. Watson, Am. Ceram. Soc. Ann. Meeting, Indianapolis, 23-27 April 1989, Paper No.4-SV 1-89, 1989.
 19. J.P. Singh, H.J. Len, E. Van Vodrlees, K. Winsely, K.J. Josef Chuk and D. Shi, Am. Ceram. Soc. Ann. Meeting, Indianapolis, 23-27 April, 1989, Paper No.42-SV 1-89, 1989.
 20. D.R. Clarke, T.M. Shaw and D. Dimos, J. Am. Ceram. Soc., 72, (1989) 1103.
 21. J.S. Moya and E. Saiz, Solid State Comm., 74(12) (1990) 1291.
 22. S. Jin, Journal of Metals, 3, (1991) 7.
 23. K.B. Poeppel, S.E. Dorris, C.A. Youngdahl, J.P. Singh, M.T. Lonagan, U. Balachandran, J.T. Dusek and K.C. Gorretta, J. Mineral Met. Mater. Soc., 41, (1989) 11.

CHAPTER IV

FLASH COMBUSTION SYNTHESIS OF YBCO

IV.1 Introduction

As has been discussed in Chapter I, the chemical methods of preparation techniques based on solutions offer a wider perspective towards the ultimate product needed for specific application. Further, the processing steps involve large volumes as well as multi stages involving elevated temperatures. In addition, although good homogeneity is maintained, the process consumes considerable reaction time. Solid state combustion processes, on the other hand, have been shown to be advantageous over the solution techniques at least in many specific cases of oxide systems because of the single stage process at faster rates. The self propagating high temperature synthesis methods are based on the strong exothermic reaction between the reactants and in most of such cases, evolution of a number of gases is involved. The combustion heat generated in such cases is too high even to produce high temperature phases instantly. A method for simultaneous synthesis and sintering of ceramics in very short time was developed earlier by Merzhanov(1). Such self propagating reactions have been used successfully to produce borides(2), carbides(3) and nitrides(4). Patil et.al.(5)

This work was published

** Journal of American Ceramic Society, 73(10) (1990) 3103.*

recently reported the use of chemical energy derived from decomposition of metal nitrate-urea mixtures to produce a variety of ceramic materials such as alumina and related oxides. CeO_2 and rare earth doped ZnO ceramics were also synthesized by the above procedure(6,7).

IV.2 Mechanism of urea-metal nitrate decomposition

The combustion mixture consisted of a redox system involving an oxidizer (nitrate) and a fuel (urea), which emulates conventional oxidizers such as chlorides or perchlorides and fuels such as polymeric amides, esters and hydrocarbons used in explosives, propellants and pyrotechniques. Nitrates thermally decompose below 700°C with evolution of oxides of nitrogen such as NO_2 , NO and N_2O_5 . Similarly urea melts and decomposes on heating around 200°C to biuret. HCNO and NH_3 further decomposes around 300°C to an organic acid trimer $(\text{HNCO})_3$ (8), which again undergoes decomposition at higher temperatures. In metal nitrate-urea mixture, the decomposition product will be nitrogen oxides, NH_3 and HCNO . The mixture of these gases ignite, even at ambient pressures, when they reach required temperature which causes an appreciable increase in temperature of the system(9). The solid state reactions occur during this flash combustion, resulting in a considerable reduction in reaction time. The reaction sequences can be visualized as depicted in Figure IV.1. In most simple systems, the reaction is initiated at around 500°C . The

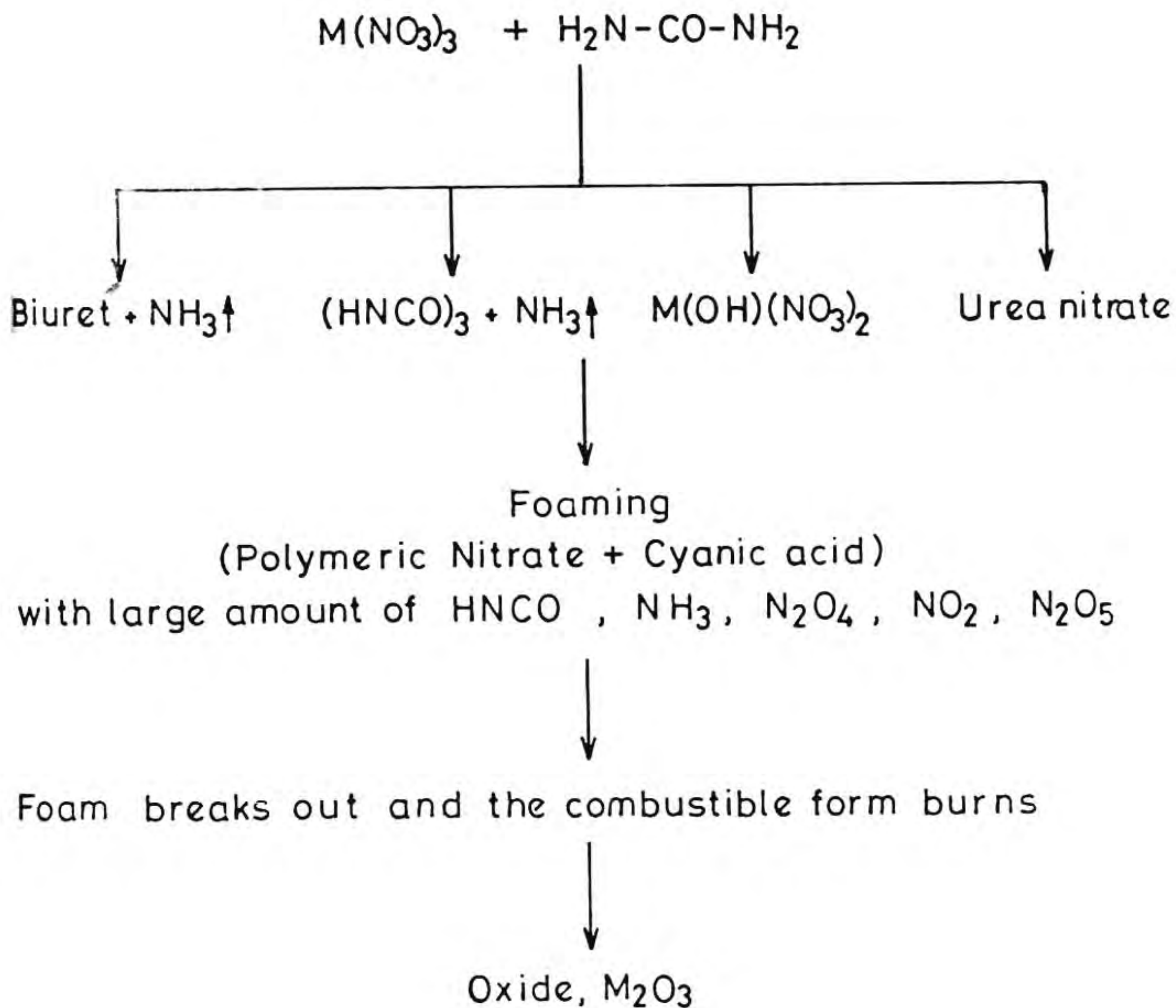


Fig. IV.1 Mechanism of metal nitrate-urea combustion reaction⁽⁹⁾

above technique has been further modified as a flash combustion synthesis for preparation of single phase YBCO starting from a mixture of nitrates of yttrium, barium and copper-urea mixtures and presented in this chapter.

IV.3 Experimental

A total of 10 gm mixture of yttrium, barium and copper nitrates (1:2:3 stoichiometry) were thoroughly mixed in an agate mortar with 5 gm of urea. The mixture was transferred into a Pt crucible. Care was taken to see that the mixture did not become highly hygroscopic. Then the crucible was placed in a furnace already heated to 900°C. First the mixture melts, and decomposes, releasing large amount of gases, and then it ignites. The reaction was over in about 5 minutes leaving black precursor which remains in the furnace for one hour. The material was then powdered in an agate mortar. The flash combustion method were also performed at 700°C and 800°C in order to study the sequence of phase formation. Sintered YBCO pellets of 10 mm diameter and 3 mm thickness were made by pressing the powder at a pressure of 100 MPa followed by firing at 930°C for 10 hours under flowing oxygen.

IV.4 Methods

Particle size analysis, BET surface area and bulk density of the powder were determined as described in Chapter II. XRD patterns using $\text{CuK}\alpha$, and SEM microstructure were also

taken for the powder as well as the sintered substance.

IV.5 Results

IV.5.i Particle size distribution

YBCO powder prepared by the present method has an average particle size of 4 microns, where a maximum particle size was around 10 microns as shown in Figure IV.2. Ball milling of the powder in acetone, with zirconia balls as the grinding media, for a period of 2 hours reduced the particle size to 2 microns.

IV.5.ii Density and surface area

The tap density of the ground powder was 2.7 gm/cm^3 . The surface area measured by BET technique was found to be $42.2 \text{ m}^2/\text{g}$. The green density of above powder when compacted at a pressure of 100 MPa was 3.9 g/cm^3 . Sintered density of these pellets were 5.61 gm/cm^3 .

IV.5.iii X-ray diffraction studies

The XRD patterns of the flash combustion powders at various temperatures are provided in Figure IV.3. The patterns show the progressive formation of YBCO phase with flash temperature. The major peak at 2θ value equal to 32.8° steadily increases with temperature and soaking time. Figure IV.3(a) shows the predominant peak of BaCO_3 ($2\theta = 23.9^\circ$) which decreases

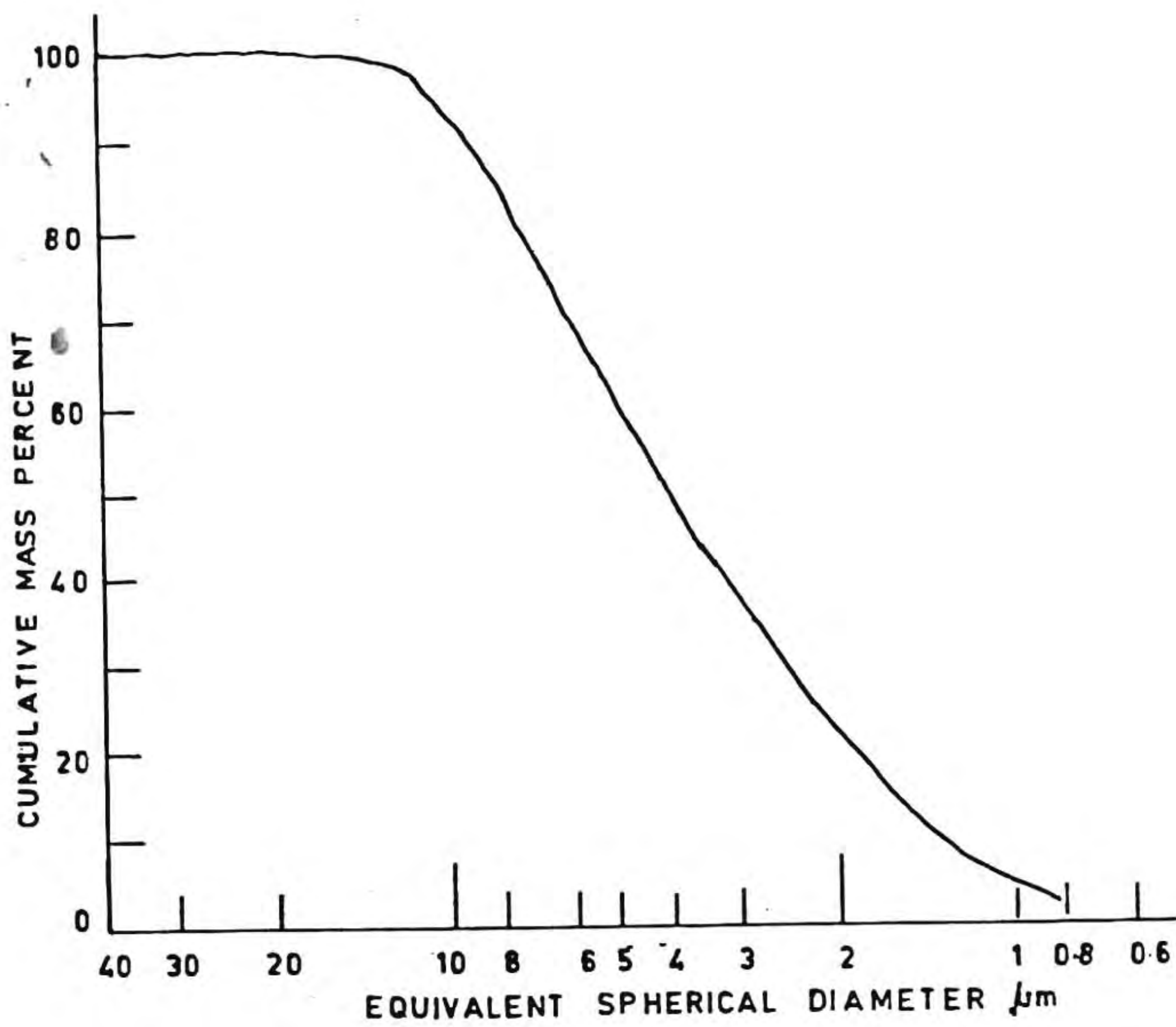


Fig. IV.2 Particle size distribution curve of flash combustion YBCO powder

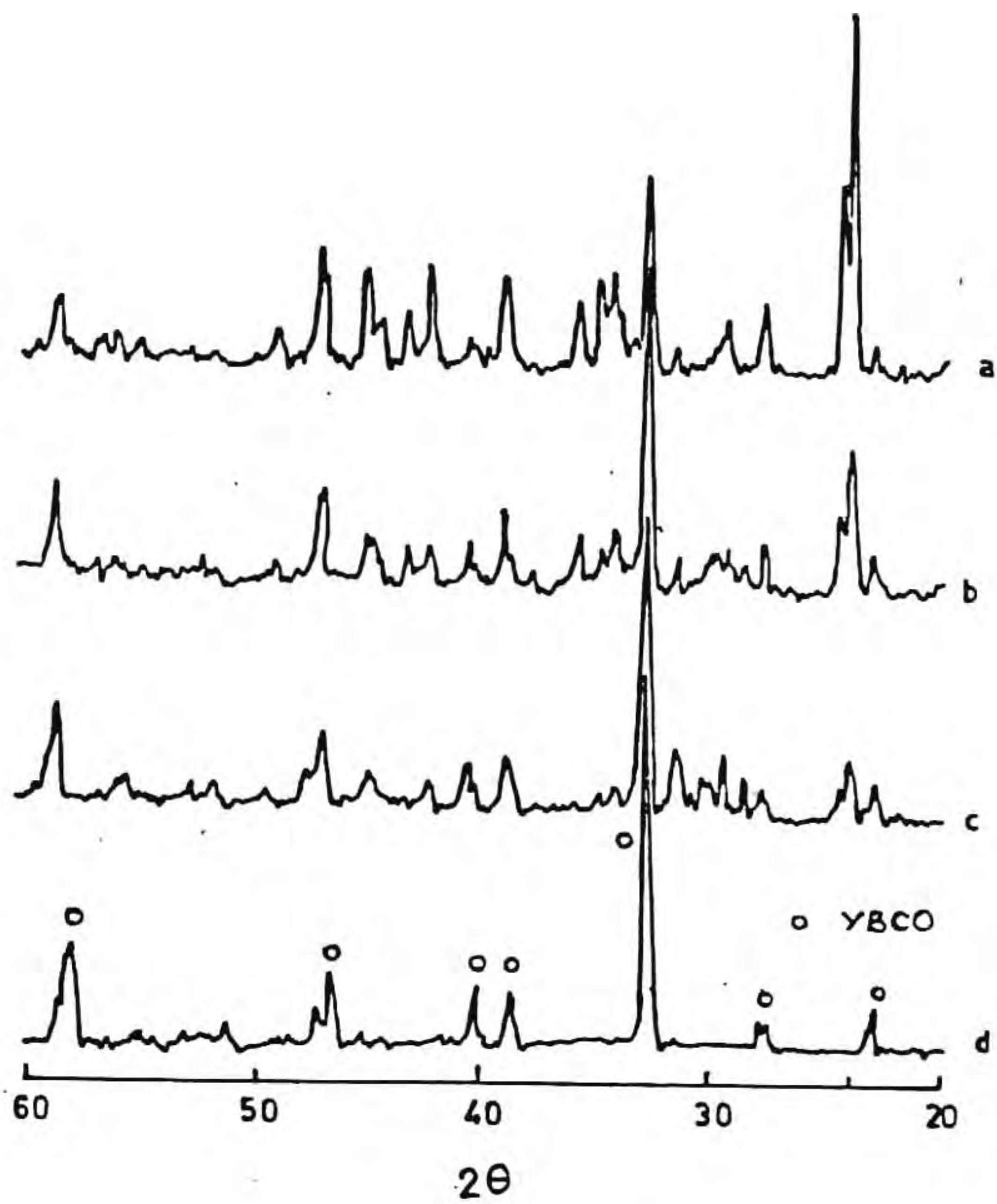


Fig. IV.3 X-ray diffraction patterns of flash combustion powder at various temperatures (a) 700°C for 5 minutes, (b) 800°C for 5 minutes, (c) 900°C for 5 minutes and (d) 900°C for 1 hour

with an increase in flash temperature. The peaks related to free CuO ($2\theta = 35.5^\circ$) and Y_2O_3 (29.1, 33.7) and $BaCuO_2$ (29.3, 40.09) and Y_2BaCuO_5 (29.8, 30.4) also show a similar trend. Figure IV.3(d) shows the pattern of single phase YBCO phase. Figure IV.4 shows the retention of $BaCO_3$ in the powders prepared at various flash temperatures calculated for the above XRD results. It decreases with increase in flash combustion temperature.

IV.5.iv SEM analysis

Figure V.5 shows the morphology of powders derived from flash combustion method prepared at $900^\circ C$ for 5 minutes. They had a finger like formation with foamy morphology. Occasional distribution of rod like particles with high aspect ratio among finer particles is seen.

Figure IV.6 shows the fractograph of a sintered YBCO sample ($>88\%$ dense). The fracture is brittle in nature. The sintered grain size were 3 to 5 microns with an aspect ratio of 4 to 6. Occasionally grains with elongated rod like shape, as seen in the basic powder, have been retained with similar morphology.

IV.5.v Electrical properties

Figure IV.7 shows the resistivity vs temperature of a sintered YBCO sample at $930^\circ C$ for 10 hours in oxygen. The T_c is 90 K with small ΔT_c . The transport current density measurements

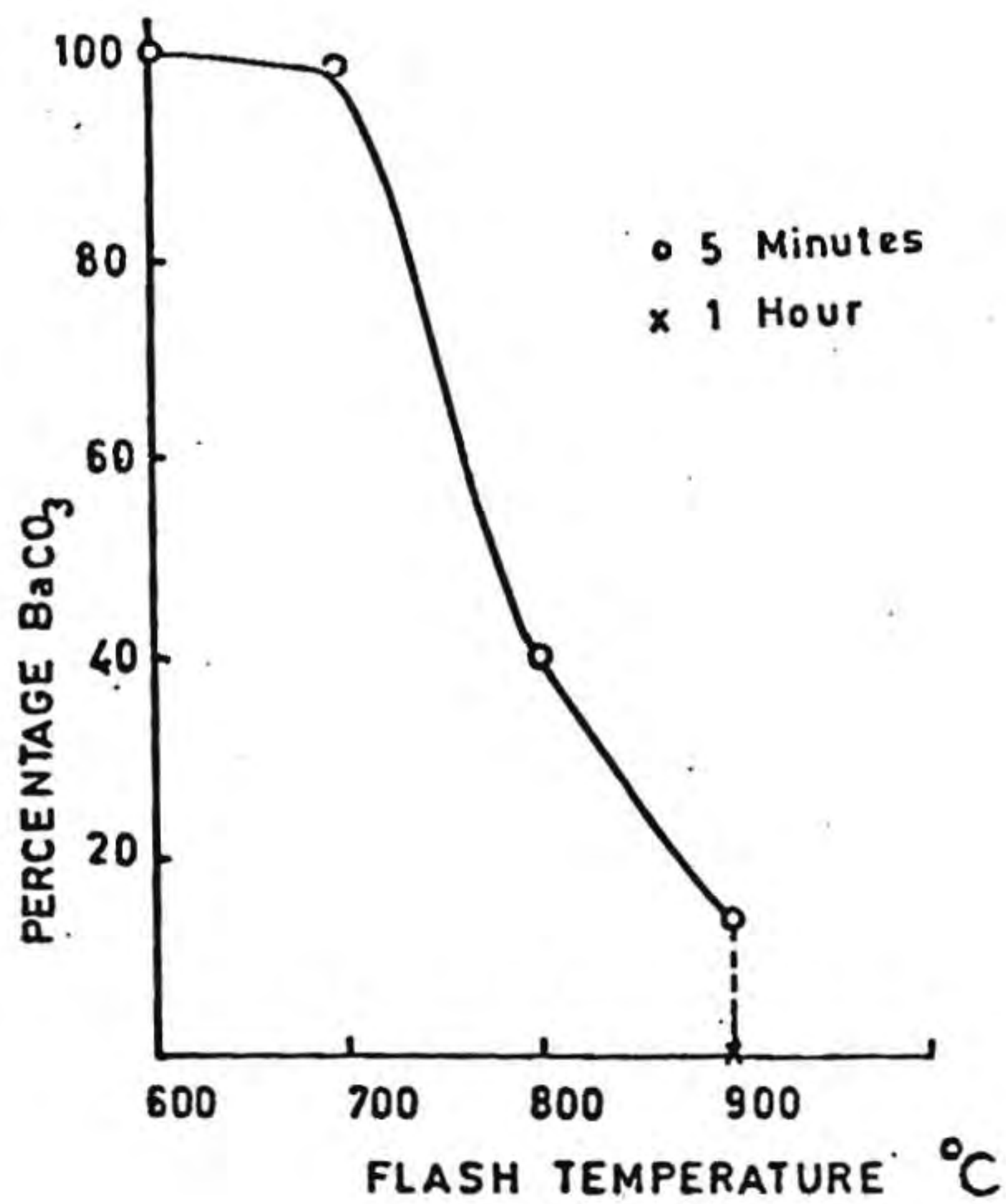


Fig. IV.4 Percentage of BaCO₃ present in the powders as a function of flash combustion temperature assuming maximum at 600°C

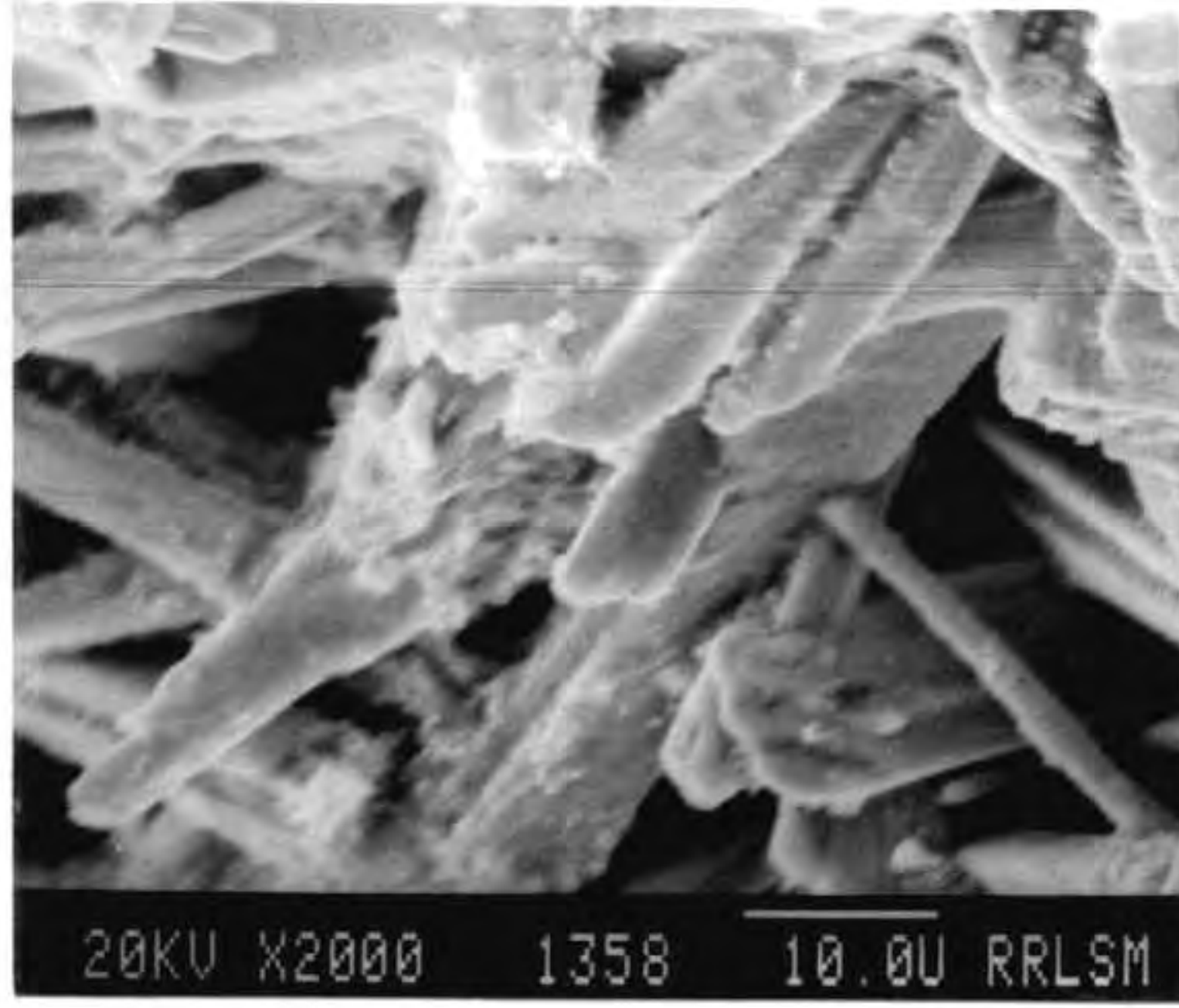


Fig. IV.5 Scanning electron micrograph of flash combustion derived YBCO powder

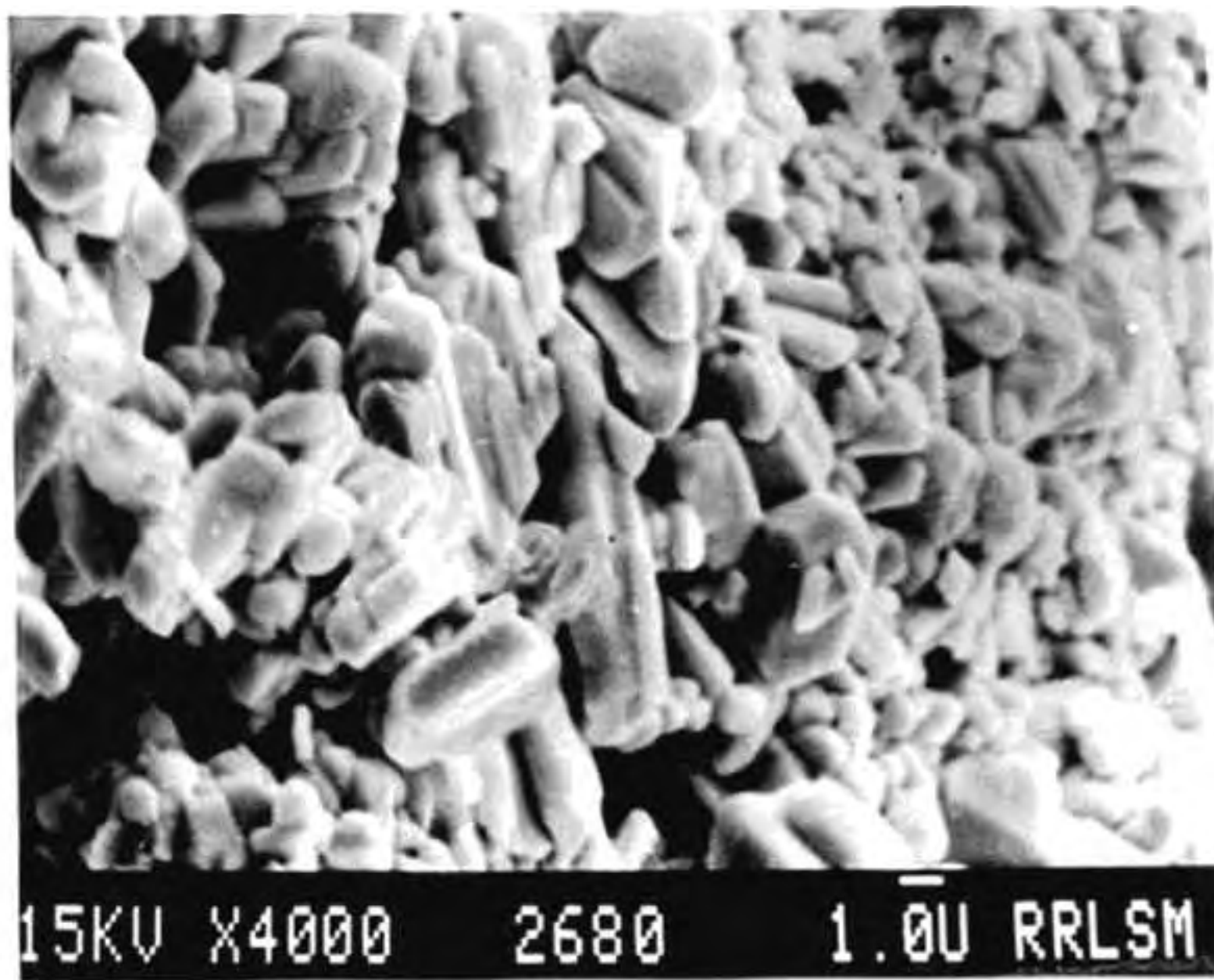


Fig. IV.6 Fractured surface of sintered YBCO sample
(930°C/10 hr)

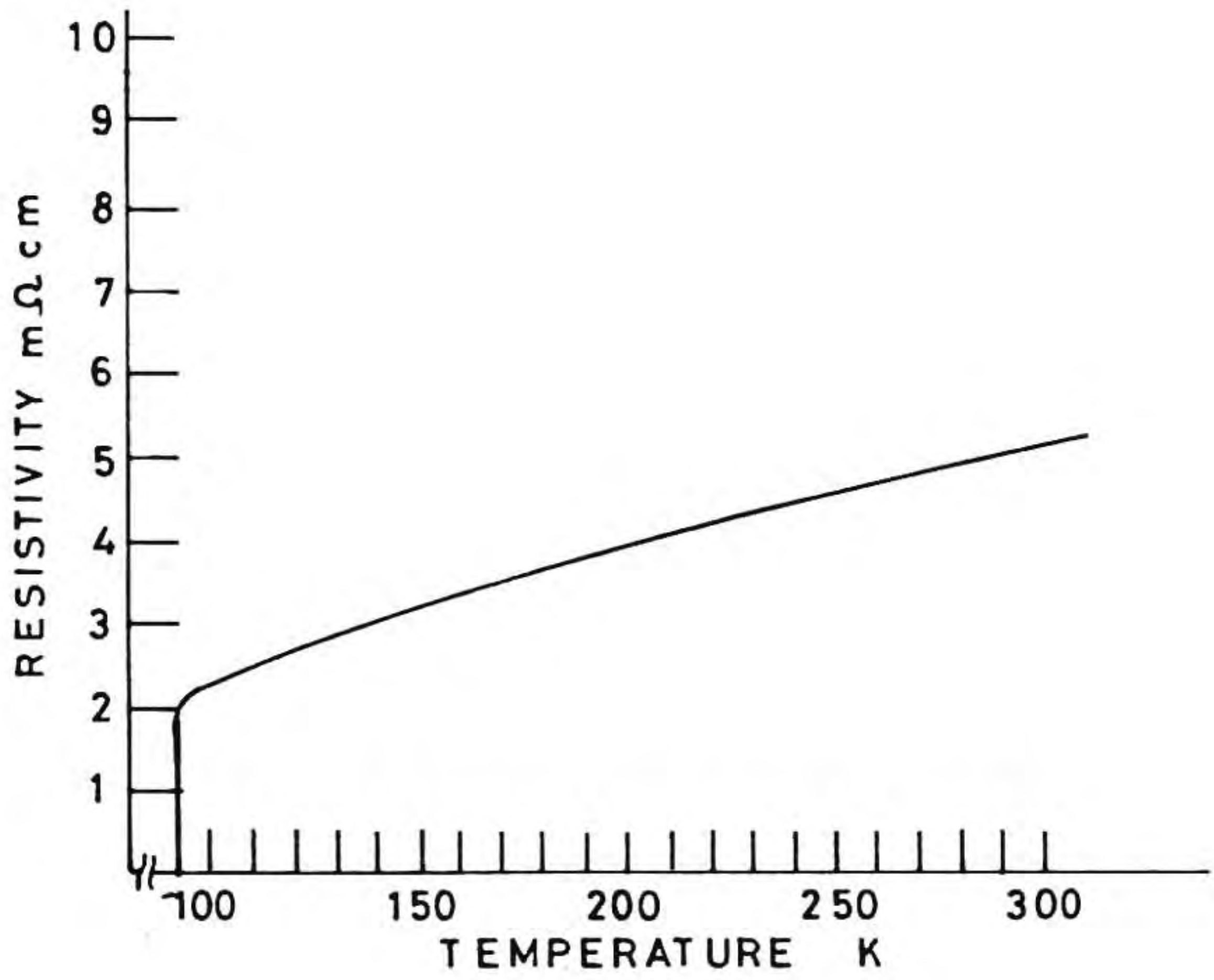


Fig. IV.7 Temperature vs resistivity for sintered YBCO derived through flash combustion route

done on rectangular sintered sample showed a J_c of 150 A/cm^2 .

IV.6 Discussion

The systematic studies reported on the reaction sequences that lead to the formation of 123 superconductor found that decomposition of BaCO_3 was the rate limiting step(10). Also these studies reported that the powders tended to agglomerate, resulting in heterogeneous product formation as a consequence of macroscopic diffusion limitations. In the present method, the nitrate-urea mixture melts first to a liquid, then dries and foams, followed by evolution of the gases combustible such as NH_3 and HCNO and as a result the temperature reaches even above 1300°C although for a short while. The reaction virtually takes place at the point of decomposition of the salts and between oxide particles at the high temperatures developed. This is the reason for the short reaction time taken to form fine crystallites. However, it is important that mixture of nitrates and urea in this case are introduced into a furnace kept at 900°C , in contrast to the usual practice of 500°C (5), to facilitate formation of the gases for the flash combustion. On the contrary, if the mixture is heated slowly in a furnace to 900°C , only decomposition takes place, but no combustion. Since the mixture melts before combustion, a high degree of mixing of constituents is achieved. This route is definitely many times shorter than the

usual ceramic route as well as simple while nitrate decomposition through heat treatment takes more than 14 hours. The urea-nitrate proportion in the mixture should be kept optimum because any excess urea may result in residual carbon, whereas incomplete combustion results when the urea content is deficient.

The physical characteristics of the YBCO powder generated through this technique showed improved properties such as high bulk and green densities. This is accomplished by the good particle size distribution of the powder.

IV.7 Conclusion

1. YBCO powder with good sinterability has been prepared for the first time by a fast and novel synthesis route.
2. Particles are mostly rod like with average particle size less than 4 microns, surface area of $42 \text{ m}^2/\text{gm}$ and can be compacted to above 55% density at 150 MPa. Sintered density as high as 88% have been obtained.
3. The urea-nitrate decomposition method is highly exothermic and hence reaction kinetics is very fast. Therefore, the formation of BaCO_3 is minimum which results in early formation of phases.

References

1. A.G. Merzhanov and I.P. Borovinskaya, Dokl. Chem. (Eng. Transl.), 204(2) (1972) 429.
2. Y. Miyamoto, M. Koizumi and O. Yamada, J. Am. Ceram. Soc., 67(11) (1984) C224.
3. R. Pampuch, J. Braloscorski and E. Walasek, Ceram. Int., 13(1) (1987) 63.
4. Z.A. Munir and J.B. Holt, J. Mater. Sci., 22(2) (1987) 710.
5. J.J. Kingsley and K.C. Patil, Mater. Lett., 6(11,12) (1988) 427.
6. H.K. Varma, P. Mukundan, K.G.K. Warriier and A.D. Damodaran, J. Mater. Sci. Lett., 9(4) (1990) 377.
7. P.M. Vipin, V.V. Sanjaynath, H.K. Varma, K.G.K. Warriier and A.D. Damodaran, J. Eur. Ceram. Soc., 5(4) (1986) 233.
8. A.M. Wynne, J. Chem. Educ., 64(2) (1987) 180.
9. J.J. Kingsley, Ph.D. Thesis, Indian Institute of Science, Bangalore, India (1990).
10. D.R. Clarke, T.M. Shaw and D. Dimos, J. Am. Ceram. Soc., 72, (1989) 1103.

CHAPTER V

MICROWAVE PROCESSING OF YBCO

V.1 Introduction

V.1.i. Microwave Dielectric Heating

The microwave dielectric heating is because of the ability of an electromagnetic field to polarize bound charges in a material and the inability of their polarization to follow this oscillating electric field of the electromagnetic radiation. Microwave region lies in the electromagnetic spectrum between infrared and radio frequencies with a wavelength of 1 mm to 1 meter corresponding to the frequencies from 0.3 to 300 GHz. When a material is exposed to an electromagnetic radiation, the total polarization affected by that will be the sum of a number of polarization mechanisms,

$$\text{ie. total polarization } \alpha_t = \alpha_e + \alpha_a + \alpha_d + \alpha_i \quad \textcircled{1}$$

Where α_e is the electronic polarization arising from the alignment of electrons around the nuclei, α_a , the atomic polarization arising from the relative displacement of charge within the nuclei, α_d represents the orientation or dipolar polarization due to the orientation of permanent dipoles and

This work was published

* *Journal of American Ceramic Society, (in press).*

* *Japanese Journal of Applied Physics Letters, 31 5A (1992) L543.*

α_i is the interfacial polarization due to the building up of charges at interface. The latter two mechanisms have got much importance when the material is experienced by an electromagnetic wave at the microwave range. Since time scale for the polarization and depolarization are much faster than microwave frequencies their effects are not contributory to the dielectric heating of the substance. But the time scale associated with α_d and α_i are comparable to microwave range.

Actually microwave absorption is due to the phenomenon in which polarization of dipoles and consequently its oscillation with the microwave frequency. The torque they get during this process makes the oscillation frequency of the dipoles lag behind the microwave frequency. In other words when the applied microwave frequency at its maximum strength, the polarization will be rising only. As it rises to a maximum, their field decreases. This lag can be visualized as absorption of microwave frequency and consequent heating of the material.

V.1.ii. Microwave interaction with matter

The dielectric heating in the microwave region of any material depends on two intrinsic properties of the materials, i.e. dielectric constant ϵ' and dielectric loss ϵ'' , which is a measure of how much effectively it can convert the radiational energy into heat. The loss mechanism can be resolved into one factor

geometry etc, and decrease with increase in wave length, there must be a compromise between all these parameters before designing a microwave absorption set up.

Finally, as both ϵ' and loss tangent ($\tan \delta$) are the two most important parameters that describe the behaviour of a dielectric under the influence of a microwave field, they both affect the power absorbed and the half-power depth and thus influence the volumetric heating behaviour in a given material. Both ϵ' and $\tan \delta$ change with temperature, the latter being generally more sensitive. It is this property of $\tan \delta$ which gives rise to very rapid rise in temperature ("thermal run away") for some materials(1-6).

A number of polar liquids are good microwave absorbers while solid materials especially ceramics show good microwave absorption characteristics in general(7,8). Microwaves cannot heat metals because metals are good reflectors(9). This is also due to their small penetration depths (narrow band semiconductors are also fall in this category). The skin depth is the depth at which the dielectric field drops to 0.368 of its surface value,

$$\text{ie., } \delta = \frac{1}{\sqrt{\pi f \mu \sigma}}$$

where $\mu \approx \mu_0$, which is permittivity of free space, σ conductivity. For example, in a metal like copper, skin depth is 1 cm at a frequency of 60 Hz which decreases to $1 \mu\text{m}$ in the microwave

range.

Ceramics are, in general, good microwave active materials and in some cases the high level of microwave absorption leads to thermal runaway in materials like doped ferrites, CuO, Co_2O_3 , NiO etc.

Recently microwave processing has received increased attention in ceramic material processing because of several reasons like (1) significant reduction in manufacturing cost due to savings in energy and time (2) improved product uniformity, (3) unique microstructure, (4) yield etc.(10-16). As shown by Roy et al.(11) today microwave energy is being used in process control where it is used to detect moisture, defects and pores. It is also used in plasma processing where the dielectric heating is effectively made use of in the synthesis of powders, in sintering and in solid state processing. It is also used for binder burnout and drying of green ceramic bodies.

V.1.iii. Ceramic superconductor powder synthesis

In 1988, Tinga(17) showed how the dielectric constant and loss factor vary with temperature in the case of CuO. As ϵ' and $\tan \delta$ increases with increase in temperature CuO is a very good microwave absorber. The Fig.V.1 shows the dielectric properties of CuO as a function of temperature.

As cited above, copper oxide couple with microwave energy exceptionally well and this property was first used by

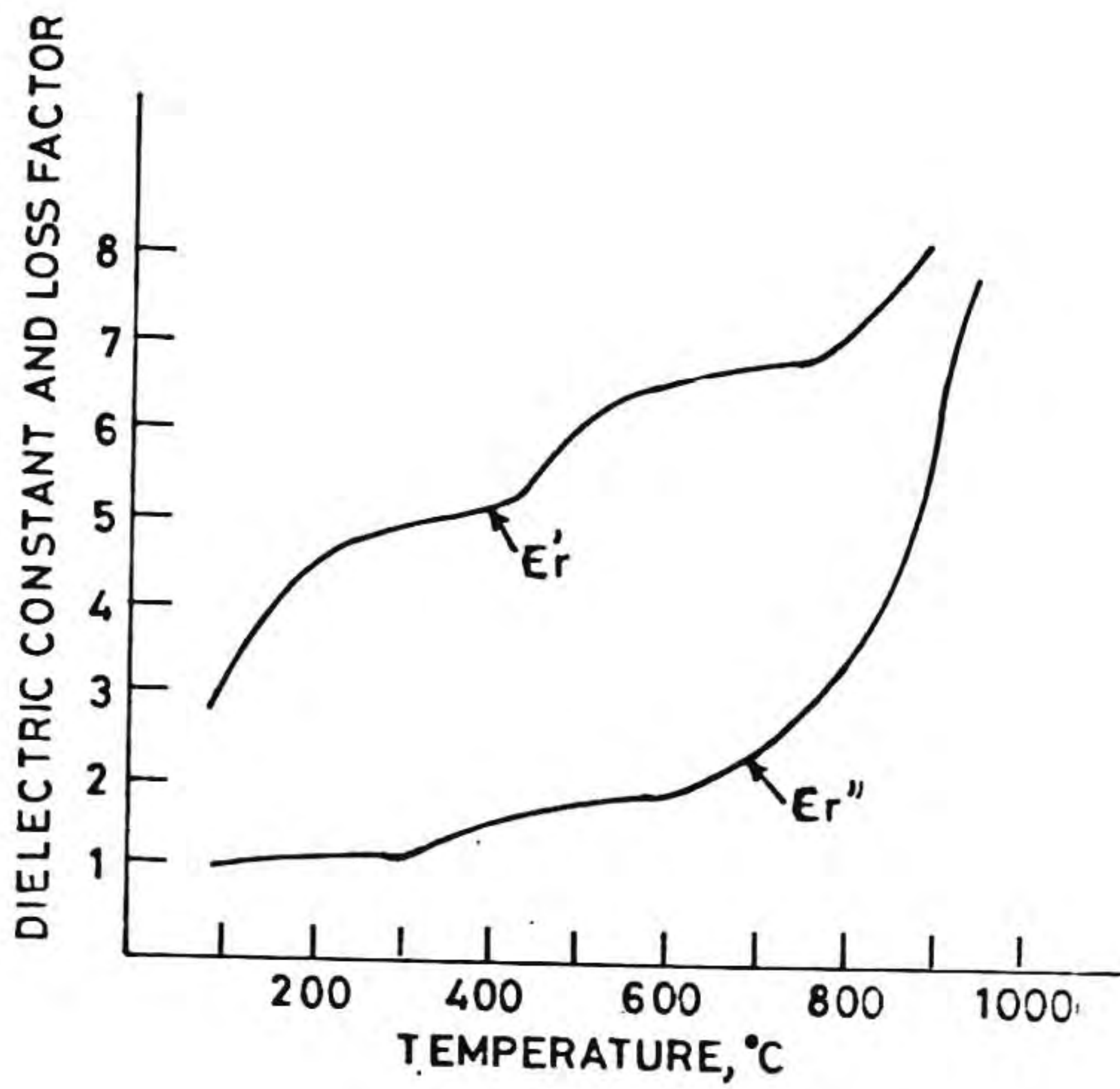


Fig. V.1 Dielectric properties of CuO as a function of temperature. ϵ_r' dielectric constant, ϵ_r'' dielectric loss factor

Baghurst et al.(18) to prepare mixed oxide high Tc superconductors. He obtained $\text{La}_{1.5}\text{Sr}_{0.5}\text{CuO}_4$ and $\text{YBa}_2\text{Cu}_3\text{O}_{7-\delta}$ from the mixture of component metal oxide/carbonate when treated with microwave radiation at a power level of 500 W. The time required for exposure to microwaves in the above experiment was 20-30 minutes with intermediate grinding before obtaining nearly single phase compounds. The regrinding process is an integral part of this process because of inhomogeneity in the mixing of component oxides. To overcome some of these problems associated with long exposure time and repeated grinding operation, a new approach has been adopted and presented in this chapter.

This chapter deals with the preparation of YBCO from the mixture of nitrates for the first time of Ba, Cu and Y when exposed to microwave energy of 600 W in a domestic oven for 4 minutes. In the above mixture, copper nitrate absorbs microwave energy efficiently and exothermically decomposes to oxide within two minutes and the already heated copper oxide couples further effectively with microwave and raises the temperature to very high levels. Also during the decomposition stage, the whole mass melts and foams due to the evolution of gases. This makes the final product more voluminous and fluffy in nature. After the exposure of 4 minutes, the resultant product was more or less uniform. The powder characteristics at various intervals of time of exposure, phase purity, surface area, sinterability and electrical and magnetic properties of the

sintered YBCO are also dealt with. In the latter section of this chapter some melt texturing process done on this precursor samples are given.

V.1.iv. Microwave oven

The main features of a modern microwave oven are a magnetron, wave guide and a microwave cavity where the material to be microwave-treated should be placed. The magnetron is the most important part where the microwaves are generated. It is a simple thermionic diode with an anode consisting of a number of cavities. As the cathode is heated, electrons are attracted towards anode and the anode cavities are turned to oscillate at the microwave frequency. These microwaves are guided through the wave guide, a rectangular channel of metal sheet, to the microwave cavity or chamber. The commercially available microwave oven has an output power of 600 W and produces microwave in the frequency 2.45 GHz. Most microwave ovens are supplied with automatic cutoffs and with a turntable which ensures that an average field experienced by the sample is approximately the same in all directions.

V.2 Experimental

Mixture of nitrates of yttrium, barium and copper in 1:2:3 stoichiometry was mixed in an agate mortar in the presence of n hexane to a paste. Typically 2.27 gm of $Y(NO_3)_3 \cdot 5H_2O$, 3.24 gm $Ba(NO_3)_2$ and 4.49 gm of $Cu(NO_3)_2 \cdot 3H_2O$ were used. This was

transferred into an alumina crucible and was introduced into the microwave oven. The blue green colour of the mixture of nitrates was turned to black within about 240 seconds. In another set of experiment, the samples were exposed for 1-4 minutes to study the phase formation. The one after being exposed for 4 minutes was heat treated in flowing oxygen for 4 hours at 900°C. The precursor powder was pressed into rectangular rods of dimension 15 mm x 4 mm x 2 mm and sintered at 940°C for 4 hours. These samples were tested for electrical properties.

V.3 Methods

Density, chemical analysis, particle size analysis, SEM, XRD, Surface area and electrical measurements were done as described in Chapters II and III.

V.4 Results and discussion

The mixture of nitrates after 120 seconds of microwave exposure starts decomposing with evolution of brown fumes of nitrogen oxides, while the solid partially melts and foams up. On further exposure to another 120 seconds, the material turns into a black mass. The Fig.V.2a shows the microwave oven and the experimental set up. The precursor as formed in the crucible is shown in Fig.V.2b. The 123 stoichiometric mixture of nitrates when subjected to thermal decomposition showed a stepwise pattern over a range of 750°C (TGA Fig.V.3) while the decomposition is complete at as low as 240 seconds in the case



Fig. V.2(a) Experimental set up



Fig. V.2(b) Precursor powder inside the crucible

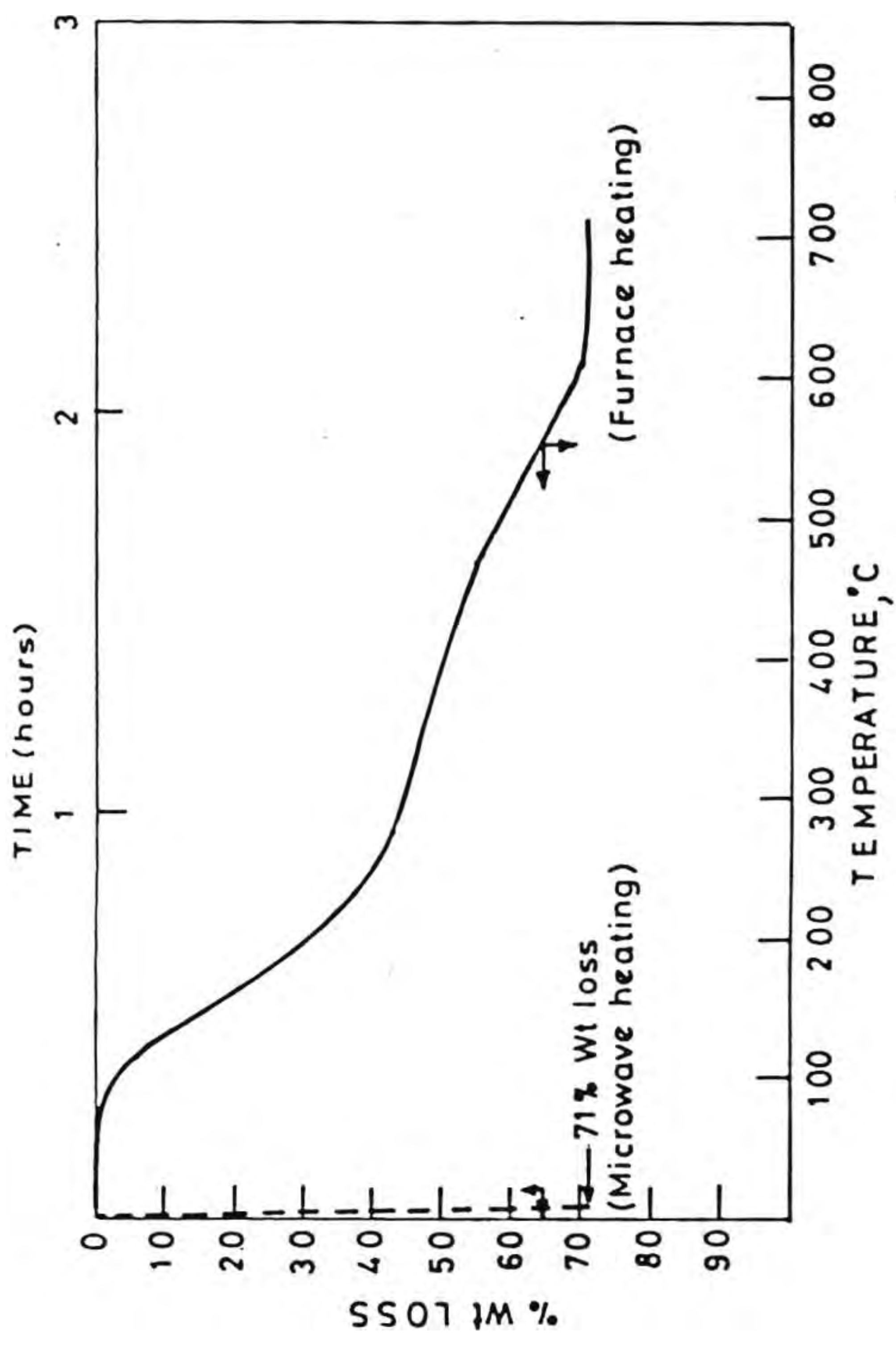


Fig. V.3 Weight loss of mixture of nitrates of 123 stoichiometry

of microwave heating. There was hardly less than 1% further weight loss even when heating above 800°C for the microwave exposed sample in a muffle furnace. This shows the completeness of microwave decomposition procedure. When observed through an optical pyrometer it was seen that the temperature reaches above 800°C within 240 seconds. However it was not possible to record the progressive weight loss with time in the present case in view of the fast kinetics of decomposition. Janney and Kimrey(19) estimated the apparent activation energy in the case of sintering of Al_2O_3 and found out that the value is one third of that of conventional sintering when microwave sintering was employed. This large difference in activation energy is explained due to the high diffusion rates induced in the microwave field. Gibson et al.(20) showed that microwave radiation greatly accelerate the diffusion of ethylene oxide (EO) in polymeric materials compared to conventional heating at the same temperature. The enhanced diffusion is due to excess in translational kinetic energy of the diffusant molecules in microwave field. The fastness in the decomposition of nitrates and the product formation can be explained using the above propositions in the present case as well. The XRD patterns of the mixture of nitrates after the exposure to microwave energy every minute upto 4 minutes and after heat treatment at 900°C for 4 hrs are presented in Fig.V.4.

There is no indication of free copper nitrate in the sample exposed for 1 minute (Fig.V.4a). Yttrium nitrate could

not be observed since the major peaks are shown outside the present range covered. Since there is no observation of Y_2O_3 peak, it is sure that yttrium nitrate does not have undergone any decomposition at this stage. The barium nitrate peaks are clearly shown in the pattern. However as the exposure time increases, the barium nitrate ($2\theta=18.9$) and copper oxide ($2\theta=38.7$) peaks get reduced followed by formation of 123 phase at as early as 3 minutes (Figs.V.4b and V.4c). There are more amounts of Y_2O_3 , Y_2BaCuO_5 and $BaCuO_2$. After exposure for 4 minutes major peak represents 123 and very small amount of 211 and $BaCuO_2$ phase. When the sample exposed to 6 minutes the peaks shown to that of a melted 123 sample, comprises of a number of compounds in this ternary system. This clearly shows the significance of optimum exposure time of 240 seconds. This sample when heat treated at $900^\circ C$ for 4 hours the XRD shows a pure 123 phase pattern.

According to the previous report(18), when the starting mixture contains CuO , Y_2O_3 and $Ba(NO_3)_2$, no free barium nitrate has been noted after 5 minutes of exposure which is in agreement with the present observation. But the 123 phase appears along with traces of 211 phase in such cases, only after sufficient exposure for more than 25 minutes. However it is interesting to note that similar observation is made after exposure to as low as 240 seconds in the present case. The powder had a bulk density of 2.25 gm/cm^3 and could be compacted to a green density of $3.92/\text{cm}^3$, when compacted to rectangular strips of dimension 15

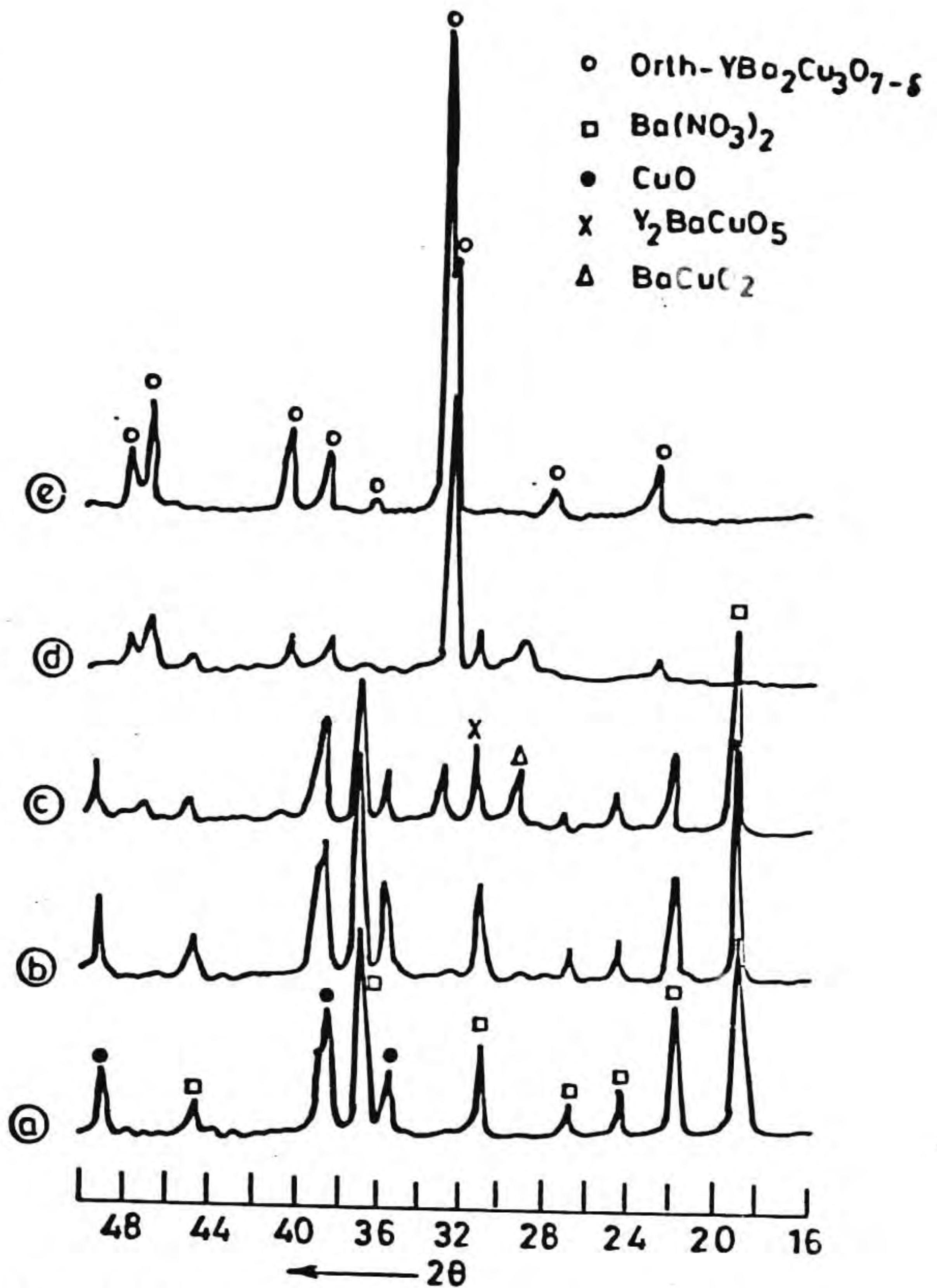


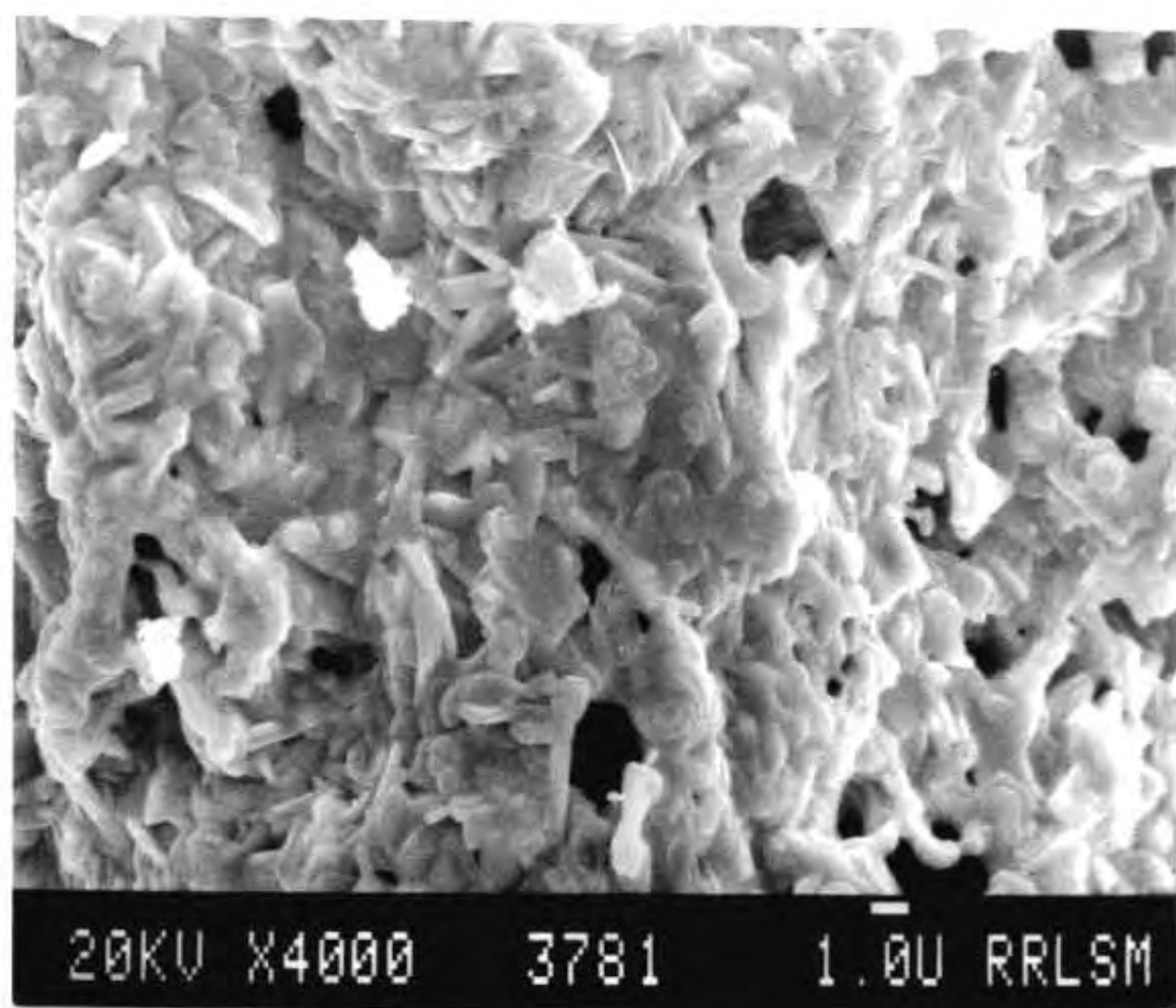
Fig. V.4 XRD patterns of the mixture of nitrates of Y, Ba and Cu after exposing to microwave for (a) 1 minute, (b) 2 minutes, (c) 3 minutes, (d) 4 minutes and (e) after heating the sample d at 900°C for 4 hours

x 4 x 2 mm at a pressure of 100 MPa. This green compaction density is 61% of theoretical density of 123 phase. When sintered the green strips at 940°C for 4 hours, the density observed was above 90% of the theoretical value.

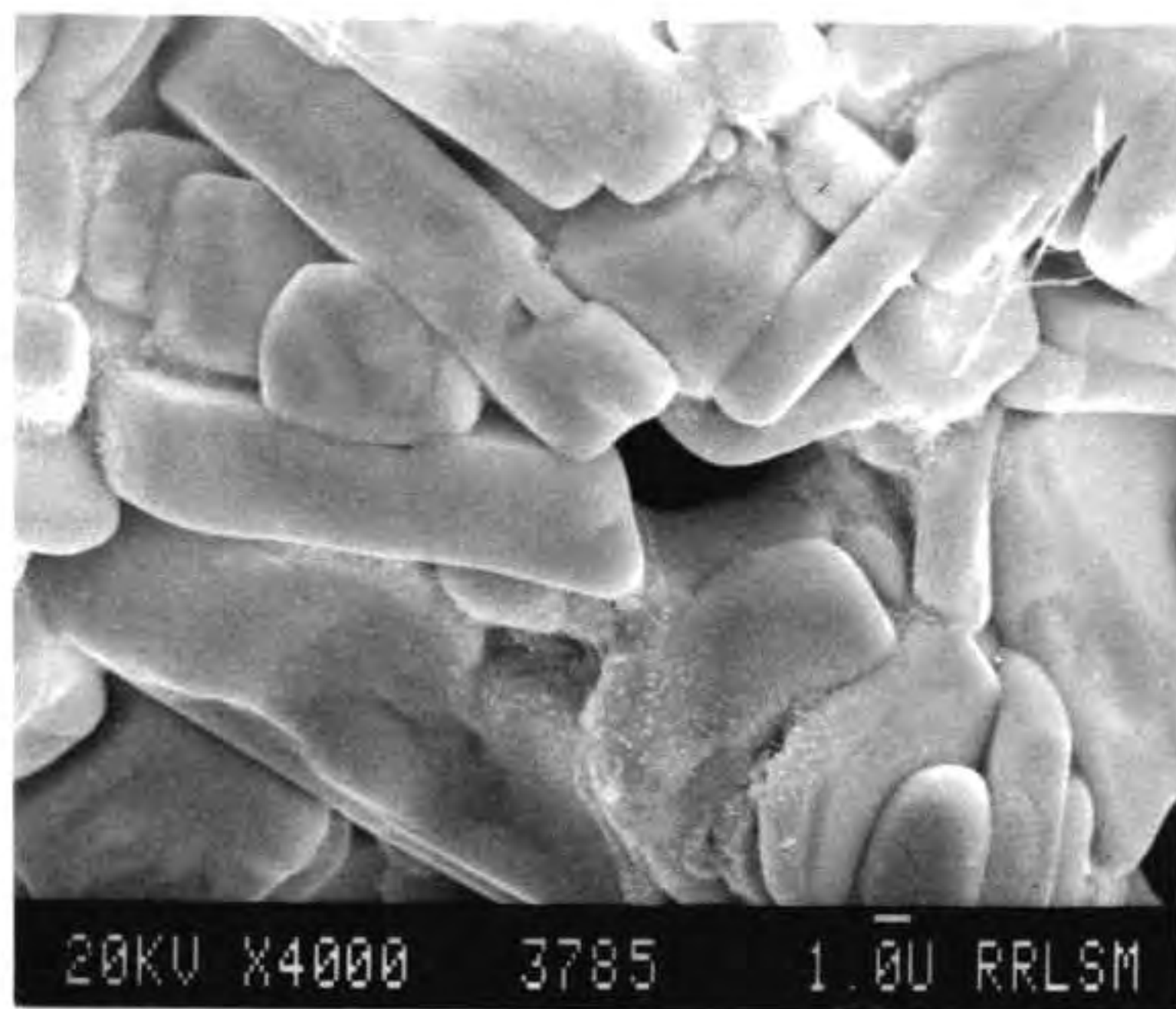
Morphological features of the powder sample obtained after microwave exposure reveals rod like formations of 123 phase. The rods are seen as embedded over a gel network showing the gel formation of mixed nitrate prior to decomposing to corresponding oxides and finally 123 phase. These particles are very fragile and could be ground easily. The sample in Fig.V.5a on annealing at 900°C for 4 hours developed large grains without showing any intermediate phase (Fig.V.5b) normally observed in samples calcined at shorter times in the conventional processes, while the ground sample powder (Fig.V.5c) sintered to high density with comparatively smaller grains (Fig.V.5d). The sample showed reasonable evidence to brittle fracture. Using the four probe technique, the critical temperature was observed and the T_c was 91 K (Fig.V.6). The transport J_c of the bulk pellet was 105 A/cm^2 .

V.5 Conclusion

The present processes described above has shown that microwaves from a domestic oven could be utilized to prepare 123 superconductors with considerable advantages. The powder could be prepared within a short time of 240 seconds and an annealing time of 4 hours, which are much lower than the conventional

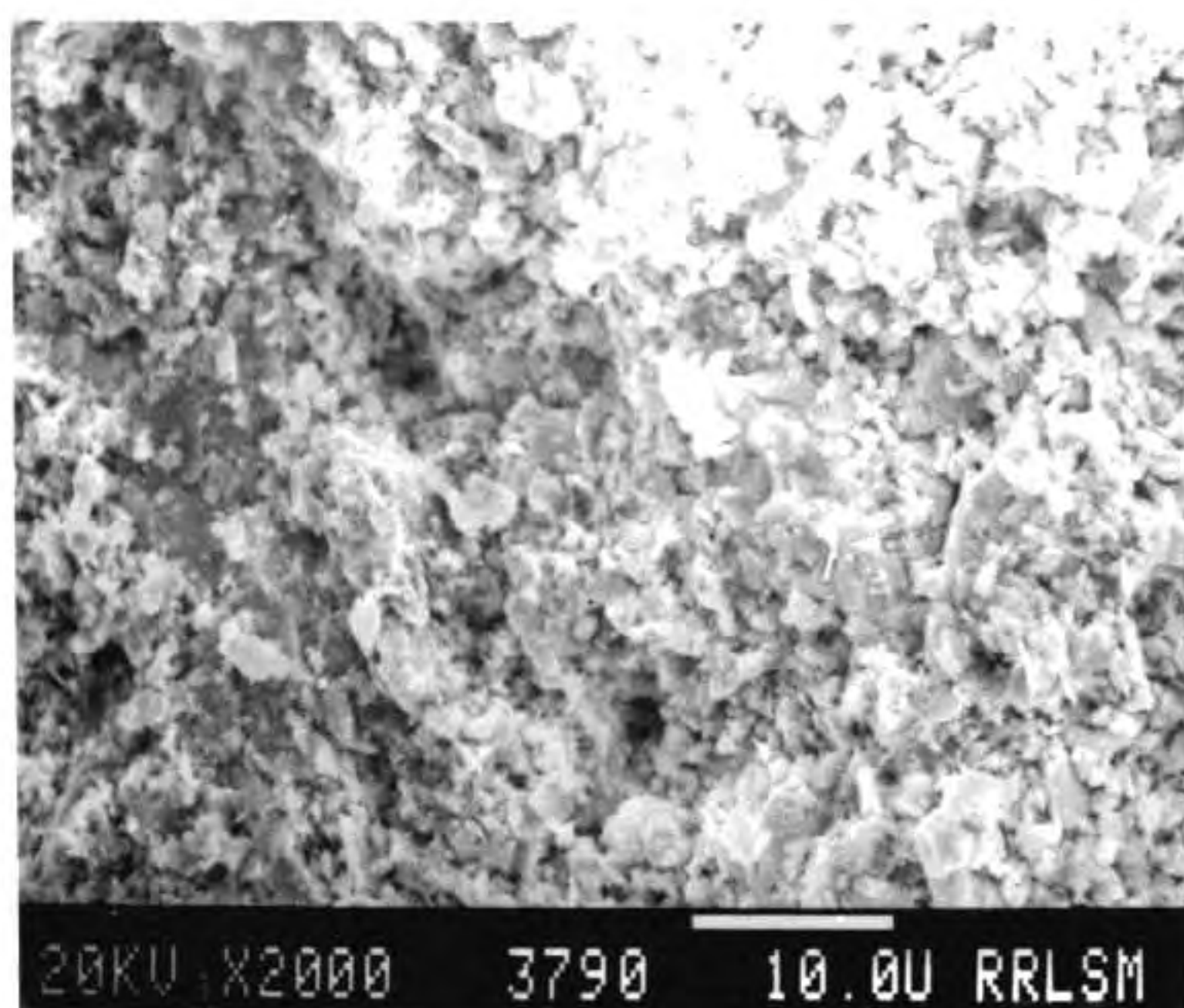


(a)

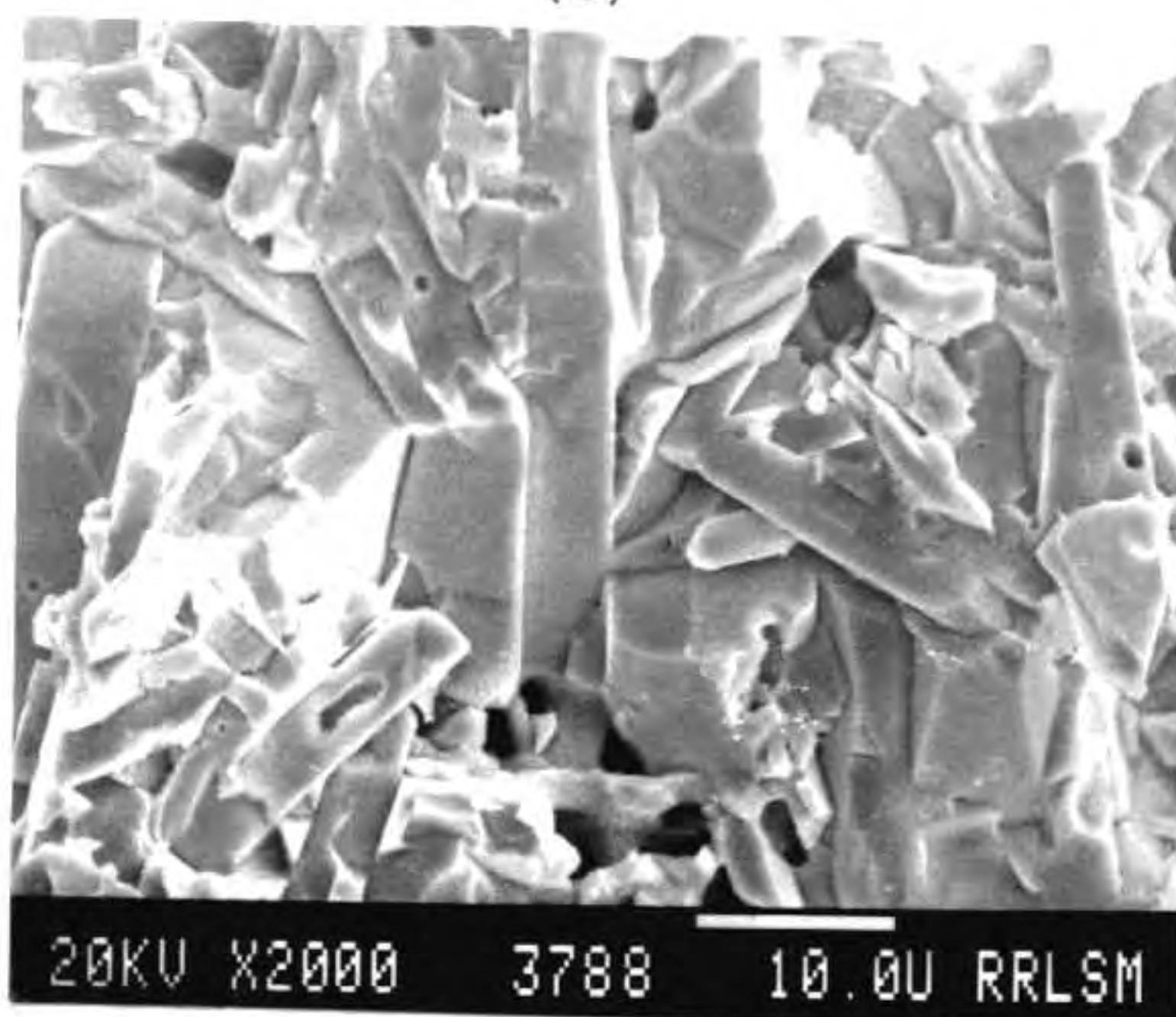


(b)

Fig. V.5 Scanning electron micrograph of sample after exposure to microwave (a) after 4 minutes, (b) above sample after annealing at 900°C for 4 hours



(c)



(d)

Fig. V.5 Scanning electron micrograph of sample after exposure to microwave (c) sample 'a' after grinding and (d) fractured surface of the sintered specimen (940°C/4 hours)

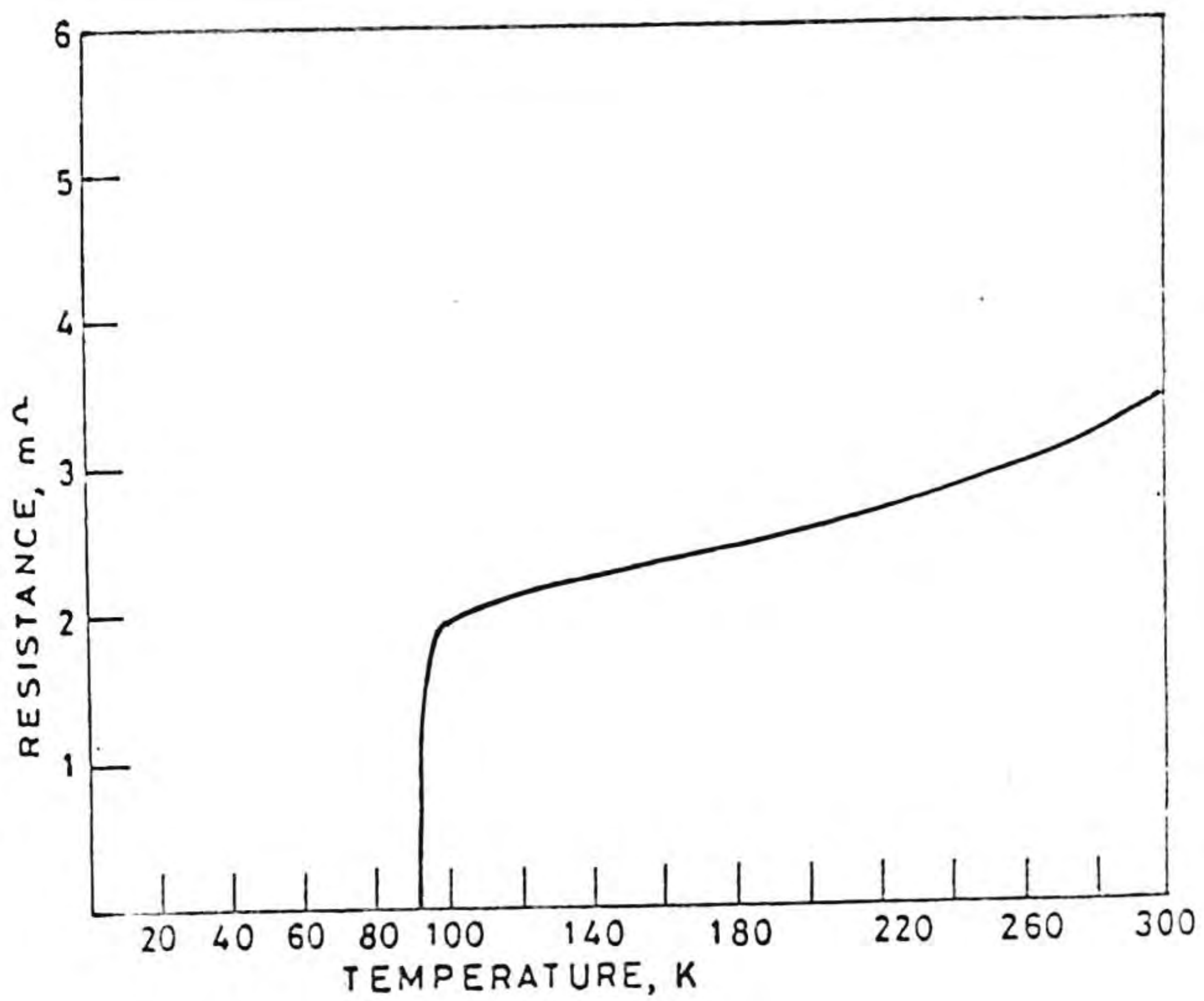


Fig. V.6 Temperature vs resistance curve of sintered 123 sample

methods. This method is unique because of the simplicity of the process and energy efficiency.

V.6 Post sintering treatments in microwave derived YBCO powder

After the discovery of YBCO compound, efforts have been made to prepare the same to improve the electrical, magnetic and microstructural features by either suitable substitution, preparation techniques or by suitable processing methods. The major problems of low critical current density and magnetic features in bulk sintered materials are identified due to the occurrence of weak links and lack of adequate flux pinning sites. The presence of weak links at the grain boundaries and flux line movement within grains, leads to low J_c values especially in strong magnetic fields(21). On the other hand, in thin films, very high J_c value in excess of 10^6 A/cm² at 77K has been achieved(22). It is established that the weak links are present at the grain boundaries and certain specially oriented grain boundaries may not behave as weak links(23). Such boundaries are low angle boundaries. So one major attempt to decrease the weak link behaviour is by introducing enhanced low angle boundaries instead of high angle boundaries usually associated with randomly oriented polycrystals of high T_c bulk sintered superconductors. This can be achieved by preferential alignment of grains parallel to the a-b conduction plane. The flux melting phenomenon associated with the high T_c materials is another detrimental factor as far as J_c at high magnetic fields

is concerned. The possible way of pinning these flux lines within the grains is by effective dispersion of uniform defects, or impurities such as non superconducting second phase compositions or by irradiation with high velocity particles such as neutrons or positrons(21). To overcome the problem associated with weak link and flux melting behaviour, two useful techniques can be adopted ie., melt texturing and zone melting(24-27). In the former method, the YBCO phase is allowed to melt, fully or partially, incongruently at a temperature range of 1000-1100°C and very slow cooling of the melt to facilitate aligned or textured growth of the large YBCO crystallites. YBCO peritectically decomposes to solid Y_2BaCuO_5 and a CuO rich liquid. In this process, the textured material contains 211 phase as a major second phase precipitate within the YBCO grains. If no temperature gradient (melt texturing process) is applied, the texturing will comprise only in large domains but these domains may not be arranged in the texturing direction so as to get a-b plane orientation all through the sample dimension.

Another way of getting high order of orientation on YBCO grains is by melt texturing in a temperature gradient (zone melting process). Because of the natural preference to crystal growth in the a-b direction of YBCO crystals, the melt processing leads to crystallites with large domains containing parallel plates if sufficiently slow cooling rates are applied. The nucleation and subsequent growth within the bulk sample

result in the formation of number of such large domains. This introduces many high angle boundaries in between these domains. Also melt texturing and quenching methods are usually associated with deformation of the original shape. To obtain aligned microstructure over extended distances (ie. in the order of sample length), recently zone melting technique has been demonstrated as one which would handle longer lengths of the sample. Very slow rate of sample movement in the heating zones and the presence of chemical inhomogeneities are found to be some of the significant aspects in this process(28). Zone melting procedure already reported in the literature have been on vertically loaded samples, while it would be better to handle low melt viscosities and liquid phase in stable horizontal sample arrangement with preferentially a moving heating zone. Further it would be adopting a faster zone movement (20-30 mm/hour) and achieving the desired microstructure by repeated operations.

V.6.i Melt texturing process

V.6.i.a Experimental:

The mixture of nitrates of Y, Ba and Cu exposed to microwave for 240 seconds as described in the above section, was crushed in an agate mortar. The powder was compacted to circular discs of 12 mm dia and 5 mm thickness at a pressure of 100 MPa. The green density was 55% theoretical. The pellets were placed in a bed of YBCO powder on an alumina substrate and placed inside

a tube furnace equipped with a programmable temperature controller. The pellet was melt processed according to the firing schedule as given in Fig.V.7. These pellets were taken out and observed for microscopy and electrical properties.

V.6.i.b Results and discussion:

Various versions of melt techniques have been reported recently, all based on rapidly heating the YBCO sample above peritectic melting point followed by slow cooling, all of which are characterized by extremely slow cooling rates. In the present study the samples were allowed to melt at 1050°C (keeping at the same temperature for 1 or 2 hours) and a slow cooling from 1020°C to 980°C by 1°C/hour, followed by oxygen annealing as given in Fig.V.7. Figure V.8 shows the magnetic levitation suspension effect shown by a melt textured YBCO superconducting pellet prepared from a microwave derived YBCO powder. The sample is suspended in air beneath a rare earth magnet because of two opposing effect, ie. diamagnetic repulsion due to the bulk of the superconducting part of the $\text{YBa}_2\text{Cu}_3\text{O}_{7-\delta}$ compound and the attractive effect by the magnetic flux induced in second phase inclusions (mainly 211 phase) within grains and grain boundaries. Stacking faults (in the order of 1-3 mm thick) and fine twins (10-50 mm spacing) also contribute to the flux trapping while the specimen is cooled in liquid nitrogen under a magnetic field. The scanning electron microscopic pictures are provided in Fig.V.9. The large domains

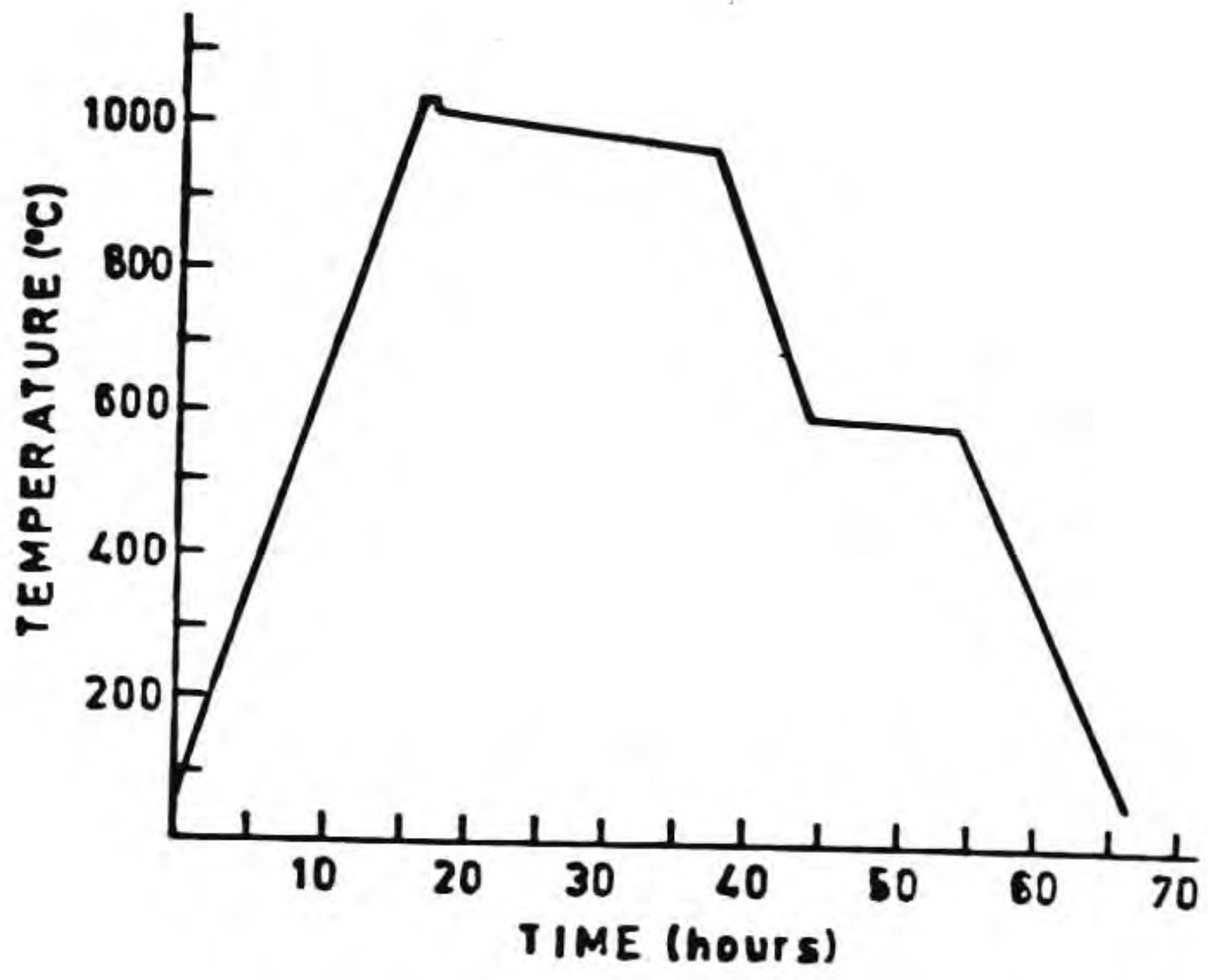


Fig. V.7 Heating schedule for the melt texturing of the microwave derived sample

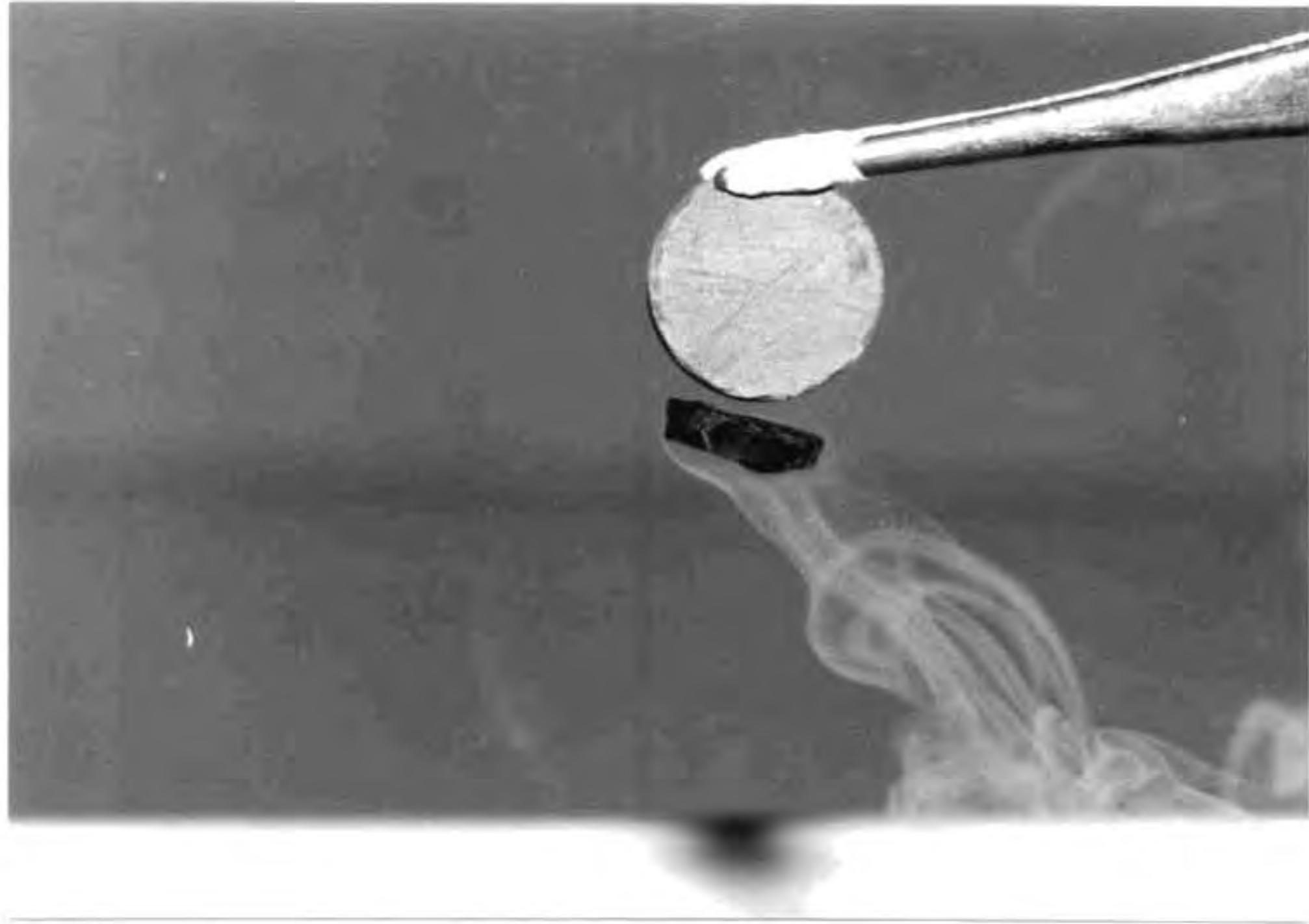


Fig. V.8 Suspension of melt-textured YBCO superconductor sample beneath a rare earth magnet

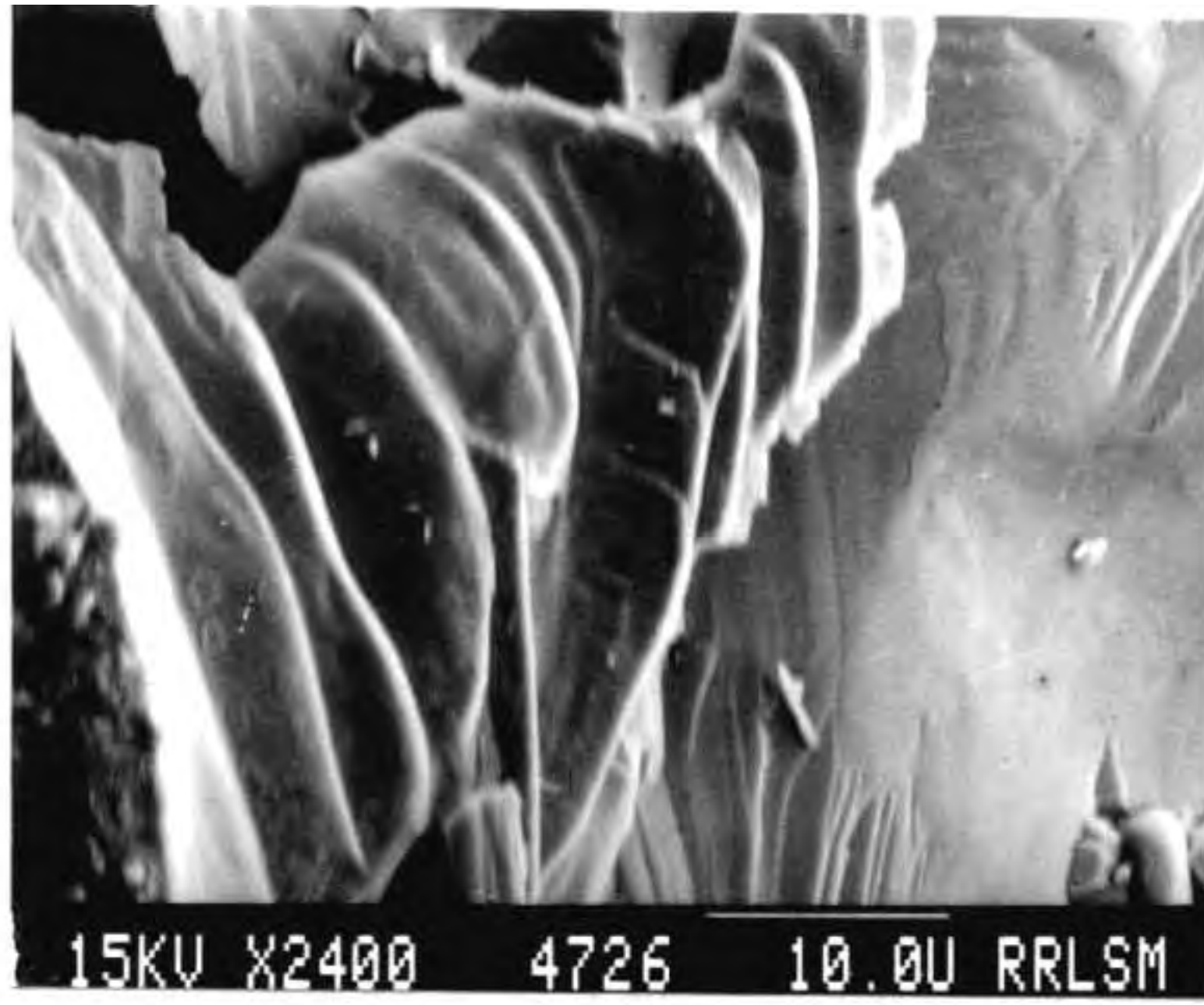
of textured YBCO is seen in the Fig.V.9a. The fractograph in Fig.V.9b shows the large (500-1000 μm) platelets stacked directionally one over the other. The optical photograph of the polished surface of the specimen revealed the large textured domains arranged in different orientation. The texturing within these domains showed the microcracks formed as a result of the various anisotropic thermal contraction and expansion during the annealing step. Also there is the presence of a number of isolated particles of 211 phase which does not interfere with the super current flow except for the volume fraction effect.

The T_c of the melt textured samples does not change from the value of 90 K as in sintered sample but there is a great leap in the critical current density, i.e., from the 105 A/cm^2 in the sintered sample the transport current measurements done in the melt textured sample showed a current density of 1000 A/cm^2 . Figure V.9c shows a demonstration frictionless bearing fabricated using melt textured YBCO superconductor. As shown in this figure schematically, the attractive force (magnetic drag) due to the trapped flux within the superconducting domains gives the stability of the bearing, the diamagnetic repulsion makes possible the bearing suspended in air.

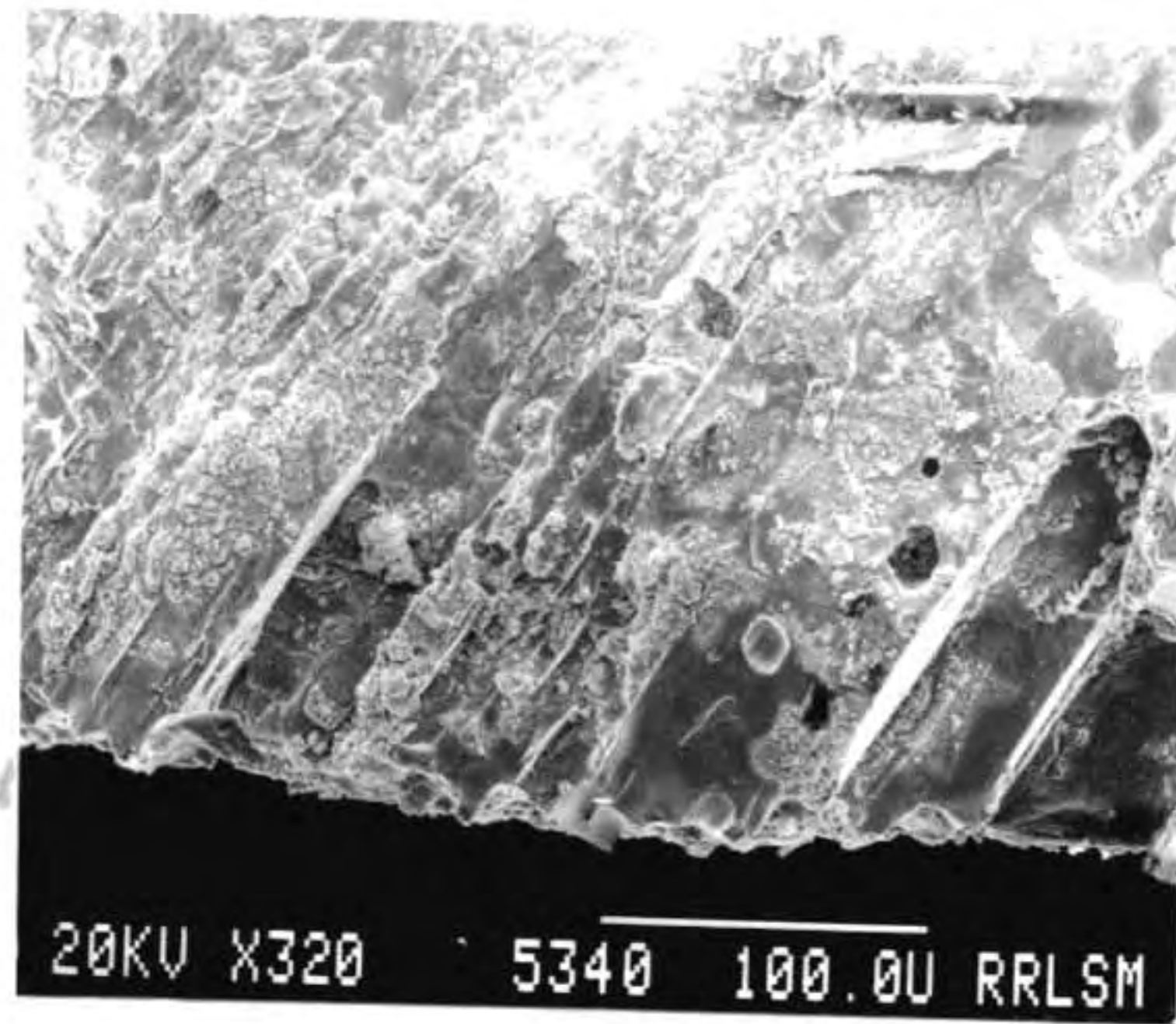
V.6.ii. Repeated Zone Melting Process

V.6.ii.a Experimental

The precursor powder formed by the above described



(a)

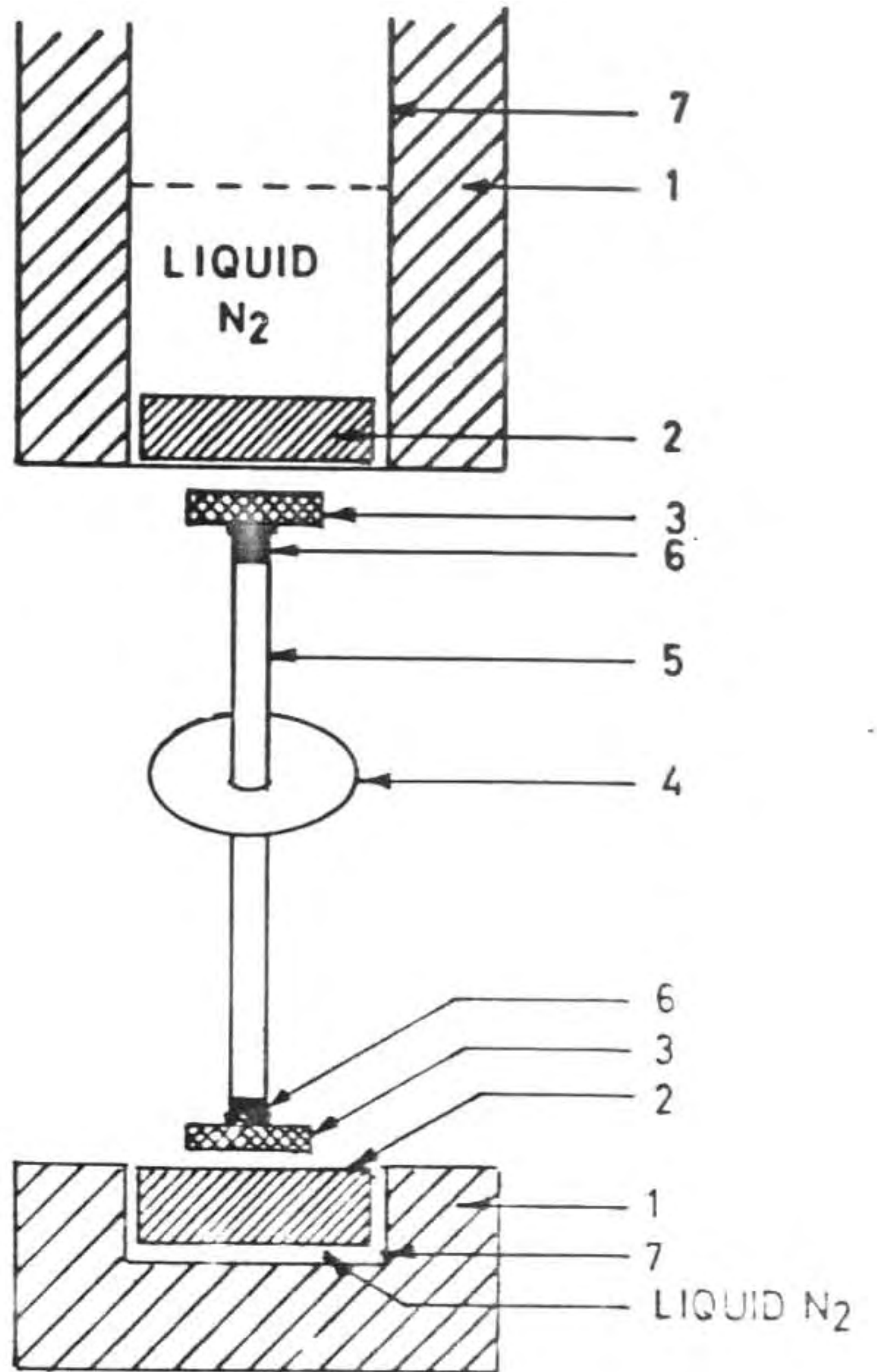


(b)

Fig. V.9 SEM pictures (a and b) of melt textured YBCO superconductor



(i)



(ii)

- 1 INSULATION
- 2 MELT TEXTURED YBCO SUPERCONDUCTOR
- 3 MAGNET
- 4 FLY WHEEL
- 5 TEFLON ROD
- 6 MILD STEEL STUD
- 7 GLASS CONTAINER

Fig. V.9c Frictionless bearing (i) experimental set up and (ii) schematic representation

microwave decomposition technique was pressed into strips of dimension 60 mm x 10 mm x 1 mm in a rectangular stainless steel die. These strips were sintered at 940°C for 5 hours, put on an alumina substrate. The sintered strips kept in the alumina substrate were introduced into the alumina tube of the three zone furnace. The furnace was moved over the alumina tube at a speed of 30 mm/hour. In the present experiment the initial and final zones were kept at 800 and 935°C and the centre zone at 1045°C.

V.6.ii.b Results and discussion:

The zone melting set up used in the present investigation is schematically presented in Fig.V.10. The rate of zone movement is fixed at 30 mm/hour in order that it is many times higher than those reported earlier. However the temperature in the three zones can be separately adjusted at an accuracy level of $\pm 2^\circ\text{C}$. The temperature profile, arrived at after repeated experiments, is also presented in Fig.V.10. The first zone is important in order to reduce thermal shock, and the third zone is important in order to avoid fast cooling, both of which contribute towards reducing microcracks. It is significant to note that YBCO is so sensitive that it may develop microcracks even due to the surface cooling of oxygen during annealing(21).

During the first step of the experiment, the furnace is moved over the sample. The sample is preheated at the rate of 30

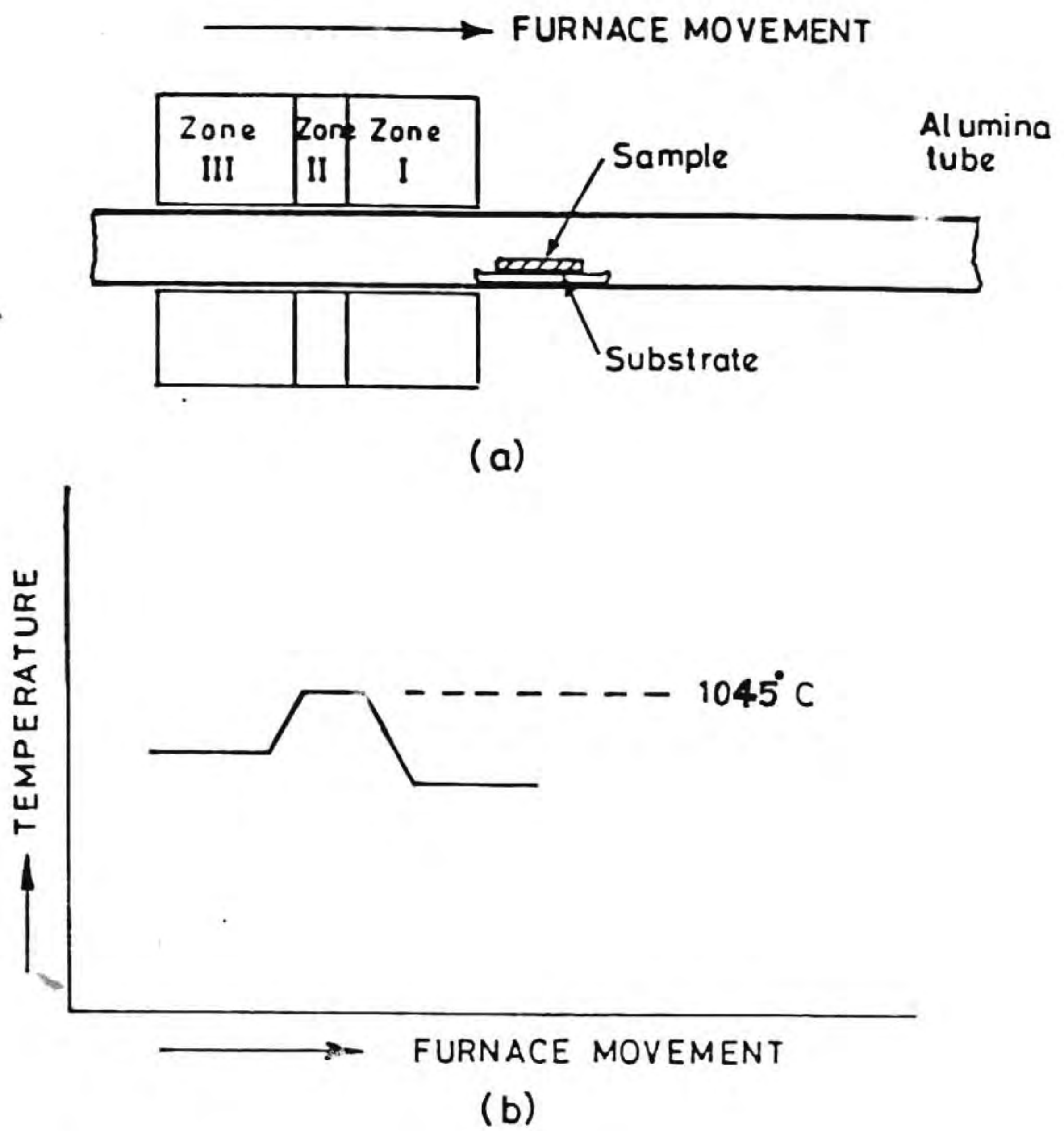
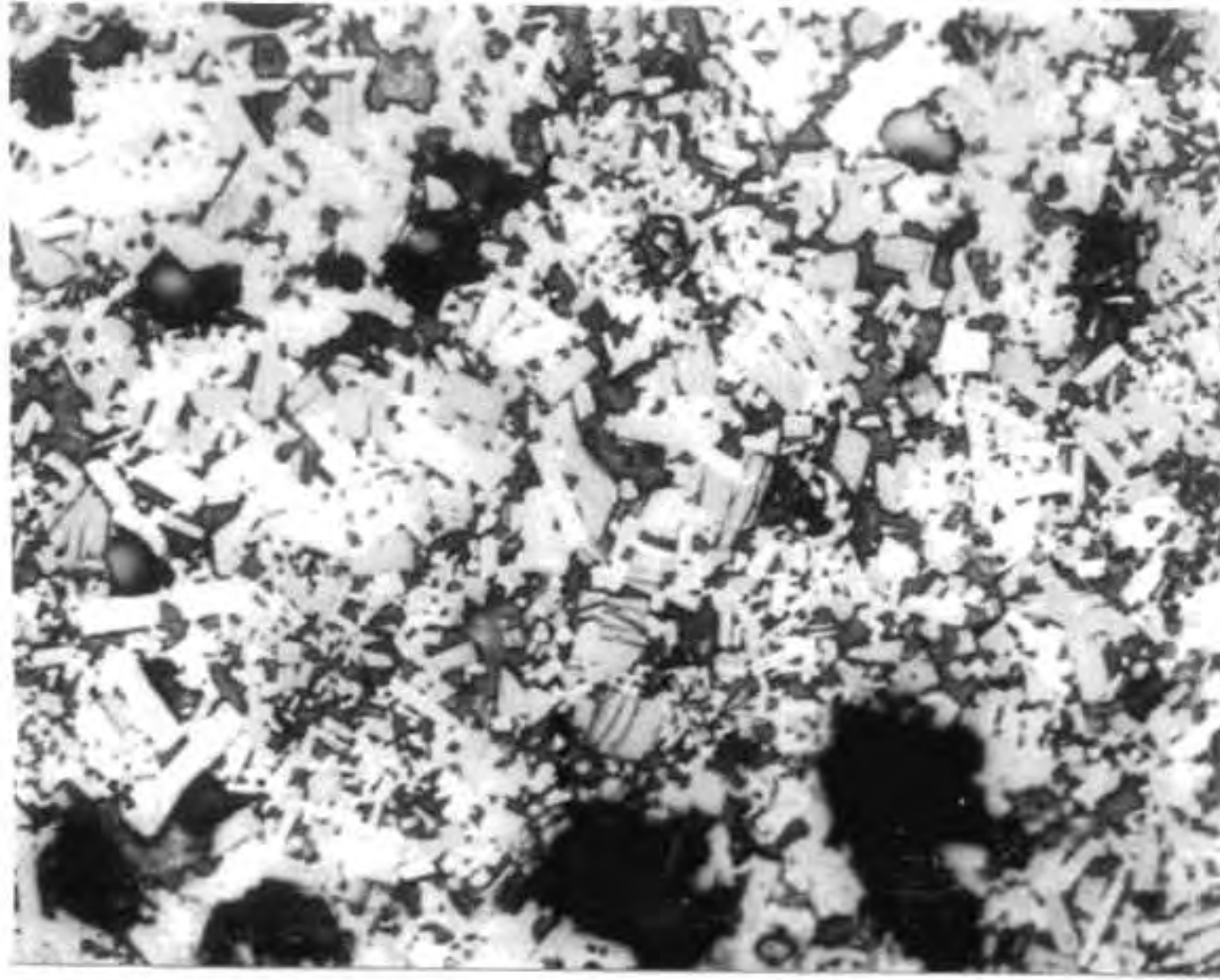


Fig. V.10 (a) Experimental set up and
(b) temperature profile

mm/hour followed partial melting by second zone and the cooling to the temperature of 935°C due to the third zone. Evidently, the whole sample does not melt as in the case of melt texturing experiments. However, repeated operations result in the remaining portions getting melted and the process repeats. In each step certain refinement of the grains and orientation takes place progressively. Optical micrographs of sample surface after the stepwise refinement provided in Figs.V.11a-f show the changes taking place in the randomly oriented dense structure to a final a-b plane oriented. It can be seen that those grains in the various domains, possesses less of intergranular cracks along the a-b plane. Figures V.12a and b show the SEM picture of the fractured surface of zone melted samples (three times). The large oriented grains of YBCO contain small second phase inclusions (211 phase). The zone melted sample after annealing in oxygen shows attractive levitation normally obtained only in the melt textured samples. By suitably selecting appropriate sintered starting microstructure and density and by adjusting the various zone temperatures judiciously, it could be possible to obtain desirable refined microstructures even under faster zone movements. The J_c value obtained in this sample was >1000 A/cm².

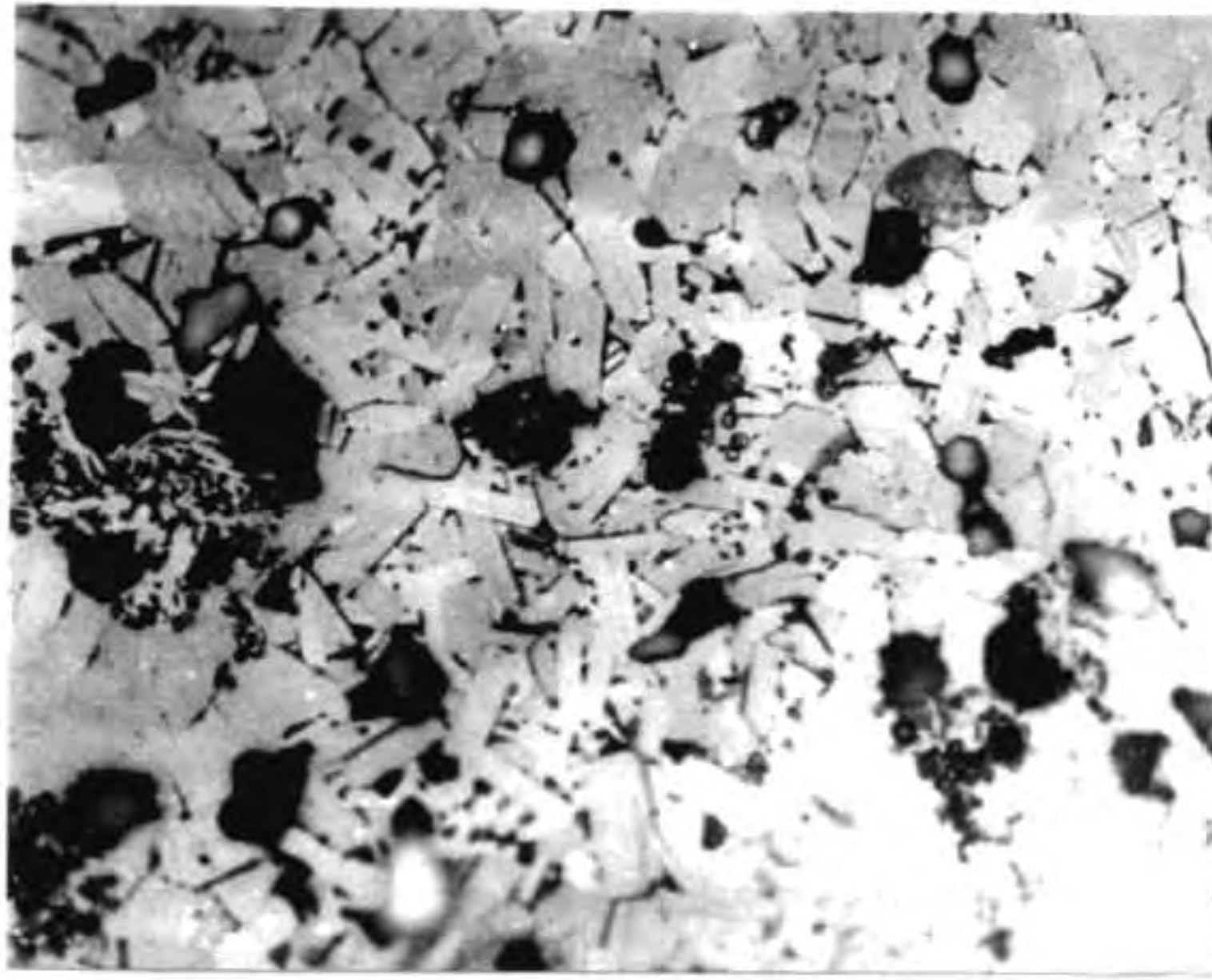
V.7 Conclusion

The rapidly formed YBCO sintered specimens obtained in the microwave decomposition technique could be subjected to



(a)

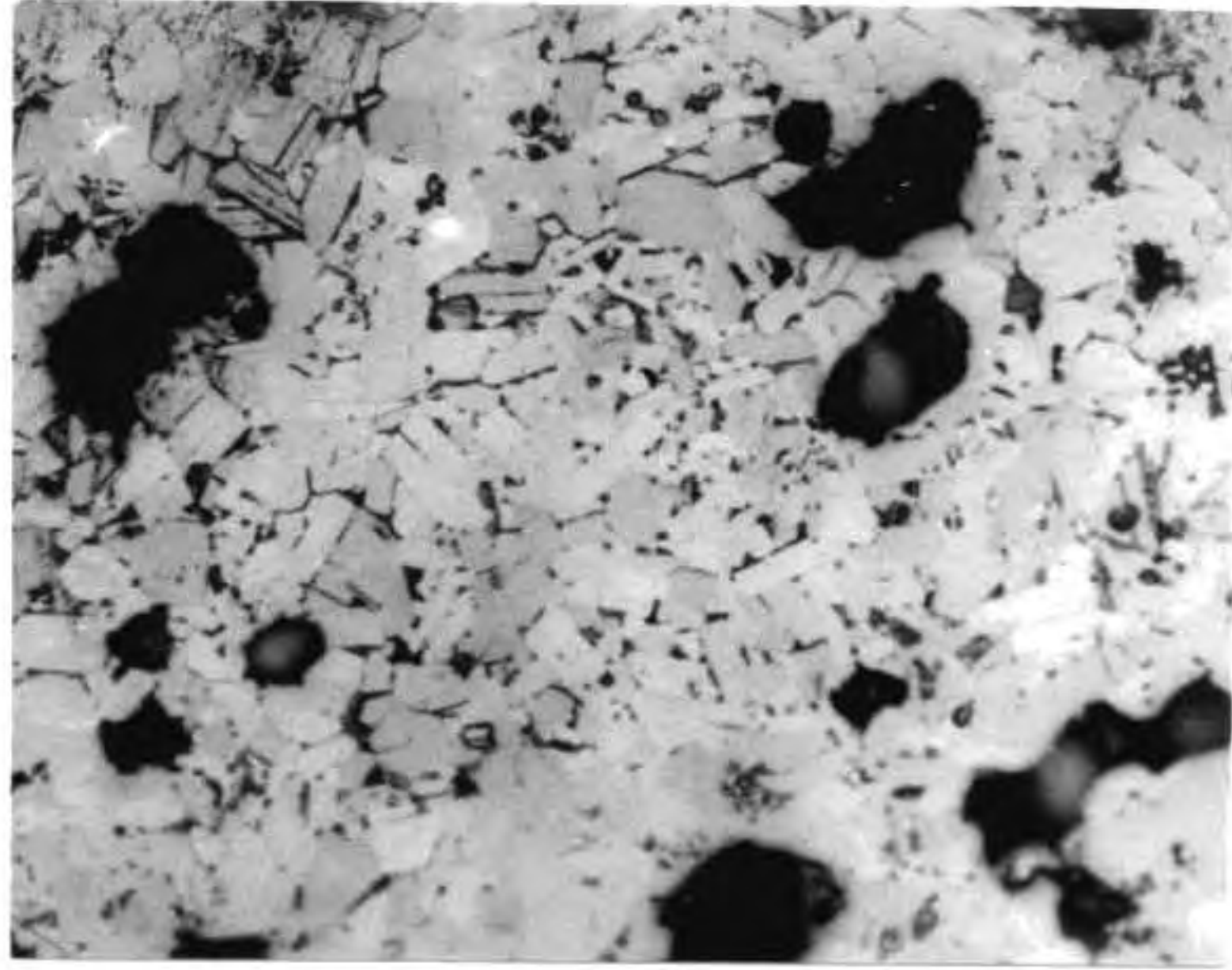
x 300



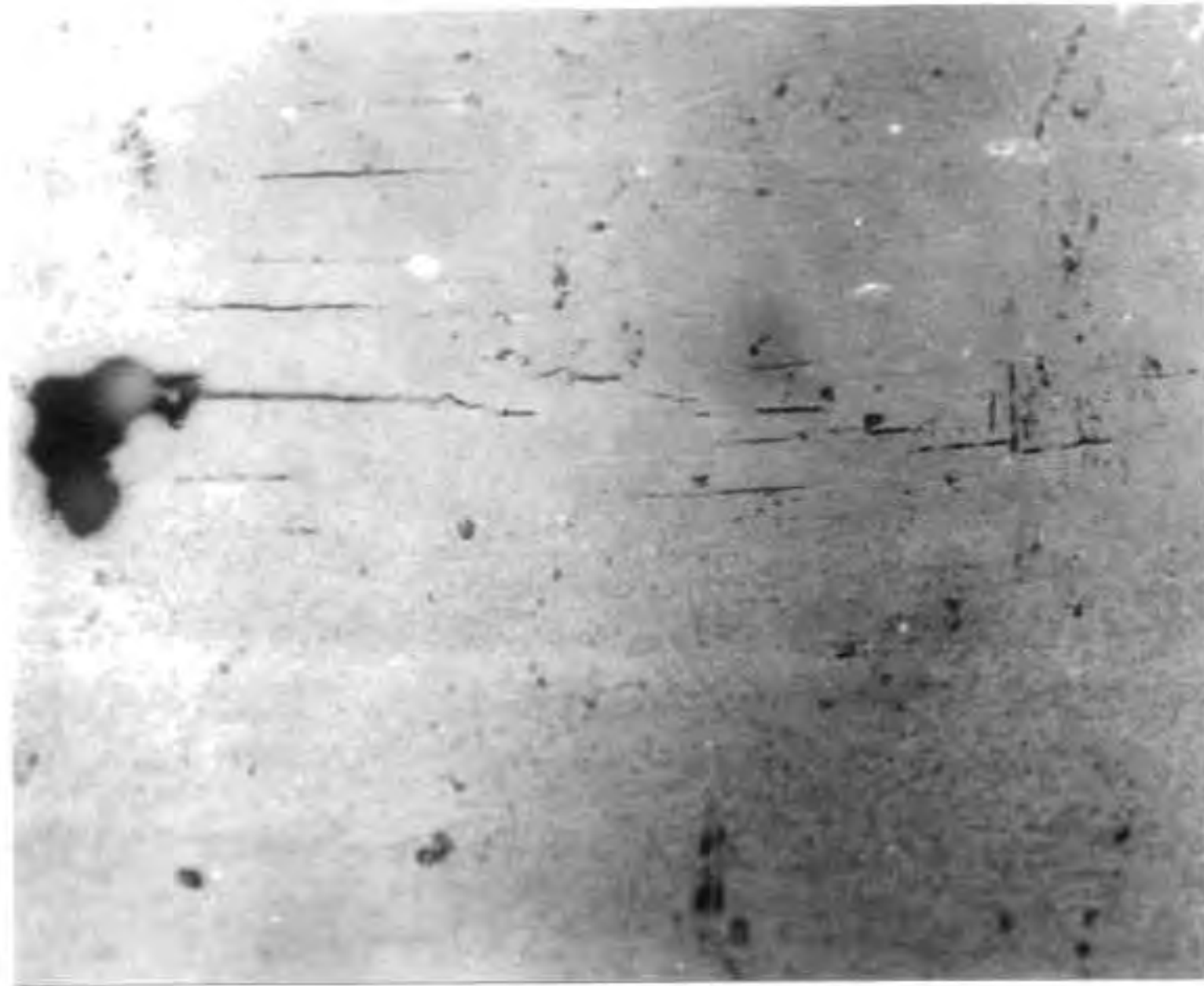
(b)

x 300

Fig. V.11 Optical micrograph of polished YBCO (a) sintered and after subjecting to zone melting for (b) one time

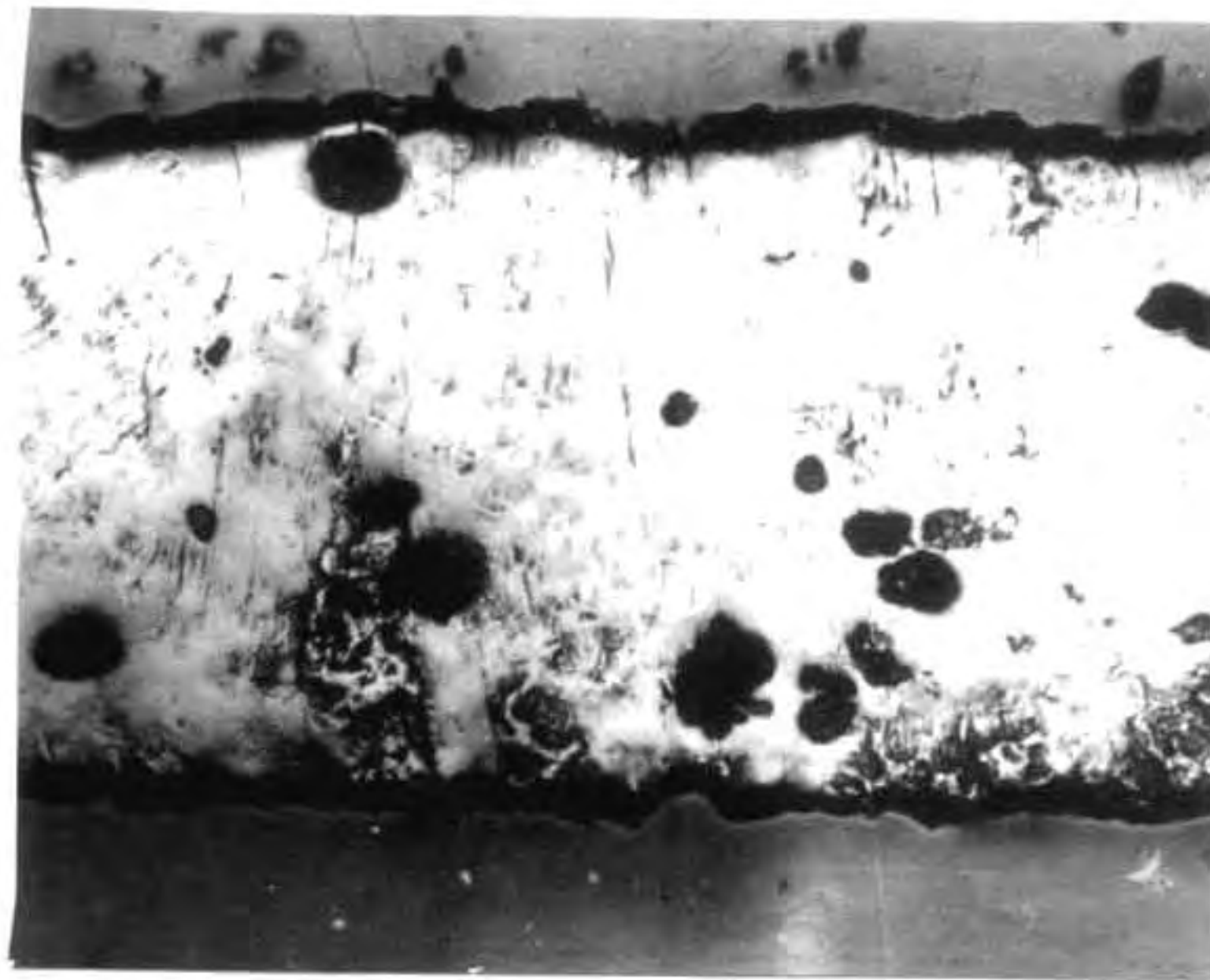


(c) x 300



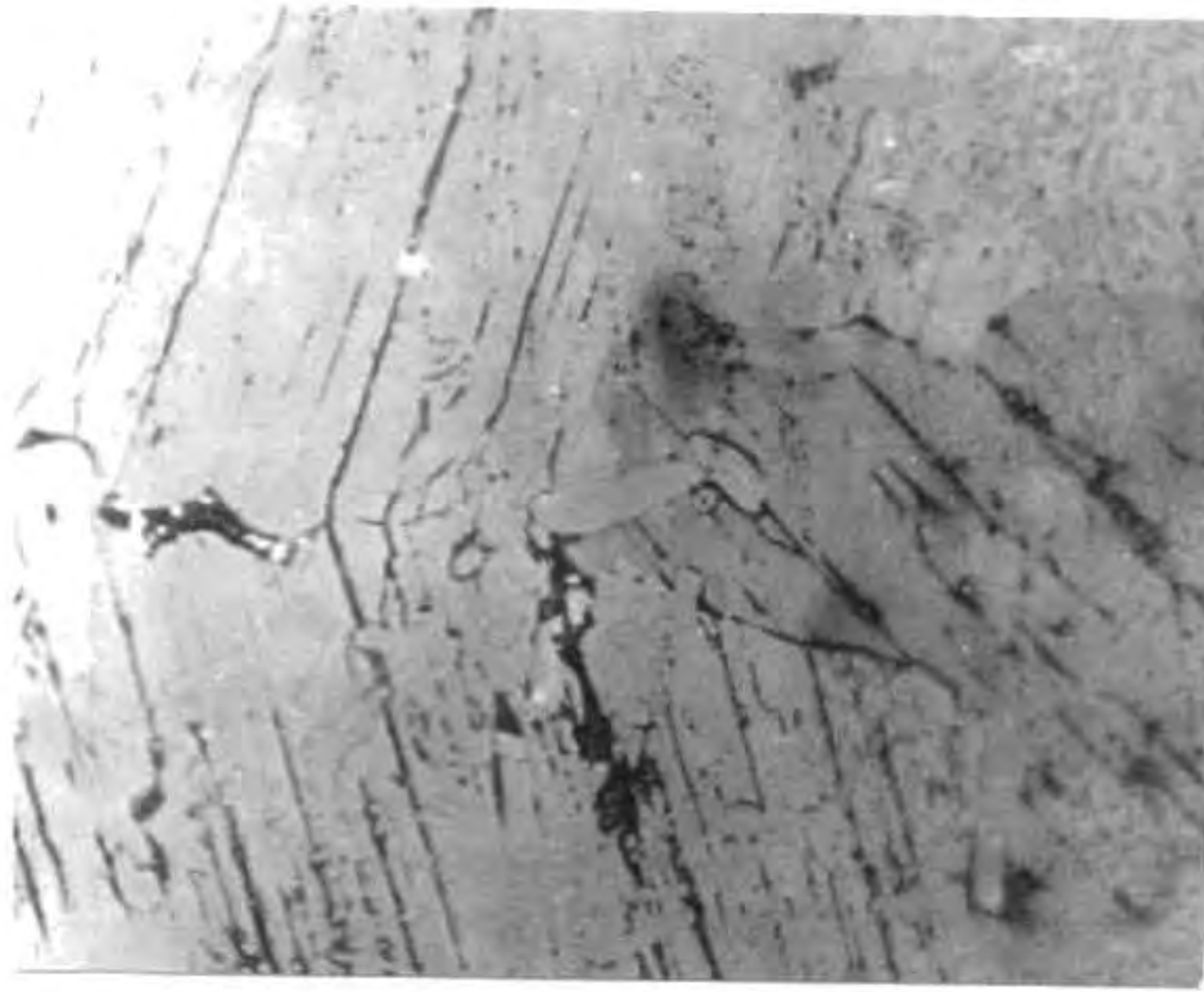
(d) x 300

Fig. V.11 Optical micrograph of polished YBCO after
subjecting to zone melting for (c) two times
and (d) three times



(e)

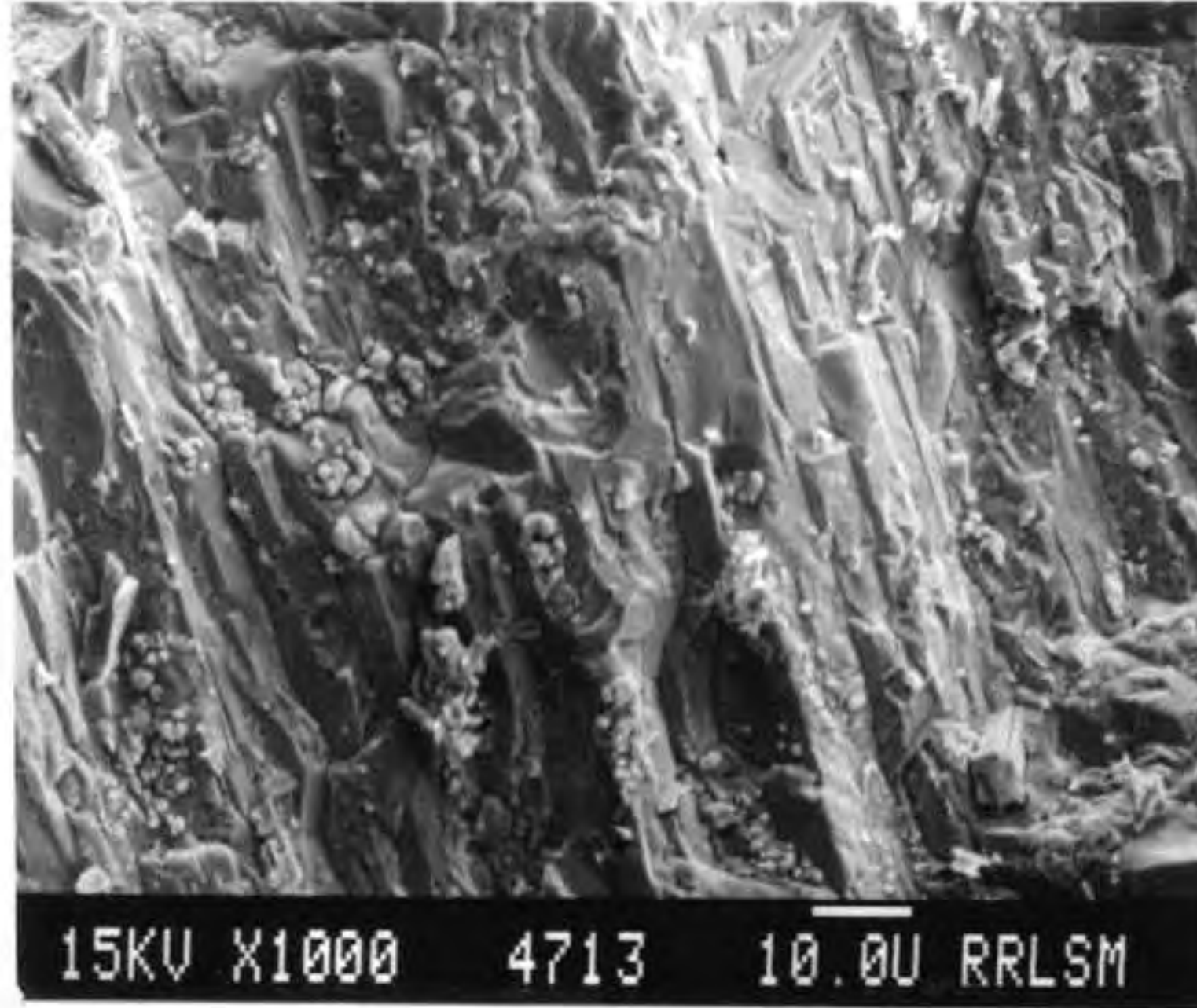
x 160



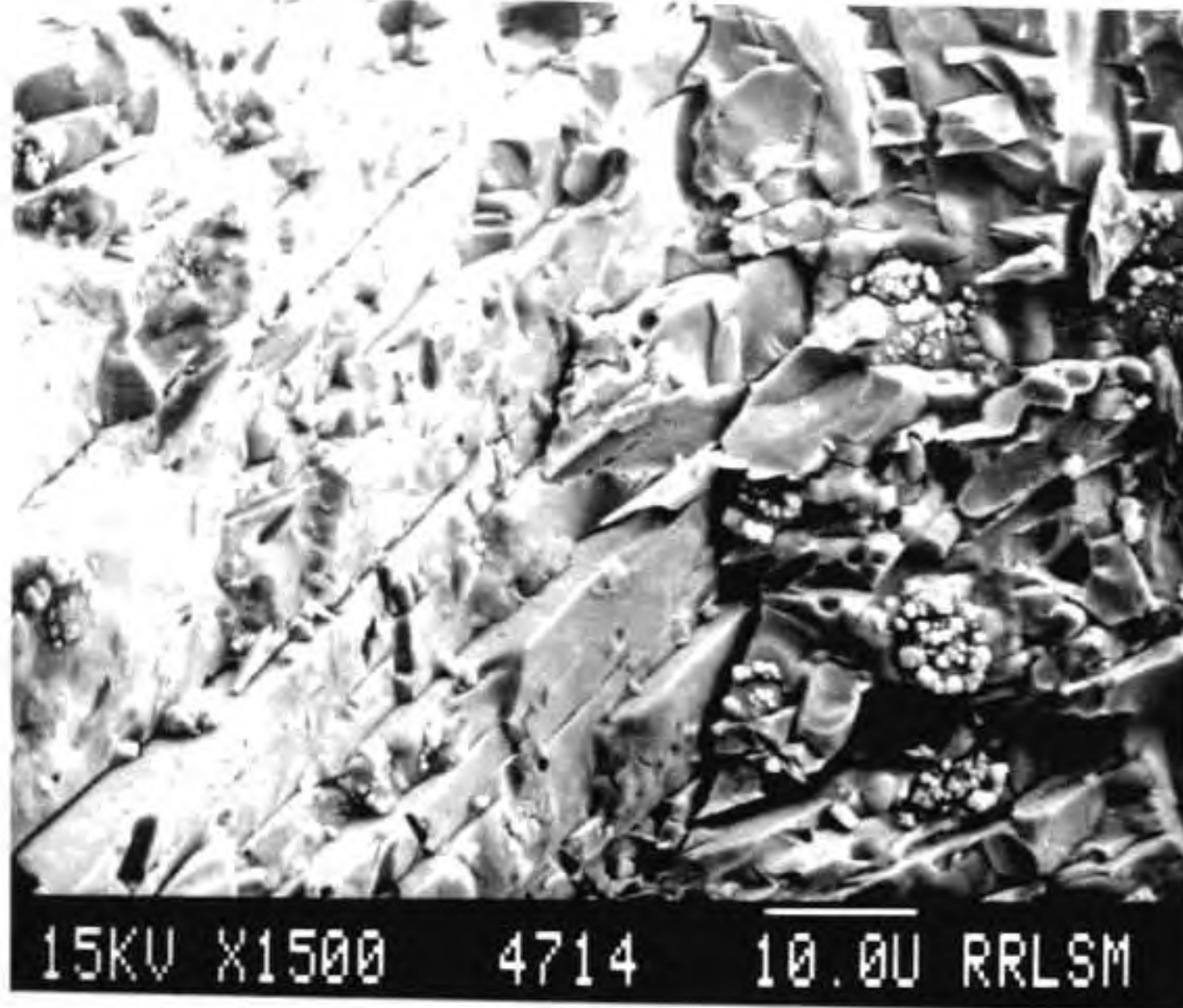
(f)

x 300

Fig. V.11 Optical micrograph of polished cross sections of three times zone refined samples (e) and (f)



(a)



(b)

Fig. V.12 SEM pictures of fractured zone refined samples showing bulk oriented YBCO grains

melt texturing and repeated zone melting operation to well developed a-b plane oriented YBCO samples at relatively fast rate of 30 mm/hr, the present work on repeated zone melting is unique with reference to fastness of preparation and processing of oriented bulk YBCO superconductors.

References

1. P. Debye, 'Polar Molecules'. Chemical Catalog, New York, 1929.
2. K.S. Cole and R.H. Cole, J. Chem. Phys., 9, (1941) 341.
3. N. Hill, W.E. Vaughan, A.H. Price and M. Davies, Dielectric Properties and Molecular Behaviour, Van Nostrand, New York, 1969.
4. I.J. Chabinsky and E.E. Eves III, Interceram., 6, (1986) 30.
5. W.W. Ho, pp.137-148 in Microwave Processing of Materials, Vol.124, Eds. W.H. Sutton, M.H. Brooks and I.J. Chabinsky, Materials Research Society, Pittsburgh, PA, 1988.
6. A.C. Metaxas and R.J. Meredith, Industrial Microwave Heating, Peter Perigrinus, London, 1983.
7. J.B. Hasted, Aqueous Dielectrics, Chapman and Hall, London, 1973.
8. Morgan and Yager, Ind. Eng. Chem., 32, (1940) 1519.
9. S.L. McGill, J.W. Walkiewicz and G.A. Smyres, Vol.124, Mat. Res. Soc., Pittsburgh, PA, 1988.
10. W.H. Sutton, Am. Ceram. Soc. Bull., 68(2) (1989) 376.
11. R. Roy, S. Komerneni and L.J. Yang, J. Am. Ceram. Soc., 68(7) (1985) 392.
12. L.M. Sheppard, Am. Ceram. Soc. Bull., 67(10) (1988) 1556.

13. R.G. Ford, *Materials in Processing Report*, 1(11) (1987) 1.
14. D.M.P. Mingos and D.R. Baghurst, *Chem. Soc. Rev.*, 20, (1991) 1.
15. M.G. Hamlyn and A.L. Bowden, *Am. Ceram. Soc. Bull.*, 69(3) 368.
16. T.T. Meek, R.D. Blake and J.J. Petrovic, *Ceram. Eng. Sci. Proc.*, 8(7-8) (1987) 861.
17. W.R. Tinga, *Electromag. Energy Rev.*, 1, (1988) 1.
18. D.R. Baghurst, A.M. Chippindale and D.M.P. Mingos, *Nature*, 332(6162) (1988) 311.
19. M.A. Janney and H.D. Kimrey, pp. 919-924 in *Ceramic Transactions, Ceramic Powder Science II*, Eds. G.L. Messing, E.R. Fuller Jr. and H. Hausner, Am. Ceram. Soc., Westerville, OH, 1988.
20. C. Gibson, I. Matthews and A. Samuel, *J. Microwave Power Electromag. Energy*, 23, (1988) 17.
21. S. Jin, *Journal of Metals*, 3, (1991) 7.
22. T. Venkatesan, X.D. Wu, B. Dutta, A. Inam, M.S. Hedge, D.M. Hwang, C.C. Chang, L. Nazar and B. Wilkens, *Appl. Phys. Lett.*, 54, (1989) 6.
23. S.E. Babcock, X.Y. Cai, D.L. Kaiser and D.C. Larbalestier, *Nature*, 347, (1990) 167.
24. S. Jin, R.C. Sherwood, T.H. Tiefel, R.B. Van Dover and D.W. Johnson, *Appl. Phys. Lett.*, 51, (1987) 203.

25. M. Murakami, M. Morita, K. Doi, K. Miyamoto and H. Hamada, *Jpn. J. Appl. Phys.*, 28, (1989) L399.
26. K. Salama, V. Selvamanickam, L. Gao and K. Sun, *Appl. Phys. Lett.*, 54 (1989) 2352.
27. P.J. McGinn, W. Chen, N. Zhu, U. Balachandran and M.T. Lanagan, *Physica C*, 165, (1990) 480.
28. R.L. Meng, Y.Y. Sun, P.H. Hor and C.W. Chu, *Physica C*, 179, (1991) 149.

CHAPTER VI

COMPARISON OF PROPERTIES OF YBCO POWDERS AND SINTERED SAMPLES DERIVED THROUGH VARIOUS ROUTES

VI.1 Introduction

The properties of polycrystalline bulk ceramic superconductors strongly depend on the microstructure of the sintered material. They also depend on the extent of oxygen content(2-5), second phase segregation at grain boundaries(6-9), nature of orientation of grains(10) etc. and they are reasonably well studied. Effect of lattice and minute region defects(11) are also investigated. The temperature of sintering and soaking time decide, to a large extent, the formation of absolute grain to grain contact and uniformly distributed grains in a well sintered specimen. It is rather well known that YBCO samples sintered above 950°C introduces slight liquid phase which may aid the sinterability and densification(11). However, temperature in the range 925-940°C is sufficient to result in well sintered microstructure guided by particle diffusion sintering in which case high green densities are most desirable(12). These parameters are decided by the history of the starting powders. Features like particle size distribution, shape, size and high green densities do play significant role in attaining densified samples which decide

the current densities, although the critical temperature is not generally affected. This chapter gives a comparison of the various non conventional powder preparation methods, their powder characteristics and sintered properties, described in previous chapters. YBCO powder was also prepared from conventional ceramic method for comparison.

VI.2 Experimental

For the preparation of $\text{YBa}_2\text{Cu}_3\text{O}_{7-\delta}$ powders, three non conventional methods described in Chapters III, IV and V were used. The powder was also prepared by conventional method. Y_2O_3 , BaCO_3 and CuO were weighed out in 1,2,3 stoichiometry (for 20 gm of YBCO) and mixed in an agate mortar for 2 hours in isopropyl alcohol medium. The thoroughly mixed powder was calcined at 950°C for 12 hours. The calcined material was crushed in the same agate mortar again and repeated the calcination and grinding steps three times. For making sintered specimens, these powders were pressed and sintered at different temperatures for different soaking times. All the powders were characterized with respect to phase purity, compaction behaviour and morphology. The dimensions of the green compact samples were 15 mm x 4 mm x 2mm. The sintered properties were also studied under the similar experimental condition.

VI.3 Results and discussion

VI.3.i Characteristics of powder preparation methods

The basic highlights of the methods are provided in Table VI.1. All the first three routes in the table give a precursor which decompose and/or react to form $\text{YBa}_2\text{Cu}_3\text{O}_{7-\delta}$ compound. In the case of citrate gel route, a uniform gel with low weight/volume ratio is formed and which on calcination at 900°C for 10 hours gives almost single phase compound in a single step. The efficiency of mixing is brought about by the dispersion of ions in atomic level within the gel network. Since the gel decomposes with evolution of a large amount of gaseous products the resulting compound was fluffy consisting of submicron particulates. The small diffusion length between the precursor particles also make the solid phase reaction fast at relatively low temperature and time.

In the case of flash combustion method, the urea-nitrate mixture first foams up . The subsequent spontaneous combustion gives the $\text{YBa}_2\text{Cu}_3\text{O}_{7-\delta}$ powder. The temperature of combustion was kept above 900°C and the powder obtained was mainly YBCO with minor phases like BaCuO_2 , CuO and Y_2BaCuO_5 . On further keeping the powder at 900°C in the furnace for another 1 hour, single phase YBCO was formed. Here also high level of mixing and fineness of particles are attributed by the decomposition of a homogeneous gel assisted by the combustible gases formed during the decomposition. The chemistry of citrate and flash

combustion route is very different, but once the precursor is formed, both follows almost same path to get reacted to $\text{YBa}_2\text{Cu}_3\text{O}_{7-\delta}$. However, the powder characteristics appear to be significantly different. Microwave decomposition method is still different from the other two routes because of the difference in energy absorption and transfer mechanism. The capacity of copper nitrate to absorb the microwave energy and its conversion into heat energy is taken into account i.e. by the selective absorption of microwave energy the copper nitrate decomposes itself to CuO and make the other two nitrates also to decomposes to the corresponding oxides. Here also the melting and decomposition of copper nitrate make mixture of nitrates into a viscous solution first and then later into a gel which within a matter of four minutes get reacted to $\text{YBa}_2\text{Cu}_3\text{O}_{7-\delta}$. Because of the enhanced absorption of copper oxide with temperature further exposure to microwave result in the melting of the compound due to thermal runaway. So further homogeneity of the powder is achieved by annealing this powder at 900°C for 4 hours. High extent of reaction of the oxides is not only due to the mixing of the components but also due to the enhanced diffusivity of the microwave active molecules. All the three methods in general, require only short reaction time and temperature to get $\text{YBa}_2\text{Cu}_3\text{O}_{7-\delta}$ compared to conventional route (Table VI.1), in which repeated grinding and calcination are essential for the completion of the reaction. It also requires high temperature (950°C) which eventually lead to

Table VI.1 Characteristics of various powder preparation techniques for YBCO

Process	Mixing of Constituent cations	Complete phase formation		Nature of products (average particle size μm)
		temperature	time(hrs)	
Citrate	Very good	900°C	10	Fluffy, fine(1-2 μm)
Flash Combustion	Good	900°C	1	Fine (4 μm)
Microwave decomposition	Good	900°C (4 minutes ex- posure to micro- waves followed by calcination at 900°C)	4	Fine (2 μm)
Conventional Solid State reaction	Moderate	925-950°C with repeated grinding and calcination	30-50	Coarse (5-25 μm)

inhomogeneous particles. The properties of powders and sintered superconductors are presented below.

VI.3.ii Powder characteristics

VI.3.ii.a Phase analysis:

The XRD patterns showed that all the powders are orthorhombic $\text{YBa}_2\text{Cu}_3\text{O}_{7-\delta}$ with less than 3% secondary unreacted phases. The lattice constants and the d values obtained for each powder are given in Table VI.2a-d. All the values match with observed values for standard $\text{YBa}_2\text{Cu}_3\text{O}_{7-\delta}$. The variation of lattice parameter is attributed to the oxygen ion concentration in the lattice. The oxygen ion concentration was determined by iodometric titration as described in Chapter III. The oxygen content data is provided in Table VI.3. The lower value of oxygen ($< \text{O}_7$) is because the powders were not oxygen annealed after calcination. Oxygen enrichment has occurred during the calcination of the precursor in air and, it is seen that the fluffier powder contain more oxygen ion concentration.

VI.3.ii.b Particle size distribution:

Figure VI.1 gives data on the particle size distribution of the four powders after ball milling for 3 hours using zirconia balls in a poly urethane container using n hexane as grinding media. As expected, citrate route gives smallest particles while conventional powder mixing route give coarse

Table VI.2 Lattice parameters and d values obtained for powders prepared by different methods (a) Citrate gel

2θ	d	I	I/I ₀
23.00	3.8668	3.4	14
23.30	3.8177	1.5	6
28.50	3.1319	1.6	7
32.60	2.7467	17	68
32.85	2.7272	25	100
35.70	2.4881	0.5	2
36.45	2.4656	1.0	4
38.65	2.3302	4.0	16
40.45	2.2305	4.8	20
46.75	1.9435	6.1	25
47.60	1.9104	3.1	12
51.60	1.7713	1.3	5
52.75	1.7353	1.2	5
53.50	1.7128	1.2	5
55.40	1.6585	0.5	2
58.35	1.5777	8.4	34
58.85	1.5694	4.0	16

a = 3.842, b = 3.902, c = 11.68

Table VI.2 Lattice parameters and d values obtained for powders prepared by different methods
(b) Flash combustion

2θ	d	I	I/I_0
22.95	3.8768	2.8	20
27.60	3.2319	1.2	9
32.60	2.7467	8.2	58
32.80	2.7305	13.8	100
35.40	2.7968	1.0	7
38.75	2.3244	2.1	15
40.20	2.2433	2.4	18
46.55	1.9519	2.8	20
47.60	1.9104	1.6	8
51.30	1.9809	1.0	7
58.05	1.58914.0	30	
58.50	1.5777	2.0	19

$a = 3.8467, b = 3.8936, c = 11.630$

Table VI.2 Lattice parameters and d values obtained
for powders prepared by different methods
(c) Microwave decomposition

2θ	d	I	I/I ₀
23.00	3.8660	2.5	15
28.00	3.1866	0.5	3
32.70	2.7402	9.0	54
32.90	2.7224	16.5	100
36.40	2.4682	0.3	2
38.75	2.3244	2.8	17
40.60	2.2221	2.6	15
46.80	1.9411	5.1	30
47.80	1.9028	1.9	11
51.65	1.7700	0.6	4
52.90	1.7308	0.3	2
58.25	1.5840	5.2	30
58.90	1.5680	2.5	15

a = 3.833, b = 3.883, c = 11.680

Table VI.2 Lattice parameters and d values obtained
for powders prepared by different methods
(d) Solid state mixing

2θ	d	I	I/I ₀
23.0	3.8630	1.5	8
27.80	3.2060	1.0	5
32.20	2.7443	11.0	59
32.90	2.7200	18.5	100
36.30	2.4720	0.4	2
38.60	2.3300	2.0	10
40.30	2.2360	2.5	14
43.10	2.0900	0.2	1
46.75	1.9410	3.5	19
47.55	1.9100	2.5	14
51.40	1.7760	0.4	2
52.60	1.7380	0.5	3
58.20	1.5830	4.5	24
58.60	1.5740	3.5	19

a = 3.820, b = 3.882, c = 11.65

Table VI.3 Oxygen content in YBCO derived through various routes

Powder preparation route	Oxygen content x ($\text{YBa}_2\text{Cu}_3\text{O}_x$)
Citrate	6.90
Flash combustion	6.82
Microwave	6.85
Conventional solid state reaction	6.82

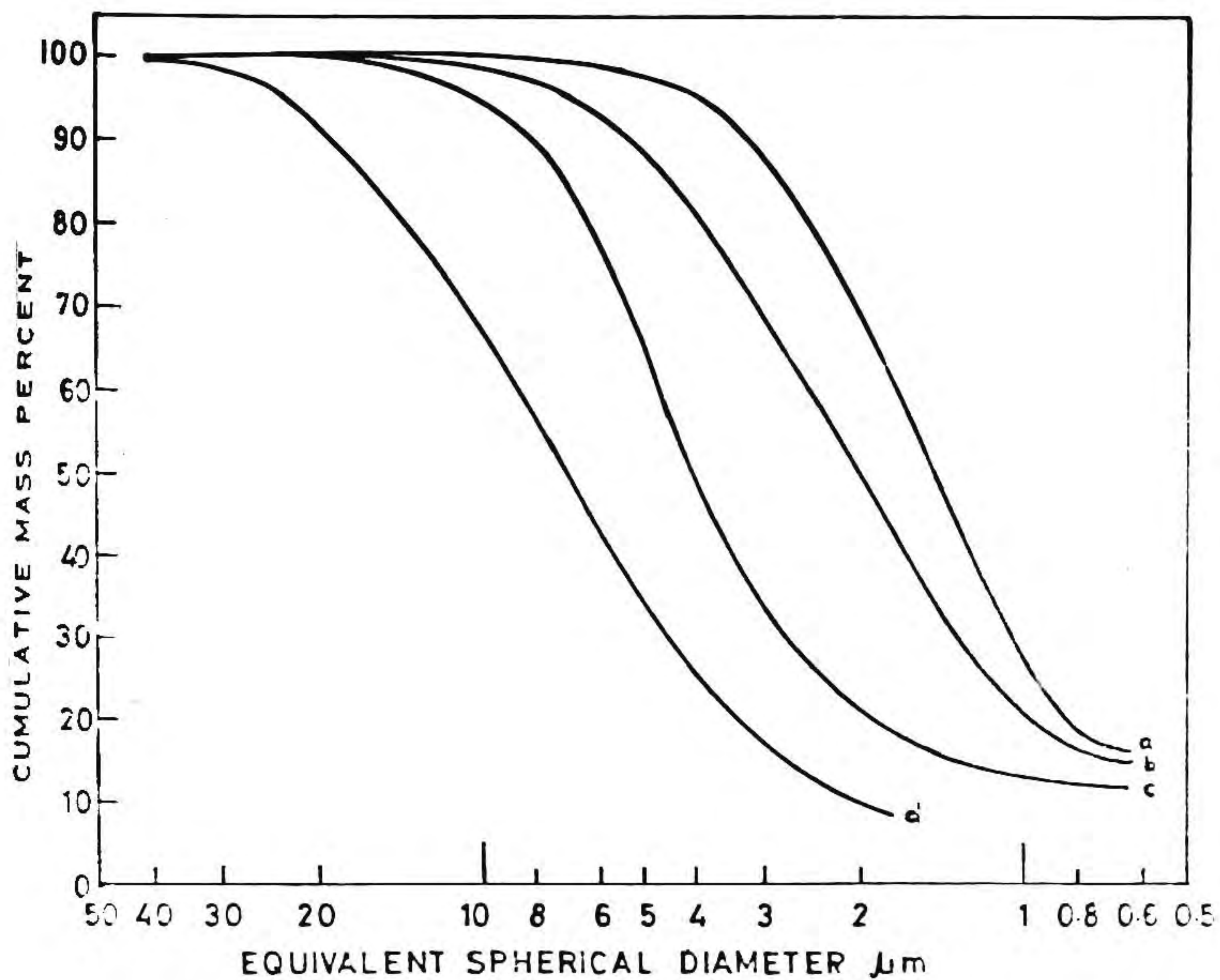


Fig. VI.1 Particle size distribution curve of various YBCO powders (a) citrate, (b) microwave, (c) flash combustion and (d) conventional solid state route

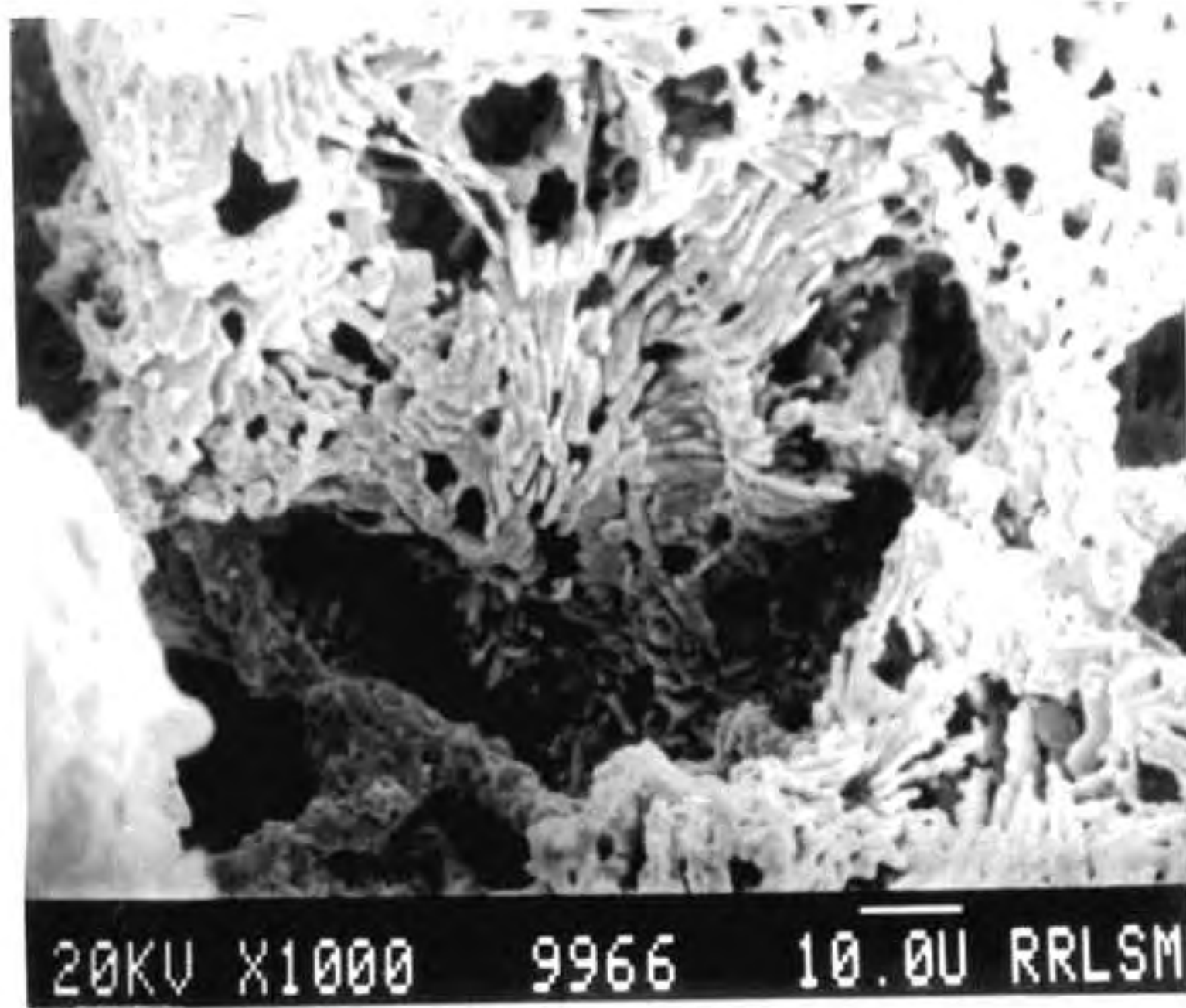
powder. The narrow size distribution of citrate, flash and microwave powder is very much pronounced to that of solid state route powder which has got a wide range of particle size and the maximum particle size is 20 microns.

VI.3.ii.c Morphology of the powders:

The crystalline morphology of citrate derived powder shows regular rod like particles with aspect ratio of 5 to 6. The interesting observation made in this route is that the powders are more or less of uniform size. In the case of flash combustion route, the powders had a finger like shape with high aspect ratio, fragile and could be crushed to fine, fluffy ones. The powder obtained from microwave decomposition also shows equisized particles having aspect ratio 4 to 5. The powder, in the low magnification, are observed as one embedded over a gel network in the very good homogeneity, both in size and shape. The particle morphology of the solid state derived powder are also provided (Fig.VI.2). As expected they are highly irregular and lot of fine as well as large particles are seen.

VI.3.ii.d Bulk density:

The tap density of the powder is a measure of the consolidation behaviour. They are provided in Table VI.4. It is clear that more fluffier the powder lesser is the tap density. This is clear from the low tap density value for citrate derived

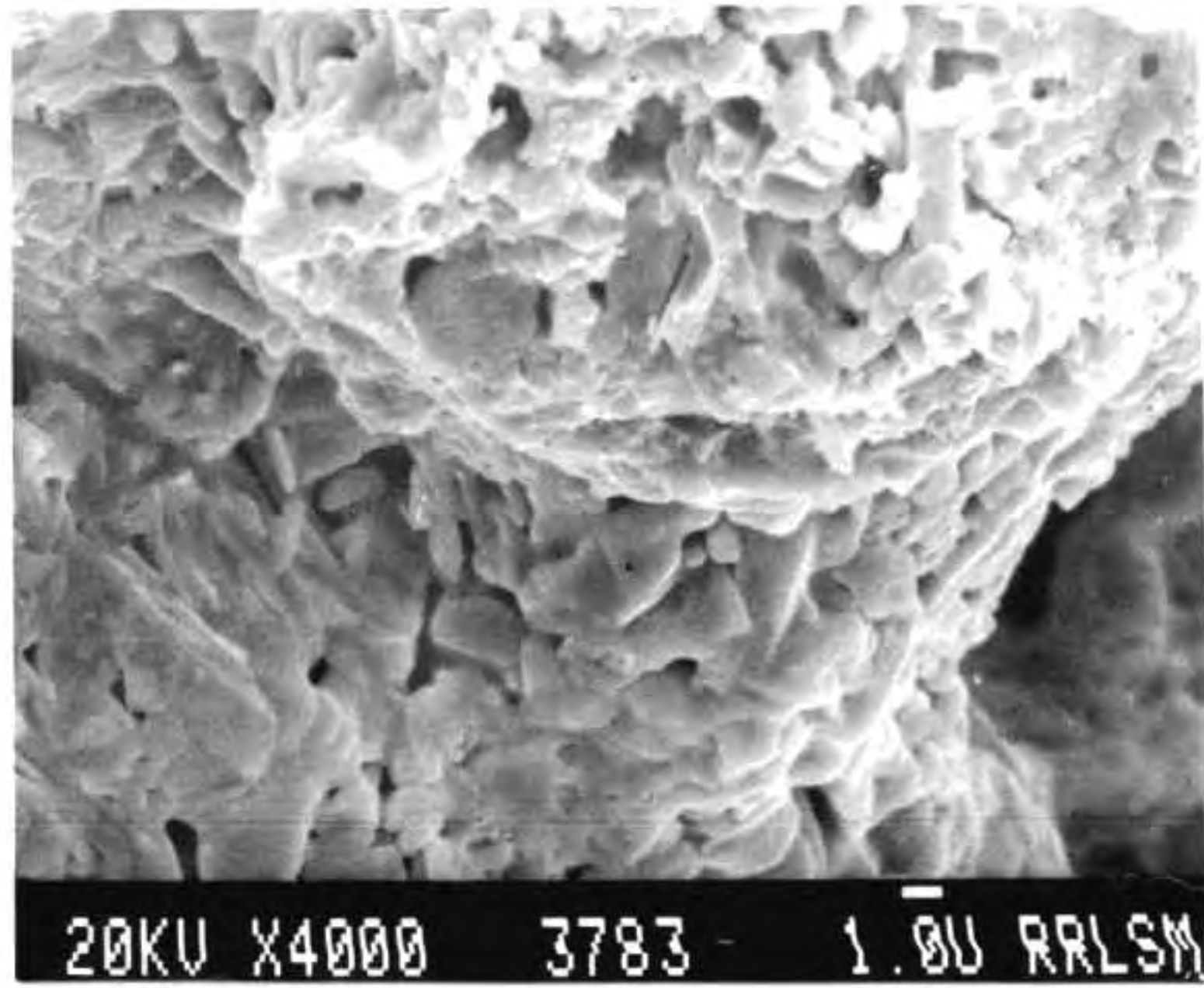


(a)

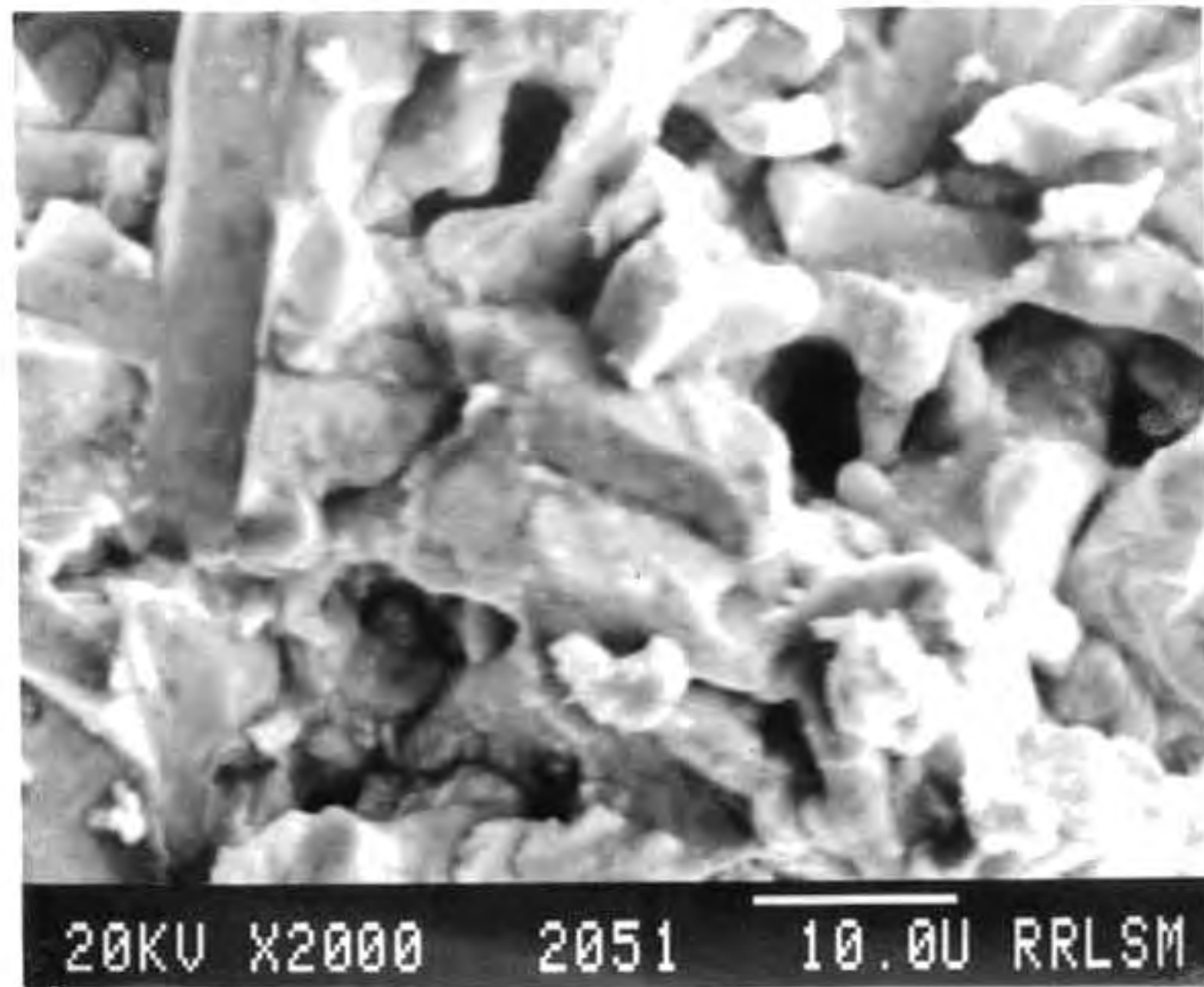


(b)

Fig. VI.2 SEM picture of the morphology of the YBCO derived through (a) Citrate and (b) Flash combustion gel decomposition



(c)



(d)

Fig. VI.2 SEM picture of the morphology of the YBCO derived through (c) Microwave decomposition and (d) Solid state mixing

Table VI.4 Tap density of YBCO powders derived through various routes

Powder preparation route	Tap density (g/cm ³)
Citrate	2.10
Flash combustion	2.7
Microwave	2.25
Conventional solid state reaction	2.6

YBCO powder. Flash combustion route gives highest tap density while other two routes gave tap density in between.

VI.3.ii.e Green compaction densities:

The green compaction densities of the powders pressed at various pressures in a rectangular stainless steel die using a uniaxial press is provided in Fig.VI.3. Highest compaction density was obtained for microwave derived ones and lowest for conventional ones. The increase of pressure increases the compaction density in a similar fashion in all the cases.

VI.3.iii Sintered characteristics

VI.3.iii.a Sintered densities:

The above pellets were sintered at two different temperatures (925°C and 940°C) and time (6 hours and 10 hours) according to the schedule given in Fig.VI.4. The development of sintered density follows a similar behaviour as in the case of green compaction behaviour (Fig. VI.5). Here the sintered density as high as 90-92% of the theoretical value was achieved in the case of citrate as well as microwave derived, when sintered at 940°C for 10 hours. The densities are lower in the case of 6 hours soaked samples as well as for samples sintered at 925°C for 10 hours. The citrate, microwave and flash combustion routes require lower temperature and time for getting higher sintered densities and the effect of high

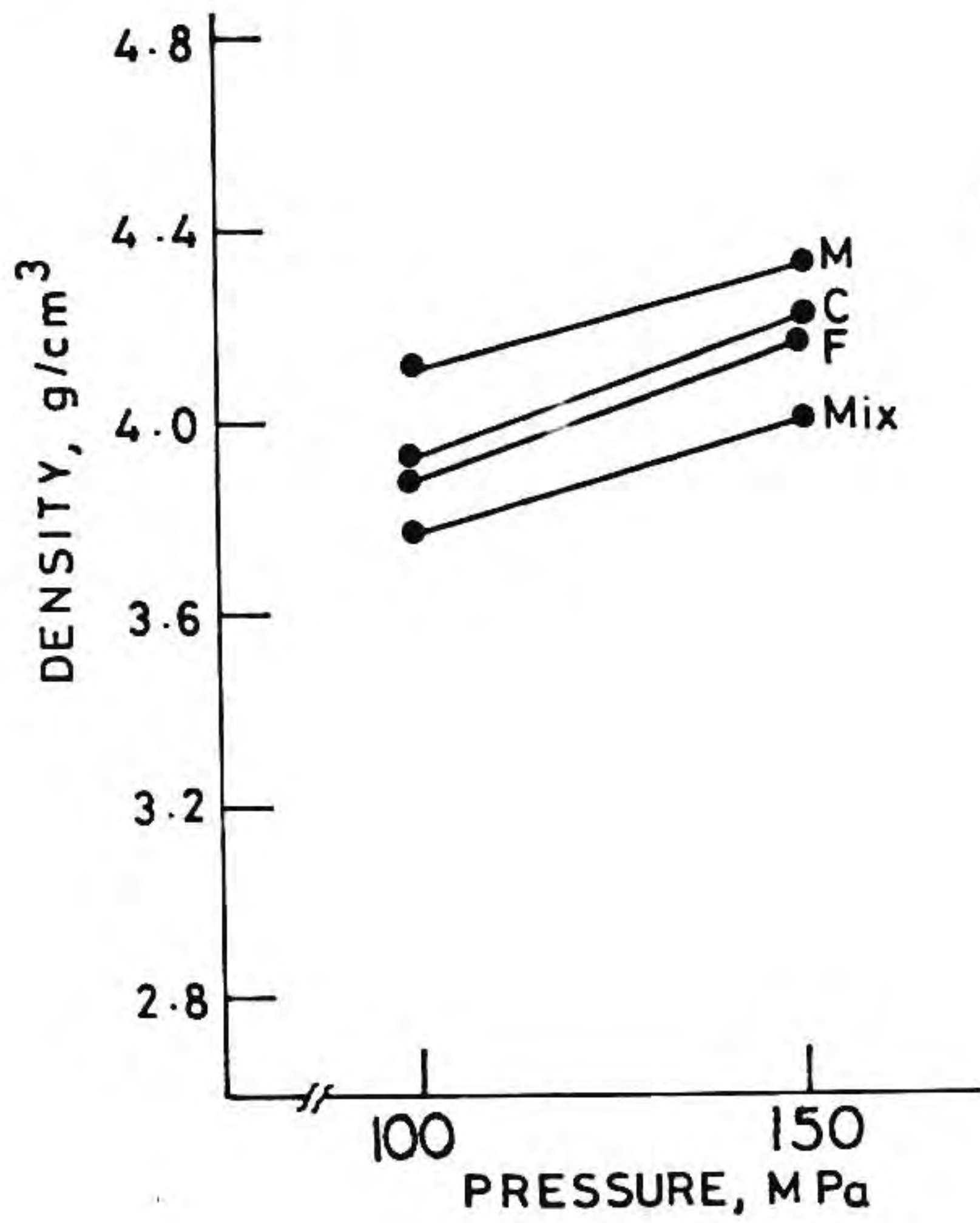


Fig. VI.3 Green density of four YBCO powders as a function of pressure

C - Citrate M - Microwave F - Flash combustion
 Mix. - Solid state mixing

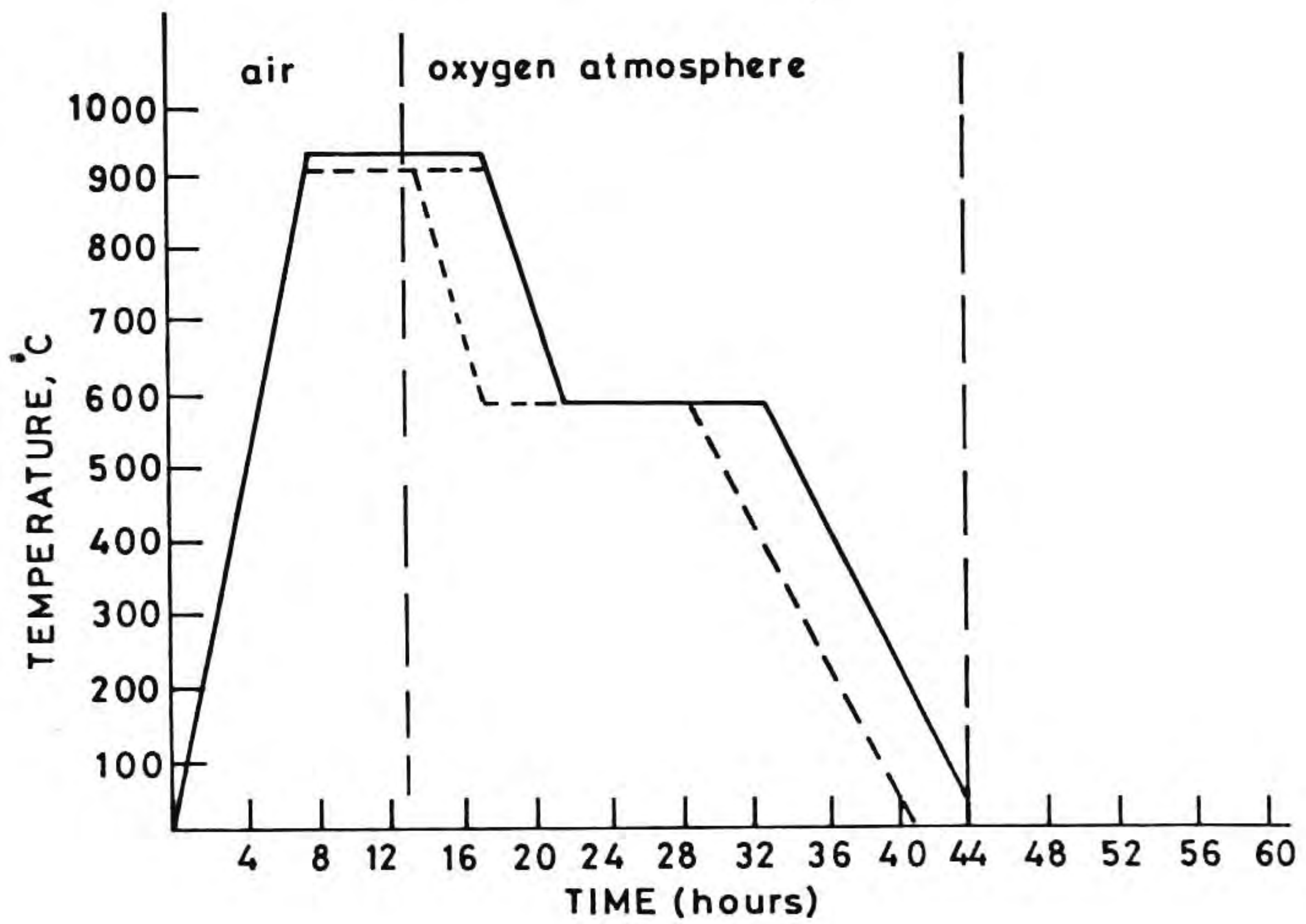


Fig. VI.4 Sintering schedule for the YBCO powder compacts

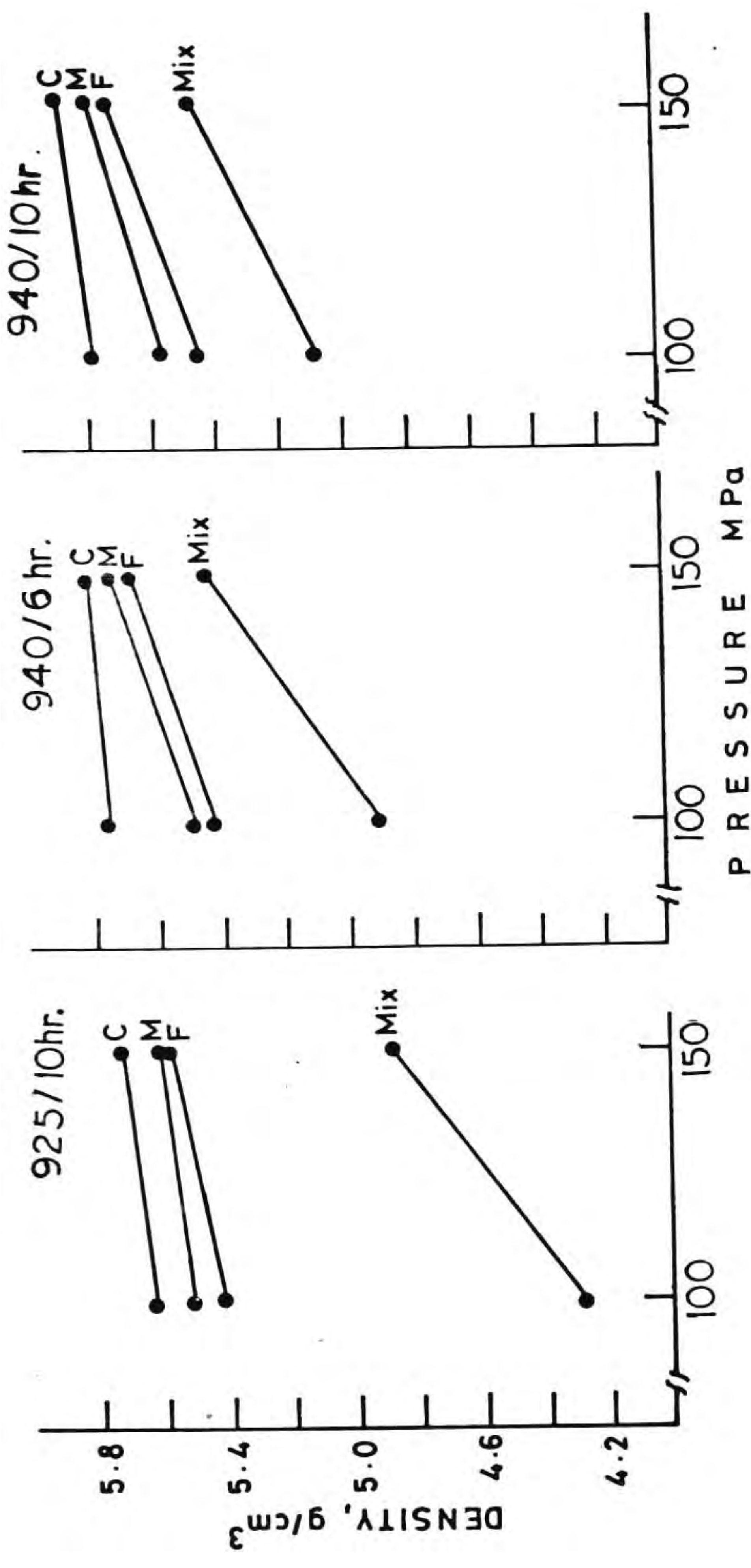


Fig. VI.5 Sintered density variation with applied pressure for the four YBCO samples sintered at different temperatures and time

C - Citrate M - Microwave F - Flash combustion
 Mix. - Solid state mixing

temperature of sintering required in the case of conventional ones are clear from the very low sintered density of that samples at 925°C (Fig.VI.5).

VI.3.iii.b Electrical properties:

The electrical measurements were done using the four probe method. The contacts were given using silver paste (described in Chapter III). The temperature vs resistivity measurements are provided in Fig.VI.6. Many authors have reported the effect of T_c , ΔT_c and J_c on the initial powder used for making sintered superconductors under the identical conditions of processing(13). It is reported that(1) ΔT_c reflects the purity of the 123 phase while the normal state resistivity reflects the quality of the grain boundary and hence the J_c is one with lower normal state resistivity expected to have higher J_c .

All the powders except the solid state derived has got the advantage of low normal state resistivity (R_{100K}) and hence the high J_c (Table VI.5). Similarly, because of the high purity of the powder they are having comparatively low ΔT_c values and T_c is also better. In the recent article Dhalle et.al.(14) explained a correlation of normal state resistivity with J_c values using the Ambegaokar-Baratoff Model. They found that the sol-gel derived powders possess very low normal state resistivity and have high J_c values.

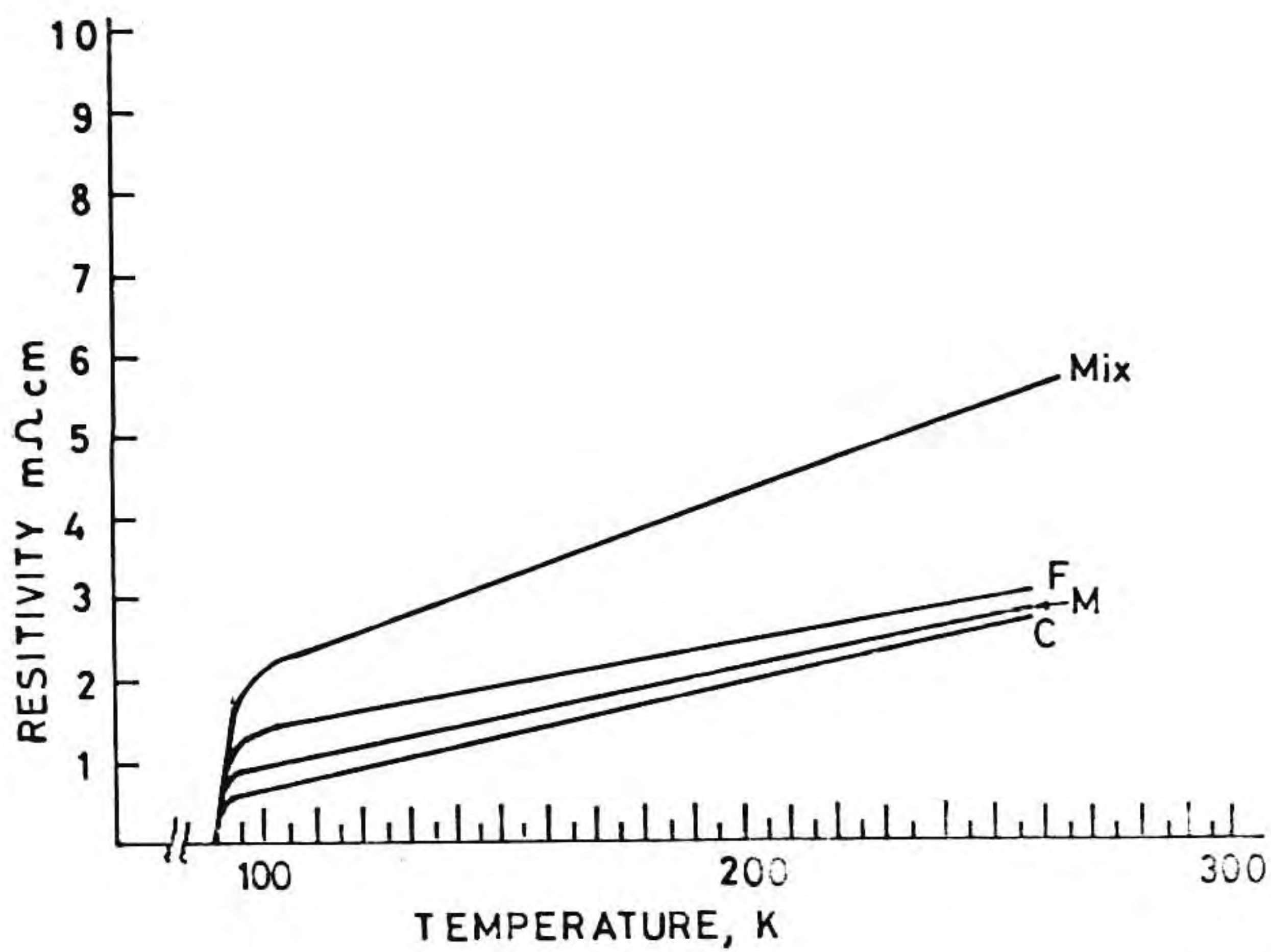


Fig. VI.6 Temperature vs resistivity of sintered YBCO samples

C - Citrate M - Microwave F - Flash combustion
 Mix. - Solid state mixing

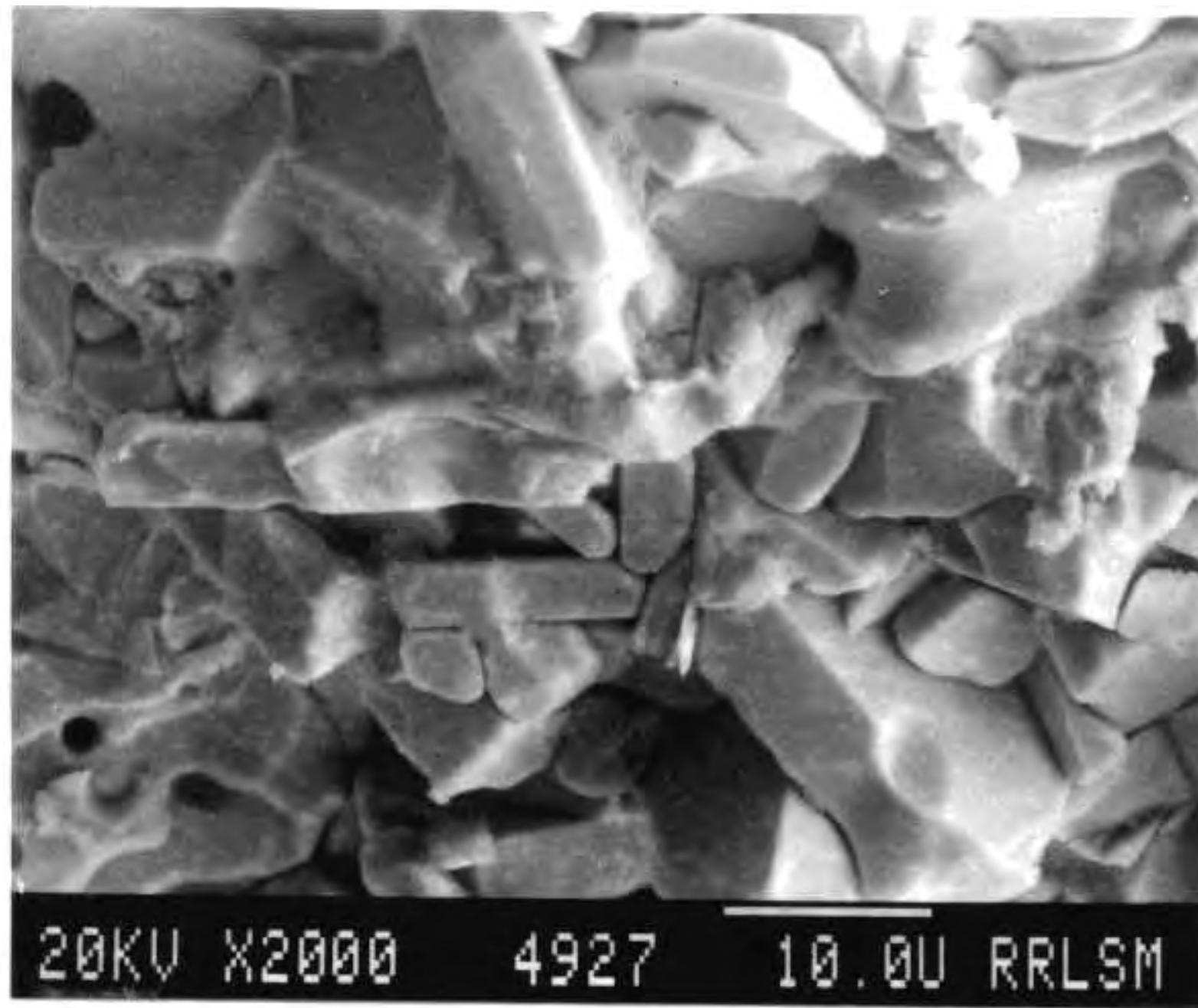
Table VI.5 Electrical properties of sintered YBCO samples

Sample	T_c _(off) K	ΔT_c K	ρ (100K) m Ω cm	J_c A/cm ²
Citrate	91.5	1.5	0.7	225
Microwave	91.0	1.8	1.1	210
Flash	91.0	1.5	1.5	190
Conventional mixing route	90.0	3.0	2.6	100-125

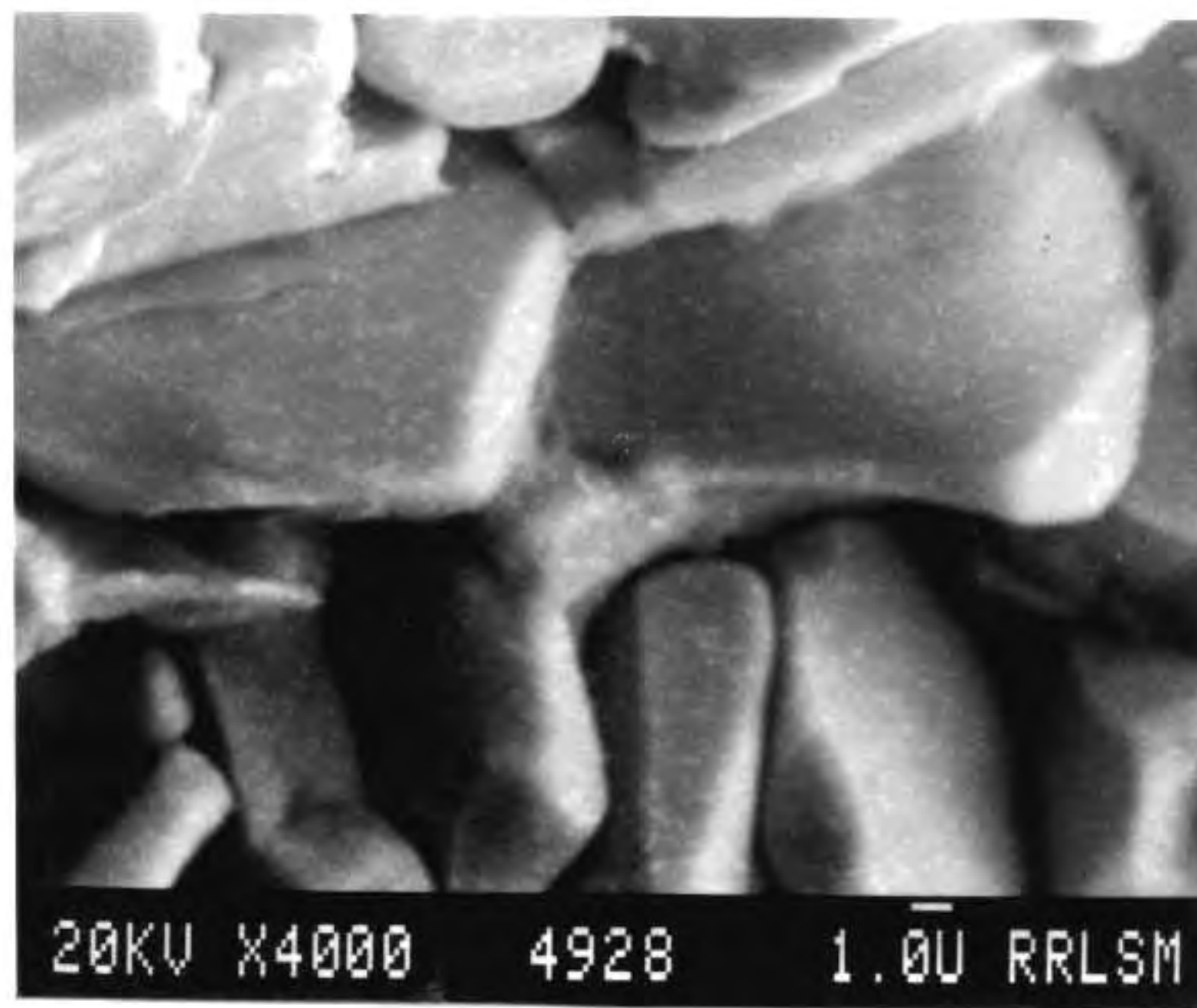
VI.3.iii.c Sintered microstructures:

A comparison of the microstructure of the sintered superconductor derived through different routes reveals interesting features which support the experimental observations regarding density, phase development and possible current densities. It appears that under the present sintering conditions all the samples have predominantly undergone diffusion based sintering with appreciably low levels of liquid phase. As generally observed the superconductor prepared through the ceramic route (prepared by mixing of individual oxides, repeated calcination, grinding and sintering) consists of rod like grains in an extremely random fashion as shown in Fig.VI.7a. However, the microstructure reveals highly scattered unreacted phases throughout the matrix. Partial decomposition of the YBCO phase also could be seen. Another significant observation is the occurrence of a wide distribution in sintered grain size.

The superconductor prepared through the novel chemical reactions in this study are significantly different from the above microstructure. For example, the citrate derived one (Fig.VI.7b) has distinct grains and grain boundaries although random orientation still persists. Average grain size can be calculated to be 10-13 microns because of the rather uniform grain size. The microstructure under higher magnification shows sort of grains tending towards platy morphology. Due to the high stoichiometric stability, deterioration of the

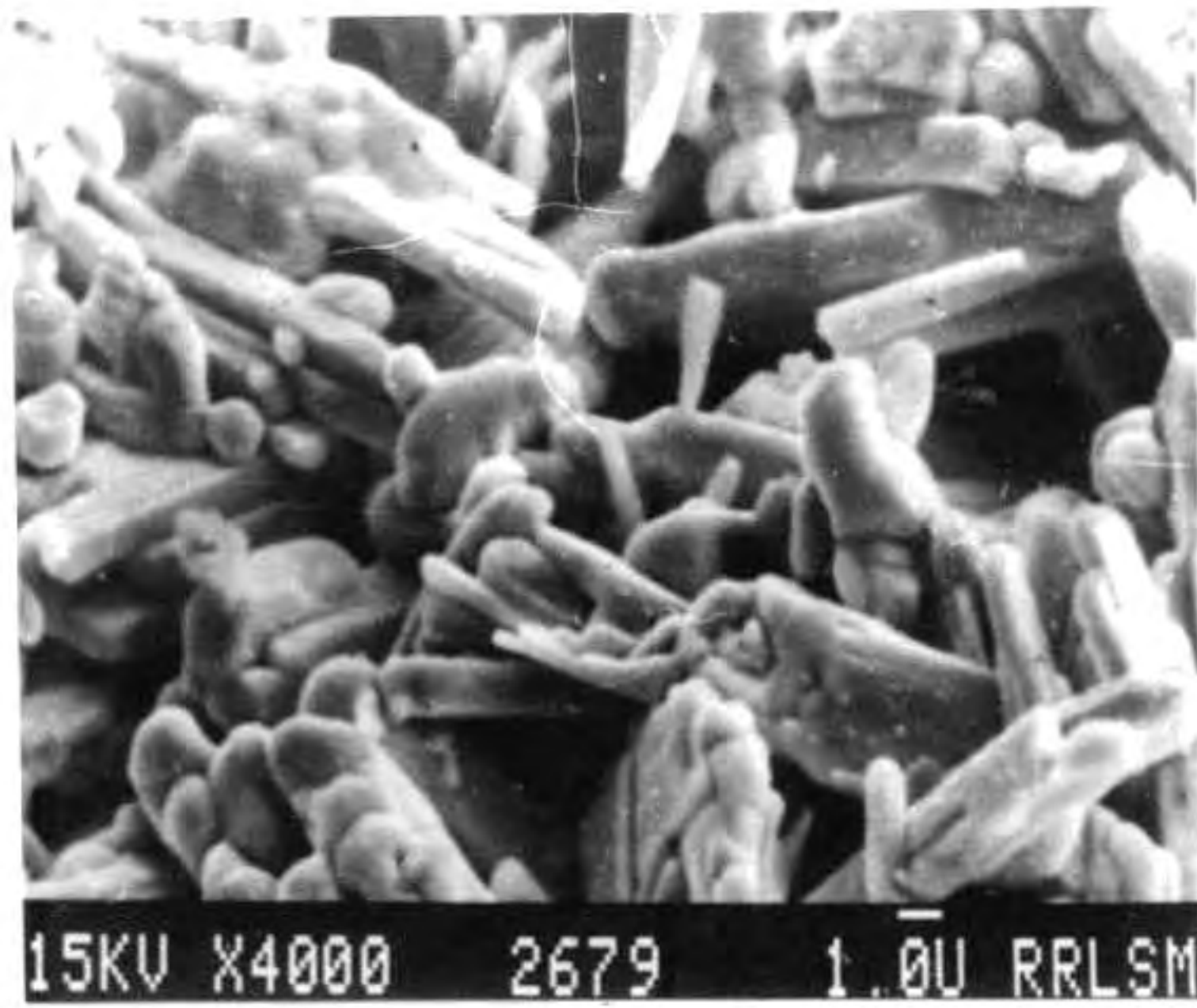


(a)

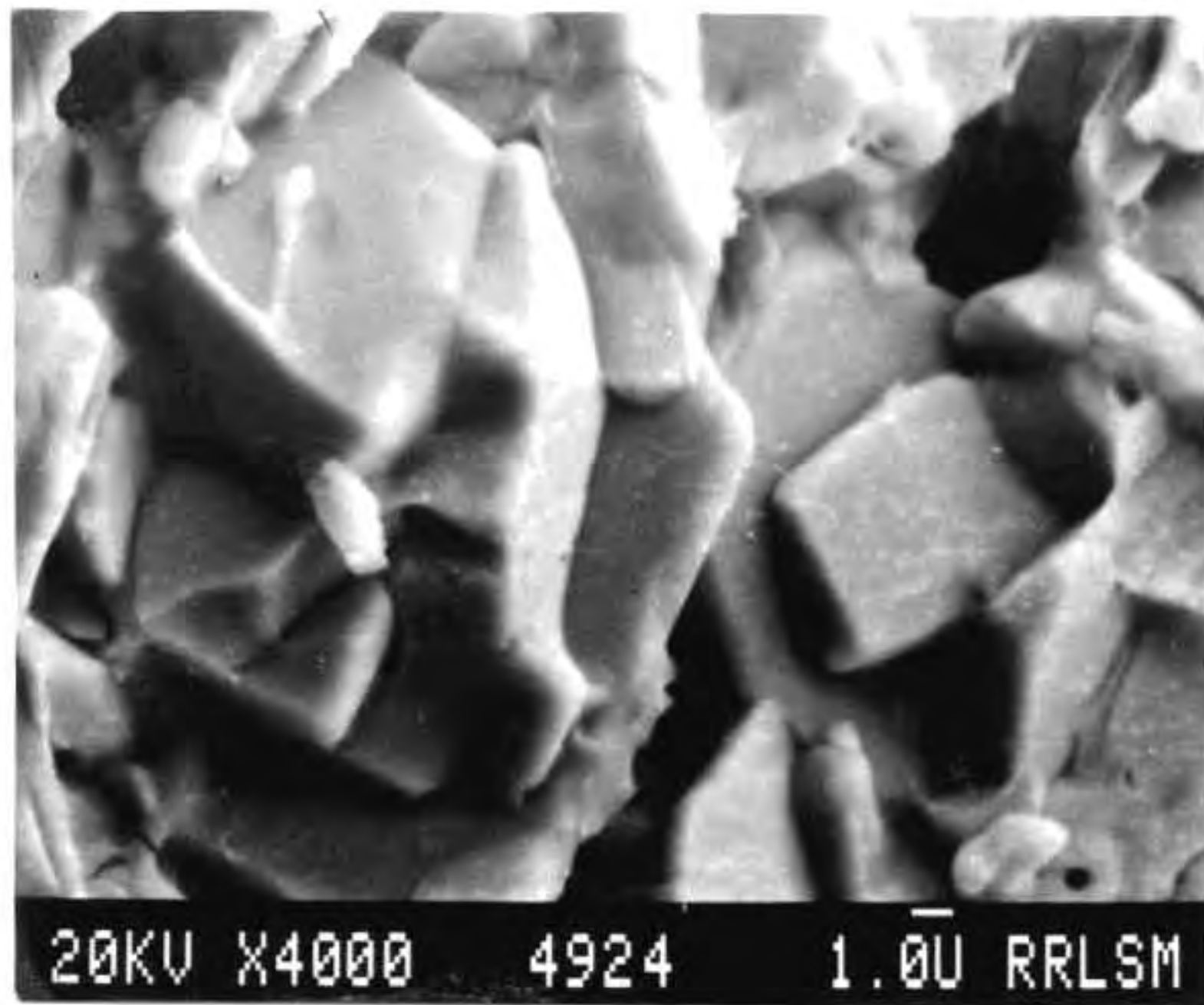


(b)

Fig. VI.7 Fractured surface of sintered YBCO sample derived through (a) solid state route, (b) citrate



(c)



(d)

Fig. VI.7 Fractured surface of sintered YBCO sample derived through (c) flash, (d) microwave methods

surface appears to be very minimum. The microstructure further reveals minimum of porosities, which is explained by the high sintered density values.

The samples prepared through flash combustion method, with its low sintered density compared to other methods, exhibits a sort of random porous microstructure while, the grain size themselves are smaller as can be seen in Fig.VI.7c. This situation arises possibly because of the high surface porosities of the particles before sintering. However, morphologically the grains are different from the citrate derived ones. On the other hand, the microwave derived YBCO exhibits a similar morphological feature as in the case of citrate derived ones. However, the grains appear to be thinner while they are more flaky in nature and no appreciable porosity is observed (Fig.VI.7d). The microstructure is very compact, dense and fully sintered with a near average grain size of 8-10 microns. The highlights of the powder characteristics, sintering behaviour and superconducting properties of the different powders are summarised in Table VI.6.

VI.4 Conclusion

This chapter deals with the comparison of physical and electrical properties of $\text{YBa}_2\text{Cu}_3\text{O}_{7-\delta}$ samples derived through different chemical methods of preparation. A powder was also synthesized by conventional solid state reaction route. The properties of non conventionally prepared powders showed

Table VI.6 Properties of YBCO powders derived through different powder preparation techniques

Properties	Citrate	Flash	Microwave	Conventional solid state
Particle size, μm	1.5	4.0	2.0	10
Green density (% theoretical)	52	44	51	42
Sintered density (% theoretical)	93	88	92	83
Sintering temp. $^{\circ}\text{C}$	940	940	940	940
Sintering time (hour)	10	10	5	10
Sintered grain size μm	8-12	5-10	10-12	15-20
Jc A/cm^2	225	190	210	110-125
Jc (Powder in tube method) A/cm^2	1650	-	885	-
Grain size (after melt texturing) mm	1-2	-	1-2	-

improved features compared to conventional one. It also showed lesser preparation time, high reproducibility, less second phase impurities and small grain size compared to the conventional counterpart. However, it appears that the above properties are specific for the method adopted. Hence the right selection of the method for the desirable end properties of the superconductor becomes extremely significant.

References

1. D.R. Clark, T.M. Shaw and D. Dimos, *J. Am. Ceram. Soc.*, 72(7) (1989) 1103.
2. E.D. Sprecht, K.J. Sparks, A.G. Dhere, J. Brynestad, O.B. Cavin, D.M. Kroeger and H.A. Oye, *Phys. Rev. B.*, 37, (1988) 7426.
3. S.X. Dou, H.K. Lin, A.J. Bourdillon, N. Savvides, J.P. Zhou and C.C. Sorrel, *Solid State Comm.*, 68, (1988) 221.
4. K.T. Tu, N.C. Yeh, S.T. Park and C.C. Tsuei, *Phys. Rev. B.*, 39, (1989) 304.
5. P.K. Gallagher, H.M. O'Bryan, S.A. Sunshine and D.W. Murphy, *Mat. Res. Bull.*, 22, (1987) 995.
6. M.F. Yan, W.W. Rhodes and P.K. Gallagher, *J. Appl. Phys.*, 63(3), (1988) 821.
7. S. Ikeda and K. Ogawa, *Hyomen-Kagaku*, 9, (1988) 17.
8. K. Kimura, A. Matisushita, H. Aoki, S. Ikeda, M. Uehara, K. Honda, T. Matsumoto and K. Ogawa, *J. Jap. Institute of Metals*, 52, (1988) 441.
9. S. Nakahara, G.J. Fisanick, M.F. Yan, R.B. Van Dover, T. Boone and R. Moore, *J. Crystal Growth*, 85, (1987) 639.
10. D. Dimos, P. Chaudhari and J. Manhart, *Phys. Rev. B.*, 41, (1990) 4038.
11. M. Endo and K. Miyashita, *J. Ceram. Soc. Inter. Edn.*, 97, (1989) 1.

12. N. Ruffer, M. Aslam, G. Kaiser, R. Groner and K. Schulze, *Supercond. Sci. Technol.*, 4, (1991) 43.
13. H. Murakami, J. Nishino, S. Yaegashi and Y. Shiohara, *J. Ceram. Soc. Jap., Int. Edition*, 98-624, (1991) 4.
14. M. Dhalle, W. Boon, E. OsQviguil, C. Van Haesendonck, Y. Brugnseraede, J. Kwarciak and O. Vander Biest, *Physica C.*, 185-189, (1991) 2447.

P a r t B

CHAPTER VII

SOL-GEL METHODS AS APPLIED TO PREPARATION OF ALUMINA AND STRONTIUM TITANATE

VII.1 Introduction

Out of the several chemical methods of preparation for the ceramic particulates, sol-gel methods are still being considered one of the most interesting in view of the advantages of superior homogeneity of phases, control of purity, particle characteristics and also low temperature processing(1). However, it requires handling of solutions, strict control over the pH and temperature of precipitation or gelation and also calls for utmost care in reducing the agglomeration of the final particulates(2). However, nanophase particulates have been easily achieved in many systems of practical importance, such as titania, iron oxide and many mixed oxides important in electronic application(3-5).

Most of the sol-gel methods for advanced materials are based on alkoxide hydrolysis-condensation-gelation reactions. Such methods, in general, are superior to all other sol-gel methods although universally accepted as expensive. Hence pure salts have also been found adequate as starting materials for the preparation of ceramic oxides depending on the quality of the ceramic particulates required for final application. For

example, aluminium nitrate and chloride can be the salt for the preparation of boehmite, monohydroxy aluminium oxide (Al-O-OH) which can further be converted into a gel as a precursor to aluminium oxide(6,7). However, the gelation characteristics are physical in nature different from the reactions involved in alkoxide systems, as seen in earlier chapters.

In the case of multi component systems, either a mixture of alkoxides can be hydrolysed together or converted into a gel, or also use a high purity salt solution to hydrolyse the alkoxide component. However, since all the alkoxides are highly unstable in aqueous environment, use of intermediate anions to stabilize alkoxide system have been looked into as in the preparation of BaTiO_3 (8). Acetic acid is generally used as such agents. The sequence of reactions proceed through an intermediate compound, which is highly stable in aqueous medium and hence facilitating easy manoeuvrability for gelation or spray drying or also for flocculation-gelation.

In all sol-gel based methods the agglomeration of fine particulates still create lot of problems. Although concepts of gel casting and sintering techniques have shown considerable improvement in solving this problem to some extent(9), the particulates still get agglomerated when separated in solid state. Surface hydroxyls remaining on the particles are found to be one of the major contributing factors for the agglomeration. The formation of agglomerates can have many sources of origin such as from Van der Waals forces,

Capillary forces etc. The Van der Waals forces exponentially increase as particle size reduces, the agglomerate in submicron powders are very much inherent(10). The tendency of agglomeration can be reduced during powder synthesis by

- (a) selection of suitable condition during precipitation(11-13)
- (b) treating precipitates before or during drying(14)
- (c) selection of suitable solvents in synthesis media(15,16)
- (d) washing the prepared powders with suitable organic solvents(17-19)
- (e) effective removal of anions(20)
- (f) hydrothermal treatments(21)
- (g) optimization of calcination temperature etc.(13)

Preferential washing of the particles with alcohol or less polar solvents seems to be one of the good solutions.

Both alumina and strontium titanate were identified to be possible candidate materials for use as substrates for the high T_c superconductors. Further, these two ceramic materials in high density sintered form has a wide range of applications. Hence the application of sol-gel technique has been made in the preparation of fine alumina and strontium titanate particulates in the present work. Alumina through boehmite intermediate is based on the spray drying of a sol starting from a high purity aluminium salt in aqueous medium, while the

strontium titanate has been prepared through the principle of chemical gelation using a water-soluble acetate intermediate starting from mixture of titanium isopropoxide and high purity strontium nitrate. Possibility of obtaining higher sintered density as well as compact microstructure by surface treatments of sol-gel derived ceramic powders are also investigated.

References

1. E.A. Barringer and H.K. Bowen, *Ceram. Eng. Sci. Proc.*, 5(5-6) (1984) 285.
2. J.D. Mackenzie, pp.113-122, *Science of Ceramic Chemical Processing*, eds. L.L. Hench and D.R. West, Wiley Interscience, New York, 1986.
3. J. Livage, M. Henry, J.P. Jolivet and C. Sanchez *MRS Bulletin*, 15(1) (1990) 18.
4. T. Sugimoto, *MRS Bulletin*, 14(12) (1989) 23.
5. M. Ozaki, *MRS Bulletin*, 14(12) (1989) 35.
6. A.C. Pierre and D.R. Uhlmann, *Ultrastructure Processing of Advanced Ceramics*, Eds. J.D. Mackenzie and D.R. Ulrich, Wiley Interscience, New York, 1988.
7. M. Le Peintre, *Compt. Rend.*, 226(7), (1948) 1370.
8. C. Sanchez, F. Babonneau, S. Doeuff and A. Leautic, pp.77, *Ultrastructure processing of Advanced Ceramics*, Eds. J.D. Mackenzie and D.R. Ulrich, Wiley Interscience, New York, 1988.
9. O.O. Omatete, M.A. Janney and R.A. Strehlow, *Am. Ceram. Soc. Bull.*, 70(10) (1991) 1651.
10. A. Roosen and H. Hausner, *Adv. Ceram. Mater.*, 3(2) (1988) 131.
11. M.A.C.G. Van de Graaf, J.H.H. ter Matt and A.J. Burggraaf, pp.783-794, *Ceramic Powders*, Ed. P. Vencenzini, Elsevier, Amsterdam, 1983.

12. E. Crucean and R. Rand, *Trans. Br. Ceram. Soc.*, 78, (1979) 58.
13. M.A.C. Van de Graff, K. Keizer and A.J. Burggraaf, pp.83-92, *Science of Ceramics*, 10, (1979).
14. W.D. Kingery, pp.3-18, *Ceramic Powders*, Ed. P. Vencenzini, Elsevier, Amsterdam, 1983.
15. H.K. Varma, K.G.K. Warriar and A.D. Damodaran, *Ceram. Inter.*, 16(2), (1990) 73.
16. H. Yamamura, A. Watanabe, S. Shirasaki, Y. Moriyoshi and M. Tanada, *Ceram. Inter.*, 11, (1985) 17.
17. K. Haberko, *Ceram. Inter.*, 5, (1979) 148.
18. M.S. Kaliszewski and A.H. Heuer, *J. Am. Ceram. Soc.*, 73(6), (1990) 1504.
19. S.LK. Dole, R.W. Scheidecker, L.E. Shiers, M.F. Benard and O. Hunter, *Mater. Sci. Eng.*, 32, (1978) 277.
20. C.E. Scott and J.S. Reed, *Am. Ceram. Soc. Bull.*, 58(6), (1979) 587.
21. E. Tani, M. Yeshimura and S. Somiya, *J. Am. Ceram. Soc.*, 66(1), (1983) 11.

CHAPTER VIII

STRONTIUM TITANATE CERAMIC FROM MODIFIED METAL ALKOXIDE PRECURSORS

VIII.1 Introduction

Strontium titanate is one of the leading titanate perovskite compounds which have extensively found application in electronic ceramic industry. The compound has a cubic structure consisting of six O^{--} , eight Sr^{++} and one Ti^{4+} in a unit cell and has a face centered cubic array of strontium plus oxygen ion, with titanium in one quarter of the octahedral interstices.

The widespread use of these titanate class of materials is due to their high polarizable crystal structure and wide range of electrical properties made possible by various chemical modifications such as doping, varied cation stoichiometry etc(1). Appropriate control over the processing conditions have also supplemented towards attaining the desirable properties. Pure strontium titanate is paraelectric at room temperature. When cooled through $-125^{\circ}C$, its unit cells become tetragonal and develops a dipole charge on their minor phases. Because of these phase change, the grain size of this sintered ceramic plays an important role with respect to its dielectric constant. Further, the easy sinterability of the

This work was published

* *British Ceramic Society Transaction and Journal*, 90 (1991) 189.

* *Journal of American Ceramic Society*, (in press).

starting strontium titanate particulates at low temperature becomes very significant. At room temperature dielectric constant is found to be around 320 which increases gradually with decreasing temperature. Strontium titanate has been recognised as an important dielectric material, especially with respect to its use in grain boundary barrier layer capacitors(2). Strontium titanate compositions with and without doping are also used for making high voltage capacitors. Further, strontium titanate has recently been found as a good substrate material for high T_c superconductor thin film because of its property of good adhesion, structural compatibility and good thermal expansion match with superconductor films. The dielectric property of strontium titanate is known to depend on a wide variety of factors including its stoichiometry, presence of impurities, sintered density and grain size and nature of dopants used(3). Conventional ceramic powder preparation techniques such as mixing, ball milling and calcination and sintering at an elevated temperature usually result in the introduction of impurity phases. Strontium titanate, however, has been prepared by hydrolysing the titanium hydroxide in a suspension of strontium carbonate followed by calcination similar to the method adopted for the preparation of aluminium titanate(4), where the titanium alkoxide was hydrolysed in a aqueous suspension containing alumina particles. Bowen et.al. used alkoxy metal carboxylate precursors for preparing spherical

strontium titanate powders(5). These methods, however, are based on hydrolysis of alkoxides which is too fast to control, although preparation of micron sized and unagglomerated powders has been reported under certain conditions(6,7). All these aspects are well described in the review appeared recently(8). Similarly the high activity of these alkoxides with water is one major problem in many of these processes. Chemical additives are often used in order to modify the reactivity of such molecular precursors. Sanchez et.al. studied, in detail, the hydrolysis-condensation reactions of titanium alkoxide in the presence of a variety of chemical additives such as acetic acid and acetyl acetone(9). These studies showed that such additives avoid TiO_2 precipitation and lead to monolithic gels or stable colloids. This type of a modification has been adopted in the case of preparation of barium titanate by sol gel technique(10,11). The titanium isopropanol reacts with excess of acetic acid to form an acetate precursor, which in presence of water, hydrolyses to a clear liquid which can be further gelled. When allowed to gel the above sol, and during drying of the gel, agglomeration occurs, although the particles will be submicron in size.

Spray drying of the sol or dispersion of a gel in a solvent would facilitate the formation of free flowing spherical agglomerates which would assist in the attainment of high compaction densities. This chapter discusses the preparation of strontium titanate powder of size less than 1

micron by spray drying of a redispersed gel and a stable sol prepared from a water solution of strontium nitrate, titanium isopropoxide and acetic acid. The powder characteristics and densification behaviour and dielectric property of the highly densified pellets were studied.

VIII.2 Spray drying of redispersed gel

VIII.2.i Experimental

Titanium isopropoxide, (Aldrich, England) was 99.9% pure. Strontium nitrate, acetic acid and isopropanol were of AR (BDH) grade.

Titanium isopropoxide (14.1 ml) was dissolved in a mixture of isopropanol (14 ml) and acetic acid (25 ml) by dropwise addition under constant stirring. To this mixture, a solution of strontium nitrate (10 g) in 50 ml double distilled water was added dropwise. The solution was gelled in petri dishes of size 20 mm dia. The gel was redispersed in water-isopropanol mixture (1:1) and spray dried through a nozzle of 0.75 mm dia. Thermal analysis of the powder was done. The powder was calcined at 1000°C, compacted at 100 MPa and sintered at 1400°C.

VIII.2.ii Methods

The characterization of the sprayed powder was done by particle size analysis, XRD, IR, BET surface area and SEM as

described in the Chapter II. The spray drying was carried out in a Buchi mini spray dryer (Switzerland). The dielectric properties were measured in an Impedance analyser, Hewlett Packard Impedance Analyser Model 4192ALF. In this, circular sintered discs of the samples were electroded with room temperature curable silver paste and the capacitance as well as electric loss was recorded. From the capacitance values dielectric constant was calculated using the equation

$$K = \frac{C d}{\epsilon_0 A}$$

where C is the capacitance, ϵ_0 is the dielectric constant of free space and A and d are the area and thickness of the sample.

VIII.2.iii Results and discussion

The TGA curve for the powder prepared by spraying the strontium titanate gel is shown in Figure VIII.1. The spray dried powder had an initial moisture content of 3-5%. However, as the temperature was raised, the decomposition of the solvents and other constituents in the gel took place with a major loss in weight between 350-500°C. The decomposition was complete below 600°C, the total loss in weight being about 35%. This is clarified further in Figure VIII.2 which shows the infrared spectra of the various samples, as-sprayed and after heating at 450°, 650° and 800°C. The important points to note from this

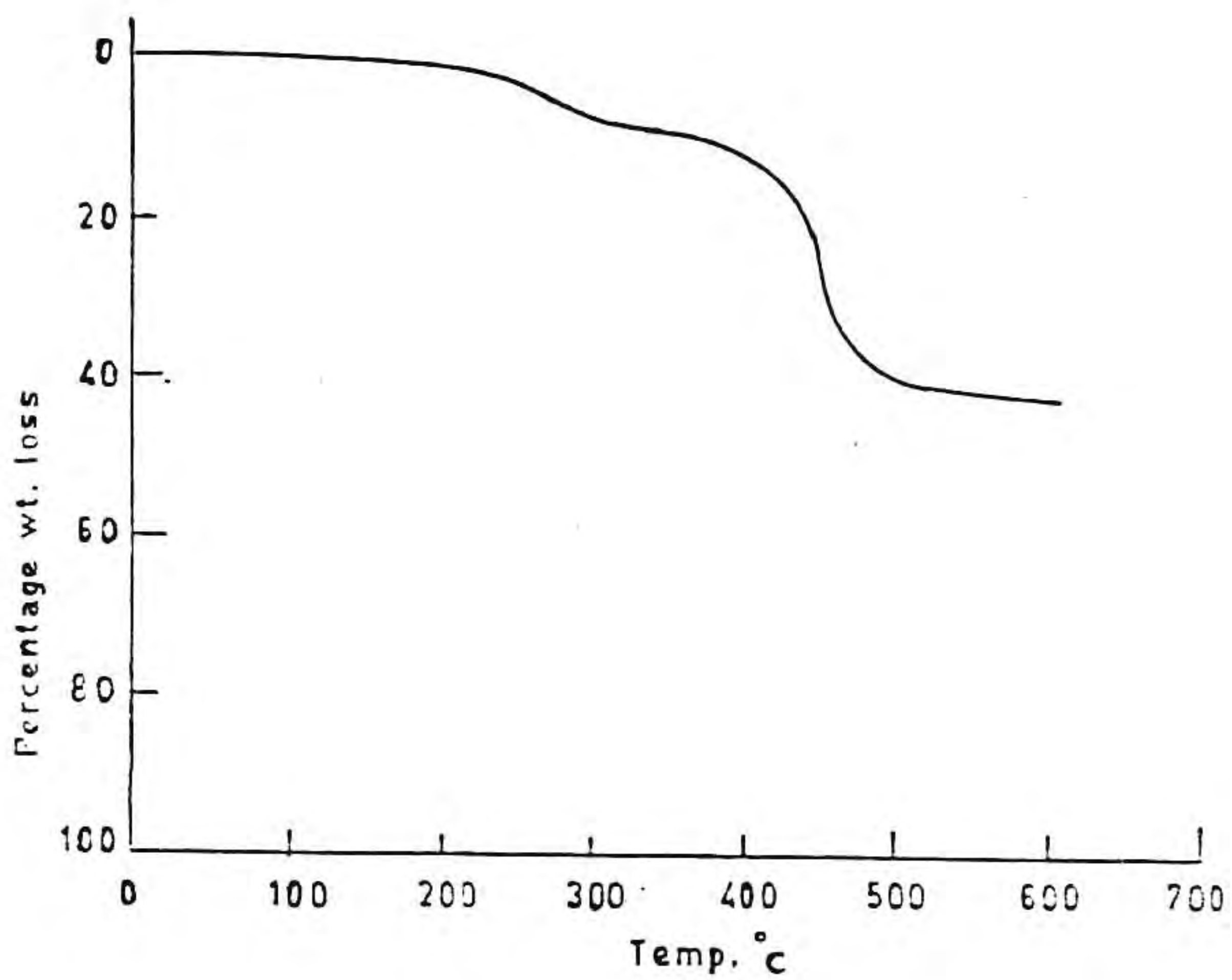


Fig. VIII.1 TGA curve of the spray dried SrTiO₃ gel

figure are the extent of removal of hydroxyls and also the possible formation of the strontium titanate phase. The peak due to the hydroxyl group appearing around 3600 cm^{-1} is very strong in the gel sprayed powder and there are complex broad absorption peaks in the range $1400\text{--}1500\text{ cm}^{-1}$ and also $600\text{--}500\text{ cm}^{-1}$ (Figure VIII.2(a)). After heating to 450°C (Figure 2(b)), there was a definite loss of hydroxyls in line with the observations obtained from the TGA analysis. The peaks between 1350 and 1500 cm^{-1} due to the COO^- stretch were reduced on increasing the temperature. However, at 650°C , the peak retained around 1450 cm^{-1} (Figure VIII.2(c)) could be due to the traces of carbonates formed during the decomposition of organics. This peak was no longer present after heating at 800°C , which resulted in complete formation of strontium titanate (Figure VIII.2(d)). The sample heated at 450°C developed a small peak around 500 cm^{-1} which increased over the range 650°C and remained almost constant up to 1400°C . This is assigned to strontium titanate(10) and demonstrates that titanate is formed at a temperature as low as 650°C .

The XRD patterns of the spray dried gel and of samples heated at various temperatures up to 1400°C are shown in Figure VIII.3. The pattern for the gel is very similar to that for strontium nitrate (Figure VIII.3(a)) alone, since the hydrolysed titanyl acetate would be in an amorphous state(12) and holding the other constituent ions in the gel network, as in the case of barium titanate prepared by acetate routes. On

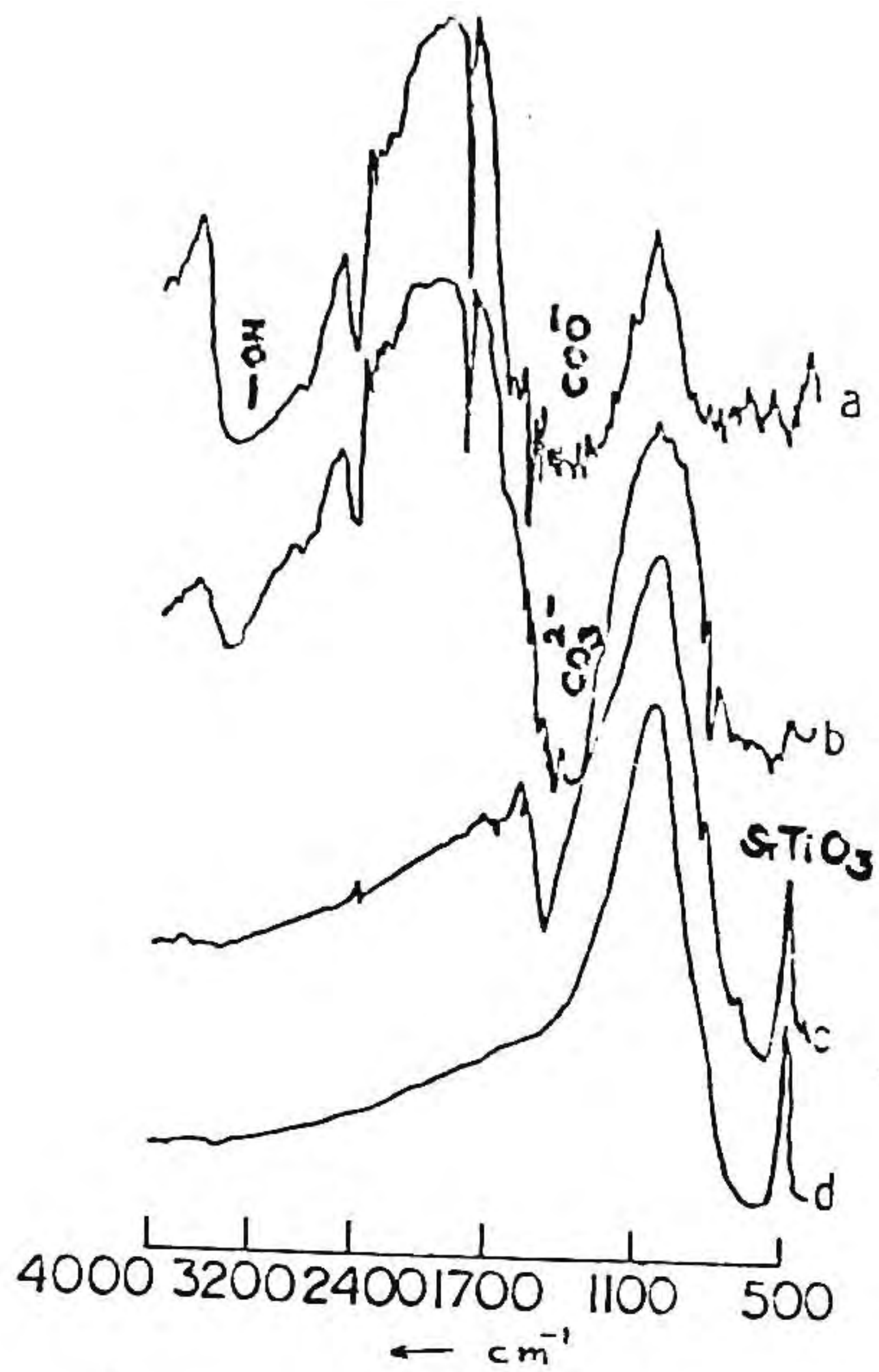


Fig. VIII.2 IR spectra of the gel sprayed powder heated to different temperature (a) as sprayed, (b) 450°C, (c) 650°C and (d) 800°C

heating the powders to 650°C the strontium titanate phase appeared (Figure VIII.3(b)) with very few impurity peaks. The decomposition reactions were complete at a temperature as low as 800°C with the formation of crystalline strontium titanate (Figure VIII.3(c)); no further change occurred in the XRD pattern after heating the gel derived strontium titanate at 1400°C (Figure VIII.3(e)). However, in separate experiments a mixture of titania and strontium carbonate in stoichiometric proportions heated at 800°C under identical conditions still retained unreacted phases, as shown in Figure VIII.3(d). The reaction of this mixture was complete only after prolonged calcination above 1200°C which caused appreciable grain growth and necessitated high sintering temperatures for increased densification. The XRD pattern of a sample of gel derived strontium titanate at 1400°C is shown in Figure VIII.3(e) which compares with Figure VIII.3(c).

In Figure VIII.4, the particle size distribution for gel sprayed powder, calcined at 1000°C, is shown and indicates average particles of 0.8 microns. About 75% consisted of particles less than 2 microns while about 40% of the powder had particles less than 0.6 microns. The powder had a tap density of 1.17 g/cm³ with good free flowing characteristics. The particles have spherical morphology consisted of sub-micron crystallites (Figure VIII.5(a)). On further calcination at 1200°C, crystallisation and particle growth occurred (Figure VIII.5(b)). Samples of powder calcined at 1000°C were



Fig. VIII.3 XRD patterns of the gel sprayed powder heated to different temperatures (a) as sprayed, (b) 650°C, (c) 800°C, (d) 800°C (solid state mixing route) and (e) 1400°C

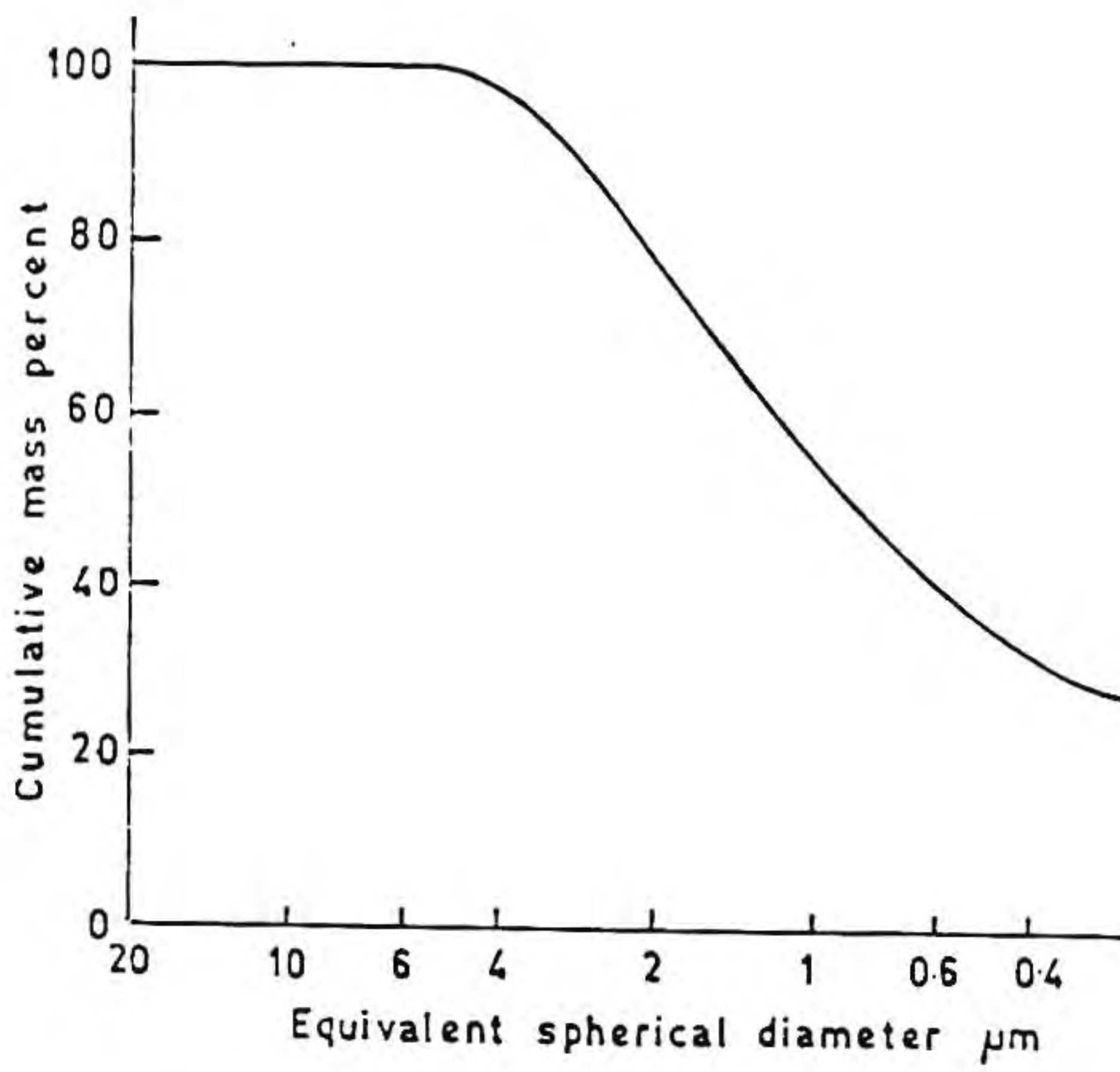
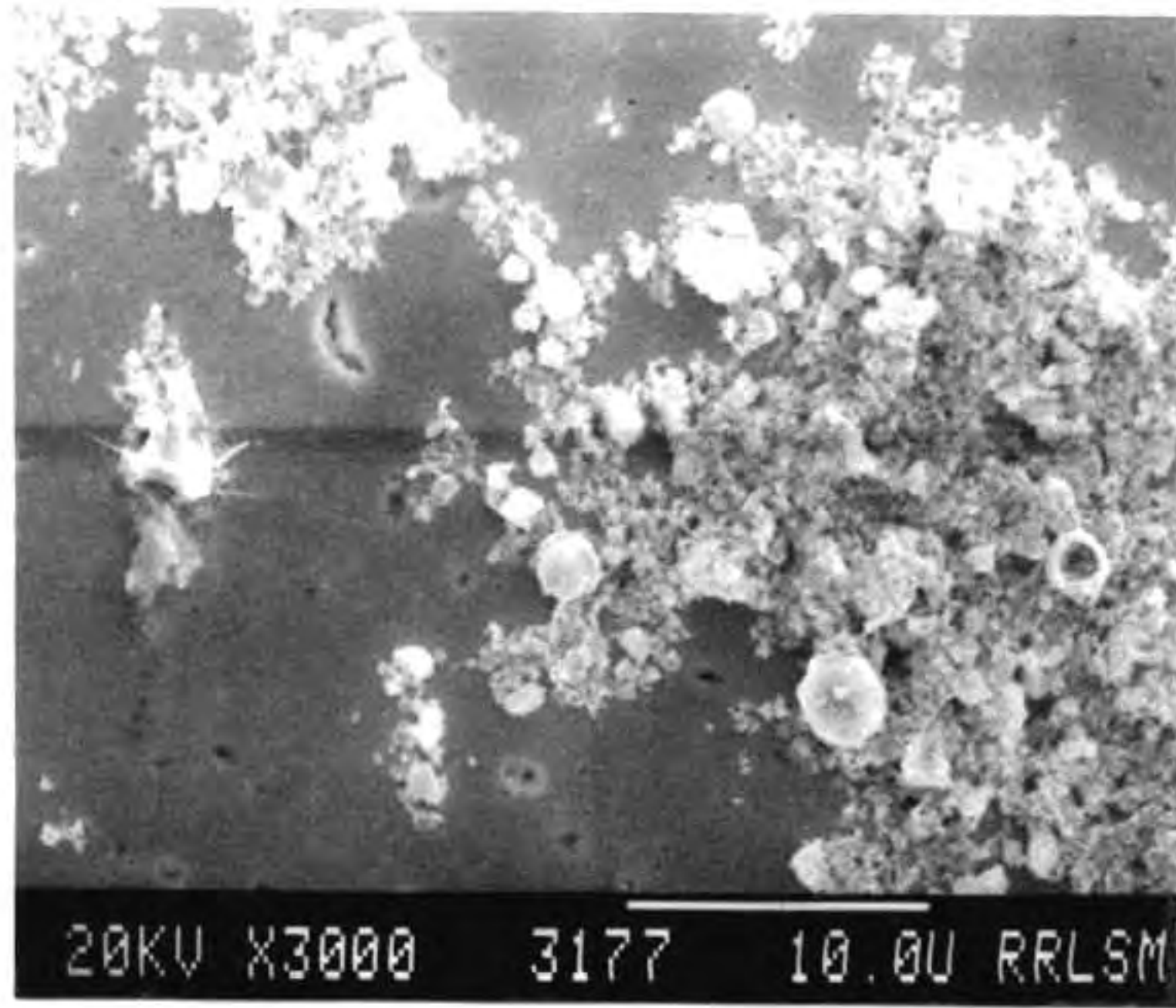
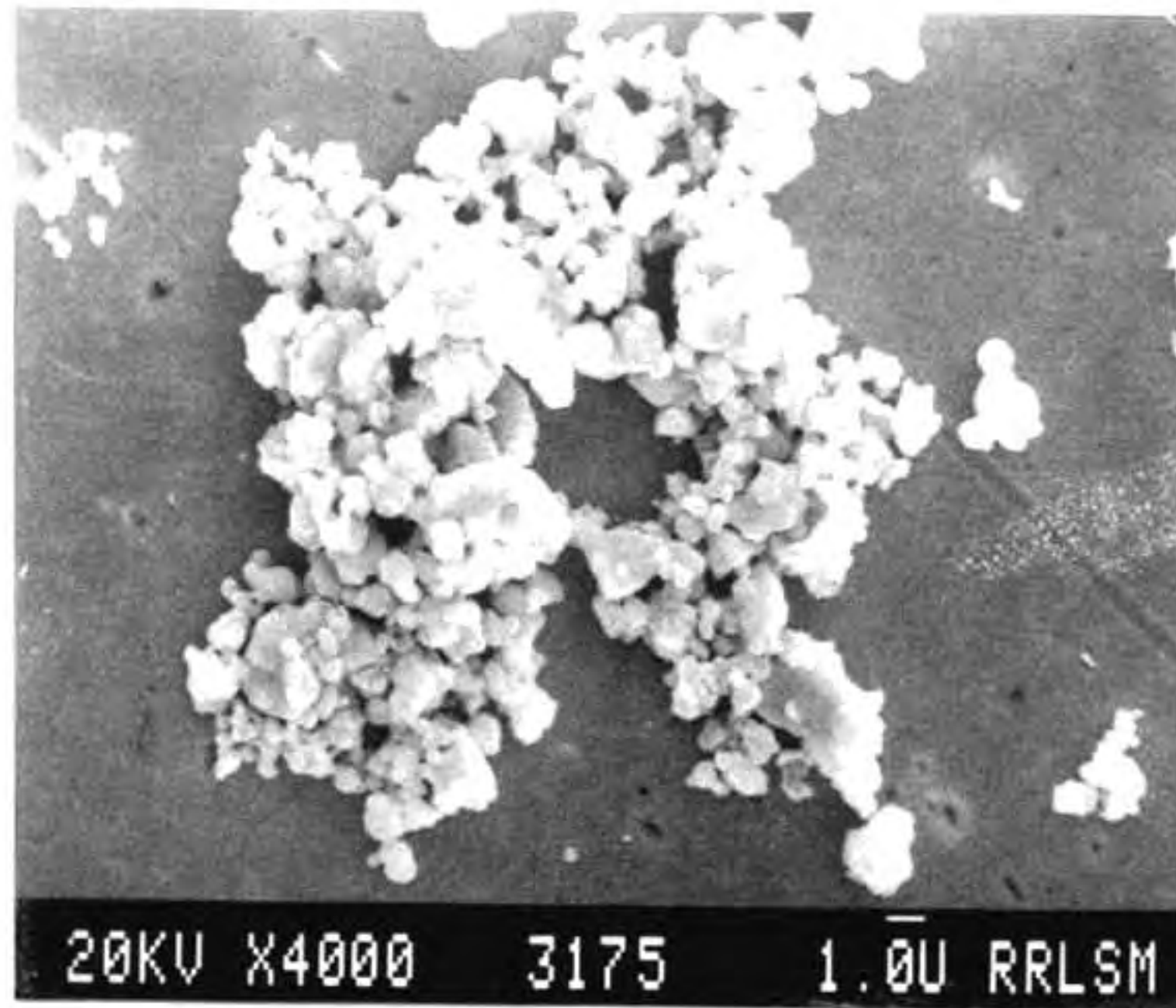


Fig. VIII.4 Particle size distribution curve of gel sprayed powder calcined at 1000°C



(a)



(b)

Fig. VIII.5 SEM pictures of (a) SrTiO_3 powder calcined at 1000°C , (b) the same at 1200°C

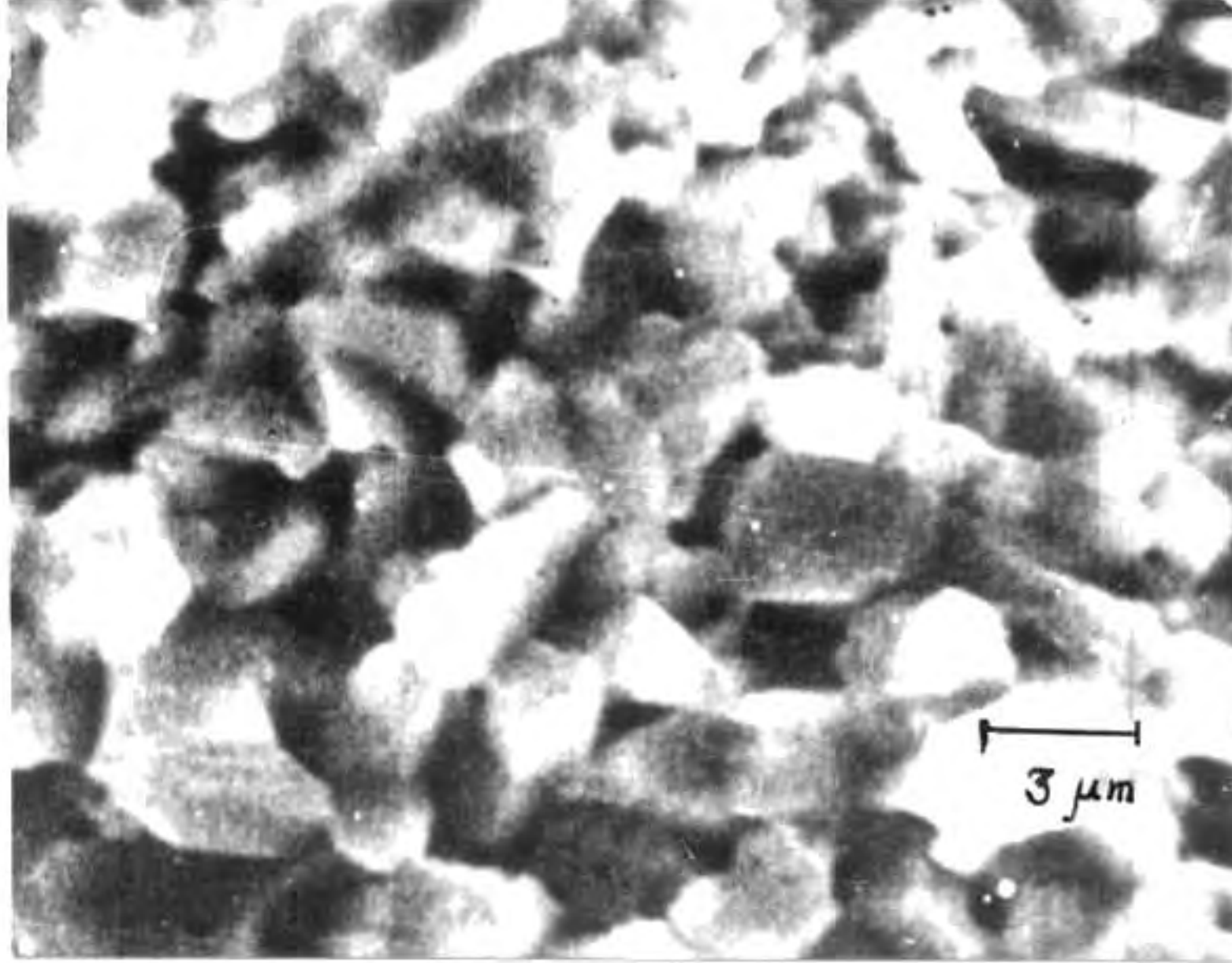


Fig. VIII.5 (c) fractograph of sintered SrTiO_3

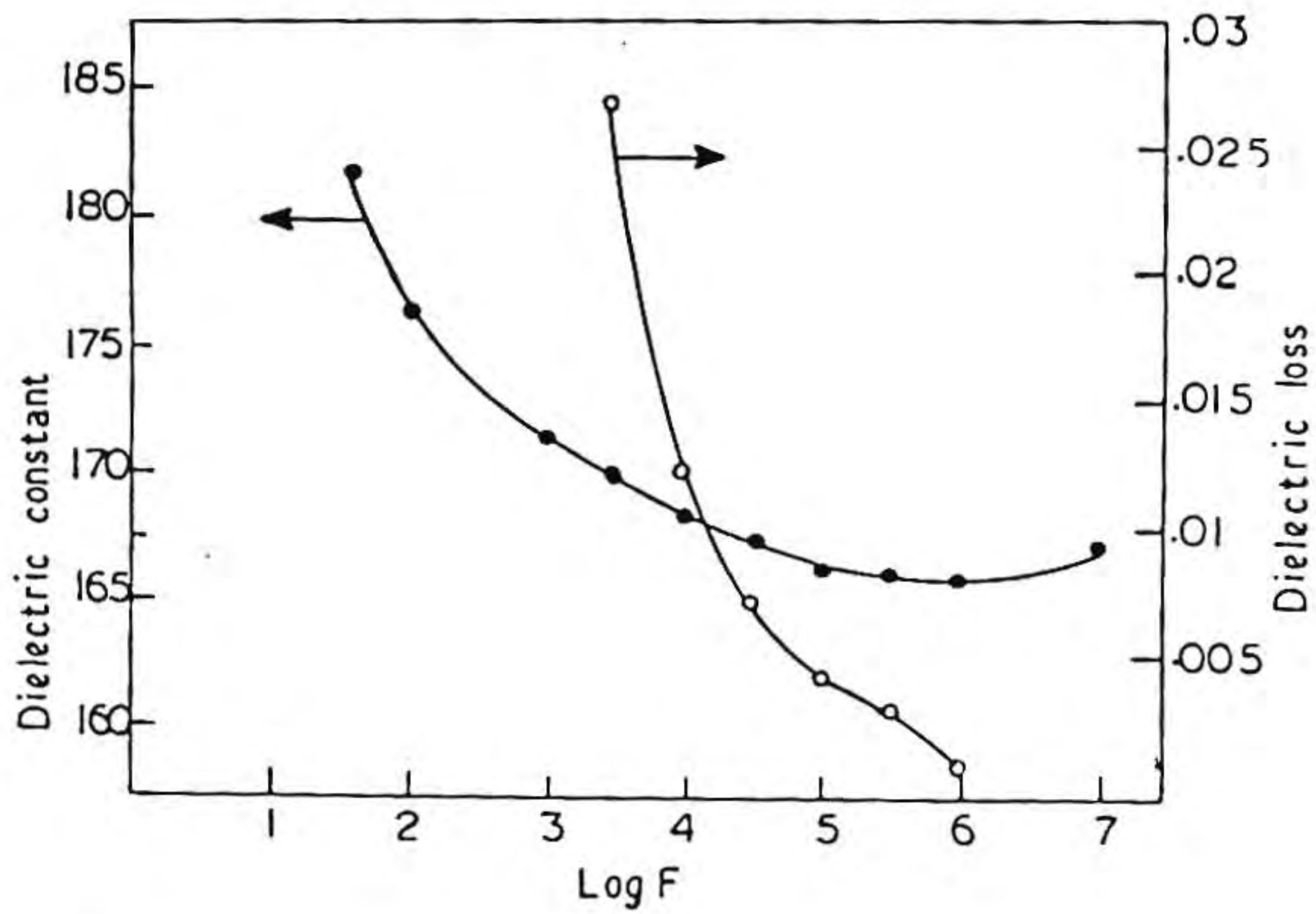


Fig. VIII.6 Frequency vs dielectric properties of sintered SrTiO_3 derived through gel spray route

fabricated to 96% theoretical density by sintering at 1400°C for 2 hrs in air and a fractograph (Figure VIII.5(c)) showed an average grain size of 2-3 microns. Sintered samples had a room temperature dielectric constant of 165 and dielectric loss of 0.0008 when measured at a frequency of 1 MHz, as shown in Figure VIII.6.

VIII.3 Spray drying of a metal alkoxide sol

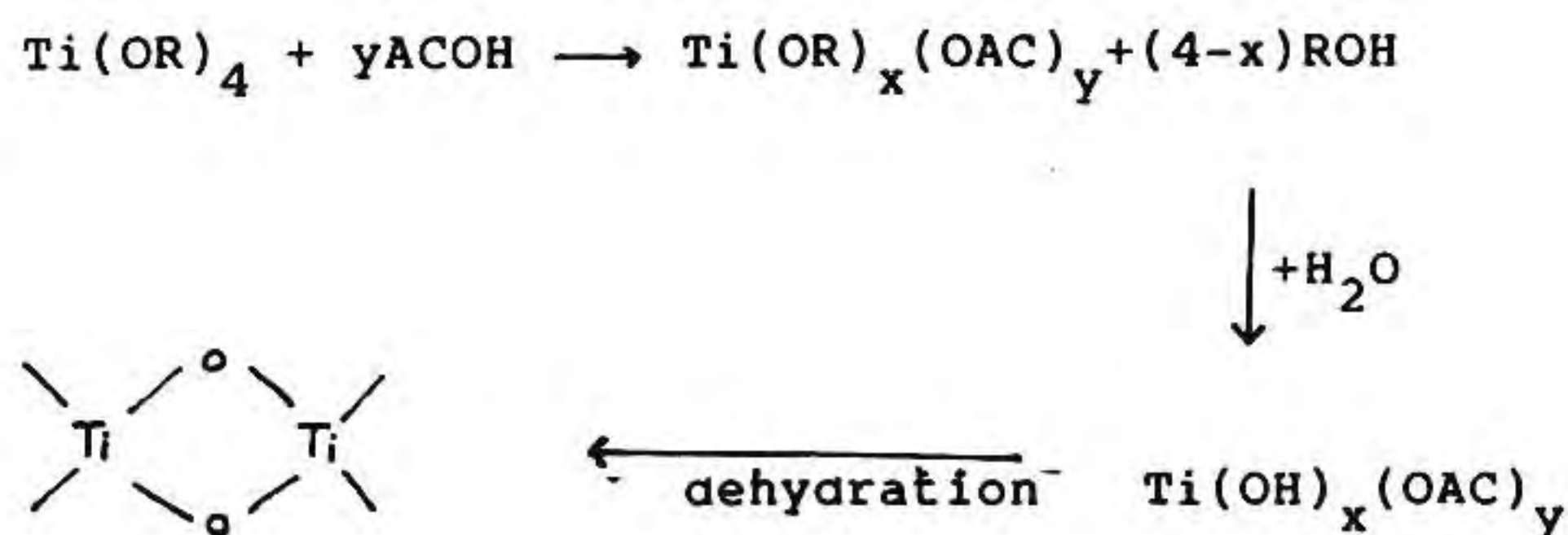
VIII.3.i Experimental

Titanium isopropoxide (14.1 ml) was dissolved in glacial acetic acid (25 ml) and was diluted with isopropyl alcohol and the ratio was varied from 1:1 to 1:3 [Ti(OR)₄:isopropyl alcohol]. A solution of strontium nitrate 10 gm dissolved in 50 ml water was then added to titanium alkoxy acetate solution. Similar batches containing strontium nitrate dissolved in 75 ml and 100 ml lots were also made. All the mixtures were allowed to gel and the rate of gelation was noted using nephelometric (light scattering) technique, by periodically measuring turbidity of 5 ml samples drawn from the bulk, using a nephelometer (Nephelometer Model CL52, Elico Pvt. Ltd., Hyderabad, India). As the gelation progresses, the aliquot sol required suitable level of dilution. This process of measuring the NTU (Nephelometric Turbidity Unit) was continued till constant values were reached indicating near complete gelation. Sol consisting of 50 ml water and 14 ml

isopropanol was used for spray drying (i.e. titanium isopropoxide : isopropanol is 1:1). The NTU value of sol was kept constant throughout the spray drying operation by keeping the sol in an ice bath. The spray drying was done in a Buchi minispray dryer having a nozzle diameter of 0.75 mm. Spray dried powder was further calcined at 250°C to 1000°C. Powder calcined at 1000°C was compacted to discs of 12 mm diameter and 3 mm thickness using a stainless steel die at a pressure of 100 MPa. Samples were sintered in the range 1350°C to 1500°C.

VIII.3.ii Results and discussion

The progress of gelation of an alkoxy derived sol is continuous and rate of gelation depends on a number of parameters like temperature, concentration, and the medium of gelation(8). The hydrolysis and polycondensation process produces polymers in solution leading to rigid gels containing cations interconnected with anion intermediates (-OH, -O-, -OAC etc). The hydrolysis and polycondensation of titanium alkoxy acetate sol can be visualized as,



As the gelation proceeds, the particle concentration increases and this can be measured using light scattering technique with reasonable accuracy as shown by Lin et.al(13). The development of turbidity of a sol is thus measured as Nephelometric Turbidity Units (NTU value) in relation to time of gelation. Figure VIII.7 gives the variation of NTU with time in sols containing different amounts of isopropyl alcohol. The rate of gelation identified by the increase in the NTU values increases with increasing proportions of solvent. The gelation time under the conditions of the present experiment took over 50 hours for a mixture of titanium isopropoxide:isopropanol 1:1 while the same value could be achieved within as low as 20 hours by increasing the ratio to 1:3.

Figure VIII.8 gives the effect of water on gelation behaviour. As is expected, when the alkoxide:water ratio is higher (1:3), gelation becomes faster and high NTU value is reached within as low as 25 hours. However, since the present method is for the preparation of a stable sol, the alkoxide:water ratio is kept minimum for ease of operation. A certain concentration is required in order to avoid the possible localised concentration of $\text{Sr}(\text{NO}_3)_2$ in the system. The optimum concentration was then chosen to have titanium isopropoxide:isopropanol as 1:1 and strontium nitrate was dissolved in 50 ml of water in order that the nephelometric values were constant and the sol could be comfortably spray

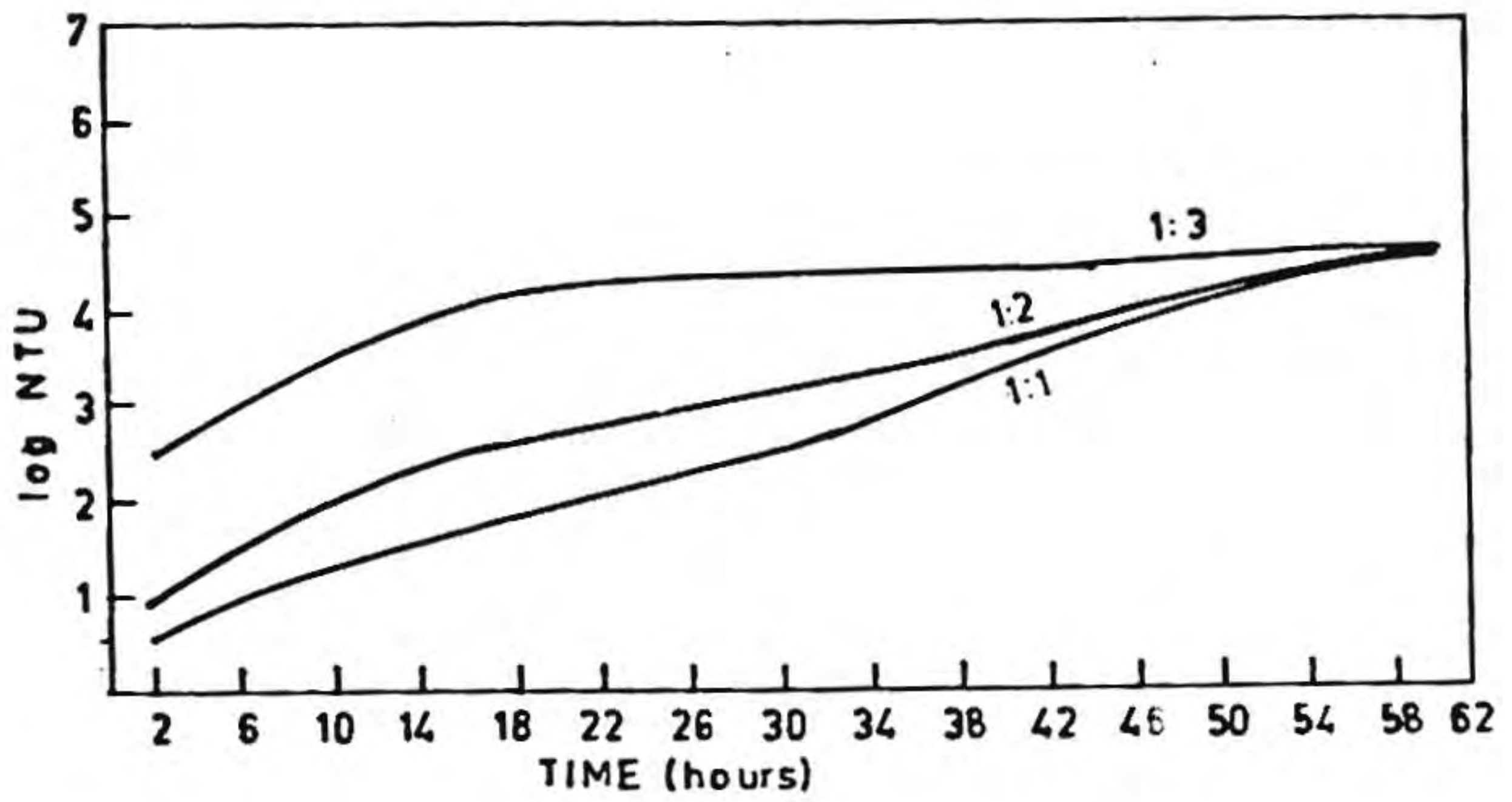


Fig. VIII.7 Variation of NTU value of sol containing different amount of solvent (isopropanol) with time

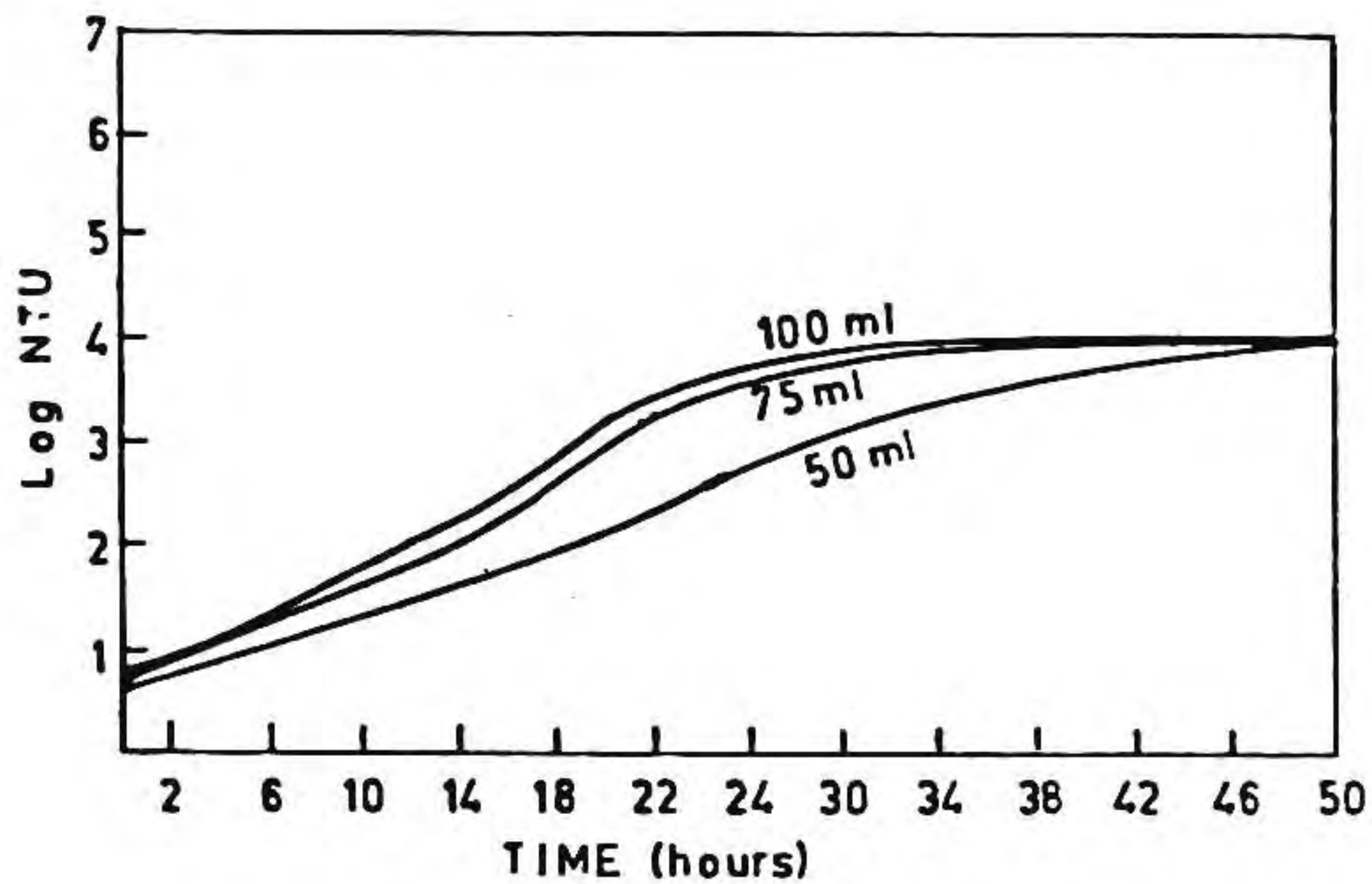


Fig. VIII.8 Variation of NTU value of sol containing different amount of solvent (water) with time

dried.

The spray drying conditions were adjusted such that the nozzle temperature was 180°C, outlet temperature 105°C. The residual moisture content in the spray dried sample was 5%. TGA of the as sprayed powder is given in Figure VIII.9. Leaving the initial weight loss due to adsorbed water, the TGA shows two major weight losses around 250-350°C and 500-575°C, due to decomposition of the organics and free solvents generated during gelation, and to decomposition of strontium nitrate respectively. The total weight loss was about 46%. The corresponding peaks in DTA substantiate these results. There is no further change accompanied by weight loss or no development of further phases at temperature higher than 553°C.

Figure VIII.10 shows the infrared spectra of the sol sprayed powder heated at 400°C to 900°C. The as sprayed powder shows strong absorption peaks for hydroxyl groups around 3600 cm^{-1} . The absorption peaks in the range 1400-1500 cm^{-1} are mainly due to carboxyl stretching. On heating the sample at 400°C, the absorption due to hydroxyls gets reduced and peaks in the range 1400-1500 cm^{-1} get sharpened (Fig. VIII.10b). A new peak starts appearing at 500-400 cm^{-1} in the sample heated at 500°C which could probably be due to oxygen stretching in SrTiO_3 . This observation is reasonably supported by the results of DTA. On further increasing the temperature, there is a gradual reduction in the peaks assigned to CO_3^{--} and $-\text{COO}^-$. The decomposition is rather complete at 800°C in bulk sample,

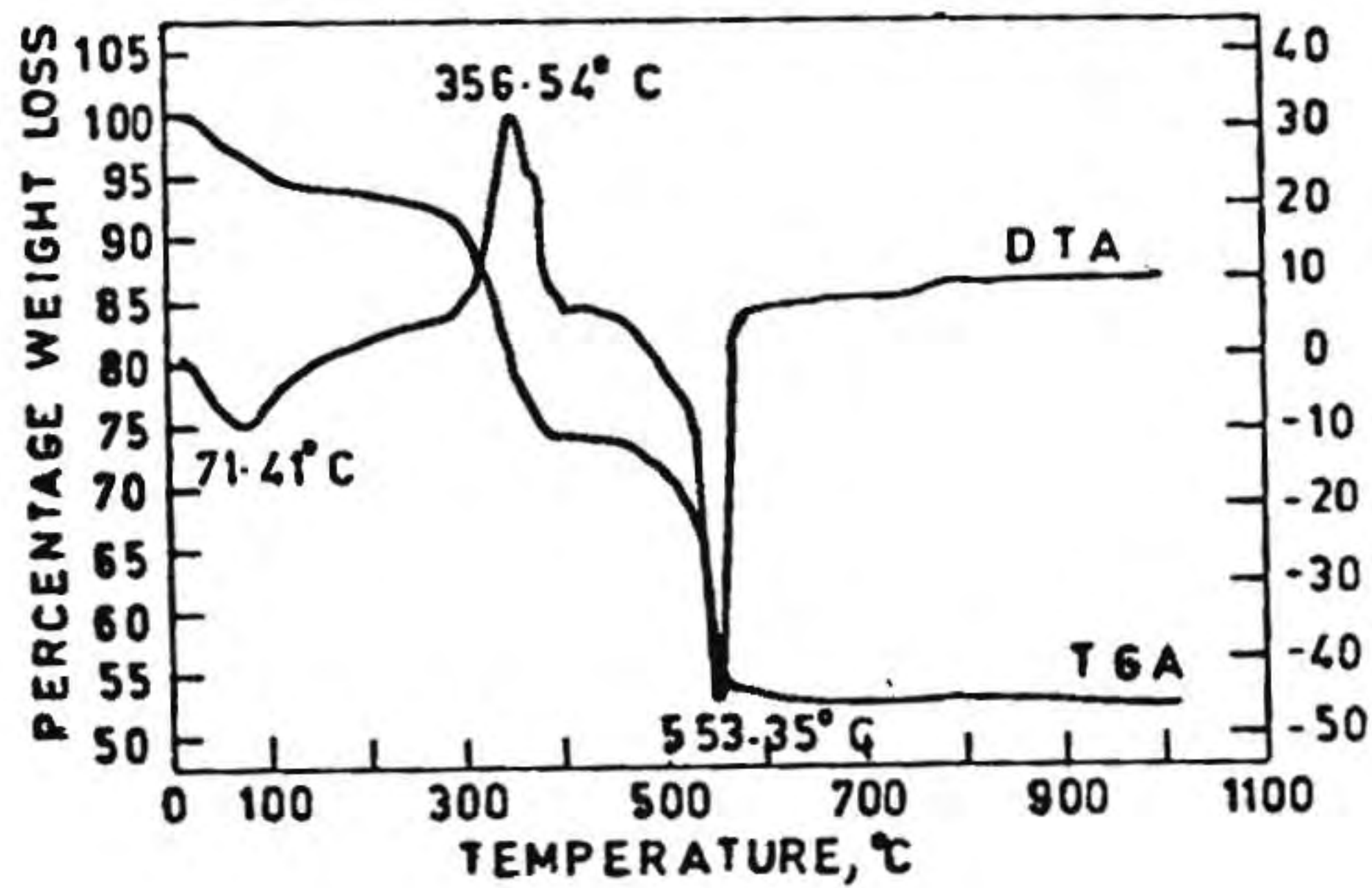


Fig. VIII.9 Thermal decomposition of sol sprayed SrTiO₃ precursor powder

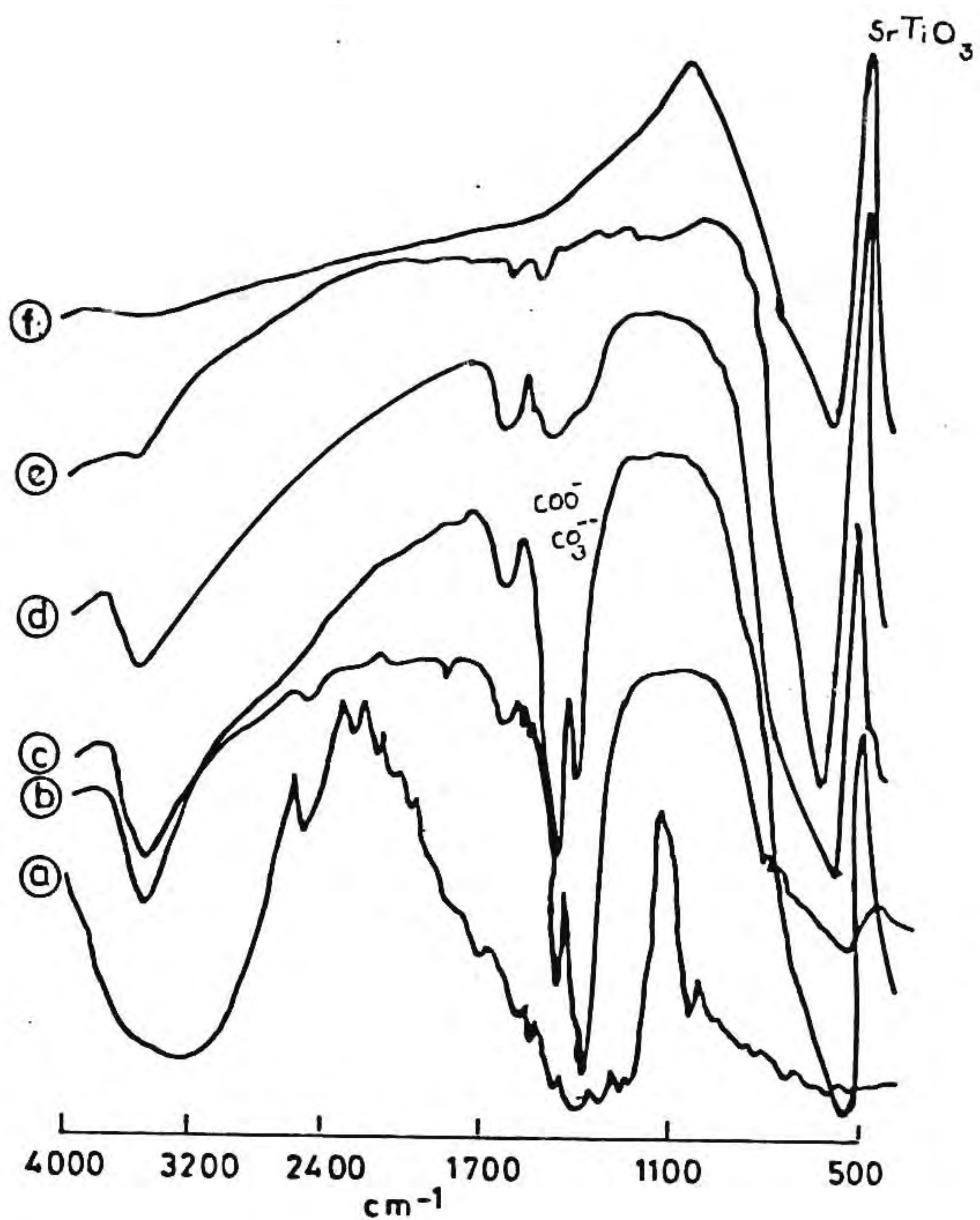


Fig. VIII.10 IR spectra of sol sprayed precursor powder calcined at various temperatures (a) spray dried powder, (b) 400°C, (c) 500°C, (d) 700°C, (e) 800°C and (f) 1200°C

because Fig.VIII.10(d) is identical with the spectra of sample heated at 1200°C. Although the strontium titanate formation has started as early as 550°C, it may require higher temperature for the complete elimination of possible carbonates.

The XRD patterns of the sol sprayed powder heated at various temperatures are given in Figure VIII.11. The XRD pattern of as sprayed powder is similar to that of strontium nitrate (Fig.VIII.11a), since the titanium oxyhydroxide should be in amorphous form. Possibly strontium ions could be attached to the surfaces of the $\text{TiO}(\text{OH})_2$ species. The structure appears to be stable upto 400°C, as is evident from XRD (Fig.VIII.11b). On heating the sample further at 550°C for one hour, the XRD pattern has peaks corresponding to SrTiO_3 phase. First strontium nitrate decomposes around 550°C, SrTiO_3 phase simultaneously forming with no predominant intermediate compounds. On heating further, there is not much change in XRD, excepting that the XRD peaks get further refined.

Figure VIII.12 gives the particle size distribution of the sol sprayed powder calcined at 1000°C. The average particle size is 0.6 microns with majority of particles having size less than 3 microns. The powder has a surface area of 12.402 m^2/g and an average pore radius of 8.32 nm from the BET surface area. The bulk density (tap density) of spray dried powder calcined at 1000°C was 1.3 gm/cc. The green and sintered densities of the strontium titanate calcined at 550°C, 800°C, 1000°C and 1200°C are presented in Table VIII.1. The compaction was done at a

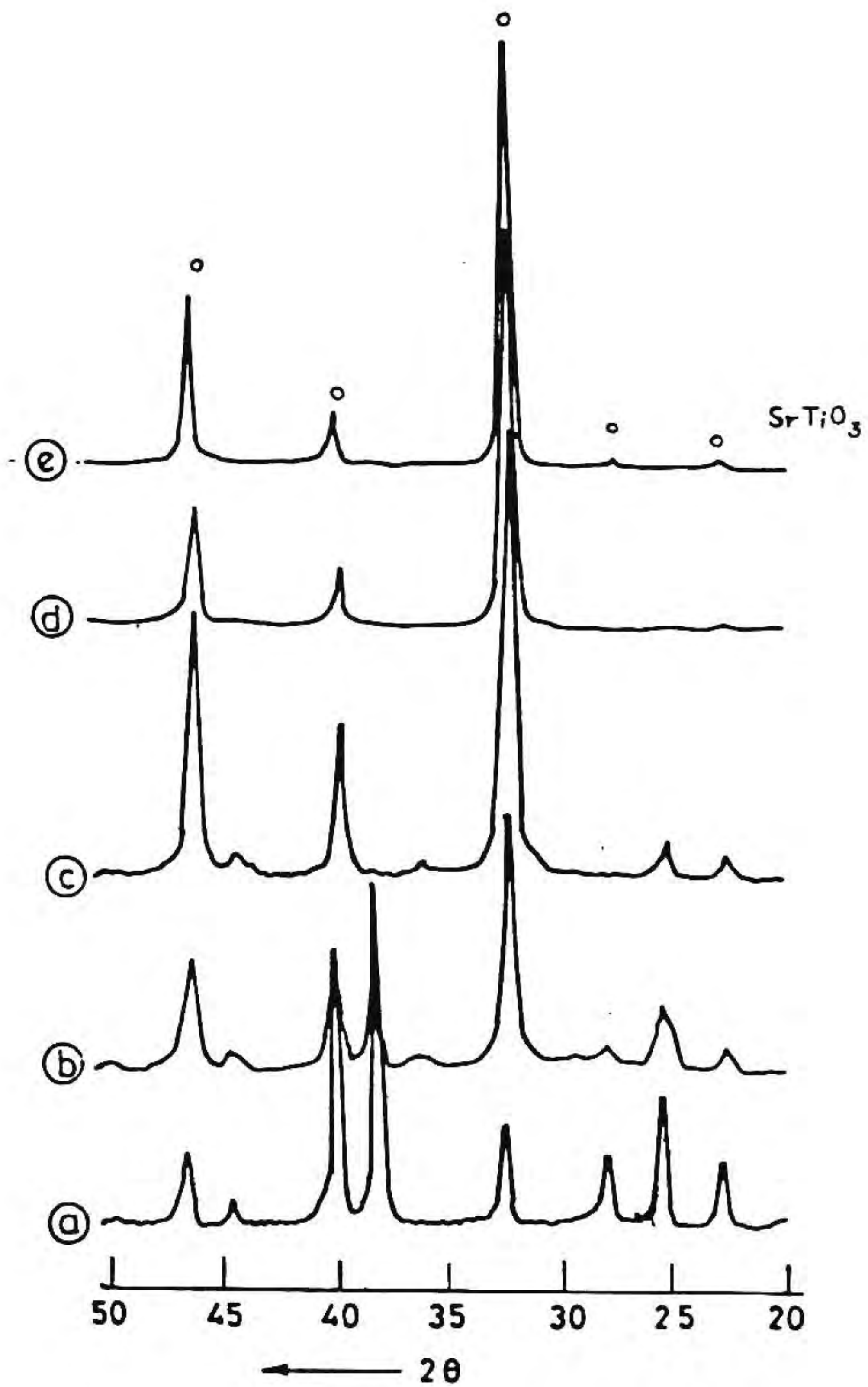


Fig. VIII.11 XRD patterns of sol sprayed precursor powder calcined at various temperatures (a) spray dried powder, (b) 400°C, (c) 550°C, (d) 800°C and (e) 1200°C

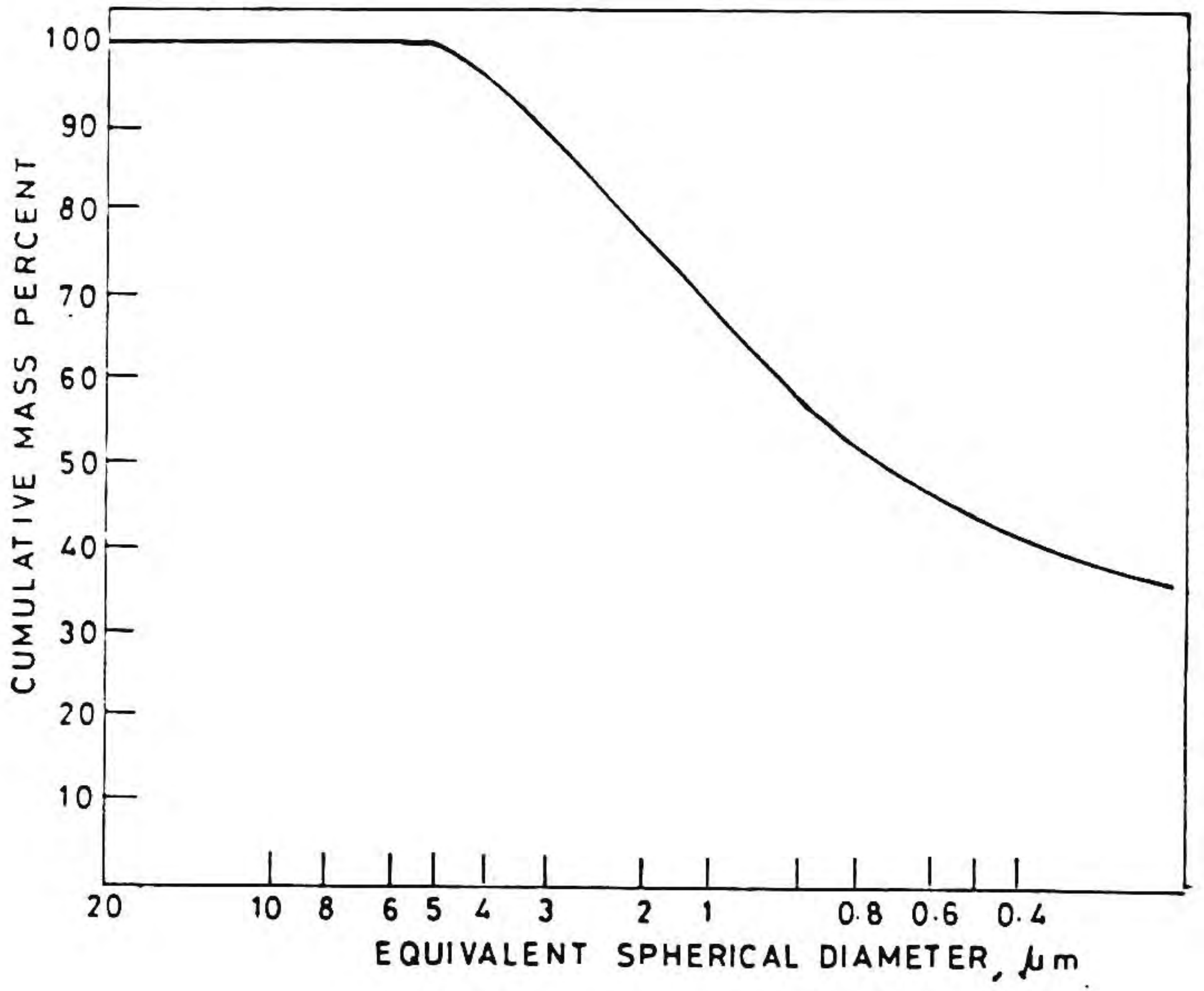


Fig. VIII.12 Particle size distribution curve of sol sprayed powder calcined at 1000°C

Table VIII.1 Densification characteristics of sol sprayed SrTiO₃ powder calcined at various temperatures

Calcination temperature	Green density % theoretical	Fired density % theoretical (1450°C)
550°C	38.0	83.0
800°C	43.3	95.0
1000°C	57.6	98.5
1200°C	62.0	98.0

pressure of 100 MPa. No binder was used.

Figure VIII.13 shows the trend of sintered density vs sintering temperature of the above green discs prepared from powders calcined at 1000°C. Sintered density reaches 98.5% at 1450°C. Further increase could not be measured under the experimental condition. Figure VIII.14 shows the dielectric behaviour of the samples sintered at 1350°C to 1500°C. It is seen that the dielectric constant increases linearly with temperature of sintering. It is also interesting to observe that the variation with respect to frequency is comparatively less in the high density samples. The values are in good approximation with the values of standard polycrystalline SrTiO_3 materials. The dielectric loss is found to be 0.008. This method easily can be extended to introduce minor dopants uniformly by adjusting the sol composition. Further, there is relatively low levels of impurity formation in this technique due to the absence of carbonate. The surface morphology of the calcined powder shows a near spherical shape which is the least disturbed under compaction conditions. However, the fractographs of the sintered samples show average grain size of less than 2 microns, but relatively of uniform distribution (Fig. VIII.15).

VIII.4 Conclusion

The present methods have shown the possibility of preparing submicron strontium titanate particulates which

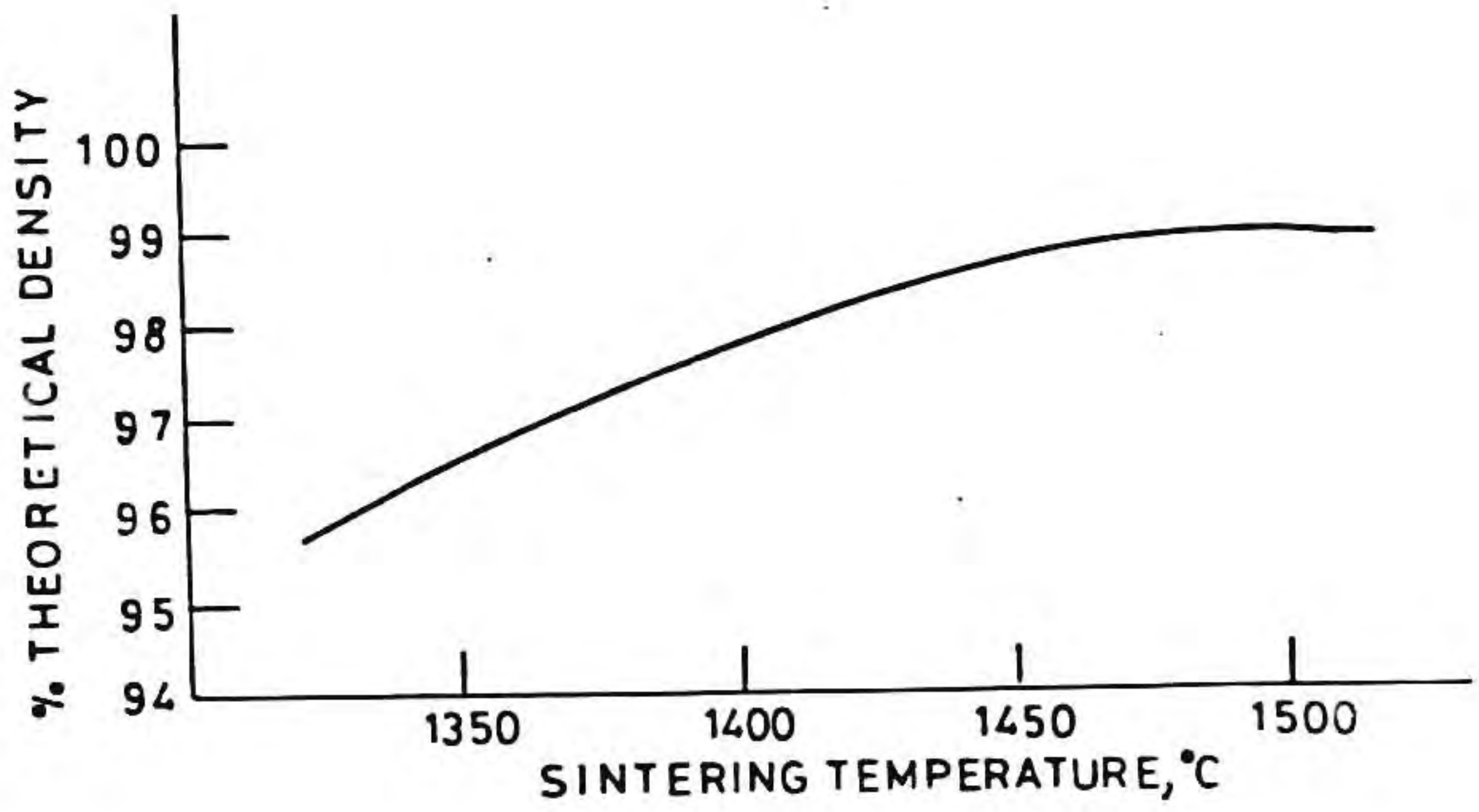


Fig. VIII.13 Variation of sintered density with sintering temperature

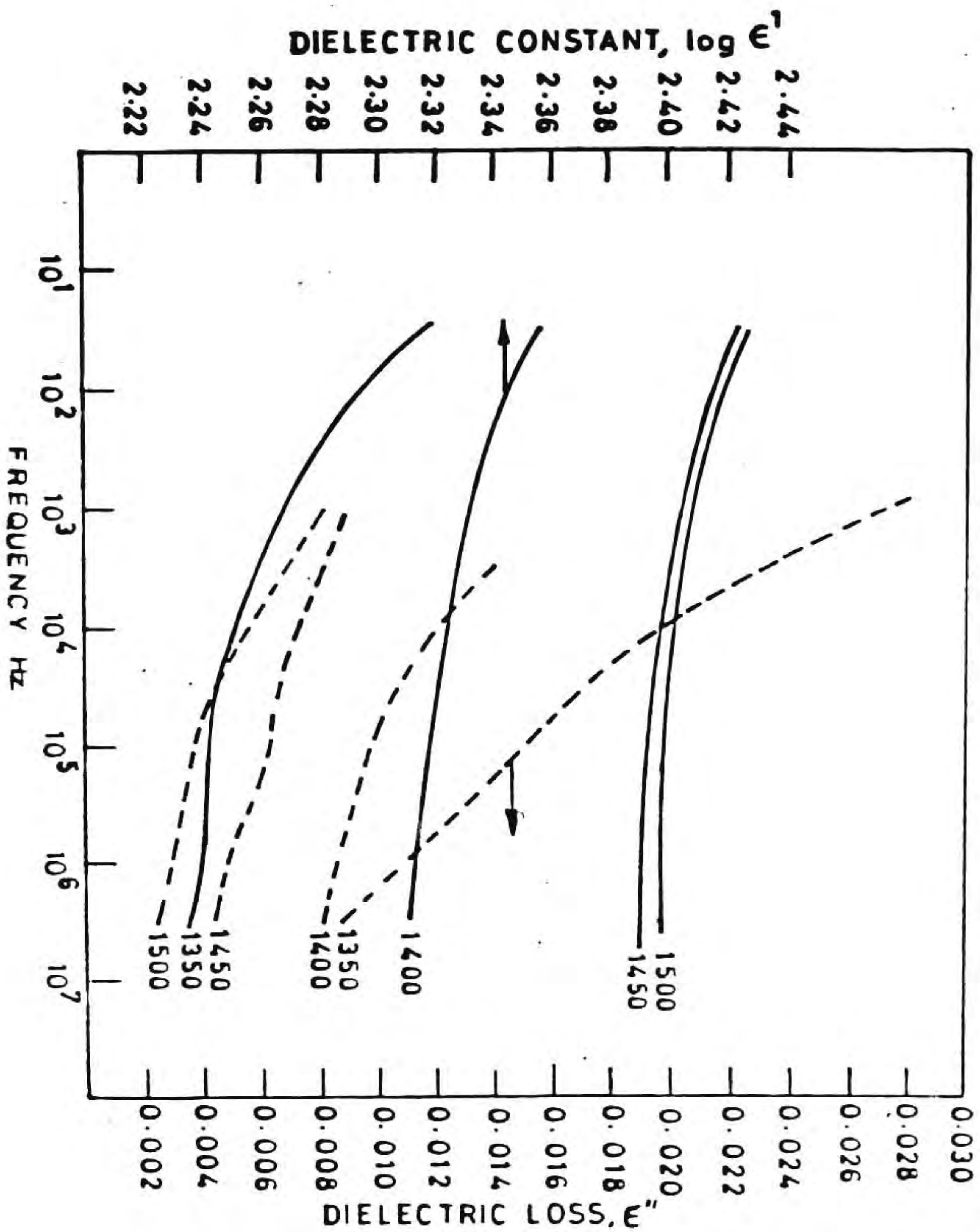
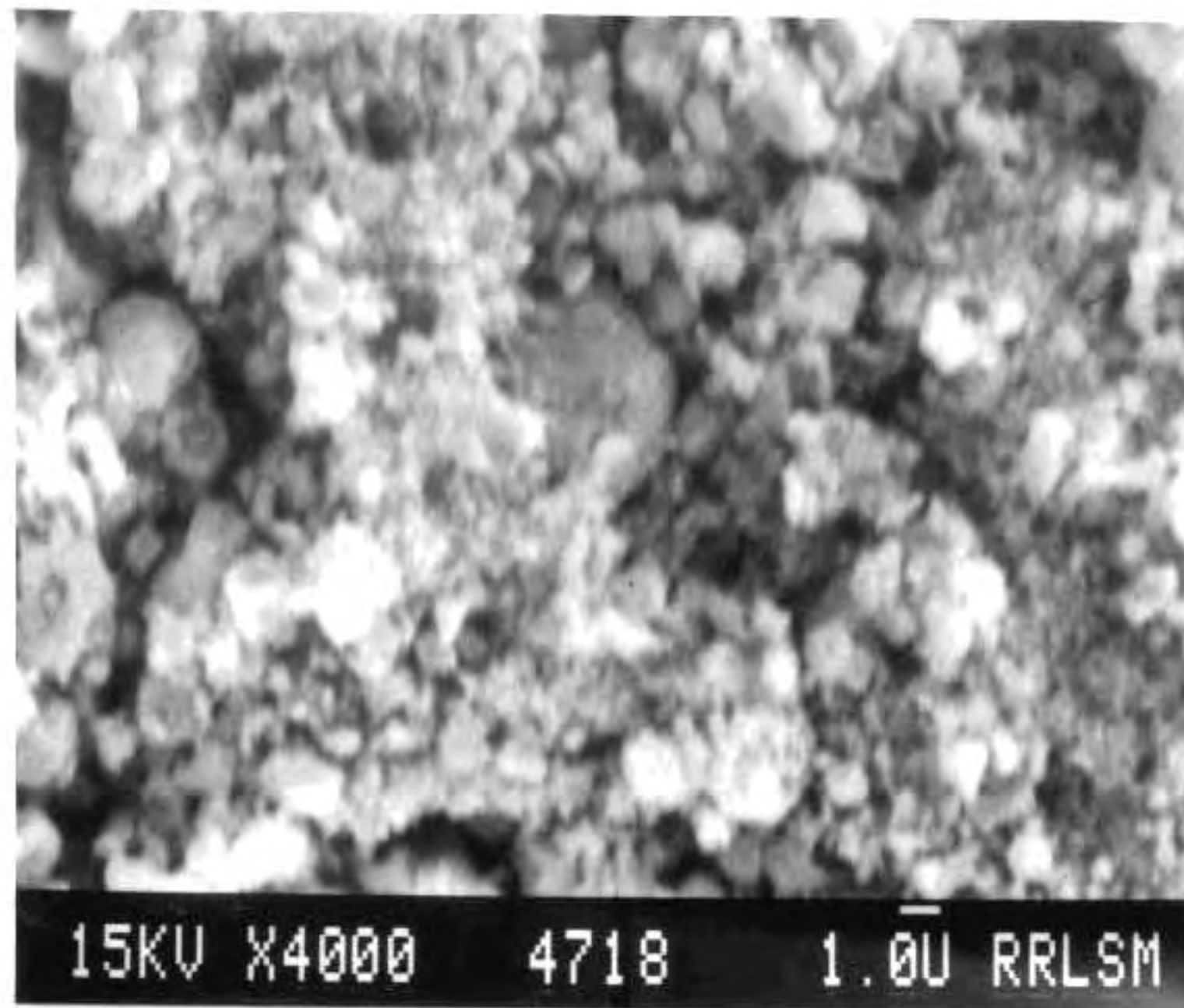
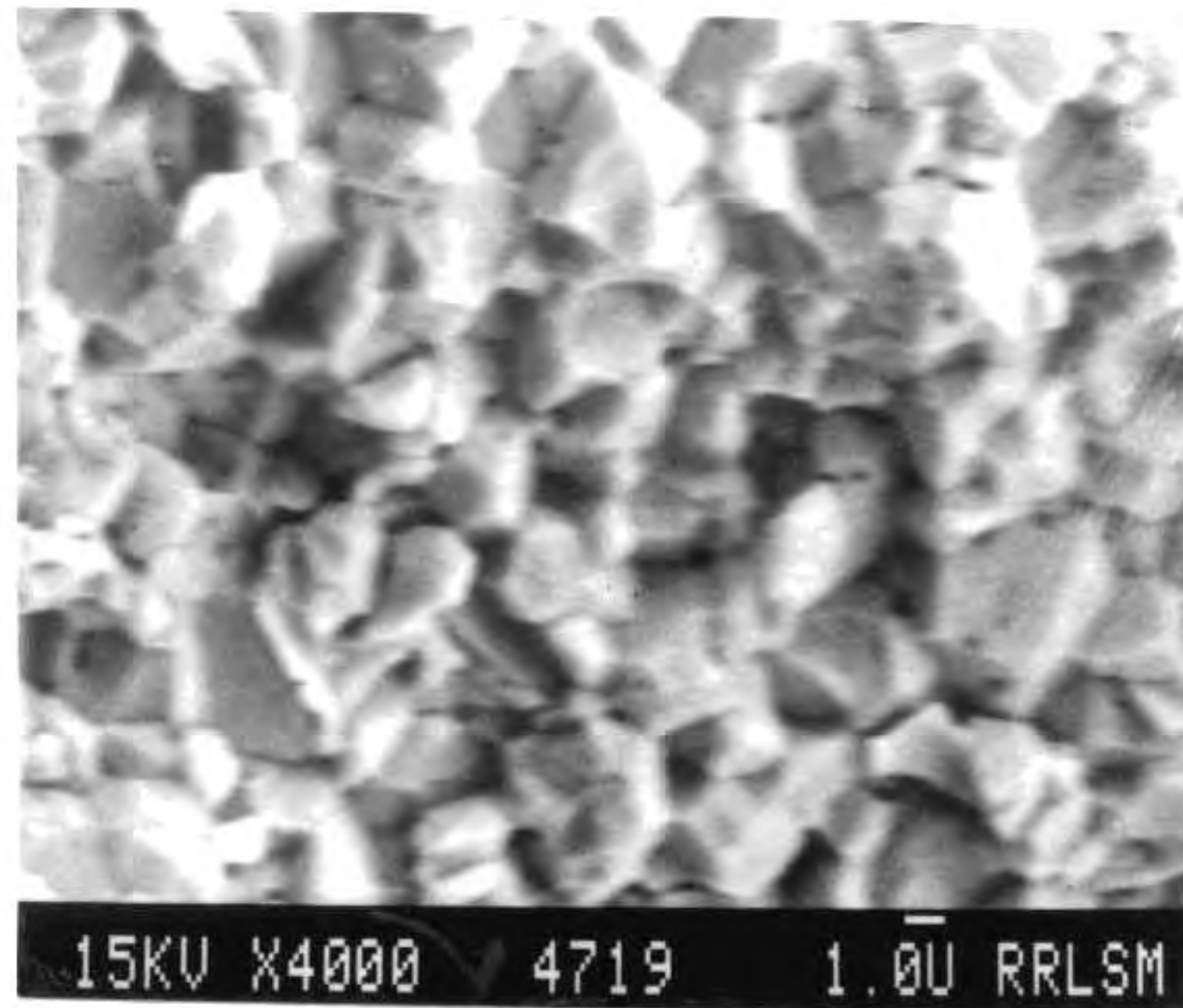


Fig. VIII.14 Dielectric behaviour of SrTiO_3 samples sintered at various temperatures as a function of frequency



(a)



(b)

Fig. VIII.15 SEM micrograph of (a) SrTiO_3 powder (calcined at 1000°C) and (b) Fractograph of SrTiO_3 sintered at 1400°C

possess high green and sintered densities by a simple spray drying technique of a redispersed gel and a sol prepared from a stabilized alkoxide derived precursor. The instantaneous precipitation of titanium alkoxide is prevented by introducing acetic acid-alcohol medium, which causes the formation of water soluble titanyl acetate $[\text{Ti}(\text{OH})_a(\text{OAC})_b]$ precursor. The strontium titanate phase was formed as early as 650°C and could be sintered to high densities. Comparing the properties of sol sprayed and gel redispersed powder, the former powder possessed better particulate and sintered properties.

References

1. K.D. Budd and D.A. Payne, pp.239, MRS Symposia Proceedings, Vol.32, Eds. C.J. Brinker, D.E. Clark and D.R. Ulrich, Elsevier Publishing Co. Inc., New York, 1984.
2. R. Wernicke, Grain Boundary Phenomenon in Electronic Ceramics, Ed. L.M. Levinson, Advances in Ceramics, 1, 261, Am. Ceram. Soc., Ohio, 1981.
3. S. Wetek, D.M. Smith and H. Pickup, J. Am. Ceram. Soc., 67(5), (1984) 372.
4. H. Okamura, E.A. Barringer and H.K. Bowen, J. Mater. Sci., 24(5), (1989) 1867.
5. R.E. Riman, R.R. Landham and H.K. Bowen, J. Am. Ceram. Soc., 72(5), (1989) 821.
6. E.A. Barringer and H.K. Bowen, J. Am. Ceram. Soc., 65(12) (1982) C199.
7. J.H. Jean, D.M. Goy and J.A. Ring, Am. Ceram. Soc. Bull., 66(10), (1987) 1517.
8. L.L. Hench and J.K. West, Chem. Rev., 90, (1990) 33.
9. C. Sanchez, F. Babonneau, S. Doeuff and A. Leautic, pp.77, Ultrastructure Processing of Advanced Ceramics, eds. J.D. Mackenzie and D.R. Ulrich, Wiley, New York, 1988.
10. D. Hennings, Electroceramics, Eds. A.J. Moulson and J. Binner, Br. Ceram. Proceedings, 41, (1989) 1.

11. P.P. Phule and S.H. Risbud, *Advanced Ceramic Materials*, 3(2), (1988) 183.
12. P.P. Phule and S.H. Risbud, *Mater. Sci. Engg.*, B3, (1989) 241.
13. K.L. Lin and H.C. Wang, *J. Mater. Sci. Lett.*, 8, (1989) 49.

CHAPTER IX

PARTICULATE CHARACTERISTICS OF ALUMINA POWDER PREPARED THROUGH SPRAY DRYING OF BOEHMITE SOL

IX.1 Introduction

Alumina is the most widely used inorganic oxide by the ceramic industry in tonnage quantities. In its high temperature form, it is classed as a neutral or amphoteric refractory having a melting point of 2050°C. The super refractoriness of alumina is due to the stability in both reducing and oxidising atmospheres. Alumina is mainly produced by Bayer process in which bauxite is digested with caustic soda and precipitated as hydrated aluminium oxide which is finally calcined. Alkali free high quality alumina is produced by a variety of chemical processes(2-9). The sol-gel processing technique offers better advantages over other routes. Precursors such as alkoxides, metal salts etc. are used in sol-gel processing. Alkoxides offer the potential of freedom from anionic counterpart while non alkoxide precursors such as metal salt offer economic advantages.

Monohydroxy aluminium oxide (boehmite) sol was investigated first by Yoldas and later by many others(10-13). Alumina-zirconia mixed sols were reported as a source for composite microspheres(14). Certain reports on compaction

This work was published

** Journal of American Ceramic Society, (in press).*

characteristics of spray dried agglomerates of alumina are available(15,16). Although submicron size particulates are possible from sol-gel methods, agglomeration of these particulates still exists as a major problem(17) which considerably limit the possible advantages of these routes. When alumina is prepared by precipitation from salts, the precipitation medium has been found to have profound influence on the particle size and surface charge of alumina powders(18). This chapter presents preparation of micron size spherical alumina particles by sol-spray technique of boehmite derived from aluminium nitrate and also the effect of post spray treatments on the properties of such particles with and without further treatment. The surface charge of powders prepared by the sol-spray route are compared.

IX.2 Experimental

Aluminium nitrate (100 gms) was dissolved in distilled water (2500 ml). Hydroxides were precipitated by addition of 25% ammonia solution drop by drop at pH 8 at 85°C. The precipitate was washed free of nitrates and then peptized by 0.3 molar HNO_3 at 90°C at pH=3.5. The clear sol thus obtained was aged for 48 hours. The final pH of the sol was 4. The sol concentration was adjusted to 3 M/lit by evaporation on a water bath. The sol concentration was followed by nephelometry(19). Visible light is passed through a colloidal suspension of solids and the intensity of scattered fraction is measured and

expressed as turbidity. The particle concentration for a specific volume increases as gelation progresses and hence results in increase of NTU (Nephelometric Turbidity Units) value. The concentrated sol was then spray dried through a nozzle of 1 mm diameter to spherical microspheres with a fixed inlet temperature of 165°C and an outlet of 105°C. The powder obtained thus was washed repeatedly (2 times) with acetone, isopropanol or tert. butanol. These powders are designated as A (as sprayed) B (acetone) C (isopropanol) and D (tert. butyl alcohol). All the powders were calcined at 500°C and then heat treated at 1100°C for physical properties. The particle size analysis, XRD and morphology were investigated.

IX.3 Methods

The characterization of the powder using the techniques particle size analysis, XRD, SEM and TGA/DTA were done as described in previous Chapter. The point of zero charge of the powders were determined as described below.

IX.3.i. Determination of point of zero charge

1 gm of alumina powder was introduced to an aqueous sol of (200 ml) 0.004 HNO_3 + KNO_3 (0.01). Then pH metric titration was carried out with 0.1 KOH at 30°C in an atmosphere of nitrogen. The addition of titrant was fixed to 0.5 to 0.05 using a microburette under continuous stirring. A blank solution was also titrated (without alumina powder) . The excess amount of

alkali was estimated from the difference between two curves plotted, pH against amount of alkali added. The surface charge density was calculated using the equation

$$\sigma_o = F (\Gamma_{H^+} - \Gamma_{OH^-})$$

$$\text{where } \Gamma_{H^+} = (n_{H^+}^s - n_{H^+}^b) / M$$

$$\Gamma_{OH^-} = (n_{OH^-}^s - n_{OH^-}^b) / M$$

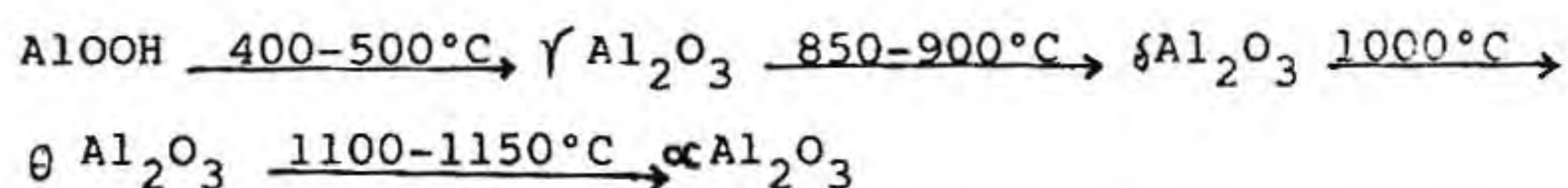
where F is faraday constant, $n_{H^+}^s$ and $n_{OH^-}^s$ are the total number of moles of H^+ and OH^- added to the suspension and $n_{H^+}^b$ and $n_{OH^-}^b$ are corresponding to the blank. M is the mass of the alumina powder.

IX.4 Results and Discussion

Usually boehmite gels are prepared by controlled hydrolysis of aluminium alkoxides(10). However, metal salts can also be a source with certain definite economic advantages, although certain anions are possibly introduced into the structure as impurities. The structure of boehmite gels derived from the salts and alkoxide are found to be different(20), but predominantly the gel formation characteristics are similar. Spray drying of the sol therefore is intended to eliminate the time required for gelling and also decrease agglomeration due to fast evaporation. In the present investigation, the anion concentration was adjusted to the optimum by carefully studying the peptization and ageing of the sols. The XRD pattern of the

sol immediately after spray drying (Fig.IX.1.a) shows the typical boehmite structure(11). Even on keeping for 48 hours no visible changes were observed in the sol. This was confirmed by measurement of particle concentration by nephelometry. The boehmite sol was concentrated to 3 M/lit [Al^{3+} concentration] to a point before it started gelation, identified by nephelometric as well as viscosity measurements.

The spray dried boehmite was decomposed to oxide at 500°C based on the thermogravimetric curve provided in the Fig.IX.2, which is similar to that of boehmite derived through alkoxide route(11). There is an initial weight loss of 12% below 200°C due to absorbed moisture followed by a major weight loss of about 35% between 150°C and 300°C attributed to decomposition of water entrapped in gel structure. Further loss of about 15% due to the conversion of $AlOOH$ to Al_2O_3 matches the theoretical loss of $AlOOH$. The decomposition is complete below 450°C as against the earlier reported ones(11). The maximum rate of water removal takes place below 300°C. The various phase changes occurring during the calcination and subsequent heating can be visualized(1) as



The conversion to alumina takes place just below 1150°C (Fig.IX.1b).

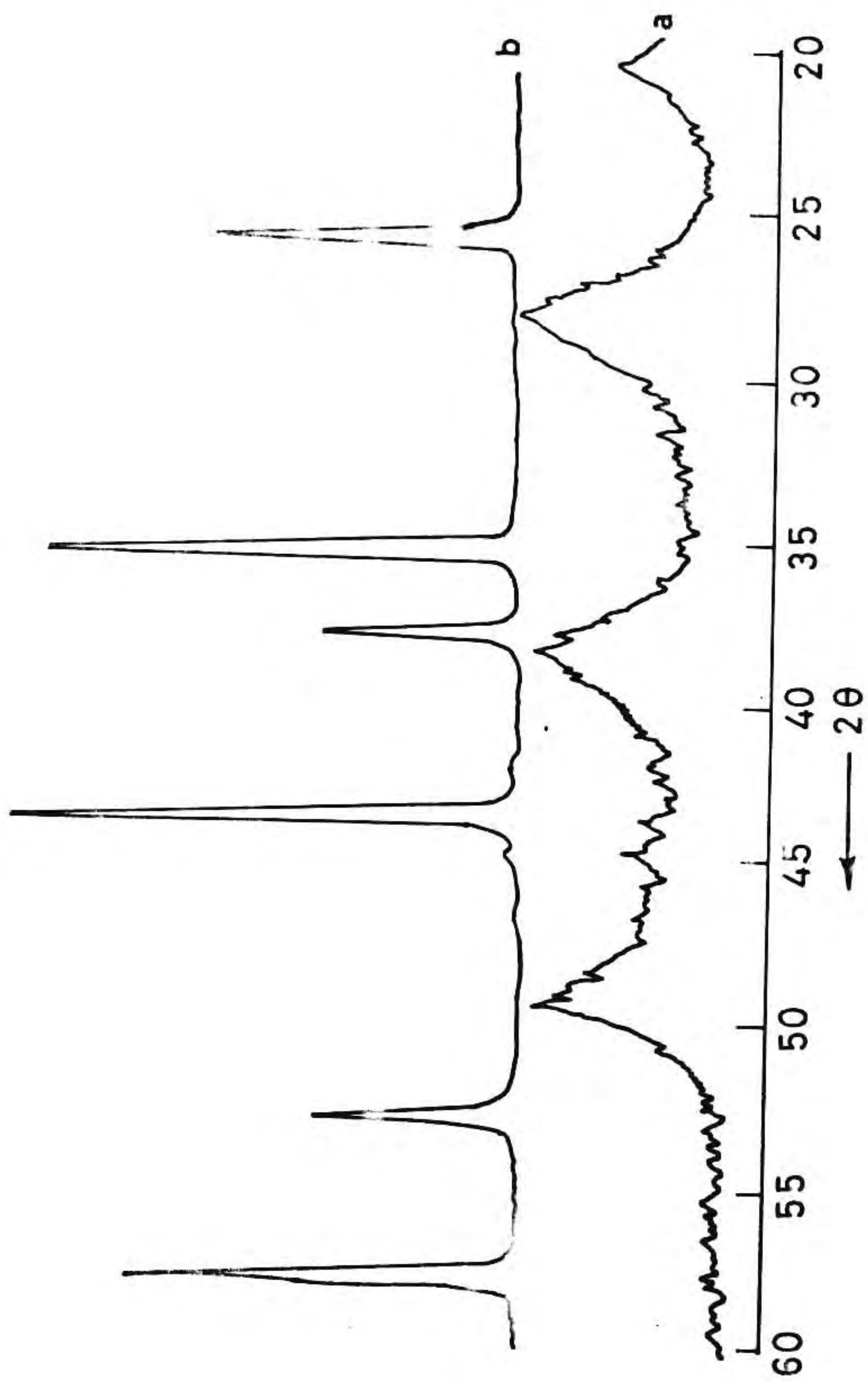


Fig. IX.1 XRD patterns of (a) spray dried powder and (b) heated at 1100°C (1 hr)

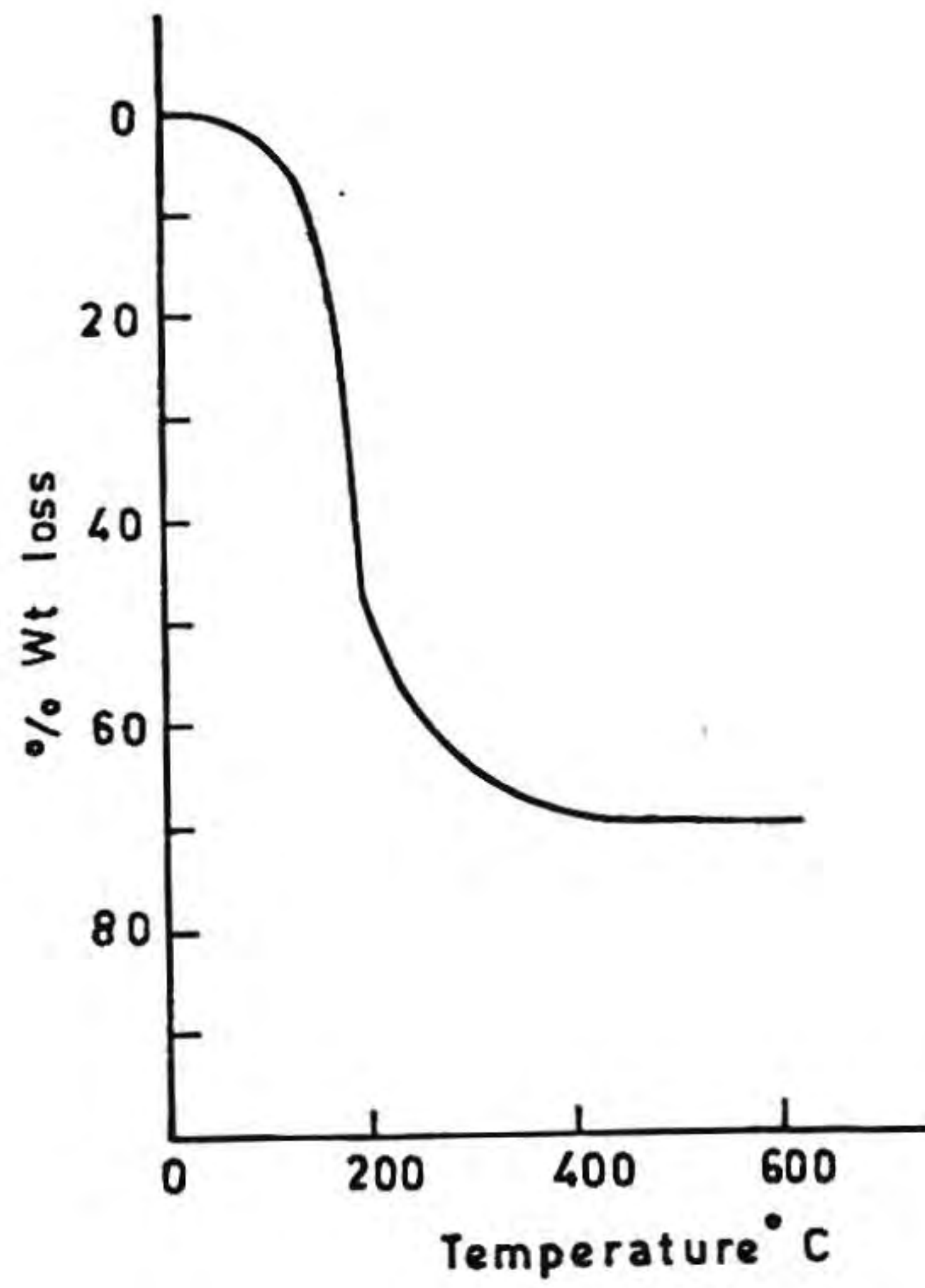


Fig. IX.2 Thermogravimetric curve of spray dried powder

Although the sol consists of particles in the nanometer range, the spray dried powder is essentially agglomerate of fine crystallites as has been reported(22). The crystallite size calculated from XRD data in this case is $0.03\mu\text{m}$. Separation of crystallites from the agglomerates or keeping these as loosely held agglomerates which can deform easily under compaction conditions can be achieved through preferential treatments by solvents having different polarities. A mechanism for reducing agglomeration in zirconia particles through washing with ethanol has been reported recently by Heuer(21). A condensation product is formed between the interaction of alcohol and the surface hydroxyls of zirconium oxide, thus separating the particles from agglomeration. However the extent of separation should depend on the intensity of hydrogen bonded OH groups on the oxide surface as well as the polarity of the solvents used for washing. The solvents used in the present investigation such as acetone, isopropyl alcohol and tert-butyl alcohol have polarities in the range 5-3.5, compared to the base powder containing water of polarity 10.3(Sanders polarity, Handbook of Physics and Chemistry CRC 59th edition). The particle size distribution as obtained on these powders is presented in Fig.IX.3. The one washed with isopropyl alcohol (Fig.IX.3c) has shown the minimum average particle size. It is significant to note that the acetone washing has resulted in increase of average as well as maximum particle sizes upto 4.2 and 15 microns respectively

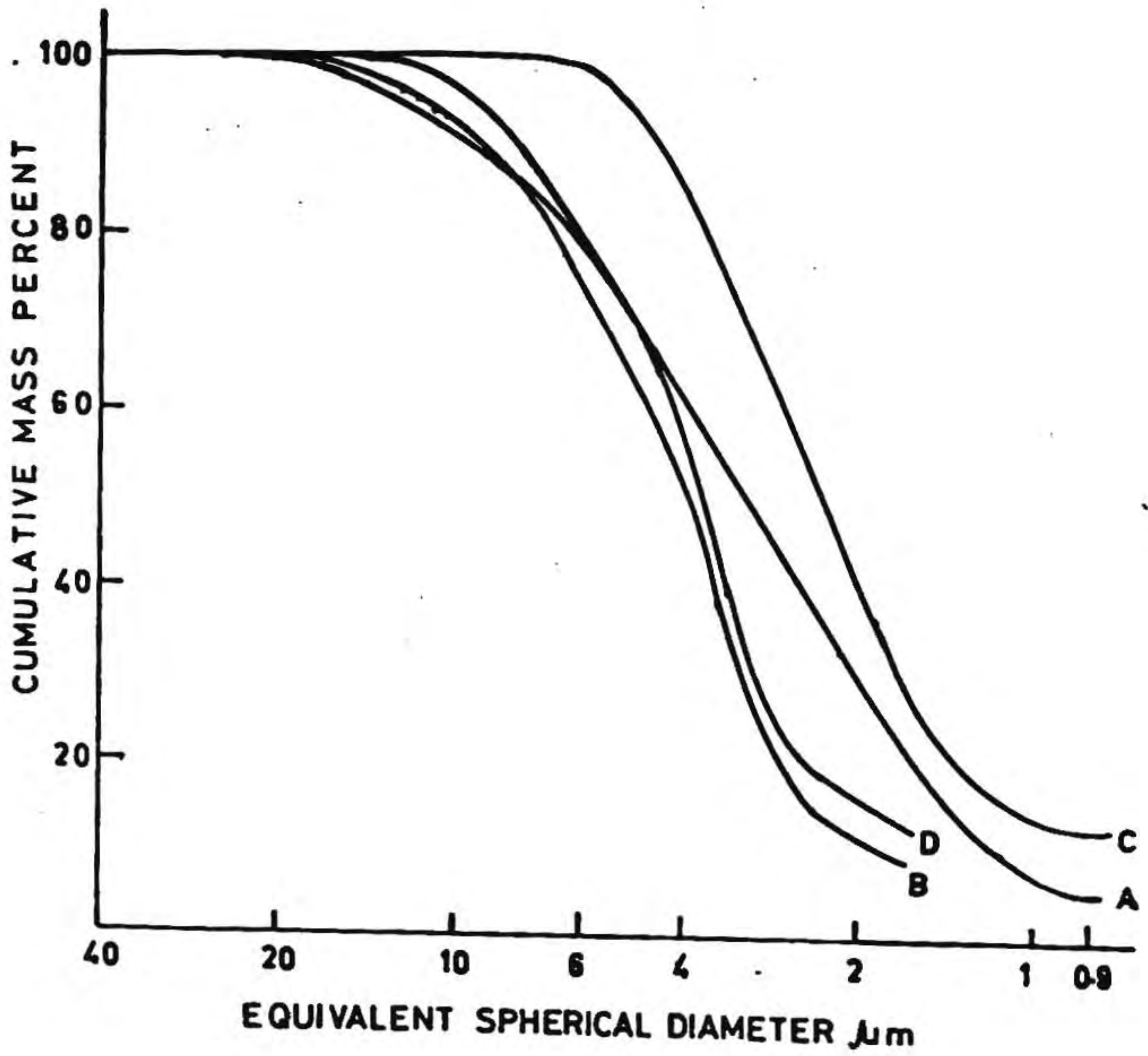


Fig. IX.3 Particle size distribution curves of calcined powders (A) powder as sprayed, (B) treated with acetone, (c) isopropanol and (D) tert. butanol

(Fig.IX.3b), while isopropanol could bring down these values correspondingly to 2.4 and 7 (Fig.IX.3c). The effect of tert-butyl alcohol is in between (Fig.IX.3d). The extent of removal of the adsorbed water on the surface of the powder would decide the strength of agglomerates. There is a notable difference in the tap densities of these powders as seen from Table IX.1 while the powder A has the highest value of 0.9 gm/cm^3 , powder C has a value of 0.85 gm/cm^3 . Further, powder A possess lowest compaction density with respect to the plot of density versus compaction pressure as shown in Fig.IX.4. The one washed with isopropanol has above 5% increase in the green density. This shows that the strength of agglomerate of the powders have been influenced by the post spray treatments. This is further clear by observing the surface morphology of the powders provided in the Fig.IX.5. While powder A has a random spherical nature with wide variation of size and clusters, powder C has a closer distribution. Further, the average particle size is $1.5 \mu\text{m}$. The powder B has a different morphology itself.

Point of zero charge of these powders were calculated by the potentiometric method(23) shows values between 7.5 for A and 8.00 for C, while the other powders have values in between (Fig.IX.6). Metal oxide surface are covered by hydroxyl groups in aqueous suspensions as already mentioned and hence possess certain surface charges(24). One method of controlling these charges is by using different media of precipitation(18). A similar behaviour can also be achieved by washing the powders

Table IX.1 Tap densities of various alumina powders derived through surface treatments of sol sprayed boehmite powder (calcination temp. 1100°C/1hour)

Sample	Tap density gm/cm ³
Without washing	0.91
Acetone washed	0.87
Isopropanol washed	0.85
Tert. butanol washed	0.86

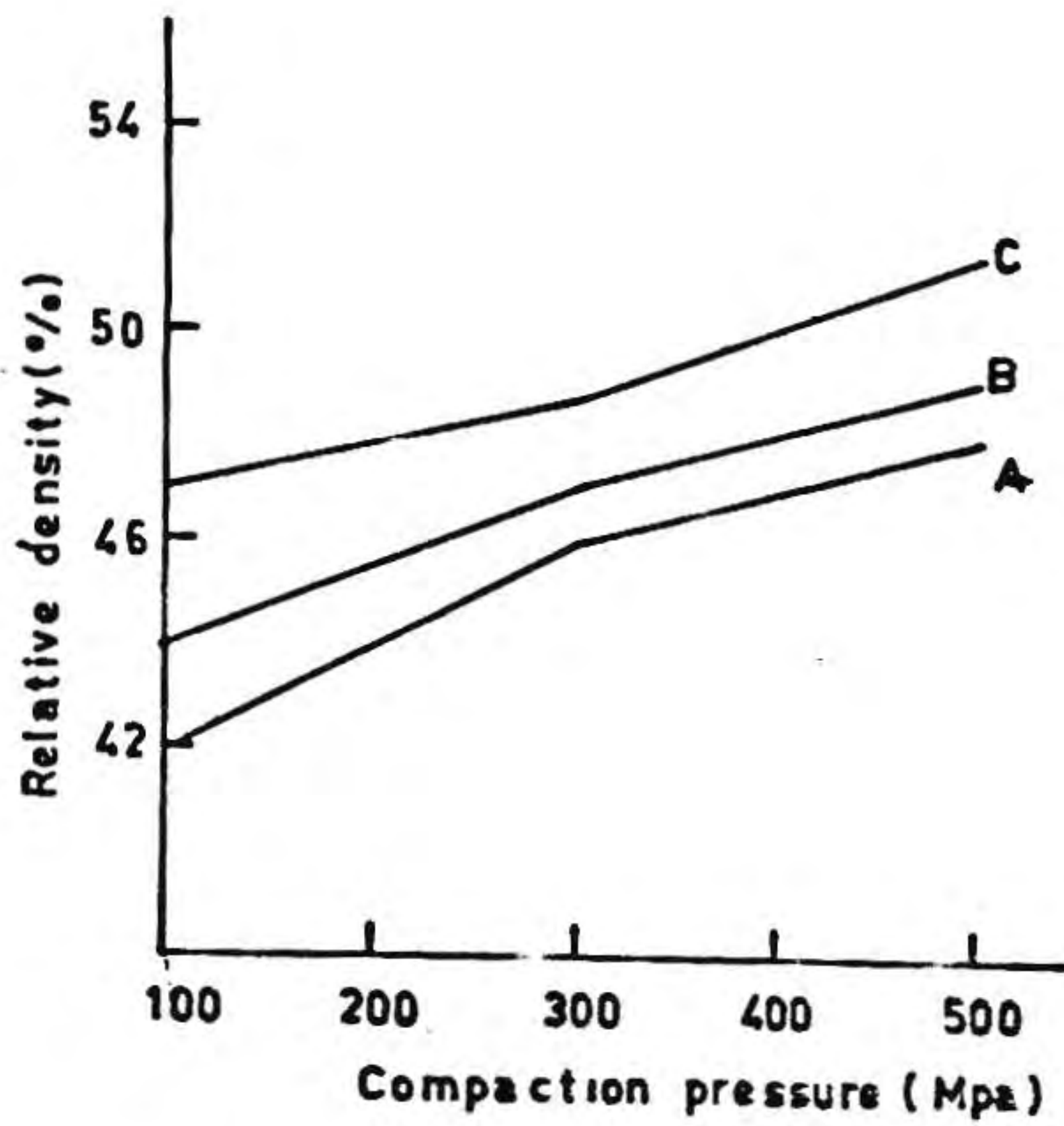
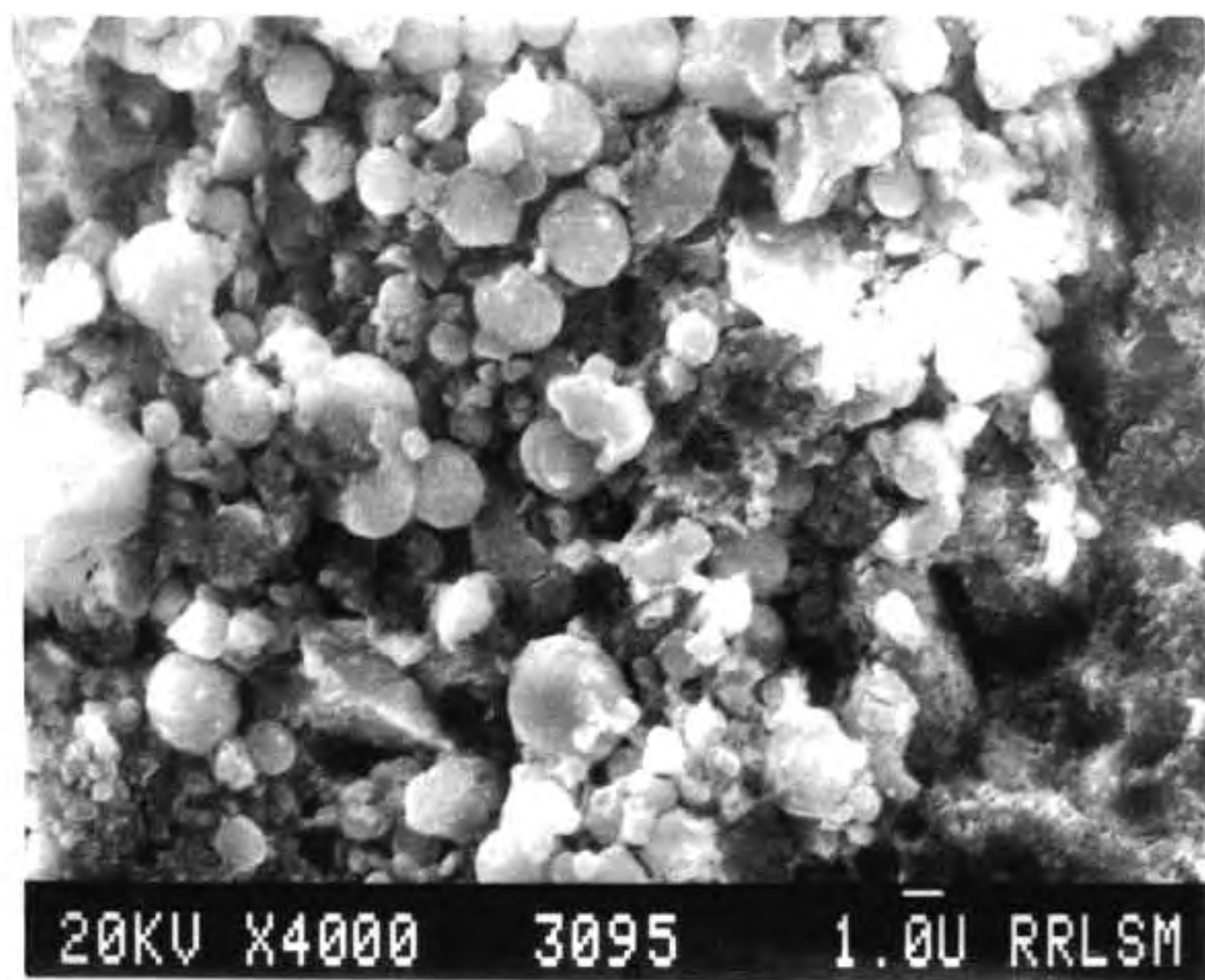
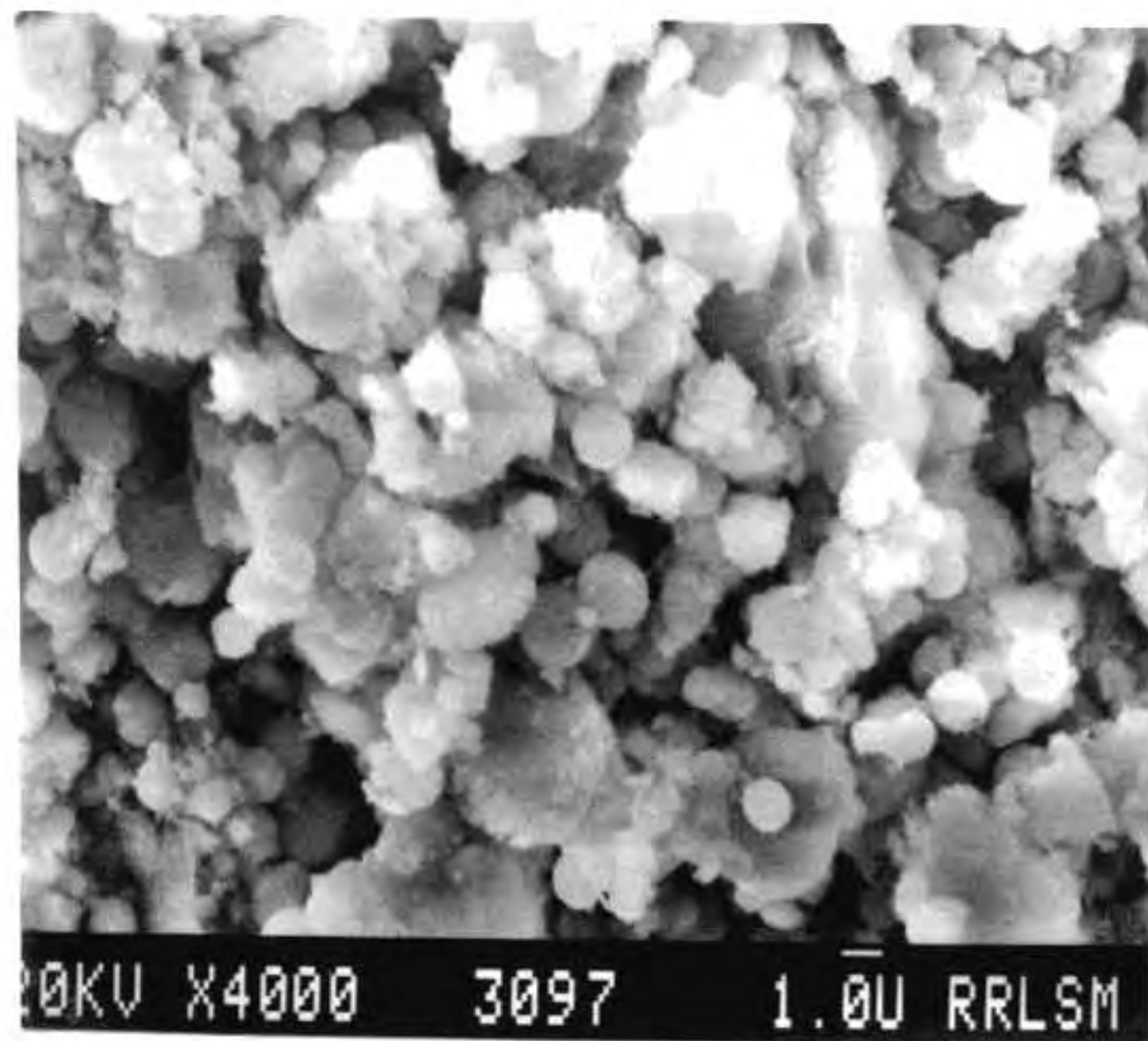


Fig. IX.4 Plot of relative density of different alumina powders as a function of compaction pressure (A) without washing, (B) acetone washed and (c) isopropanol washed

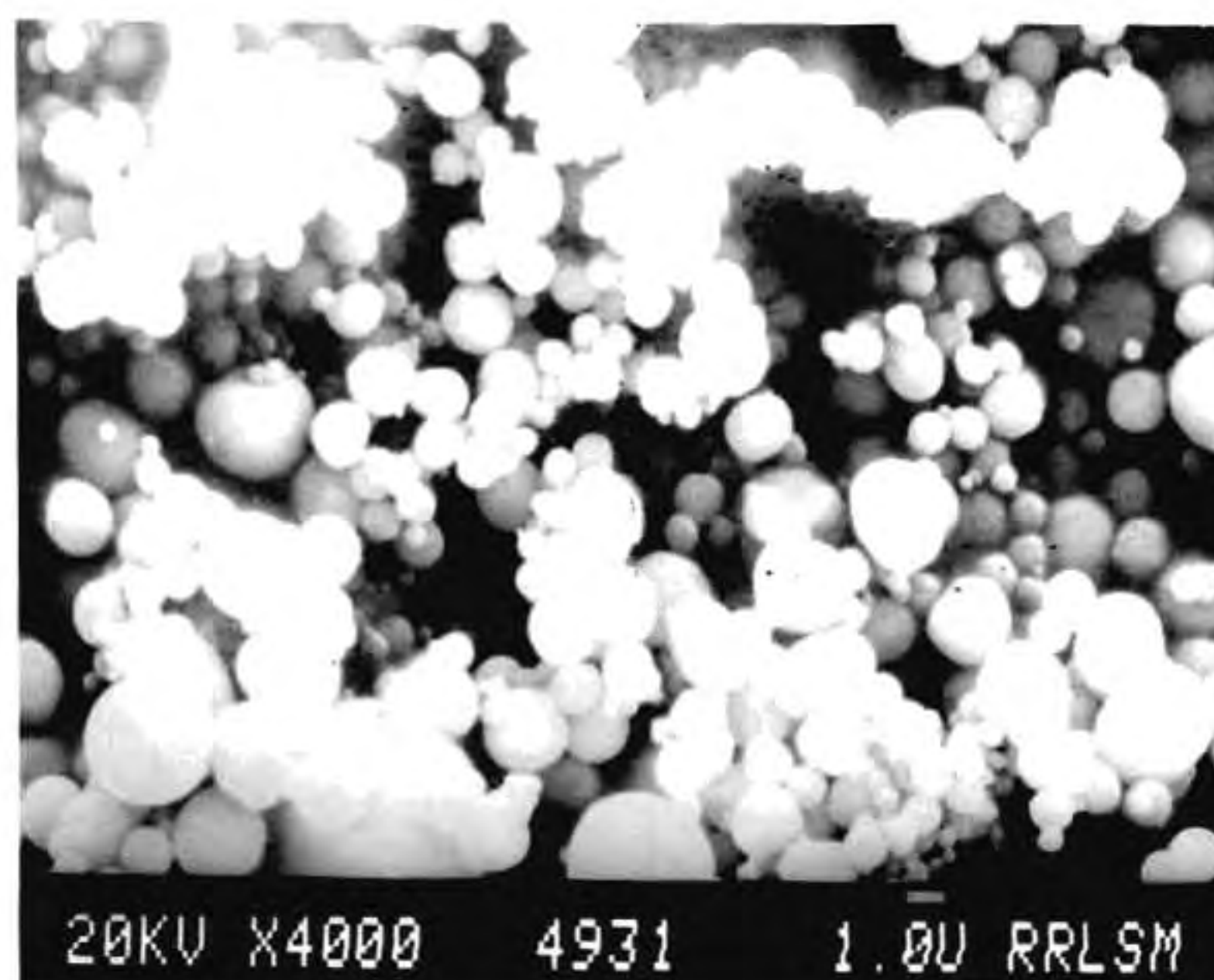


(a)

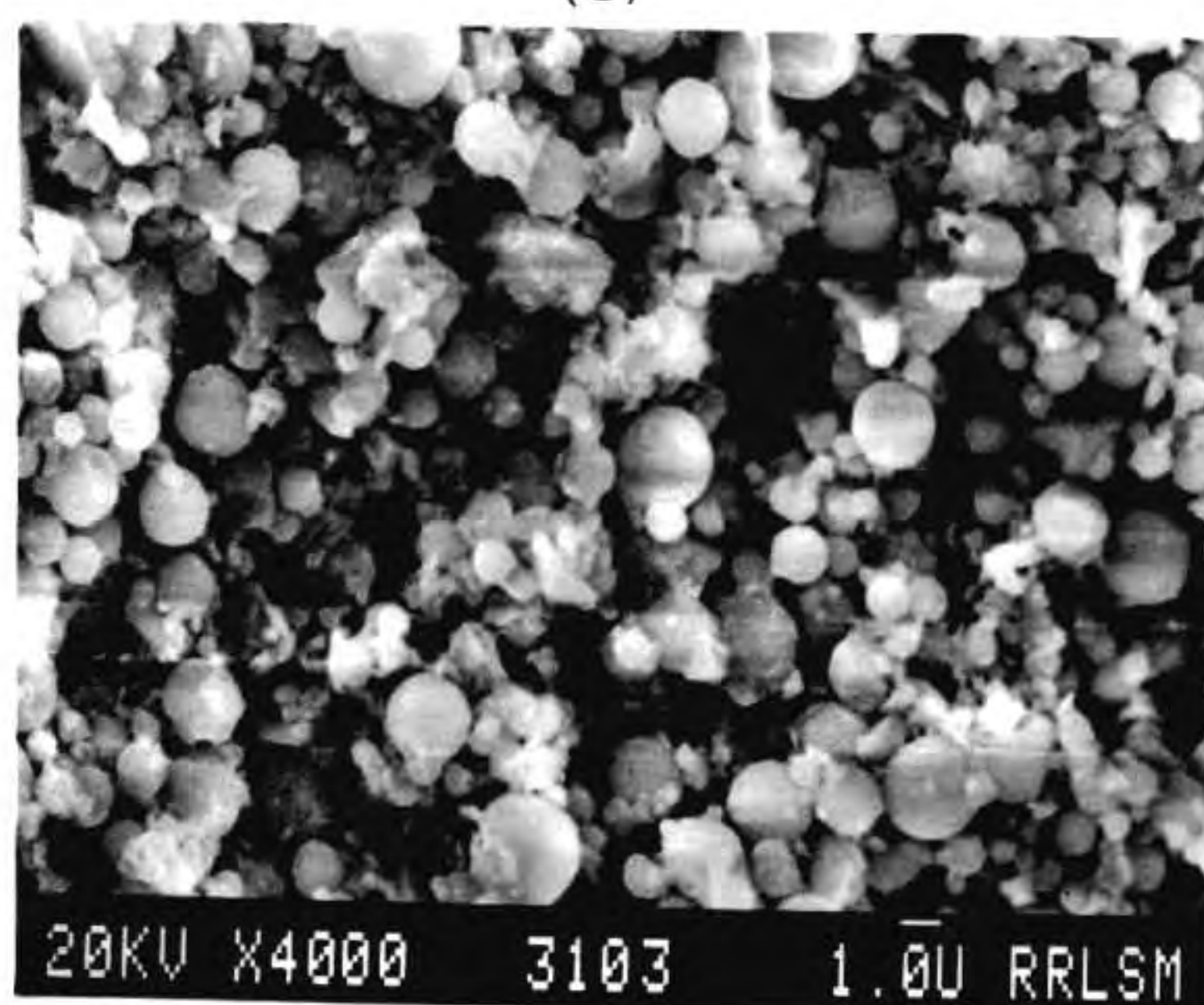


(b)

Fig. IX.5 SEM picture of the alumina samples obtained after various treatments (a) as sprayed and (b) after washing in acetone



(c)



(d)

Fig. IX.5 SEM picture of the alumina samples obtained after various treatments (c) isopropanol and (d) tert. butanol

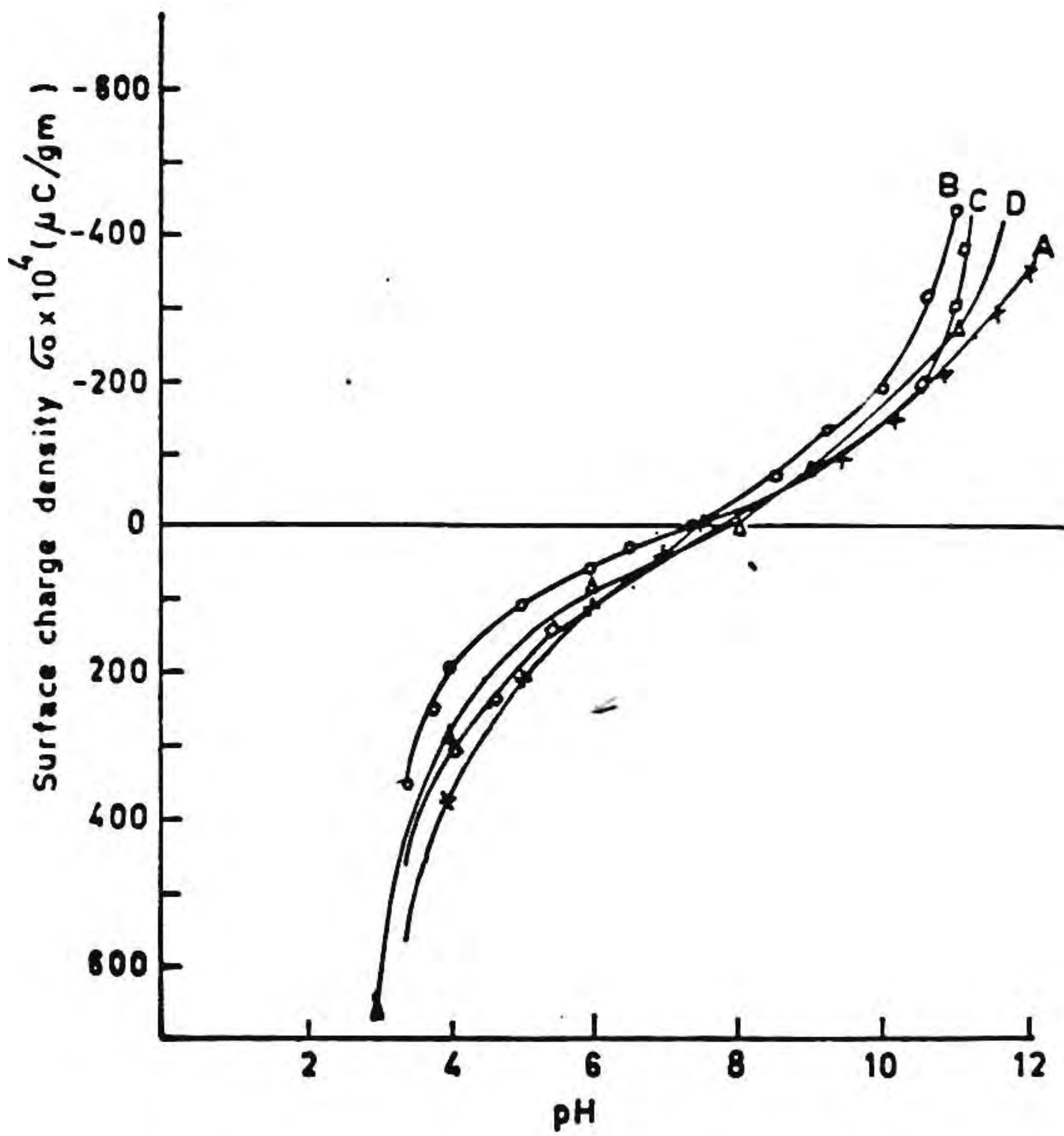
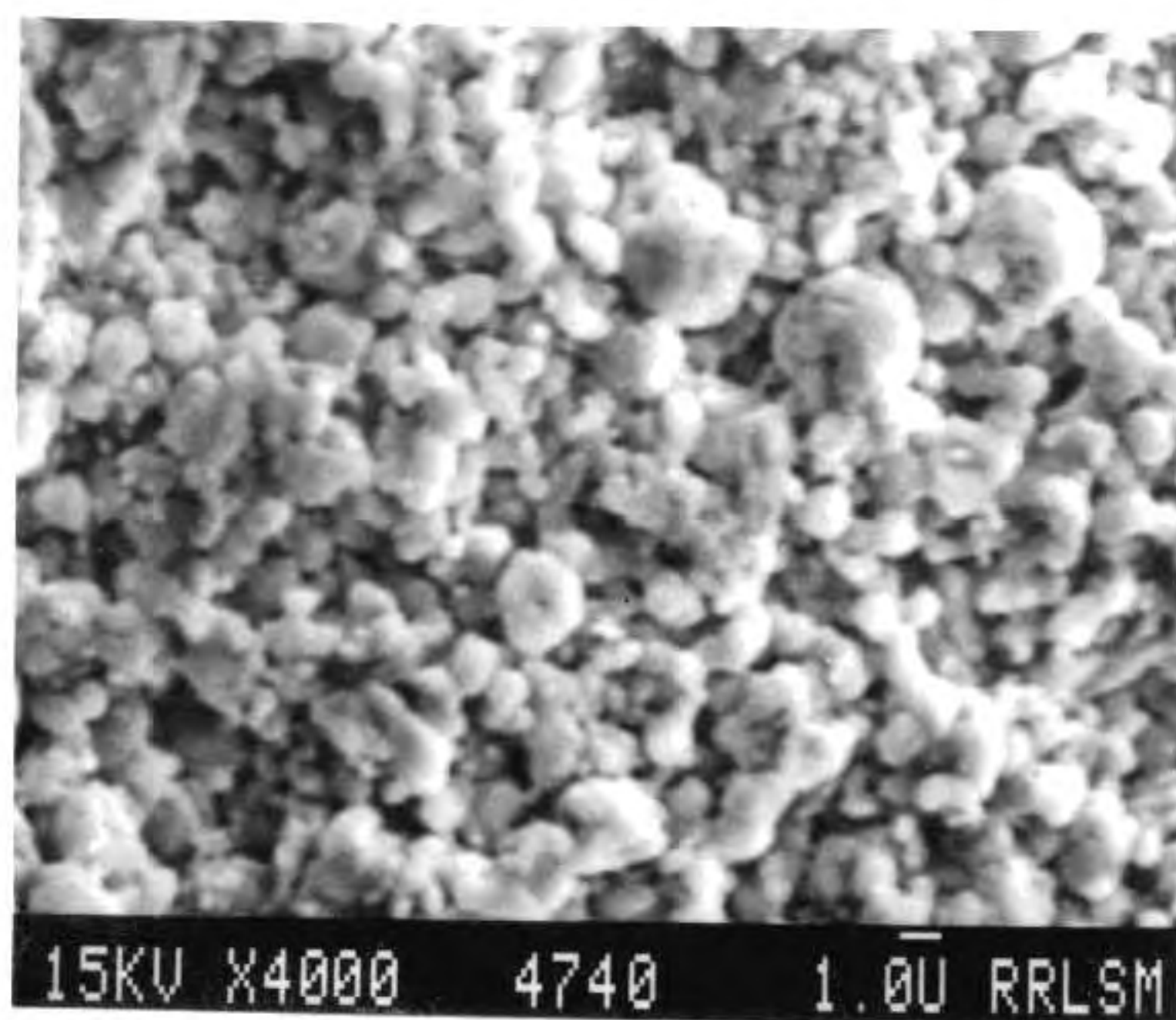
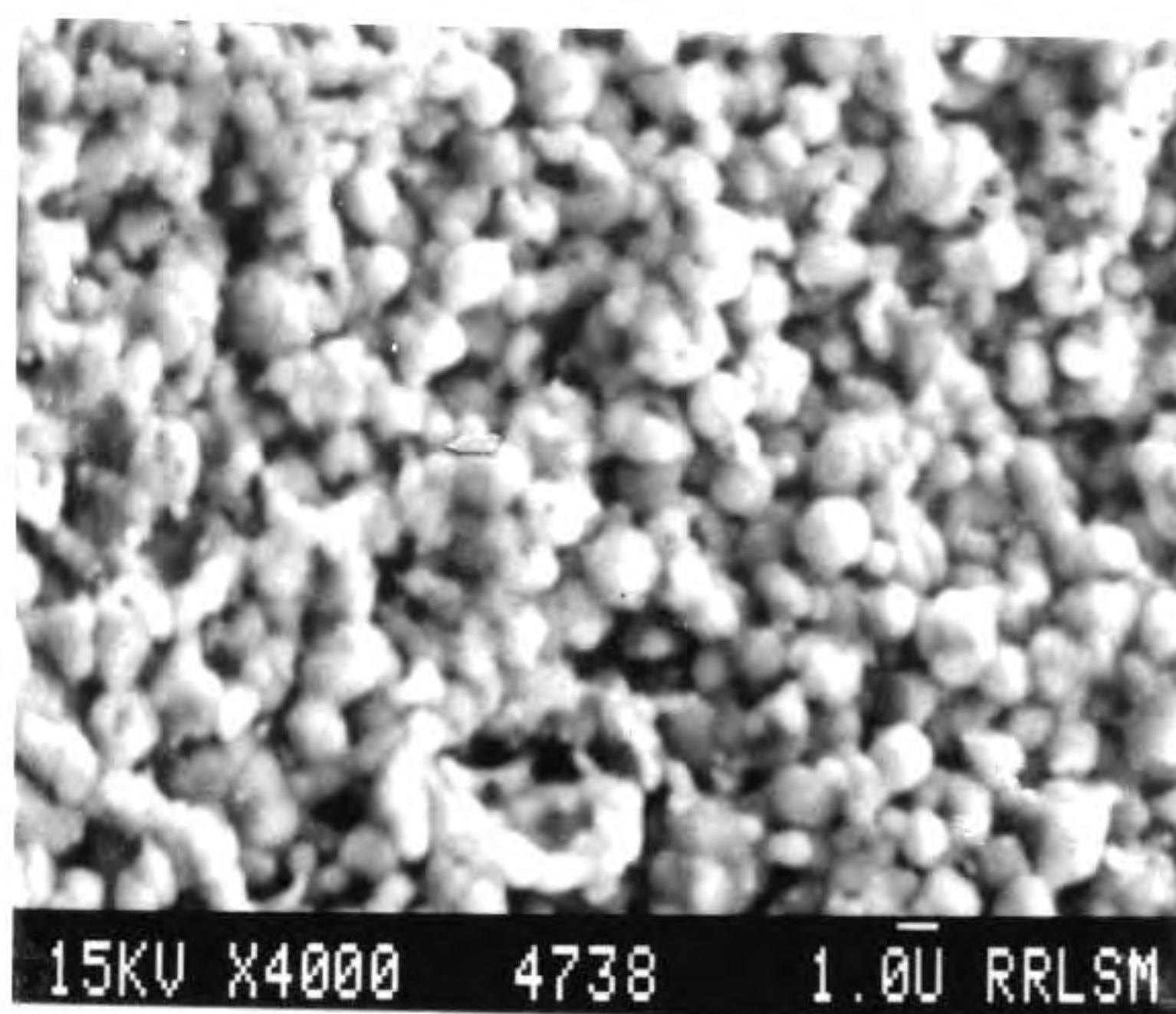


Fig. IX.6 Variation of point of zero charge as a function of pH for calcined alumina powders (A) without washing, (B) acetone washed, (C) isopropanol washed and (D) tert. butanol washed



(a)



(b)

Fig. IX.7 Sintered surface microstructure of alumina (1400°C for 3 hours) derived from boehmite (a) without washing and (b) after washing with isopropanol

with specific solvents, as has been seen in the present investigation. The effect of washing can be further visualized from the sintered alumina (at 1400°C for 3-hours) surfaces given in Figs. IX.7a and b. While the powder without washing showed scattered agglomerated grains in the microstructure, the alumina powder derived from the isopropanol washed boehmite showed a uniform microstructure for the alumina grains.

IX.5 Conclusion

The present investigation, therefore, indicates the possibility of preparing free flowing spherical alumina particles by spray drying of boehmite sol. These agglomerates having 2-2.25 micron average particle size still contain submicron crystallites. Further, the agglomerates can be broken up by careful removal of OH groups through washing with solvents. Such powders possess good compaction characteristics. The point of zero charge also changes by the post spray drying treatment, facilitating these powders for easy dispersion. Hence, it has been possible to obtain spherical alumina powders of average particle size of 2-2.4 micron having bulk density of 0.85 gm/cm³, maximum compaction density of above 52% and point of zero charge 8, starting from an alumina sol derived from aluminium nitrate.

References

1. W.H. Gitzen, *Alumina as a ceramic material.*, The American Ceramic Society Inc., Columbus, Ohio, 1970.
2. B.C. Cornilsen and J.S. Reed, *Am. Ceram. Soc. Bull.*, 58(12), (1979) 1199.
3. C.A. Rachwal, *Ceram. Engg. Sci. Proc.*, 40(1-2), (1983) 28.
4. T. Mitsushiro, *Yogyo Kyokaishi*, 86(16), (1978) 506.
5. J.E. Blendell and H.K. Bowen, *Am. Ceram. Soc. Bull.*, 63(6), (1984) 797.
6. K. Fujita, *Yogyo Kyokaishi*, 83(12), (1975) 586.
7. S.K. Sarkar, *J. Am. Ceram. Soc.*, 67(9), (1984) C172.
8. T. Sato, *J. Appl. Chem. Bio. Tech.*, 28(12), (1978) 811.
9. J. Cavino and R.A. Nissan, *Mater. Res. Bull.*, 21(3), (1986) 337.
10. B.E. Yoldas, *Am. Ceram. Soc. Bull.*, 54(3), (1975) 289.
11. R.D. Dwivedi and G. Gowda, *J. Mater. Sci. Lett.*, 4, (1985) 331.
12. Ph. Colomban, *J. Mater. Sci.*, 24, (1989) 3002.
13. A.C. Pierre and D.R. Uhlmann, *J. Amer. Ceram. Soc.*, 70(1), (1987) 28.
14. L. Mondanaro and B. Guilhot, *Am. Ceram. Soc. Bull.*, 68(5), (1989) 1017.
15. R.G. Fray and J.W. Halloran, *J. Am. Ceram. Soc.*, 67(3), (1984) 199.

16. S.J. Lukasiewicz and J.S. Reed, *Am. Ceram. Soc., Bull.*, 57(9), (1978) 798.
17. A. Roosen and H. Hausner, *Advanced Ceram. Mater.*, 3(2), (1988) 131.
18. H.K. Varma, K.G.K. Warriier and A.D. Damodaran, *Ceramic International*, 16(2), (1990) 73.
19. K.L. Lin and H. Wang, *J. Mat. Sci. Lett.*, 8, (1989) 49.
20. A.C. Pierre and D.R. Uhlmann, Aging of an alumina gel made from aluminium nitrate, pp.865-872, *Ultrastructure processing of advanced ceramics*, Eds. J.D. Mackenzie and D.R. Ulrich, Wiley Interscience Publications, New York, 1988.
21. M.S. Kaliszewski and A.H. Heuer, *J. Am. Ceram. Soc.*, 73(6), (1990) 1504.
22. D. Vollath, *J. Mat. Sci.*, 25, (1990) 2227.
23. H. Kita, N. Henni, K. Shimazu, H. Hattori and K. Tanabe, *J. Chem. Soc., Faraday Trans., I*, 7, (1981) 2451.
24. R.O. James and A.R. Parks, *Surface and colloid science*, pp.119-124, Vol.12, Ed. E. Matijevic, Plenum, New York, 1988.

SUMMARY

Chemical methods of preparation of ceramic powders from solid phase, gas phase and solution phase reactions are generally employed in order to achieve high purity small unagglomerated, uniform sized particulates with good reproducibility. Some of the important properties of fine ceramic particulates depend a large extent on the method of preparation as well as preparative conditions. Hence it becomes very important to select a definite chemical route for a particular range of end properties.

The present investigation, in this background, is an attempt to prepare a range of ceramic oxide particulates through different routes and compare their properties. The different routes attempted are the citrate precursor method, urea-nitrate combustion method and the microwave decomposition method. The oxide systems selected are single, binary and ternary compounds, Al_2O_3 , SrTiO_3 and $\text{YBa}_2\text{Cu}_3\text{O}_{7-\delta}$ respectively. The important findings are summarised below.

Citrate gel method for the preparation of $\text{YBa}_2\text{Cu}_3\text{O}_{7-\delta}$ and $\text{Ag}/\text{YBa}_2\text{Cu}_3\text{O}_{7-\delta}$ compounds is simple and results in high order of homogeneity of phases in powders. It has been observed that $\text{YBa}_2\text{Cu}_3\text{O}_{7-\delta}$ phase starts forming as early as 550°C . Single phase $\text{YBa}_2\text{Cu}_3\text{O}_{7-\delta}$ compound prepared at 900°C showed an average particle size of $1.5\ \mu\text{m}$. $\text{Ag}/\text{YBa}_2\text{Cu}_3\text{O}_{7-\delta}$ composite prepared through this route does not require separate oxygen annealing

step to make it superconducting, probably due to high order of oxygen diffusivity in presence of finely distributed silver in the $\text{YBa}_2\text{Cu}_3\text{O}_{7-\delta}$ matrix.

$\text{YBa}_2\text{Cu}_3\text{O}_{7-\delta}$ superconductor has been prepared by a fast combustion technique involving a mixture of nitrates of Y, Ba and Cu and urea. Single phase $\text{YBa}_2\text{Cu}_3\text{O}_{7-\delta}$ compound could be formed when the combustion was conducted at 900°C followed by annealing at the same temperature for one hour. The average particle size of $\text{YBa}_2\text{Cu}_3\text{O}_{7-\delta}$ was $4\ \mu\text{m}$ with surface area as high as $42\ \text{m}^2/\text{gm}$. This method has been shown to reduce the processing time of $\text{YBa}_2\text{Cu}_3\text{O}_{7-\delta}$ superconductors considerably.

A novel microwave decomposition technique has been attempted for the easy and fast method of preparation of $\text{YBa}_2\text{Cu}_3\text{O}_{7-\delta}$ from a mixture of nitrates of the constituent cations. Appreciable amount of YBCO phase was formed on exposing the nitrate mixture of Y, Ba and Cu for 4 minutes to microwaves. Single phase YBCO has been obtained when the above mixture was further annealed at 900°C for 4 hours. The average particle size was 2 microns. The microwave exposed precursor of YBCO powder could be melt textured to highly a-b plane oriented samples.

A comparative study has been made on the properties of $\text{YBa}_2\text{Cu}_3\text{O}_{7-\delta}$ powders prepared by citrate gel method, flash combustion technique and microwave decomposition route along with a powder prepared by conventional solid state mixing route. All the three nonconventional methods require

processing time less than 10 hours while the conventional one requires 30 hours. Average particle size of the powders range from 1.5 to 4 μm in the case of former three routes while the latter route produces powders with broad particle size distribution i.e., 5-25 μm . Compaction density and sintered density were also high for the three powders from chemical routes. Superconducting property of citrate, flash and microwave derived sintered samples are markedly improved compared to conventional one with reference to T_c , J_c and ΔT_c .

Submicron strontium titanate particulate has been prepared by a modified sol-gel technique. Highly uniform sol or dispersed gel derived from titanium isopropoxide-acetic acid-strontium nitrate solutions were spray dried and decomposed at 550-600°C to generate 0.6 to 0.8 μm uniform SrTiO_3 powders. Sintered SrTiO_3 prepared from powder derived through sol spray route possesses improved dielectric property compared to gel derived counterpart.

Free flowing spherical alumina powder has been prepared from spray dried boehmite sol derived from aluminium nitrate. Effect of post preparation treatments on the spray dried boehmite powder were investigated. Preferential washing with non aqueous solvents has shown improved characteristics to the final alumina powders since considerable deagglomeration of the powders could be achieved.